Mnemonic architecture of a mini-brain: determining the wiring diagram of the larval mushroom body of *Drosophila melanogaster* using EM reconstruction

Doctoral thesis for obtaining the academic degree Doctor of Natural Sciences

submitted by
Katharina Eichler

at the

Universität Konstanz

Faculty of Sciences

Department of Biology

Konstanz, 2017

Konstanzer Online-Publikations-System (KOPS)
URL: http://nbn-resolving.de/urn:nbn:de:bsz:352-2--tu38tavwp4ml4

Date of the oral examination: 29. September 2017
1. Reviewer: Prof. Dr. Andreas S. Thum
2. Reviewer: Prof. Dr. C. Giovanni Galizia
3. Reviewer: Prof. Dr. Michael Pankratz

To my parents Monika and Stefan
and my sister Janina.

Table of contents

1 Summary

1.1 Deutsche Version

In der vorliegenden Doktorarbeit untersuche ich Lernen und Gedächtnis in *Drosophila* Larven. Die Fruchtfliege *Drosophila melanogaster* hat sich in den letzten Jahren zunehmend als geeigneter Modellorganismus zur Erforschung von neuronalen Netzwerken und Verhalten etabliert. *Drosophila* als Modellsystem bringt große Vorteile mit sich, so ist zum Beispiel das gesamte Genom sequenziert. Dies ermöglichte die Entwicklung eines umfangreichen genetischen Toolkits, welches erlaubt einzelne Gene und auch einzelne Zellen in beinahe unlimitierter Art und Weise zu manipulieren. Zusätzlich verfügt das Fliegengehirn nur über 100.000 und das larvale Gehirn sogar nur über 10.000 Nervenzellen. Somit wird die Erforschung der Aufgaben, welche Neurone in bestimmten Verhalten übernehmen, auf der Einzelzellebene in adulten sowie in larvalen *Drosophila* handhabbar.

Es wurde gezeigt, dass verschiedene assoziative Lernprozesse von mehreren Reizen im Pilzkörper stattfinden, dieser ist eine Struktur im Zentralgehirn von Insekten. Der Pilzkörper besteht aus parallelen Fasern, den sogenannten Kenyon-Zellen, in denen das gemeinsame Auftreten von konditionierten und unkonditionierten Reizen ermittelt wird. Während der konditionierte Reiz den Pilzkörper über die Haupteingangsstruktur, der sogenannten Calyx, erreicht, signalisieren die Eingangsneurone der Loben den unkonditionierten Reiz. Von den Loben senden Pilzkörper-Ausgangsneurone die gelernte Information zu prämotorischen Gehirnzentren weiter. Jedoch waren die Details über die Verknüpfungen, die Nervenzellen in dieser Gehirnregion miteinander machen, zu Beginn meiner Arbeit unbekannt.

Folglich ist ein zentrales Ziel meiner Doktorarbeit die Feinstruktur des Zentrums für Lernen und Gedächtnis, in einem Larvengehirn mit einer Auflösung auf Synapsenebene, zu erstellen. Weiterhin charakterisiert die vorliegende Doktorarbeit die neuronale Or-

ganisation von unkonditionierten Reizen, welche zum Pilzkörper signalisiert werden.
Zunächst beschreibe ich in *Kapitel I* eine elektronmikroskopische Studie, welche sich der Charakterisierung des Pilzkörpers im Detail widmet. Hierfür habe ich alle Pilzkörper intrinsischen Kenyon-Zellen und alle ihre pre- und postsynaptischen Partner von Hand rekonstruiert. Diese Arbeit wurde im Gehirn einer Larve im ersten Lebensstadium durchgeführt in einem Datensatz, welcher von Albert Cardona zur Verfügung gestellt wurde. Der Antennallobus ist das Duftzentrum, welches die Duftinformation in andere Gehirnzentren sendet, so auch in den Pilzkörper. Die Rekonstruktion des larvalen Antennallobus von Berck und Kollegen im selben Datensatz ermöglichte mir die Charakterisierung des Eingangs von konditionierten Reizen, welche die Kenyon-Zellen auf ihren Dendriten erhalten. In diesem Kapitel präsentiere ich das Konnektom des larvalen Lernzentrums, welches nun erstmalig die Verschaltungen im Pilzkörper in einer Detailgenauigkeit beschreibt, die zuvor nicht erreichbar war.
Während alle Verhaltensstudien in dieser Doktorarbeit Larven im dritten Stadium nutzen, wurde die Rekonstruktion mit einer Larve im ersten Stadium durchgeführt. Deswegen beschäftigt sich *Kapitel II* mit dem Vergleich dieser beiden Lebensstadien von *Drosophila* im Bezug auf angeborenes und gelerntes Verhalten. Hierbei konnte ich eine hohe Übereinstimmung der beschriebenen Verhalten feststellen, somit lassen sich Studien zur Anatomie und zum Verhalten der Larve über ihre Entwicklung hinweg vergleichen.
Anschließend führe ich ein aversives assoziatives Duftlernen in *Kapitel III* ein. Hier benutze ich einen mechanosensorischen Stimulus als Bestrafung und zeige, dass dieser angeborenes und erlerntes Fluchtverhalten in *Drosophila* Larven im dritten Stadium verursacht.
In *Kapitel IV* beschreibe ich die Organisation des Belohnungssystems im Pilzkörper. Hier dokumentiere ich die Rolle von Eingangs- und Ausgangsneuronen des Pilzkörpers

in appetitiven assoziatives Duftlernen in Larven im dritten Stadium. Hierfür wurden diese Zellen aktiviert oder deren Informationsübertragung an Synapsen ausgeschaltet. In *Kapitel V* beschreibe ich noch einmal den aktuellen Stand der Lern- und Gedächtnisforschung in *Drosophila* Larven in Form eines Reviews.

Zusammenfassend, zeige ich in meiner Doktorarbeit, dass die *Drosophila* Larve ein geeigneter Modellorganismus für die Erforschung von assoziativen Duftlernen und dessen zugrunde liegenden Mechanismen ist. Das Konnektom des Pilzkörpers wird die Gedächtnisforschung weiter vorantreiben und als Grundlage neuer Experimente dienen. Somit rückt ein Verstehen von erfahrungsabhängigen Verhaltensweisen durch die Integration von sensorischen Stimuli, um so mit der gelernten Information zum Beispiel leichter Futter zu finden und Fressfeinde zu vermeiden, in greifbare Nähe.

1.2 English Version

In my thesis, I studied learning and memory in the *Drosophila* larva. In the recent years the fruit fly *Drosophila melanogaster* was established as a suitable model organism for understanding neuronal networks and the expression of behavior. Using the fruit fly model system has great advantages due to its fully sequenced genome. This allowed for the development of an extensive genetic toolkit, which enables researchers to manipulate single genes and single cells in an almost unlimited fashion. Moreover the fruit fly brain contains only about 100,000 neurons and the larval brain has about an order of magnitude less. This makes investigating the role neurons play in particular behaviors manageable on the single-cell level in both the larva and the adult fly.

Associative learning of multiple stimuli is a process known to occur in the mushroom body (MB), an insect central brain structure. The MB consists of parallel fibers, the so-called Kenyon cells (KCs), which are coincidence detectors for the conditioned (CS, in my case olfactory stimuli) and unconditioned stimulus (US, relevant for this work: appetitive and aversive stimuli like sugar or vibration, respectively) during learning. The CS enters the MB at its main input structure the calyx and the US connects to the lobes of the MB. Output neurons from the lobes convey the learned information to premotor areas in the brain. However, the details of how the neurons wire together in the MB was largely unknown at the beginning of my thesis work.

Thus a central aim of this thesis is to reveal the ultrastructure of the learning and memory center in a larval brain in single-synapse resolution. This thesis work also further characterizes the organization of reward and punishment stimuli (US) signaling onto the MB.

First, in *Chapter I* I describe the electron microscopy effort to characterize the MB neuropile in a connectome study. I manually reconstructed all MB intrinsic KCs, and

all of their pre- and postsynaptic partners. For this work I used the whole first instar larval brain volume made available by Albert Cardona. The larval antennal lobe (AL) is the olfactory center that conveys odor information to higher order brain areas (MB and lateral horn). Recently Berck and colleagues have reconstructed the AL in the same volume enabling me to characterize the CS inputs KCs receive on their dendrites. In this chapter I reveal the connectome of the larval learning and memory center, showing the connections in the MB at a resolution that previously could not have been achieved. While the behavioral studies in this thesis employ third instar larvae, the connectome was reconstructed in a first instar larva dataset. Thus *Chapter II* deals with the comparison of innate and learned behavior of first and third instar larvae. I show a high degree of concordance which enables the comparison of anatomical and behavioral studies across the life stages of larvae.

Chapter III introduces an aversive olfactory learning paradigm using a mechanosensory stimulus as punishment. I show that such a stimulus can elicit innate and learned escape response behavior in third instar *Drosophila* larvae.

In *Chapter IV* I characterize the organization of the reward system of the MB. By activating or acutely silencing MB input and output neurons this chapter reveals the importance of these neurons for appetitive olfactory learning in third instar larvae.

Finally in *Chapter V* I review the current findings in the field of learning and memory in *Drosophila* larvae.

In summary, my thesis shows that the *Drosophila* larva is a suitable model organism to study the underlying mechanisms and networks of conditioned behavior. The accessibility of the MB connectome will guide future investigation into how a small brain integrates sensory stimuli to learn about the environment and to find food sources and avoid predators based on acquired knowledge.

2 General introduction

2.1 *Drosophila* as a suitable model organism

The fruit fly *Drosophila melanogaster* is a well established model organism offering a wide range of tools allowing for genetic manipulations. The adult fruit fly brain consists of a relatively small amount of neurons (about 100,000 [Iyengar et al., 2006]) yet is capable of complex behaviors such as courtship (reviewed in Pavlou and Goodwin [2013]), circadian rhythm and sleep (reviewed in Yamamoto and Koganezawa [2013]) and learning and memory (reviewed in Guven-Ozkan and Davis [2014]). The fruit fly also has a short life cycle (reviewed in Markow [2015]) and is easy to rear in the laboratory (reviewed in Stocker and Gallant [2008]).

The *Drosphila* genome contains many gene homologues of the human genome and thus shows a high degree of evolutionary conservation (reviewed in Bier [2005]). This makes the fly a model organism for studying the genetic processes underlying heritable diseases in humans [Hu et al., 2011]. Additionally, the fruit fly has been utilized to investigate cellular and molecular mechanisms that when failing lead to neurodegenerative diseases including Parkinson's and Alzheimer's as well as neurological diseases, such as amyotrophic lateral sclerosis (reviewed in Ugur et al. [2016]). Furthermore, the *Drosophila* olfactory system was found to be surprisingly similar to the mammalian one in respect of anatomical organization and its functional logic [Buck and Axel, 1991].

The complete sequencing of the fairly small *Drosophila* genome of about 13,600 genes in the year 2000 [Adams et al., 2000] allowed for a multitude of genetic tools to be developed. One of these tools is the GAL4 system published in 1993 by Brand and Perrimon [Brand and Perrimon, 1993] and has since been developed further based on the sequenced genome and gained significant importance in the field of neuroscience. The GAL4 system allows for targeted gene expression in *Drosophila* (for details see *section 2.3*). To restrict the GAL4 expression pattern even further another tool, the Split

GAL4 system was developed (Luan et al. [2006]; see *section 2.3*). The advantage of genetic accessibility enables large-scale genetic screens with behaving animals and makes *Drosophila melanogaster* an attractive model organism for studying behavior and its underlying neuronal mechanisms and networks.

2.2 The *Drosophila* life cycle

Drosophila melanogaster is a holometabolous insect with a short life cycle of around 10 days when reared at 25 °C [Demerec and Kaufmann, 1965]. Female flies can lay up to 3,000 eggs throughout their adult life [Ashburner et al., 2005]. During the first 24 hours after egg-laying embryogenesis occurs and a larva will hatch from its egg. Larvae undergo two molts, at 48 and 72 hours after egg-laying, resulting in three larval stages, so-called instars (Fig. 1). Two days later, after leaving the food substrate in the wandering stage for about one day, larvae pupate within the last larval skin [Demerec and Kaufmann, 1965]. In the subsequent four to five days metamorphosis takes place in the pupa to transform the larval body into the imago. The adult fly ecloses about 10

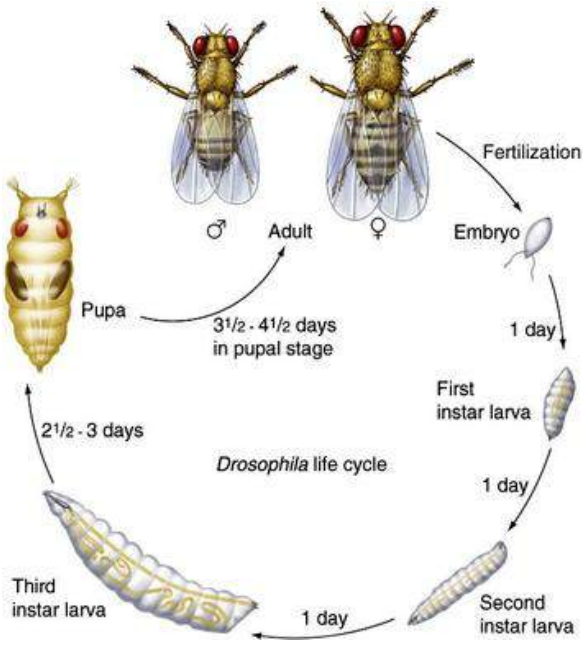

Figure 1: The *Drosophila melanogaster* life cycle
A larva hatches one day after egg-laying and goes through three larval stages over the course of about four days. The *Drosophila* larva pupates and after metamorphosis the imago ecloses. From http://www.creative-diagnostics.com/Drosophila.htm.

days after egg-laying. Female flies are fertile 8-12 hours after eclosure [Ashburner et al., 2005].

2.3 The GAL4/UAS-system

The GAL4/UAS-system developed by Brand and Perrimon [1993] allows expression of genes of interest in *Drosophila* in a cell- and tissue-specific manner (Fig. 2A).
Taking advantage of this genetic tool requires two fly strains, driver (containing the GAL4 construct) and effector (containing the UAS construct) strain (Fig. 2A). The *gal4* gene is coding for a yeast transcription factor that binds to its binding site, the UAS (**U**pstream **A**ctivation **S**equence). In the presence of the GAL4 transcription activator protein the UAS is activated and a gene downstream of UAS is transcribed.
A fly-specific promoter upstream of *gal4* restricts the expression pattern to a defined subset of cells expressing the transcription factor that drives the particular promoter [Brand and Perrimon, 1993]. In the offspring of the driver and effector strain cross GAL4 drives the transcription of a gene of interest only in a specific set of cells. Any gene of interest can be expressed under the control of UAS transcription. The possibility of diversifying the fly-specific promoter and the gene of interest makes this genetic tool very adaptable (reviewed in Yoshihara and Ito [2012]; Hudson and Cooley [2014]; Sivanantharajah and Zhang [2015]).
An approach to restrict the GAL4 expression pattern to just a few or even to single cells in the brain can be achieved by the Split GAL4 system (Fig. 2B). This tool uses the modular nature of GAL4, which consists of two domains, DNA binding (DBD) and activation domain (AD) to be functional. Each domain is fused to a heterodimerizing leucine zipper fragment, so that both domains are binding tightly together when expressed in the same cell [Luan et al., 2006] and thus creating the functional GAL4 transcription factor

(Fig. 2B). Both constructs can be under the control of a different promoter fragment. By crossing a DBD and an AD GAL4 strain one can generate a new fly strain in which the functional GAL4 is restrained to cells overlapping in both expression patterns.

The Janelia Research Campus hosts a collection of GAL4 and Split GAL4 driver and UAS effector fly strains that enable researchers to time-dependently gain control over a specific set of neurons in the *Drosophila* brain [Pfeiffer et al., 2008]. For example, neurons can be made visible by expressing a green fluorescent protein (GFP, reviewed in Tsien [1998]), silenced by a temperature sensitive protein *shibire* [Kitamoto, 2001] or activated with a channelrhodopsins like Chronos and Chrimson [Klapoetke et al., 2014]. Moreover, the activity of neurons can be monitored with a genetically encoded calcium indicator (GCaMP) [Tian et al., 2009].

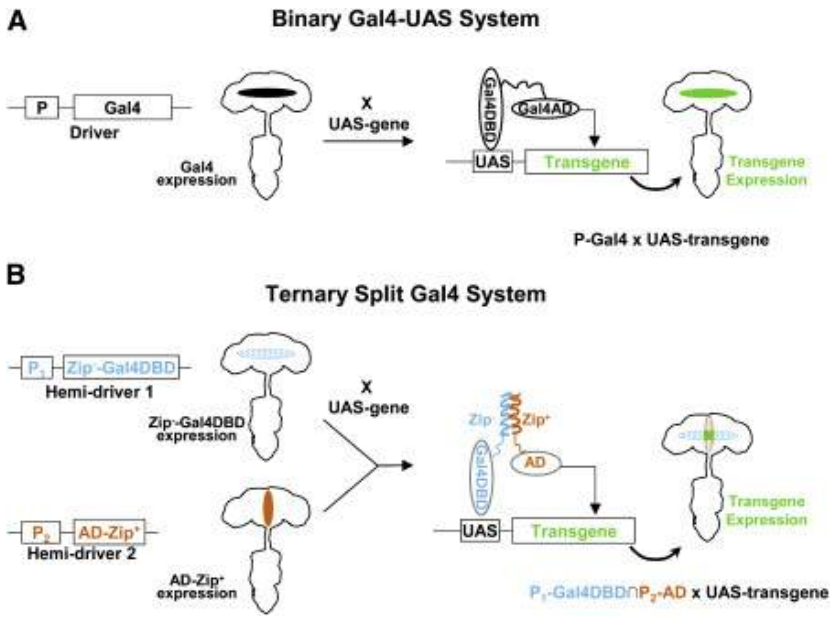

Figure 2: The Split GAL4 system restricts the expression pattern further
A The GAL4/UAS-system in *Drosophila* for targeted gene expression. The driver strain contains the *gal4* gene expressing the GAL4 transcription factor driven by the control of a genomic promotor (P) in a driver-specific expression pattern (*in black*). The UAS effector strain carries the upstream activation sequence (UAS) and the gene of interest (transgene, *in green*). When both strains are crossed together the GAL4 transcription factor can bind to the UAS and enables driver-specific expression of the gene of interest (*in green*).
B The Split GAL4 system uses the modular nature of the GAL4 protein. It consists of two separable domains, the DNA-binding (DBD) and transcription-activation (AD) domain. To ensure that both domains bind together when expressed they are fused to a leucine zipper (Zip^+ or Zip^-). Using different promotors for the two GAL4 domain constructs expresses the domains in different cell populations. Only in the intersection ($\cap$) of these two expression patterns domains are able to fuse and thus create a functional GAL4 transcription factor restricting the transgene expression to these cells.
From Luan et al. [2006].

2.4 Olfactory pathways in *Drosophila*

Olfaction is one of the most important senses for flies at any stage. It is key to finding mating partners, tracking down food sources and locating suitable sites for egg-laying. Adult *Drosophila* sense odors and pheromones with about 1,300 olfactory receptor neurons (ORNs, Fig. 3). These are located in the third antennal segment and the maxillary palp where they express olfactory receptors (ORs) (reviewed in Gerber et al. [2009]). The fly *Or* gene family consists of 60 genes encoding for 62 ORs [Robertson et al., 2003]. ORNs project to 50 glomeruli (reviewed in Gerber et al. [2009]) in the antennal lobe (AL), while ORNs expressing the same OR exist in multiple copies and target the same glomerulus. Odors activate multiple different ORNs and olfactory information is encoded as an activity pattern in the AL (reviewed in Hallem and Carlson [2004]). 150 projection neurons (PNs), about three from each glomerulus, send the olfactory information (in form of an activity pattern of PNs) to two higher brain centers: the mushroom body (MB) and lateral horn (LH) (reviewed in Gerber et al. [2009]). These two target areas of the PNs are thought to be involved in distinct tasks. While the MB is the center for learning and memory [Quinn et al., 1974] the LH was shown to be involved in innate olfactory behavior [De Belle et al., 1994; Tanaka et al., 2004; Jefferis et al., 2007]. PNs connect to approximately 2,000 MB intrinsic Kenyon cells (KCs; Kenyon [1896]) [Ito and Hotta, 1992; Aso et al., 2014a] in the calyx (Yasuyama et al. [2002]; Leiss et al. [2009]; for more detail see *section 2.7*).

The larval olfactory pathway has the same building plan as the adult pathway, however neuron numbers are reduced [Ramaekers et al., 2005; Kreher et al., 2005]. The 21 larval ORNs are located in the dome of the dorsal organ, a paired structure on each site of the larval head [Heimbeck et al., 1999; Kreher et al., 2005]. They each express their individual OR and send their axons to their individual glomerulus in the antennal lobe

[Ramaekers et al., 2005]. From there 21 PNs project to the larval LH and MB (where they connect to about 600 KCs; Stocker [2009]; reviewed in Gerber et al. [2009]) like in adult flies (Fig. 3).

While the adult olfactory pathway consists of converging and diverging connections [Stocker, 2009] the larval pathway relates the olfactory information in a one-to-one fashion [Ramaekers et al., 2005].

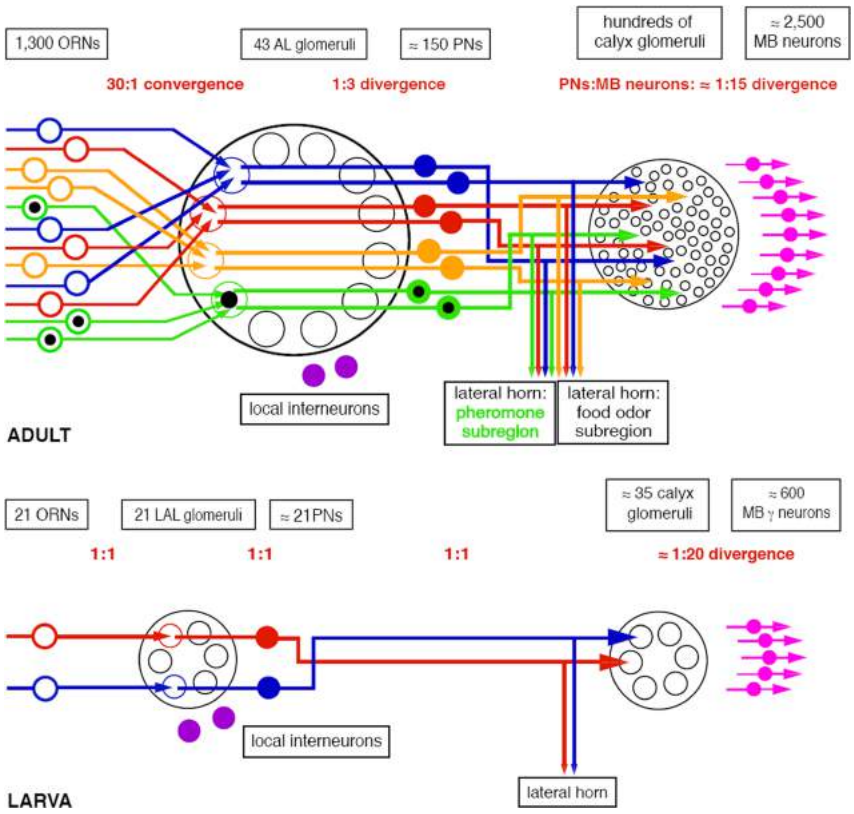

Figure 3: Olfactory pathways in adult and larval *Drosophila melanogaster*
The design of the olfactory pathways of adult and larval *Drosophila* is similar. However, larvae have drastically reduced numbers of neurons in each level of the pathway. There are multiple copies of adult olfactory receptor neurons (ORNs) and projection neurons (PNs). The adult olfactory pathway has layers of convergence and divergence, while the pathways in larvae are characterized by one-to-one connections. Larvae have only one ORN per expressed OR and a unique PN per glomerulus in the antennal lobe (AL). PNs signal olfactory information into two higher order brain centers, the mushroom body (MB) and the lateral horn in adult and larval *Drosophila*. Additionally, adult flies have a pheromone subsystem (black dots) that is missing in larvae. From Stocker [2009].

2.5 Gustatory pathways in *Drosophila*

The gustatory sense enables animals to navigate their chemosensory environment by physical contact and to distinguish between harmful and safe food. The taste system controls eating and drinking behavior. In *Drosophila* tastes are categorized into relatively few modalities, like sweet, salt and bitter (reviewed in Vosshall and Stocker [2007];

Gerber et al. [2009]). Taste sensilla, which are hairlike structures, are found at the tarsi, labellum, wing margins and in the pharynx of adult flies (reviewed in Stocker [1994]; Singh [1997]). Gustatory receptor neurons (GRNs) are organized in two to four neurons per sensilla. The circuitry of the gustatory system is not as well understood as the olfactory pathways. From the sensory organs on the labellum, pharynx and tarsi GRNs project to their first-order processing center, the subesophageal zone (SEZ) (Wang et al. [2004]; reviewed in Stocker [1994]). GRNs that express the same GR and derive from different taste organs do not project to the same brain area like the ORNs do in the AL. The projections of GRNs are constrained by the nerve through which they enter the brain and thus they segregate into different parts of the SEZ depending on the taste organ they originated from [Stocker and Schorderet, 1981; Scott et al., 2001; Wang et al., 2004].

A gene family related to the *Or* family consisting of 60 members (*Gr* family) encodes for 68 gustatory receptors [Clyne et al., 2000; Scott et al., 2001]. In this family *Gr5a*, *Gr64a-f* and *Gr66a* are the best understood genes and code for sweet and bitter taste sensing receptors (reviewed in Gerber et al. [2009]). *Gr5a* encodes a trehalose receptor that binds to a variety of sugars (for example: trehalose, arabinose, fructose, and sucrose; reviewed in Gerber et al. [2009]) and activates the neuron expressing the receptor [Tanimura et al., 1988]. Surprisingly, *Gr5a* neurons are also activated by low concentrations of salt (NaCl; Marella et al. [2006]). Neurons expressing *Gr64a* have been found to be activated by other sugars like maltotriose or stachyose [Dahanukar et al., 2007]. Both receptors *Gr5a* and *Gr64a* were proposed to be complementary in detecting different types of sugar and might be expressed in the same cell acting as independent sensors (Dahanukar et al. [2007]; reviewed in Gerber et al. [2009]). Recently *Gr43a* was found to be a fructose receptor in the hemolymph of adult flies [Miyamoto et al., 2012]. While these receptors seem to be activated by positive taste

experiences, the *Gr66a* receptor bind to negative tastants [Moon et al., 2006]. *Gr66a* neurons are activated by bitter compounds like caffeine, quinine and limonin, as well as high concentrations of salt, but not by sweet compounds [Marella et al., 2006]. Interestingly, salt can be sensed by sweet and bitter receptors dependent on the salt concentration, suggesting the existence of two different salt sensors. In both cases members of the *pickpocket* (*ppk*) gene family are involved in the process. One *ppk* gene, *ppk11*, might mediate the appetitive response to low salt concentrations and another one, *ppk19*, is involved in the aversive responses to high concentrations of salt [Liu et al., 2003]. Furthermore GRNs have been found to sense water, however the underlying processes and neurons involved are largely unknown (Inoshita and Tanimura [2006]; reviewed in Gerber et al. [2009]).

Interestingly larvae behave very similar to the adult fly towards different tastants. They avoid high concentrations of salt and bitter compounds and prefer sugars and low salt concentrations [Liu et al., 2003; Niewalda et al., 2008]. Larvae have two more external sense organs (terminal and ventral organs) and four pharyngeal organs [Gendre et al., 2004] in addition to the aforementioned dorsal organ involved in olfaction. Most of these organs are suggested to be involved in gustation (Singh and Singh [1984]; Python and Stocker [2002]; reviewed in Gerber et al. [2009]). Food search is the main task of a larva (reviewed in Tennessen and Thummel [2011]) and therefore it is important to evaluate putative food sources. Unsurprisingly different studies estimated there to be 90 GRNs per body side (Python and Stocker [2002]; Colomb et al. [2007]; reviewed in Apostolopoulou et al. [2015]), outnumbering the ORNs by large. This is consistent with a feeding focused larval life style dug into the food, while flying adult flies have 1,300 ORNs (reviewed in Stocker [2001]) and only 600 GRNs (reviewed in Stocker [1994]). Like in adult flies, larvae express the *Gr66a* gene and it encodes for bitter receptors [Kwon et al., 2011; Apostolopoulou et al., 2014, 2016]. Also neurons expressing the

ppk11 gene were found in larvae, which are activated by low salt concentrations [Liu et al., 2003; Colomb et al., 2007]. Recently, the receptor gene *GR43a* was described as the major larval sugar receptor [Mishra et al., 2013]. Moreover it has been found that a set of GRNs expresses a gene called *serrano* as well as *ppk19* and *Gr66a* which are all required for high-salt perception [Alves et al., 2014]. Interestingly GRNs project to similar regions in the SEZ in larvae as observed in adult *Drosophila* [Scott et al., 2001; Colomb et al., 2007].

Candidate target neurons of GRNs have been reported to express the *hugin* gene and send processes to the protocerebrum and the ventral nerve cord in larvae [Colomb et al., 2007; Bader et al., 2007; Melcher and Pankratz, 2005]. In adult flies as well as in larvae further gustatory pathways in the brain remain largely unknown (for detail see *section 2.6*)

2.6 Other sensory pathways in *Drosophila* larvae

In addition to olfactory and gustatory stimuli adult flies as well as larvae can detect other sensory cues like mechanosensory, temperature, nociceptive and visual stimuli. I will focus on the larval pathways due to their relevance to *Chapter I*. Recently Ohyama et al. [2015] described a multimodal sensory pathway involved in escape behavior as a response to an attack of a predatory wasp [Tracey et al., 2003]. While so-called multi-dendritic class IV neurons sense the nociceptive stimuli of the wasps sting, chordotonal neurons react to mechanosensory cues like vibration resulting from the wasps wing motions. Nociceptive and mechanosensory stimuli are integrated in the larval brain to enhance the selection of the fastest mode of escape locomotion [Ohyama et al., 2015]. Furthermore larvae can sense air-currents [Ohyama et al., 2013; Jovanic et al., 2016] and respond with startle behavior or explore the environment further with a head-turn

[Ohyama et al., 2013]. This gentle mechanical stimulus activates the mentioned chordotonal neurons [Ohyama et al., 2013; Jovanic et al., 2016].

Drosophila larvae can also navigate temperature gradients moving up the gradient between 15 °C and 23 °C and down the gradient at temperatures above 30 °C. Three sensory neurons in each dorsal organ at the larval head have been found to be involved in cold avoidance behavior, while neurons for warm avoidance behavior remain unknown [Klein et al., 2015].

Moreover larvae show light avoidance behavior for which the Bolwig's organs (BO) [Hassan et al., 2000] and class IV multidendritic (md) [Xiang et al., 2010] neurons are required. The BO contains of 12 photoreceptors (PR) that express Rhodopsin (eight express Rh6 and four express Rh5) and is involved in phototaxis at low light levels. PRs send their axons to the larval optical neuropil and contact three classes of neurons: three optic lobe pioneer neurons, a serotonergic cell cluster and five lateral neurons (LNs) which are essential for light avoidance behavior [Sprecher et al., 2011; Kane et al., 2013]. The md neurons express Rhodopsin only in very small amounts and respond to high light levels like the sun light (Sokabe et al. [2016]; reviewed in Keene and Sprecher [2012]).

In summary larvae can navigate their environment based on olfactory, gustatory, mechanosensory, nociceptive, temperature and visual cues. These stimuli can be associated with one another in a central brain structure to learn about features of the larval world to make predictions about the future (see next section).

2.7 Associating different sensory modalities

Association of different sensory stimuli gives organisms the advantage of learning about their environment and predicting future events. Learning and memory is an

activity-dependent process described to require a central-brain structure in insects called the mushroom body (MB) [Heisenberg et al., 1985]. Adult *Drosophila* show Pavlovian learning by associating odors with a reward (sugar; Tempel et al. [1983]) or a punishment (electric shock; Tully and Quinn [1985]). In a classical conditioning paradigm flies receive an electric shock in the presence of an odor A. Subsequently flies are presented another odor B and no electric shock occurs. To control for innate preference of the flies towards the odors or any other odor-specific effects, another group of flies is trained reciprocally (odor A, no shock; odor B with shock). After training flies face a choice test in which they avoid the previously punished odor (reviewed in Gerber et al. [2009]). But how does this memory come about?

The mushroom body is where these associations occur. Here the unconditioned stimulus (US; e.g. electric shock) and the conditioned stimulus (CS; e.g. odor) are integrated and processed to establish the conditioned response (e.g. odor avoidance) [Heisenberg et al., 1985]. In flies the CS enters the MB in its main input structure, the so-called calyx (Fig. 4A). Olfactory projection neurons (PNs) form large presynaptic boutons in the calyx [Yasuyama et al., 2002; Leiss et al., 2009]. MB Intrinsic Kenyon cells (KCs) [Kenyon, 1896], wrap their dendritic branches around the PN boutons forming claw-like structures. KCs were found to typically have about 6 claws with different PNs in the larva [Masuda-Nakagawa et al., 2005] and five to six in adult *Drosophila* [Leiss et al., 2009]. The connectivity between PNs and KCs has previously been suggested to be random [Masuda-Nakagawa et al., 2005; Murthy et al., 2008; Caron et al., 2013]. However one study in larvae found a high degree of stereotypy in the connectivity between AL and calyx glomeruli [Ramaekers et al., 2005]. Another study in adult *Drosophila* found a regionalized and probabilistic connectivity [Gruntman and Turner, 2013]. Additionally to olfactory input (for adult reviewed in Heisenberg [2003]; Waddell [2013]; Owald and Waddell [2015]; Schürmann [2016] and larvae *Drosophila* Berck et al. [2016]; Masuda-

Nakagawa et al. [2005]; reviewed in Gerber et al. [2009]) KCs were reported to receive gustatory, visual and thermal input in the adult *Drosophila* calyx (Bang et al. [2011]; Vogt et al. [2014]; reviewed in Owald and Waddell [2015]; Schürmann [2016]; for larvae see *Chapter I*).

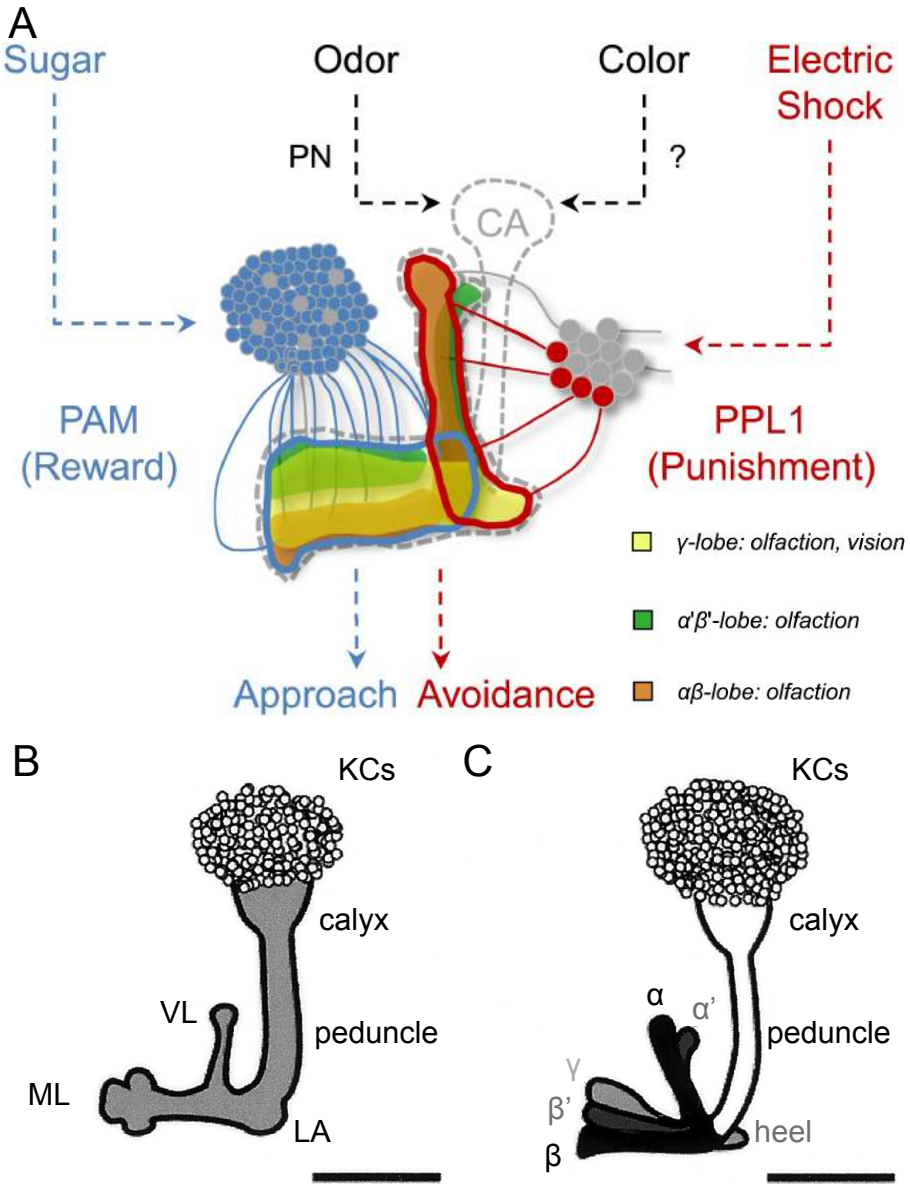

Figure 4: The mushroom body (MB) of *Drosophila melanogaster*
A Schematic of the reward and punishment pathways in an adult *Drosophila* MB. Odor information is signaled to the MB calyx via projection neurons (PN). Also visual information enters the MB at the calyx. The reward is mediated by dopaminergic PAM-cluster neurons onto the horizontal lobe and punishment is signaled via PPL1-cluster neurons onto the vertical lobe. γ Kenyon cells are involved in visual and olfactory memory, while α/β and α'/β' Kenyon cells mediate olfactory learning. Adapted from Vogt et al. [2014].
B Schematic of the larval MB. KC send dendrites into the calyx and parallel axons through the peduncle and bifurcate at the lower peduncle into medial (ML) and vertical lobe (VL). There they also send extensions into the lateral appendix (LA). Scale bar is 50 µm.
C Schematic of the adult fly MB. The horizontal lobe consists of three parallel structures: β, β' and γ lobe. The vertical lobe is divided into α and α' lobes. KCs send their dendrites into the calyx and axons into the lobes in three distinct morphological patterns. They either bifurcate into α/β or α'/β' or innervate only the γ lobe. Scale bar is 60 µm.
B and C adapted from Kurusu et al. [2000].

As mentioned before KCs have their dendrites in the calyx of the MB. Furthermore they form parallel axons in the peduncle and bifurcate into the horizontal (called medial lobe

in larvae) and the vertical lobe [Aso et al., 2014a; Kunz et al., 2012] (Fig. 4B and C). MB extrinsic dopaminergic (DANs) and octopaminergic modulatory neurons (OANs) connect to KCs in the lobes defining separate compartments. Dopamine and octopamine are neurotransmitter that have been shown to be involved in signaling the US during learning in insects. DANs and OANs convey the rewarding and punishing signals to the MB KCs in insects (adult insects; Schwaerzel et al. [2003]; Vergoz et al. [2007] reviewed in Waddell [2013]; Owald and Waddell [2015]; Schürmann [2016], larval *Drosophila*; Selcho et al. [2009]; Pauls et al. [2010]; Selcho et al. [2014]; Rohwedder et al. [2016]; reviewed in Gerber et al. [2009]; Diegelmann et al. [2013]) and tile the MB into distinct compartments [Pauls et al., 2010; Aso et al., 2014a]. DANs from the PAM-cluster connect to the horizontal lobe and have been shown to be involved in appetitive (reward) learning [Liu et al., 2012]. PPL1-cluster DANs innervate the vertical lobe and were reported to play a role in aversive (punishment) learning [Aso et al., 2012] (Fig. 4A). MB output neurons (MBONs) send their dendritic arborizations into the lobe compartments respecting the boundaries formed by the DANs/OANs (adult; Aso et al. [2014a]; Owald et al. [2015]; reviewed in Owald and Waddell [2015], larvae *Drosophila*; Pauls et al. [2010]). Thus each compartment is characterized by DAN-to-KC and KC-to-MBON connections. It has been shown that simultaneous activation of KCs and DANs can modulate the KC-MBON synapses (reviewed in Owald and Waddell [2015]; Schürmann [2016]). Interestingly MBONs from the horizontal lobe drive aversive behavior when optogenetically activated, even though their DANs/OANs encode reward [Owald et al., 2015; Aso et al., 2014b]. Similarly activating MBONs from the vertical lobe drives appetitive behavior, while the DANs/OANs from these compartments signal punishment [Aso et al., 2014b]. The current model in the field is that synaptic depression occurs at the KC-MBON synapses. Associating an odor with a punishment “weakens” the KC-MBON synapses in the active DAN compartment and causes the flies to subsequently

approach this odor less.

Interestingly, the MB has been compared to the cerebellum in the mammalian brain due to consisting of granule cells organized in parallel fibers (KCs) [Kenyon, 1896] and the synaptic connections between extrinsic afferent and efferent elements (MBINs/MBONs) with the intrinsic fibers [Schürmann, 1974].

2.8 Similarities and differences of adult and larval MBs

The MB KCs derive from four neuroblasts that divide consistently from the embryonic to the end of the pupal stage forming the larval and adult MB [Ito and Hotta, 1992; Kunz et al., 2012]. While first instar larvae have a relatively small number of KC ($\sim$100; see *Chapter I*), the adult MB consists of approximately 2,000 KCs [Ito and Hotta, 1992; Aso et al., 2014a]. The principal architecture of the MB shares similar features. KC axons form the peduncle in a parallel bundle and later bifurcate into vertical and horizontal (medial) lobes [Kurusu et al., 2002]. While the larva has only one medial and one vertical lobe system, the adult MB is organized in seven KC subunits in three horizontal and 2 vertical lobes (Fig. 4) [Lee et al., 1999; Tanaka et al., 2008; Aso et al., 2014a]. MB input neurons have been shown to be octopaminergic or dopaminergic (adult Schwaerzel et al. [2003]; Aso et al. [2014a]; reviewed in Waddell [2013], larva Selcho et al. [2009, 2014]). DANs/OANs and MBONs tile the MB into a relatively small number of compartments in both larval [Pauls et al., 2010] and adult MB [Aso et al., 2014a]. In the calyx KC wrap around PN boutons in both life stages forming “claw”-like structures (adult Yasuyama et al. [2002]; Leiss et al. [2009], larva Masuda-Nakagawa et al. [2005]; Ramaekers et al. [2005]. While the larval MB has KCs that only present one claw in the calyx [Ramaekers et al., 2005], these single-claw KCs have not been found yet in the adult MB. Another important difference is that a key neuron for memory consolidation in the adult MB,

the DPM neuron [Waddell et al., 2000; Haynes et al., 2015], has not been found in larval *Drosophila*. However, a paired GABAergic feedback neuron innervating most MB compartments, called the APL neuron, was found in both larval [Masuda-Nakagawa et al., 2014] and adult MB [Liu and Davis, 2009].

2.9 Comprehensive electron microscopy (EM) reconstruction is fast in the *Drosophila* larva

Neurons connect to each other through synapses, building circuits in which they send and process information. Mapping the neural connections in a circuit is important for understanding the possible flow of information within a circuit - and in determining the circuit motifs that could implement neural computations. With serial section transmission electron microscopy [Hayworth et al., 2006; Anderson et al., 2009; Cardona et al., 2010] one can generate images of brain tissues, which can be analyzed for synapses and neuron structure [Cardona et al., 2010; Schürmann, 2016] subsequently. The *Drosophila* larval MB is very similar in organization and function to the adult MB but has an order of magnitude less KCs (reviewed in Gerber et al. [2009]) and each neuron is an order of magnitude smaller. Hence reconstruction of an entire MB is two orders of magnitude faster and thus becomes very feasible. In *Chapter I* we reconstructed neurons in a first instar larval brain EM volume, made available by the lab of Albert Cardona at Janelia Research Campus (USA). After dissecting the brain from the larva it was cut into thin slices (50 nm) using an ultramicrotome, these sections were imaged with an electron microscope (for more detail see *Chapter I Material and Methods*) as mosaics with slightly overlapping image areas. The overlap allows for assembly of individual sections computationally. Moreover, cutting the sections can deform them and destroys the continuity between them [Saalfeld et al., 2012]. Thus the deformations have to be

removed and the sections need to be aligned. Assembly and alignment of the sections generates a 3D representation of the imaged brain tissue [Cardona et al., 2012; Saalfeld et al., 2012]. This dataset is embedded into a browser-based reconstruction software called CATMAID (**C**ollaborative **A**nnotation **T**oolkit for **M**assive **A**mounts of **I**mage **D**ata; Fig. 5, Saalfeld et al. [2009]; Cardona et al. [2012]; Schneider-Mizell et al. [2016]) for manual reconstruction of neurons and networks.

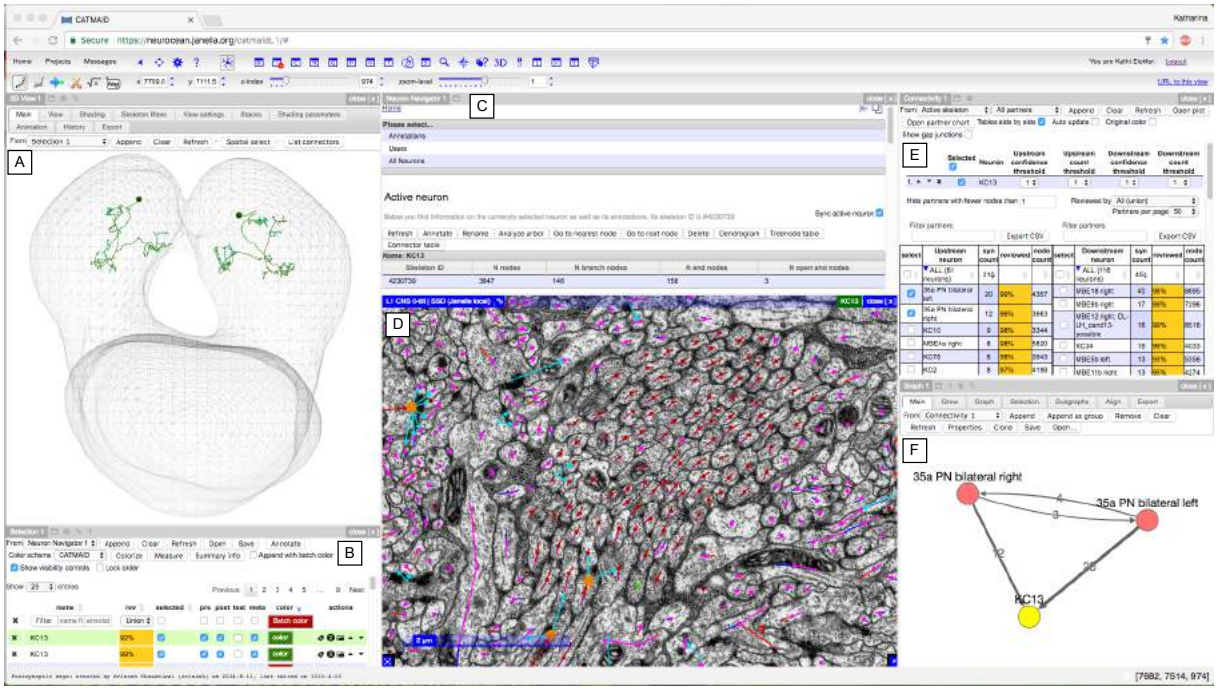

Figure 5: Collaborative Annotation Toolkit for Massive Amounts of Image Data (CATMAID)
Screenshot of the browser-based annotation toolkit with some representative widgets shown that are employed for reconstruction of neurons.
A The 3D widget allows for visualization of reconstructed neurons (here two KCs in green) and the whole larval CNS (grey mesh).
B Neurons can be listed in the Selection widget, visual features can be changed here to be presented in the 3D widget (A).
C The Neuron Navigator allows for organization of the reconstruction effort. Neurons can be given meaningful tags, so-called annotations. This tool helps with searching for neurons by their name or annotations.
D The EM stacks are manually reconstructed (colored dots on top of black-and-white EM images). This is a cross section of the larval MB peduncle with reconstructed KCs in dark red.
E The Connectivity widget lists all pre- and postsynaptic partners of neurons of interest by the connection strength (here a KC of the right brain hemisphere). This tool helps with targeted reconstruction of connected neurons. All listed neurons and synapses are ”clickable” and lead the user to the respective location in the EM stacks in (D).
F Connections between neurons can be made visible in the Graph widget. Again connections are ”clickable” and lead to the respective synapse location in (D).
After reconstruction neurons can be reviewed branch by branch with the help of the Review widget (not shown), to ensure reconstruction accuracy. The widgets in CATMAID support fast reconstruction of neurons and their visualization for comparison purposes with light microscopy data.

Starting the reconstruction of a neuron in this environment begins with the soma of a neuron of interest or at a synapse up- or downstream of a reconstructed neuron. Subsequently, the user follows all the branches of the neuron and marks all the synapses. A user documentation on how to trace neurons is available at http://catmaid.readthedocs.io/en/stable/#. The tools provided by CATMAID allow for fast neuron reconstruction with a single-cell and -synapse resolution and help with accuracy.

For example, visualizing homologous neurons of both brain hemispheres in the 3D widget (Fig. 5A) helps with detection of missing branches when comparing the two neurons. Analyzing reconstructed networks in both brain hemisphere in the Graph widget (Fig. 5F) allows identification of missing connections in one hemisphere and further investigation of the neurons missing that connection. Furthermore, CATMAID's tools help with analyzing the reconstructed neuronal network and allow for export of neuronal features into different file formats (tables showing connection strength between neurons, lists of all 3D coordinates of a neuron and its synapses) for further investigation.

2.10 Introduction to Chapters I - V

2.10.1 Chapter I

For my thesis I focus on uncovering the ultrastructure of a learning and memory center. It has been shown that a central brain structure, the so-called mushroom body (MB), is required in insects in general for establishing and retrieving an olfactory memory [Heisenberg et al., 1985]. The MB has been extensively characterized in light microscopic and behavioral studies recently in adult (Aso et al. [2014a,b] reviewed in Owald and Waddell [2015]) as well as larval *Drosophila* [Rohwedder et al., 2016]; reviewed in Diegelmann et al. [2013]; Schleyer et al. [2011]). However no wiring diagram of this brain area in single-neuron- and single-synapse-resolution has been available to this date.

Such a map could guide further behavioral analysis and assist in the understanding of learning processes.

As mentioned before the MB in adult *Drosophila* consists of ∼2,000 intrinsic and ∼200 extrinsic elements [Aso et al., 2014a]. Like in the adult the MB is crucial for associative learning in larvae, yet has about an order of magnitude less neurons (reviewed in Gerber et al. [2009]). It has been shown that even the earliest stages of larvae can form associative memories with their embryonic born KCs [Pauls et al., 2010]. Due to the relatively small size of larval neurons, complete circuit reconstruction can be achieved quickly [Berck et al., 2016; Ohyama et al., 2015; Jovanic et al., 2016; Schneider-Mizell et al., 2016].

Thus I set out to manually reconstruct all MB intrinsic KCs and their pre- and postsynaptic partners in the first instar larva brain dataset from Albert Cardona (see *section 2.9*). This chapter analyzes the resulting connectome of the first instar larval MB and describes its implication in associative learning behavior.

2.10.2 Chapter II

The MB connectome described in *Chapter I* was reconstructed in a first instar larva, due to the much smaller size of its nervous system compared to third instar larvae. However most behavioral studies (see *Chapter III and IV*) are performed in third instar larvae, because their body size makes them easier to handle. This chapter aims to compare innate and learned behaviors in these larval stages to provide confidence in relating functional studies in third instar with circuit reconstruction data acquired in first instar larvae.

2.10.3 Chapter III

Chapter III describes the behavior of third instar *Drosophila* larvae in response to vibration, a mechanosensory disturbance. This stimulus ('buzz') is presented through a loud speaker located beneath a agarose-filled petri dish on which the larvae crawl and is equivalent to the natural sound of predatory wasps attacking larvae. I study the impact of three different buzz frequencies on locomotion and innate olfactory behavior. Moreover I show that certain buzz frequencies can serve as a punishing stimulus in olfactory learning in larvae. This chapter investigates the behavior first reported in Eschbach et al. [2011] further.

2.10.4 Chapter IV

Based on the connectome described in *Chapter I* I analyze the function of MB extrinsic (in- and output) neurons (MBEs) in this chapter. This study focuses on the behavioral architecture of MBEs and their specific function for associative odor-taste reward learning. I acutely block synaptic output of MBEs or optogenetically activate these neurons during odor-fructose learning employing the GAL4/UAS-system. I reveal the function of nearly all MBEs in innate olfactory and gustatory behavior as well as in odor-taste associative learning in third instar larvae.

2.10.5 Chapter V

In this review I summarize the current progress in the field of larval olfactory learning. I relate the recent findings from the circuit reconstruction of the larval MB (*Chapter I*) to behavior reported by other studies. Moreover I review the current findings about the molecular network of learning and memory in *Drosophila* larvae.

2.11 References

Adams, M. D., Celniker, S. E., Holt, R. A., Evans, C. A., Gocayne, J. D., Amanatides, P. G., Scherer, S. E., Li, P. W., Hoskins, R. A., Galle, R. F., et al. (2000). The genome sequence of drosophila melanogaster. *Science*, 287(5461):2185–2195.

Alves, G., Sallé, J., Chaudy, S., Dupas, S., and Manière, G. (2014). High-nacl perception in drosophila melanogaster. *Journal of Neuroscience*, 34(33):10884–10891.

Anderson, J. R., Jones, B. W., Yang, J.-H., Shaw, M. V., Watt, C. B., Koshevoy, P., Spaltenstein, J., Jurrus, E., Kannan, U., Whitaker, R. T., et al. (2009). A computational framework for ultrastructural mapping of neural circuitry. *PLoS Biol*, 7(3):e1000074.

Apostolopoulou, A. A., Köhn, S., Stehle, B., Lutz, M., Wüst, A., Mazija, L., Rist, A., Galizia, C. G., Lüdke, A., and Thum, A. S. (2016). Caffeine taste signaling in drosophila larvae. *Frontiers in Cellular Neuroscience*, 10.

Apostolopoulou, A. A., Mazija, L., Wüst, A., and Thum, A. S. (2014). The neuronal and molecular basis of quinine-dependent bitter taste signaling in drosophila larvae. *Frontiers in behavioral neuroscience*, 8:6.

Apostolopoulou, A. A., Rist, A., and Thum, A. S. (2015). Taste processing in drosophila larvae. *Frontiers in integrative neuroscience*, 9:50.

Ashburner, M. et al. (2005). *Drosophila. A laboratory handbook.* Cold Spring Harbor Laboratory Press.

Aso, Y., Hattori, D., Yu, Y., Johnston, R. M., Iyer, N. A., Ngo, T.-T., Dionne, H., Abbott, L., Axel, R., Tanimoto, H., et al. (2014a). The neuronal architecture of the mushroom body provides a logic for associative learning. *Elife*, 3:e04577.

Aso, Y., Herb, A., Ogueta, M., Siwanowicz, I., Templier, T., Friedrich, A. B., Ito, K., Scholz, H., and Tanimoto, H. (2012). Three dopamine pathways induce aversive odor memories with different stability. *PLoS Genet*, 8(7):e1002768.

Aso, Y., Sitaraman, D., Ichinose, T., Kaun, K. R., Vogt, K., Belliart-Guérin, G., Plaçais, P.-Y., Robie, A. A., Yamagata, N., Schnaitmann, C., et al. (2014b). Mushroom body output neurons encode valence and guide memory-based action selection in drosophila. *Elife*, 3:e04580.

Bader, R., Colomb, J., Pankratz, B., Schröck, A., Stocker, R. F., and Pankratz, M. J. (2007). Genetic dissection of neural circuit anatomy underlying feeding behavior in drosophila: Distinct classes of hugin-expressing neurons. *Journal of Comparative Neurology*, 502(5):848–856.

Bang, S., Hyun, S., Hong, S.-T., Kang, J., Jeong, K., Park, J.-J., Choe, J., and Chung, J. (2011). Dopamine signalling in mushroom bodies regulates temperature-preference behaviour in drosophila. *PLoS Genet*, 7(3):e1001346.

Berck, M. E., Khandelwal, A., Claus, L., Hernandez-Nunez, L., Si, G., Tabone, C. J., Li, F., Truman, J. W., Fetter, R. D., Louis, M., et al. (2016). The wiring diagram of a glomerular olfactory system. *Elife*, 5:e14859.

Bier, E. (2005). Drosophila, the golden bug, emerges as a tool for human genetics. *Nature Reviews Genetics*, 6(1):9–23.

Brand, A. H. and Perrimon, N. (1993). Targeted gene expression as a means of altering cell fates and generating dominant phenotypes. *development*, 118(2):401–415.

Buck, L. and Axel, R. (1991). A novel multigene family may encode odorant receptors: a molecular basis for odor recognition. *Cell*, 65(1):175–187.

Cardona, A., Saalfeld, S., Preibisch, S., Schmid, B., Cheng, A., Pulokas, J., Tomancak, P., and Hartenstein, V. (2010). An integrated micro-and macroarchitectural analysis of the drosophila brain by computer-assisted serial section electron microscopy. *PLoS Biol*, 8(10):e1000502.

Cardona, A., Saalfeld, S., Schindelin, J., Arganda-Carreras, I., Preibisch, S., Longair, M., Tomancak, P., Hartenstein, V., and Douglas, R. J. (2012). Trakem2 software for neural circuit reconstruction. *PloS one*, 7(6):e38011.

Caron, S. J., Ruta, V., Abbott, L., and Axel, R. (2013). Random convergence of olfactory inputs in the drosophila mushroom body. *Nature*, 497(7447):113–117.

Clyne, P. J., Warr, C. G., and Carlson, J. R. (2000). Candidate taste receptors in drosophila. *Science*, 287(5459):1830–1834.

Colomb, J., Grillenzoni, N., Ramaekers, A., and Stocker, R. F. (2007). Architecture of the primary taste center of drosophila melanogaster larvae. *Journal of Comparative Neurology*, 502(5):834–847.

Dahanukar, A., Lei, Y.-T., Kwon, J. Y., and Carlson, J. R. (2007). Two gr genes underlie sugar reception in drosophila. *Neuron*, 56(3):503–516.

De Belle, J. S., Heisenberg, M., et al. (1994). Associative odor learning in drosophila abolished by chemical ablation of mushroom bodies. *Science-AAAS-Weekly Paper Edition-including Guide to Scientific Information*, 263(5147):692–694.

Demerec, M. and Kaufmann, B. P. (1965). *Drosophila guide: introduction to the genetics and cytology of Drosophila melanogaster*. Carnegie Institution of Washington Washington, DC.

Diegelmann, S., Klagges, B., Michels, B., Schleyer, M., and Gerber, B. (2013). Maggot learning and synapsin function. *Journal of Experimental Biology*, 216(6):939–951.

Eschbach, C., Cano, C., Haberkern, H., Schraut, K., Guan, C., Triphan, T., and Gerber, B. (2011). Associative learning between odorants and mechanosensory punishment in larval drosophila. *Journal of Experimental Biology*, 214(23):3897–3905.

Gendre, N., Lüer, K., Friche, S., Grillenzoni, N., Ramaekers, A., Technau, G. M., and Stocker, R. F. (2004). Integration of complex larval chemosensory organs into the adult nervous system of drosophila. *Development*, 131(1):83–92.

Gerber, B., Stocker, R. F., Tanimura, T., and Thum, A. S. (2009). Smelling, tasting, learning: Drosophila as a study case. In *Chemosensory Systems in Mammals, Fishes, and Insects*, pages 187–202. Springer.

Gruntman, E. and Turner, G. C. (2013). Integration of the olfactory code across dendritic claws of single mushroom body neurons. *Nature neuroscience*, 16(12):1821–1829.

Guven-Ozkan, T. and Davis, R. L. (2014). Functional neuroanatomy of drosophila olfactory memory formation. *Learning & Memory*, 21(10):519–526.

Hallem, E. A. and Carlson, J. R. (2004). The odor coding system of drosophila. *TRENDS in Genetics*, 20(9):453–459.

Hassan, J., Busto, M., Iyengar, B., and Campos, A. R. (2000). Behavioral characterization and genetic analysis of the drosophila melanogaster larval response to light as revealed by a novel individual assay. *Behavior genetics*, 30(1):59–69.

Haynes, P. R., Christmann, B. L., and Griffith, L. C. (2015). A single pair of neurons links sleep to memory consolidation in drosophila melanogaster. *Elife*, 4:e03868.

Hayworth, K., Kasthuri, N., Schalek, R., and Lichtman, J. (2006). Automating the collection of ultrathin serial sections for large volume tem reconstructions. *Microscopy and Microanalysis*, 12(S02):86.

Heimbeck, G., Bugnon, V., Gendre, N., Häberlin, C., and Stocker, R. F. (1999). Smell and taste perception in drosophila melanogasterlarva: Toxin expression studies in chemosensory neurons. *Journal of Neuroscience*, 19(15):6599–6609.

Heisenberg, M. (2003). Mushroom body memoir: from maps to models. *Nature Reviews Neuroscience*, 4(4):266–275.

Heisenberg, M., Borst, A., Wagner, S., and Byers, D. (1985). Drosophila mushroom body mutants are deficient in olfactory learning: Research papers. *Journal of neurogenetics*, 2(1):1–30.

Hu, Y., Flockhart, I., Vinayagam, A., Bergwitz, C., Berger, B., Perrimon, N., and Mohr, S. E. (2011). An integrative approach to ortholog prediction for disease-focused and other functional studies. *BMC bioinformatics*, 12(1):357.

Hudson, A. M. and Cooley, L. (2014). Methods for studying oogenesis. *Methods*, 68(1):207–217.

Inoshita, T. and Tanimura, T. (2006). Cellular identification of water gustatory receptor neurons and their central projection pattern in drosophila. *Proceedings of the National Academy of Sciences of the United States of America*, 103(4):1094–1099.

Ito, K. and Hotta, Y. (1992). Proliferation pattern of postembryonic neuroblasts in the brain of drosophila melanogaster. *Developmental biology*, 149(1):134–148.

Iyengar, B. G., Chou, C. J., Sharma, A., and Atwood, H. L. (2006). Modular neuropile organization in the drosophila larval brain facilitates identification and mapping of central neurons. *Journal of Comparative Neurology*, 499(4):583–602.

Jefferis, G. S., Potter, C. J., Chan, A. M., Marin, E. C., Rohlfing, T., Maurer, C. R., and Luo, L. (2007). Comprehensive maps of drosophila higher olfactory centers: spatially segregated fruit and pheromone representation. *Cell*, 128(6):1187–1203.

Jovanic, T., Schneider-Mizell, C. M., Shao, M., Masson, J.-B., Denisov, G., Fetter, R. D., Mensh, B. D., Truman, J. W., Cardona, A., and Zlatic, M. (2016). Competitive disinhibition mediates behavioral choice and sequences in drosophila. *Cell*, 167(3):858–870.

Kane, E. A., Gershow, M., Afonso, B., Larderet, I., Klein, M., Carter, A. R., De Bivort, B. L., Sprecher, S. G., and Samuel, A. D. (2013). Sensorimotor structure of drosophila larva phototaxis. *Proceedings of the National Academy of Sciences*, 110(40):E3868–E3877.

Keene, A. C. and Sprecher, S. G. (2012). Seeing the light: photobehavior in fruit fly larvae. *Trends in neurosciences*, 35(2):104–110.

Kenyon, F. (1896). The brain of the bee. a preliminary contribution to the morphology of the nervous system of the arthropoda. *Journal of Comparative Neurology*, 6(3):133–210.

Kitamoto, T. (2001). Conditional modification of behavior in drosophila by targeted expression of a temperature-sensitive shibire allele in defined neurons. *Journal of neurobiology*, 47(2):81–92.

Klapoetke, N. C., Murata, Y., Kim, S. S., Pulver, S. R., Birdsey-Benson, A., Cho, Y. K., Morimoto, T. K., Chuong, A. S., Carpenter, E. J., Tian, Z., et al. (2014). Independent optical excitation of distinct neural populations. *Nature methods*, 11(3):338–346.

Klein, M., Afonso, B., Vonner, A. J., Hernandez-Nunez, L., Berck, M., Tabone, C. J., Kane, E. A., Pieribone, V. A., Nitabach, M. N., Cardona, A., et al. (2015). Sensory determinants of behavioral dynamics in drosophila thermotaxis. *Proceedings of the National Academy of Sciences*, 112(2):E220–E229.

Kreher, S. A., Kwon, J. Y., and Carlson, J. R. (2005). The molecular basis of odor coding in the drosophila larva. *Neuron*, 46(3):445–456.

Kunz, T., Kraft, K. F., Technau, G. M., and Urbach, R. (2012). Origin of drosophila mushroom body neuroblasts and generation of divergent embryonic lineages. *Development*, 139(14):2510–2522.

Kurusu, M., Awasaki, T., Masuda-Nakagawa, L. M., Kawauchi, H., Ito, K., and Furukubo-Tokunaga, K. (2002). Embryonic and larval development of the drosophila mushroom bodies: concentric layer subdivisions and the role of fasciclin ii. *Development*, 129(2):409–419.

Kurusu, M., Nagao, T., Walldorf, U., Flister, S., Gehring, W. J., and Furukubo-Tokunaga, K. (2000). Genetic control of development of the mushroom bodies, the associative learning centers in the drosophila brain, by the eyeless, twin of eyeless, and dachshund genes. *Proceedings of the National Academy of Sciences*, 97(5):2140–2144.

Kwon, J. Y., Dahanukar, A., Weiss, L. A., and Carlson, J. R. (2011). Molecular and cellular organization of the taste system in the drosophila larva. *Journal of Neuroscience*, 31(43):15300–15309.

Lee, T., Lee, A., and Luo, L. (1999). Development of the drosophila mushroom bodies: sequential generation of three distinct types of neurons from a neuroblast. *Development*, 126(18):4065–4076.

Leiss, F., Groh, C., Butcher, N. J., Meinertzhagen, I. A., and Tavosanis, G. (2009). Synaptic organization in the adult drosophila mushroom body calyx. *Journal of Comparative Neurology*, 517(6):808–824.

Liu, C., Plaçais, P.-Y., Yamagata, N., Pfeiffer, B. D., Aso, Y., Friedrich, A. B., Siwanowicz, I., Rubin, G. M., Preat, T., and Tanimoto, H. (2012). A subset of dopamine neurons signals reward for odour memory in drosophila. *Nature*, 488(7412):512–516.

Liu, L., Leonard, A. S., Motto, D. G., Feller, M. A., Price, M. P., Johnson, W. A., and Welsh, M. J. (2003). Contribution of drosophila deg/enac genes to salt taste. *Neuron*, 39(1):133–146.

Liu, X. and Davis, R. L. (2009). The gabaergic anterior paired lateral neuron suppresses and is suppressed by olfactory learning. *Nature neuroscience*, 12(1):53–59.

Luan, H., Peabody, N. C., Vinson, C. R., and White, B. H. (2006). Refined spatial manipulation of neuronal function by combinatorial restriction of transgene expression. *Neuron*, 52(3):425–436.

Marella, S., Fischler, W., Kong, P., Asgarian, S., Rueckert, E., and Scott, K. (2006). Imaging taste responses in the fly brain reveals a functional map of taste category and behavior. *Neuron*, 49(2):285–295.

Markow, T. A. (2015). The secret lives of drosophila flies. *Elife*, 4:e06793.

Masuda-Nakagawa, L. M., Ito, K., Awasaki, T., and O'Kane, C. J. (2014). A single gabaergic neuron mediates feedback of odor-evoked signals in the mushroom body of larval drosophila. *Frontiers in neural circuits*, 8:35.

Masuda-Nakagawa, L. M., Tanaka, N. K., and O'Kane, C. J. (2005). Stereotypic and random patterns of connectivity in the larval mushroom body calyx of drosophila. *Proceedings of the National Academy of Sciences of the United States of America*, 102(52):19027–19032.

Melcher, C. and Pankratz, M. J. (2005). Candidate gustatory interneurons modulating feeding behavior in the drosophila brain. *PLoS Biol*, 3(9):e305.

Mishra, D., Miyamoto, T., Rezenom, Y. H., Broussard, A., Yavuz, A., Slone, J., Russell, D. H., and Amrein, H. (2013). The molecular basis of sugar sensing in drosophila larvae. *Current Biology*, 23(15):1466–1471.

Miyamoto, T., Slone, J., Song, X., and Amrein, H. (2012). A fructose receptor functions as a nutrient sensor in the drosophila brain. *Cell*, 151(5):1113–1125.

Moon, S. J., Köttgen, M., Jiao, Y., Xu, H., and Montell, C. (2006). A taste receptor required for the caffeine response in vivo. *Current biology*, 16(18):1812–1817.

Murthy, M., Fiete, I., and Laurent, G. (2008). Testing odor response stereotypy in the drosophila mushroom body. *Neuron*, 59(6):1009–1023.

Niewalda, T., Singhal, N., Fiala, A., Saumweber, T., Wegener, S., and Gerber, B. (2008). Salt processing in larval drosophila: choice, feeding, and learning shift from appetitive to aversive in a concentration-dependent way. *Chemical senses*, 33(8):685–692.

Ohyama, T., Jovanic, T., Denisov, G., Dang, T. C., Hoffmann, D., Kerr, R. A., and Zlatic, M. (2013). High-throughput analysis of stimulus-evoked behaviors in drosophila larva reveals multiple modality-specific escape strategies. *PLoS One*, 8(8):e71706.

Ohyama, T., Schneider-Mizell, C. M., Fetter, R. D., Aleman, J. V., Franconville, R., Rivera-Alba, M., Mensh, B. D., Branson, K. M., Simpson, J. H., Truman, J. W., et al. (2015). A multilevel multimodal circuit enhances action selection in drosophila. *Nature*, 520(7549):633–639.

Owald, D., Felsenberg, J., Talbot, C. B., Das, G., Perisse, E., Huetteroth, W., and Waddell, S. (2015). Activity of defined mushroom body output neurons underlies learned olfactory behavior in drosophila. *Neuron*, 86(2):417–427.

Owald, D. and Waddell, S. (2015). Olfactory learning skews mushroom body output pathways to steer behavioral choice in drosophila. *Current opinion in neurobiology*, 35:178–184.

Pauls, D., Selcho, M., Gendre, N., Stocker, R. F., and Thum, A. S. (2010). Drosophila larvae establish appetitive olfactory memories via mushroom body neurons of embryonic origin. *Journal of Neuroscience*, 30(32):10655–10666.

Pavlou, H. J. and Goodwin, S. F. (2013). Courtship behavior in drosophila melanogaster: towards a 'courtship connectome'. *Current opinion in neurobiology*, 23(1):76–83.

Pfeiffer, B. D., Jenett, A., Hammonds, A. S., Ngo, T.-T. B., Misra, S., Murphy, C., Scully, A., Carlson, J. W., Wan, K. H., Laverty, T. R., et al. (2008). Tools for neuroanatomy and neurogenetics in drosophila. *Proceedings of the National Academy of Sciences*, 105(28):9715–9720.

Python, F. and Stocker, R. F. (2002). Adult-like complexity of the larval antennal lobe of d. melanogaster despite markedly low numbers of odorant receptor neurons. *Journal of Comparative Neurology*, 445(4):374–387.

Quinn, W. G., Harris, W. A., and Benzer, S. (1974). Conditioned behavior in drosophila melanogaster. *Proceedings of the National Academy of Sciences*, 71(3):708–712.

Ramaekers, A., Magnenat, E., Marin, E. C., Gendre, N., Jefferis, G. S., Luo, L., and Stocker, R. F. (2005). Glomerular maps without cellular redundancy at successive levels of the drosophila larval olfactory circuit. *Current biology*, 15(11):982–992.

Robertson, H. M., Warr, C. G., and Carlson, J. R. (2003). Molecular evolution of the insect chemoreceptor gene superfamily in drosophila melanogaster. *Proceedings of the National Academy of Sciences*, 100(suppl 2):14537–14542.

Rohwedder, A., Wenz, N. L., Stehle, B., Huser, A., Yamagata, N., Zlatic, M., Truman, J. W., Tanimoto, H., Saumweber, T., Gerber, B., et al. (2016). Four individually identified paired dopamine neurons signal reward in larval drosophila. *Current Biology*, 26(5):661–669.

Saalfeld, S., Cardona, A., Hartenstein, V., and Tomančák, P. (2009). Catmaid: collaborative annotation toolkit for massive amounts of image data. *Bioinformatics*, 25(15):1984–1986.

Saalfeld, S., Fetter, R., Cardona, A., and Tomancak, P. (2012). Elastic volume reconstruction from series of ultra-thin microscopy sections. *Nature Methods*, 9:717–20.

Schleyer, M., Saumweber, T., Nahrendorf, W., Fischer, B., von Alpen, D., Pauls, D., Thum, A., and Gerber, B. (2011). A behavior-based circuit model of how outcome expectations organize learned behavior in larval drosophila. *Learning & Memory*, 18(10):639–653.

Schneider-Mizell, C. M., Gerhard, S., Longair, M., Kazimiers, T., Li, F., Zwart, M. F., Champion, A., Midgley, F. M., Fetter, R. D., Saalfeld, S., et al. (2016). Quantitative neuroanatomy for connectomics in drosophila. *Elife*, 5:e12059.

Schürmann, F. (1974). On the functional anatomy of the corpora pedunculata in insects (author's transl). *Experimental brain research*, 19(4):406–432.

Schürmann, F.-W. (2016). Fine structure of synaptic sites and circuits in mushroom bodies of insect brains. *Arthropod Structure & Development*, 45(5):399–421.

Schwaerzel, M., Monastirioti, M., Scholz, H., Friggi-Grelin, F., Birman, S., and Heisenberg, M. (2003). Dopamine and octopamine differentiate between aversive and appetitive olfactory memories in drosophila. *Journal of Neuroscience*, 23(33):10495–10502.

Scott, K., Brady, R., Cravchik, A., Morozov, P., Rzhetsky, A., Zuker, C., and Axel, R. (2001). A chemosensory gene family encoding candidate gustatory and olfactory receptors in drosophila. *Cell*, 104(5):661–673.

Selcho, M., Pauls, D., Han, K.-A., Stocker, R. F., and Thum, A. S. (2009). The role of dopamine in drosophila larval classical olfactory conditioning. *PLoS One*, 4(6):e5897.

Selcho, M., Pauls, D., Huser, A., Stocker, R. F., and Thum, A. S. (2014). Characterization of the octopaminergic and tyraminergic neurons in the central brain of drosophila larvae. *Journal of Comparative Neurology*, 522(15):3485–3500.

Singh, R. N. (1997). Neurobiology of the gustatory systems of drosophila and some terrestrial insects. *Microscopy research and technique*, 39(6):547–563.

Singh, R. N. and Singh, K. (1984). Fine structure of the sensory organs of drosophila melanogaster meigen larva (diptera: Drosophilidae). *International Journal of Insect Morphology and Embryology*, 13(4):255–273.

Sivanantharajah, L. and Zhang, B. (2015). Current techniques for high-resolution mapping of behavioral circuits in drosophila. *Journal of Comparative Physiology A*, 201(9):895–909.

Sokabe, T., Chen, H.-C., Luo, J., and Montell, C. (2016). A switch in thermal preference in drosophila larvae depends on multiple rhodopsins. *Cell reports*, 17(2):336–344.

Sprecher, S. G., Cardona, A., and Hartenstein, V. (2011). The drosophila larval visual system: high-resolution analysis of a simple visual neuropil. *Developmental biology*, 358(1):33–43.

Stocker, H. and Gallant, P. (2008). Getting started: an overview on raising and handling drosophila. *Drosophila: Methods and Protocols*, pages 27–44.

Stocker, R. and Schorderet, M. (1981). Cobalt filling of sensory projections from internal and external mouthparts in drosophila. *Cell and tissue research*, 216(3):513–523.

Stocker, R. F. (1994). The organization of the chemosensory system in drosophila melanogaster: a rewiew. *Cell and tissue research*, 275(1):3–26.

Stocker, R. F. (2001). Drosophila as a focus in olfactory research: mapping of olfactory sensilla by fine structure, odor specificity, odorant receptor expression, and central connectivity. *Microscopy research and technique*, 55(5):284–296.

Stocker, R. F. (2009). The olfactory pathway of adult and larval drosophila. *Annals of the New York Academy of Sciences*, 1170(1):482–486.

Tanaka, N. K., Awasaki, T., Shimada, T., and Ito, K. (2004). Integration of chemosensory pathways in the drosophila second-order olfactory centers. *Current biology*, 14(6):449–457.

Tanaka, N. K., Tanimoto, H., and Ito, K. (2008). Neuronal assemblies of the drosophila mushroom body. *Journal of Comparative Neurology*, 508(5):711–755.

Tanimura, T., Isono, K., and Yamamoto, M.-T. (1988). Taste sensitivity to trehalose and its alteration by gene dosage in drosophila melanogaster. *Genetics*, 119(2):399–406.

Tempel, B. L., Bonini, N., Dawson, D. R., and Quinn, W. G. (1983). Reward learning in normal and mutant drosophila. *Proceedings of the National Academy of Sciences*, 80(5):1482–1486.

Tennessen, J. M. and Thummel, C. S. (2011). Coordinating growth and maturation—insights from drosophila. *Current Biology*, 21(18):R750–R757.

Tian, L., Hires, S. A., Mao, T., Huber, D., Chiappe, M. E., Chalasani, S. H., Petreanu, L., Akerboom, J., McKinney, S. A., Schreiter, E. R., et al. (2009). Imaging neural activity in worms, flies and mice with improved gcamp calcium indicators. *Nature methods*, 6(12):875–881.

Tracey, W. D., Wilson, R. I., Laurent, G., and Benzer, S. (2003). painless, a drosophila gene essential for nociception. *Cell*, 113(2):261–273.

Tsien, R. Y. (1998). The green fluorescent protein. *Annual review of biochemistry*, 67(1):509–544.

Tully, T. and Quinn, W. G. (1985). Classical conditioning and retention in normal and mutant drosophila melanogaster. *Journal of Comparative Physiology A*, 157(2):263–277.

Ugur, B., Chen, K., and Bellen, H. J. (2016). Drosophila tools and assays for the study of human diseases. *Disease models & mechanisms*, 9(3):235–244.

Vergoz, V., Roussel, E., Sandoz, J.-C., and Giurfa, M. (2007). Aversive learning in honeybees revealed by the olfactory conditioning of the sting extension reflex. *PloS one*, 2(3):e288.

Vogt, K., Schnaitmann, C., Dylla, K. V., Knapek, S., Aso, Y., Rubin, G. M., and Tanimoto, H. (2014). Shared mushroom body circuits underlie visual and olfactory memories in drosophila. *Elife*, 3:e02395.

Vosshall, L. B. and Stocker, R. F. (2007). Molecular architecture of smell and taste in drosophila. *Annu. Rev. Neurosci.*, 30:505–533.

Waddell, S. (2013). Reinforcement signalling in drosophila; dopamine does it all after all. *Current opinion in neurobiology*, 23(3):324–329.

Waddell, S., Armstrong, J. D., Kitamoto, T., Kaiser, K., and Quinn, W. G. (2000). The amnesiac gene product is expressed in two neurons in the drosophila brain that are critical for memory. *Cell*, 103(5):805–813.

Wang, Z., Singhvi, A., Kong, P., and Scott, K. (2004). Taste representations in the drosophila brain. *Cell*, 117(7):981–991.

Xiang, Y., Yuan, Q., Vogt, N., Looger, L. L., Jan, L. Y., and Jan, Y. N. (2010). Light-avoidance-mediating photoreceptors tile the drosophila larval body wall. *Nature*, 468(7326):921–926.

Yamamoto, D. and Koganezawa, M. (2013). Genes and circuits of courtship behaviour in drosophila males. *Nature Reviews Neuroscience*, 14(10):681–692.

Yasuyama, K., Meinertzhagen, I. A., and Schürmann, F.-W. (2002). Synaptic organization of the mushroom body calyx in drosophila melanogaster. *Journal of Comparative Neurology*, 445(3):211–226.

Yoshihara, M. and Ito, K. (2012). Acute genetic manipulation of neuronal activity for the functional dissection of neural circuits—a dream come true for the pioneers of behavioral genetics. *Journal of neurogenetics*, 26(1):43–52.

Chapter I: The complete connectome of a learning and memory centre in an insect brain

Katharina Eichler[1,2*], Feng Li[1*], Ashok Litwin-Kumar[3*], Youngser Park[4], Ingrid Andrade[1], Casey Schneider-Mizell[1], Timo Saumweber[5], Annina Huser[2], Claire Eschbach[1], Bertram Gerber[5,6,7], Richard D. Fetter[1], James W. Truman[1], Carey Priebe[4], L. F. Abbott[3,8,c], Andreas S. Thum[2,c], Marta Zlatic[1,c], Albert Cardona[1,c]

[1] HHMI Janelia Research Campus, 19700 Helix Dr., Ashburn, VA 20147.

[2] Department of Biology, University of Konstanz, 78464 Konstanz, Germany.

[3] Department of Neuroscience, Columbia University.

[4] Department of Applied Mathematics and Statistics, Whiting School of Engineering, Johns Hopkins University.

[5] Abteilung Genetik von Lernen und Gedächtnis, Leibniz Institut für Neurobiologie (LIN), 39118 Magdeburg, Germany.

[6] Otto von Guericke Universität Magdeburg, Institut für Biologie, Verhaltensgenetik, Universitätsplatz 2, 39106 Magdeburg, Germany.

[7] Center for Behavioral Brain Sciences (CBBS), 39106 Magdeburg, Germany.

[8] Department of Physiology and Cellular Biophysics, Columbia University.

[*] equal contribution. [c] corresponding authors.

Nature (2017) 548, 175-182

doi: 10.1038/nature23455

3.1 Abstract

Associating stimuli with positive or negative reinforcement is essential for survival, but a complete wiring diagram of a higher-order circuit supporting associative memory has not been previously available. We report the full reconstruction at synaptic resolution of one such circuit, the mushroom body of *Drosophila* larva. Our results reveal that Kenyon cells not only integrate random combinations of inputs, but that a subset of them receives stereotyped inputs from single projection neurons. Combining these two kinds of Kenyon cells maximizes the performance of a model output neuron on a stimulus discrimination task. Memories are formed when co-activation of Kenyon cells and modulatory neurons (mostly dopaminergic) alters the strength of Kenyon cell synapses onto output neurons within mushroom body compartments. We found a novel canonical circuit in these compartments with previously unidentified connections: reciprocal Kenyon cell to modulatory neuron connections, modulatory neuron to output neuron connections, and a surprisingly high number of recurrent connections between Kenyon cells. We also report a comprehensive set of connections between output neurons that could enhance the selection of learned responses. The complete circuit map of the mushroom body should guide future functional studies of this learning and memory center.

3.2 Introduction

Massively parallel, higher-order neuronal circuits such as the cerebellum and insect mushroom body serve to form and retain associations between stimuli and reinforcement in vertebrates and higher invertebrates [Heisenberg, 2003; Menzel, 2012; Waddell, 2013; Owald and Waddell, 2015; Schürmann, 2016]. Although these systems provide a

biological substrate for adaptive behavior, no complete synapse-resolution wiring diagram of their connectivity has been available to guide analysis and inspire understanding. The mushroom body (MB) is a higher-order parallel fiber system in many invertebrate brains, including hemimetabolous as well as holometabolous insects and their larval stages [Schürmann, 2016]. MB function is essential for associative learning in adult insects [Heisenberg, 2003; Waddell, 2013; Menzel, 2012; Owald and Waddell, 2015] and in *Drosophila* larvae [Gerber et al., 2009; Diegelmann et al., 2013; Rohwedder et al., 2016], from the earliest larval stages onward [Gerber et al., 2009; Pauls et al., 2010]. Indeed, the basic organization of the adult and the larval MB and their afferent circuits is very similar, however, the number of neurons is less by about an order of magnitude in larvae [Gerber et al., 2009]. Thus, to systematically investigate the organizational logic of the MB, we used serial section electron microscopy (EM) to map with synaptic resolution the complete MB connectome in a first instar *Drosophila* larva (L1; Fig. 1a). L1 are foraging animals capable of all behaviors previously described in later larval stages, including their modulation by associative learning [Gerber et al., 2009; Pauls et al., 2010] (Fig. 1b). Their smaller neurons enable fast EM imaging of the entire nervous system and reconstruction of complete circuits [Ohyama et al., 2015; Berck et al., 2016].

Models of sensory processing in many neural circuits feature neurons that fire in response to combinations of sensory inputs, generating a high-dimensional representation of the sensory environment [Babadi and Sompolinsky, 2014]. The intrinsic MB neurons, the Kenyon cells (KCs), receive dendritic input from combinations of projection neurons (PNs) that encode various stimuli, predominantly olfactory in both adult [Heisenberg, 2003; Waddell, 2013; Owald and Waddell, 2015; Schürmann, 2016], and larva [Masuda-Nakagawa et al., 2005; Gerber et al., 2009; Berck et al., 2016], but also thermal, gustatory and visual in adult [Bang et al., 2011; Owald and Waddell, 2015; Schürmann,

2016] and larva (reported here for the first time). Previous analyses in adults [Murthy et al., 2008; Caron et al., 2013] and larvae [Masuda-Nakagawa et al., 2005] suggest that the connectivity between olfactory PNs and KCs in the calyx is random, but they do not eliminate the possibility of some degree of bilateral symmetry [Gruntman and Turner, 2013], which requires access to the full PN-to-KC wiring diagram in both hemispheres. The MB contains circuitry capable of associating reward or punishment with the representation of the sensory environment formed by KCs. KCs have long parallel axons that first run together forming the peduncle and then extend collaterals to form the so-called lobes, in both larvae [Gerber et al., 2009] and adults [Heisenberg, 2003; Waddell, 2013; Schürmann, 2016]. KCs receive localized inputs along their axonal fibers from dopaminergic as well as octopaminergic modulatory neurons (DANs and OANs, respectively) that define separate compartments. DANs and OANs have been shown to convey reinforcement signals in adult insects [Waddell, 2013; Lin et al., 2014b; Das et al., 2014; Galili et al., 2014; Huetteroth et al., 2015; Ichinose et al., 2015; Cohn et al., 2015; Owald and Waddell, 2015; Menzel, 2012; Schürmann, 2016] and larval *Drosophila* [Gerber et al., 2009; Diegelmann et al., 2013; Rohwedder et al., 2016]. The dendrites of the mushroom body output neurons (MBONs) respect the DAN compartments in adult [Aso et al., 2014a; Owald et al., 2015; Bouzaiane et al., 2015; Owald and Waddell, 2015] and larvae [Pauls et al., 2010]. It has been shown in adult *Drosophila* that co-activation of KCs and DANs can associatively modulate the KC-MBON synapse [Owald and Waddell, 2015; Bouzaiane et al., 2015; Cohn et al., 2015; Hige et al., 2015; Perisse et al., 2016; Schürmann, 2016]. Thus, the compartments represent anatomical and functional MB units where sensory input (KCs) is integrated with internal reinforcement signals (DANs/OANs) to modulate instructive output for behavioral control (MBONs). However, the synaptic connectivity of KCs, DAN/OANs, and MBONs at this crucial point of integration was previously unknown.

Furthermore, studies in adult *Drosophila* have shown that despite the compartmental organisation of the MB, many MBONs interact with MBONs from other compartments, suggesting that the MB network functions combinatorially during memory formation and retrieval [Aso et al., 2014a; Owald et al., 2015; Perisse et al., 2016]. However, a comprehensive account of all MBON-to-MBON/DAN connections is lacking. Thus, to provide a basis for understanding how the MB, a prototypical parallel fiber learning and memory circuit, functions as an integrated whole, we provide a full, synapse-resolution connectome of all MB neurons of an L1 *Drosophila* larva.

3.3 Results

We reconstructed all the KCs in both brain hemispheres of an L1 *Drosophila* larva and identified all of their pre- and postsynaptic partners (Fig. 1a, d, Fig. 3a; Supp. Table 1). We found 223 KCs (110 on the left, 113 on the right), of which 145 are mature (73 on the left, 72 on the right). Immature KCs either lack or have tiny dendrites, and their axons terminate early with filopodia typical of axon growth cones. Every mature KC presents a well-developed dendrite, and its axon innervates all of the MB compartments. Although the number of KCs is different between the two sides (Fig. 1a), we found exactly 24 MBONs, 7 DANs, 2 paired and 2 unpaired OANs and 5 additional modulatory input neurons (which we call MBINs or mushroom body input neurons, a term we also use to refer to all the modulatory neurons collectively) of unknown neurotransmitter identity (Supp. Fig. 1a, Supp. Table 3). An additional pair of GABAergic neurons (one per side), homologous to the APL neurons in the adult fly [Liu and Davis, 2009; Masuda-Nakagawa et al., 2014], synapse reciprocally with all mature ipsilateral KCs (Ext. Data Fig. 1).

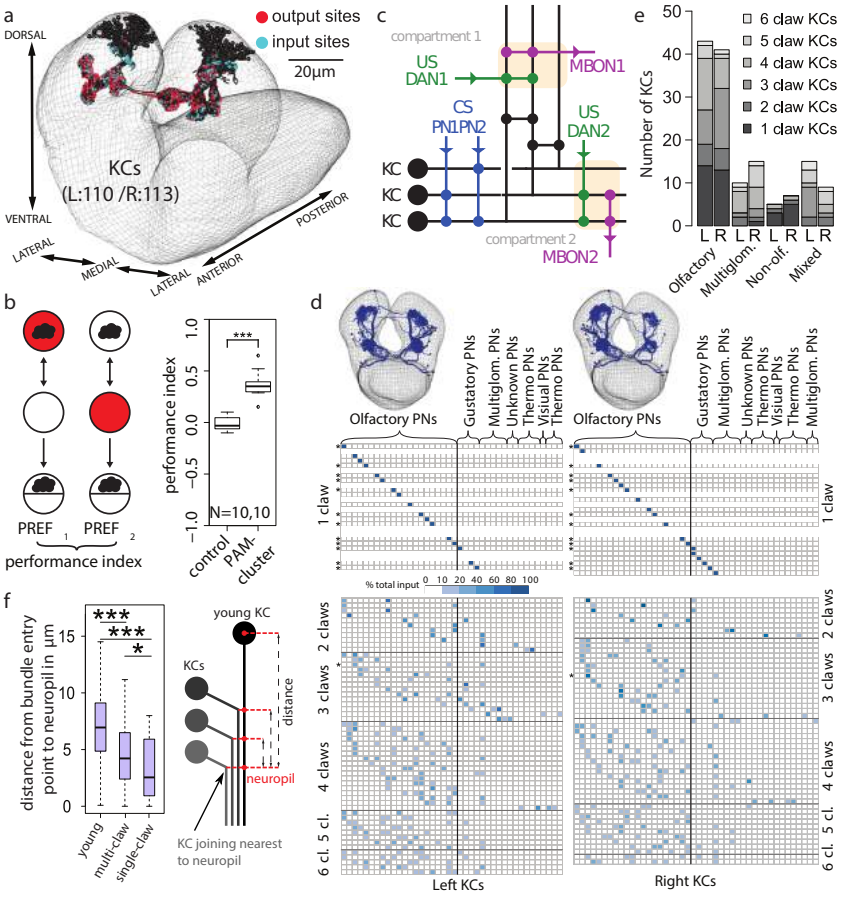

Figure 1: Mushroom bodies of a first instar *Drosophila* larva.
a Kenyon cells (KCs) from a whole-CNS EM volume.
b Associative learning in first instar larvae: in a Petri dish, we presented an odor (cloud) and red light, either paired (left) or unpaired (right), and computed the performance index. Control larvae (attP2; UAS-CsChrimson) receiving paired stimuli did not learn, whereas larvae in which optogenetic activation of dopaminergic (PAM cluster) neurons (GMR58E02-GAL4; UAS-CsCrimson) was paired with odor showed robust appetitive learning ($p < 0.0001$).
c Diagram of the current MB circuitry model. Projection neurons (PN) relay sensory stimuli to KC dendrites. MBON dendrites and DAN/OAN/MBIN axons tile the parallel KC axons, defining compartments (*grey boxes*). DAN/OAN/MBIN signal reward or punishment, and KCs synapse onto output neurons (MBONs).
d PN-to-KC connectivity matrix, color-coded by percent of inputs on KC dendrites. Uniglomerular olfactory PNs (Olfactory PNs) and other PNs from other sensory modalities synapse onto single-claw or multi-claw KCs. Stars indicate KCs with identical input patterns on the left and right hemispheres. For the PNs on the right of the black vertical lines, first 18 columns are left-right homologous PNs, last column (left) and last five columns (right) are hemisphere-specific PNs.
e Number of KCs integrating inputs from uniglomerular olfactory, multiglomerular olfactory, non-olfactory or a mixture of these PN types.
f Earlier-born KCs join the lineage bundle closer to the neuropil surface than later-born ones, meaning older KCs present less claws than younger ones. Distances span from the point where the KC joins the bundle to the joining point of the KC nearest to the neuropil. Differences between all groups are significant (*** p-values smaller than 0.0001; single-claw and multi-claw KC comparison p-value: 0.0237).

PN inputs to the KCs

The reconstruction enabled us to identify all the sensory PNs and their connections onto KCs. KC dendrites have claw-like structures that wrap around PN axon boutons

in the MB calyx [Schürmann, 2016] (Ext. Data Fig. 2b). We identified input from 21 uniglomerular olfactory PNs on each side, 5 and 7 multiglomerular PNs [Berck et al., 2016], and 14 and 18 non-olfactory PNs on the left and right sides, respectively. Non-olfactory PNs include thermal, visual, gustatory, mixed olfactory, and possibly other modalities (Fig. 1d, e; Supp. Table 1). A subset of mature KCs receives input from only one PN (single-claw KCs), while the remaining KCs (multi-claw KCs, as in the adult fly [Caron et al., 2013]) receive input from 2–6 PNs [Masuda-Nakagawa et al., 2005] (Fig. 1d, Ext. Data Fig. 2c). Interestingly, single-claw KCs are born earlier than multi-claw KCs (Fig. 1f). KCs with different numbers of claws receive roughly the same number of synapses summed across claws (Ext. Data Fig. 2a). This suggests that multi-claw KCs may require input from multiple PNs to respond, assuring combinatorial selectivity [Honegger et al., 2011; Gruntman and Turner, 2013].

Two features of the PN-to-KC connectivity are immediately visible (Fig. 1d): the contrast between the ordered and apparently disordered connections onto single-claw KCs and multi-claw KCs, respectively, and the existence of KCs that do not receive any uni-glomerular PN input. Most KCs (77%) receive exclusively olfactory input from uni- or multi-glomerular PNs, while the others receive non-olfactory input (Fig. 1d, e). Prominent among these are two KCs per side that exclusively receive thermal information and one per side that carries visual signals.

No structure is apparent in the olfactory PN input to multi-claw KCs (Fig. 1d; see Ext. Data Fig. 3b-e for further analysis), consistent with previous analyses in adults [Murthy et al., 2008; Caron et al., 2013] and larvae [Masuda-Nakagawa et al., 2005]. Structure was found, however, when all the PNs were included in the analysis, reflecting the presence of specialized non-olfactory KCs (Ext. Data Fig. 3a). We also examined whether PN connections onto multi-claw KCs in the left and right hemispheres are independent. Only one bilateral pair of multi-claw KCs receives input from the same

set of homologous PNs (marked by asterisks in Fig. 1d), no more than predicted by a random model ($p = 0.69$; Ext. Data Fig. 3e). Such asymmetry has not been observed previously in the first instar larva where strongly connected presynaptic partners of identified neurons have always been seen to have left and right homologs [Ohyama et al., 2015; Schneider-Mizell et al., 2016; Berck et al., 2016].

In contrast to the randomness of multi-claw KCs, the number of single-claw KCs is significantly greater than predicted by random models (Fig. 2a) and Fig. 1d shows clear structure in their wiring. If single-claw KCs sampled random PNs, we would expect to find about 5 pairs of single-claw KCs innervated by the same PN per hemisphere ("duplicates"). The data indicate zero left-hemisphere and one right-hemisphere duplicate ($p < 0.002$ and $p < 0.005$ in the random model, respectively). In contrast, the random model predicts that duplicates should be rare for multi-claw KCs, and the data reveal only two ($p = 0.93$). The fact that single-claw KCs appear earliest in development suggests that a top priority, initially, is to assure that a complete set of signals is relayed to the MBONs, which is not guaranteed with random wiring. Indeed, we found that 27 (44) randomly wired multi-claw KCs, on average, were needed to achieve the same level of coverage of PN inputs as the 17 (19) single-claw KCs in the left (right) hemisphere (see Methods).

PN-to-KC connectivity optimizes the KC odor representation for associative learning

The lack of duplication in PN-to-KC connections suggests that MB wiring is well-suited to promote KC diversity. We hypothesized that this diversity produces a high-dimensional odor representation that supports stimulus discrimination. To test this idea, we developed a model in which KCs produce sparse responses to random combinations of odor-evoked PN activity (see Methods). We compared the performance on a stimulus classification task of a model MBON in networks with the observed PN-to-KC connectivity and completely randomly connected models with varying degrees of connectivity

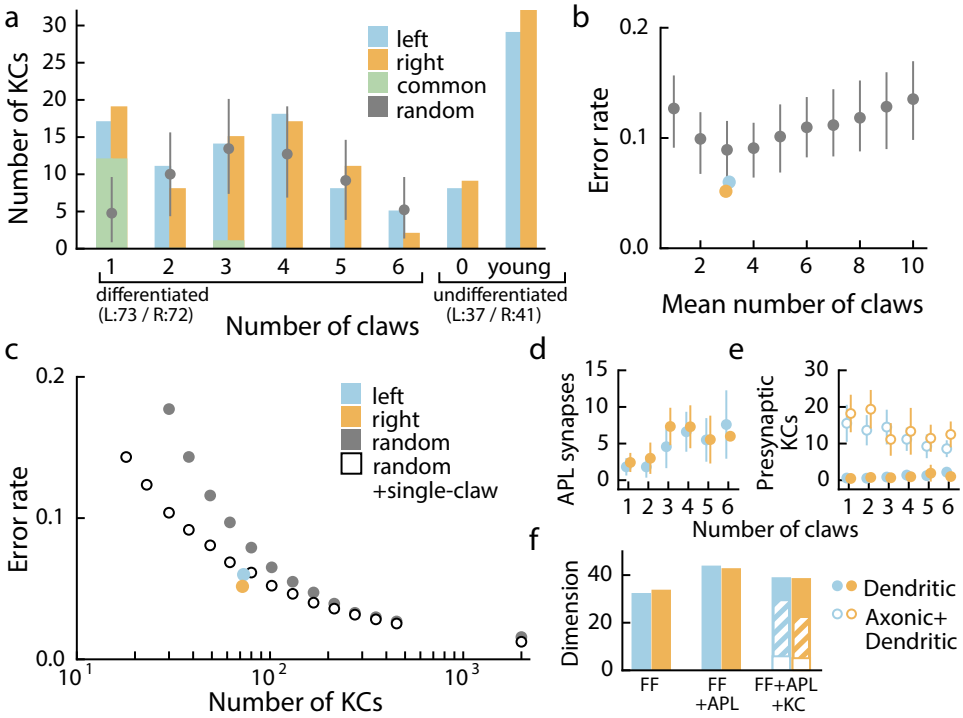

Figure 2: KC connectivity reduces redundancy and optimizes stimulus discrimination.
a Distribution of KC claw numbers compared to random models (grey). Random models have significantly fewer single-claw KCs ($p < 10^{-5}$). Grey circles and lines denote mean and 95% confidence intervals. Random models for both hemispheres gave similar results and were pooled.
b Classification error rate of a readout of the KC representation trained on a stimulus discrimination task. Observed connectivity (blue and orange) is compared to random models in which KCs have different distributions of average claw numbers (grey).
c Average performance of models with purely random connectivity (grey) or random multi-claw plus non-random single-claw KCs (white). S.E.M. is smaller than the marks. **d** Number of APL-to-KC synapses, which is correlated with claw number.
e Number of presynaptic KC-to-KC connections, which is inversely related to postsynaptic claw number. Data is shown for dendritic synapses in the calyx (filled circles) or all synapses (open circles).
f Dimension of KC representation in models with only feedforward PN-to-KC connections (FF), with APL-mediated inhibition (FF+APL), or with inhibition and excitatory KC-to-KC connections (FF+APL+KC). Dimension is slightly reduced by dendritic KC-to-KC connections (right, filled bars) but strongly reduced by axonic KC-to-KC connections (open bars). Facilitatory axonic KC-to-KC connections (hatched bars) yield an intermediate reduction.

(see Methods). Fully random networks have few of the single-claw KCs observed in the reconstruction (Fig. 2a).

The observed connectivity leads to performance superior to the average performance of purely random model networks (Fig. 2b). Motivated by the observation that unique single-claw KCs are born early in MB development (Fig. 1f), we hypothesized that their presence may be particularly important when the number of KCs is small. We therefore compared the performance of networks with only randomly connected KCs to that of networks with the same total number of KCs but containing a subpopulation

of unique single-claw KCs. In networks with few KCs, the presence of single-claw KCs substantially improves performance (Fig. 2c). As additional KCs are added, the advantage of single-claw KCs diminishes. For networks constructed using estimates of adult *Drosophila* KC connectivity, where single-claw KCs have not been identified [Caron et al., 2013], unique single-claw KCs provide only a small benefit.

Inhibitory KC interactions via the APL neuron

The MB is innervated by the GABAergic APL neuron [Liu and Davis, 2009; Masuda-Nakagawa et al., 2014] that synapses reciprocally with all mature KCs (Ext. Data Fig. 1a). Although APL receives most of its input from multi-claw KCs, individual single-claw KCs typically have more synapses onto APL dendrites than multi-claw KCs (Ext. Data Fig. 1b,c). Conversely, APL connects more strongly to KCs with more claws (Fig. 2d, Ext. Data Fig. 1c). We extended our model to include APL-mediated feedback inhibition and assessed its effect on the dimension of the KC representation, which quantifies the level of decorrelation of KC responses [Litwin-Kumar et al., 2017] (see Methods). The addition of recurrent APL inhibition increases the dimension by approximately 30% (Fig. 2f), consistent with the proposed role of APL in maintaining sparse, decorrelated KC responses [Luo et al., 2010; Papadopoulou et al., 2011; Lin et al., 2014a; Masuda-Nakagawa et al., 2014]. The increased inhibition received by multi- compared to single-claw KCs may reflect a greater need for decorrelation of their responses given the larger overlap of their PN inputs.

Recurrent KC interactions

We next examined whether KCs directly interact with each other, a possibility suggested by previous studies in *Drosophila* and other species [Schürmann, 2016]. Surprisingly, we found that, on average, 60% of the synapses received by KCs come from other KCs (on average, 10 presynaptic partners) and 45% of output synapses made by KC are onto other KCs (Fig. 2e, Ext. Data Fig. 2d–g). Most KC-to-KC synapses are

axo-axonic and located in the peduncle and MB lobes; a much smaller fraction are dendro-dendritic and located in the calyx (Ext. Data Fig. 2h). The largest number of KC-to-KC connections occurs between the two thermosensory KCs (Supp. Table 1), but these KCs also make large numbers of connections to olfactory and visual KCs. Single-claw KCs make more recurrent connections, on average, than multi-claw KCs, and both single- and multi-claw KCs tend to connect reciprocally to KCs of the same type (Ext. Data Fig. 4a–d). However, we found no relationship between the similarity of the PN inputs to KC pairs and the number of KC-to-KC synapses formed between them (correlation coefficients 0.016 and -0.014 for left and right hemispheres; $p > 0.4$, comparison to shuffled network).

KCs have been shown to be cholinergic in the adult [Barnstedt et al., 2016], so it is likely that KC-to-KC connections are depolarizing. Even when strong dendro-dendritic KC connections are added to our model, dimension only decreases slightly (Fig. 2f). Additional subthreshold axo-axonic KC-to-KC connections also have a weak effect (Fig. 2f, hatched bars). However, if we also assume that the strength of axo-axonic connections is equal to that of the dendro-dendritic connections we model, the dimension collapses due to the large correlations introduced by this recurrence (Fig. 2f, open bars). While our model does not reveal a functional role for KC-to-KC connections, it is possible that processes that we did not model, such as experience-dependent modulation of their synaptic strengths, may modify the representation to favor either behavioral discrimination or generalization. Further characterization of these connections is needed to assess this hypothesis.

A canonical circuit motif in each MB compartment

We next identified the MBONs and modulatory neurons (MBINs) associated with every MB compartment. Each compartment is innervated by 1–5 MBONs and 1–3 MBINs (most often DAN/OANs), except for the shaft compartment of the medial lobe that lacks

MBINs in L1 larvae (but has them in L3; [Rohwedder et al., 2016]). Most MBONs and MBINs innervate a single MB compartment (although most MBINs present a bilateral axon,innervating both the left and right homologous compartments), with few exceptions (MBIN-l1 and 5/24 MBONs; Fig. 3d, Ext. Data Fig. 5). Most MBINs (over 80%) are primarily presynaptic to other MB neurons, but some allocate 50% or more of their presynaptic sites to non-MB neurons (Ext. Data Fig. 6a, Supp. Table 2b). We also found a positive correlation between the number of output sites on the MBIN axons or the number of input sites on the MBON dendrites and the number of synapses with KCs (Ext. Data Fig. 6b, c).

Antibody labeling of GFP-labeled neurons showed seven MBINs are dopaminergic (DAN-c1, d1, f1, g1, i1, j1 and k1; Ext. Data Fig. 5, four are octopaminergic (OAN-a1, -a2, -e1 and -g1), three others are neither dopaminergic nor octopaminergic (MBIN-e1, -e2 and -l1), and two were not technically accessible (MBIN-b1 and -b2) (Supp. Fig. 2a). MBONs can be glutamatergic, cholinergic or GABAergic (Supp. Fig. 2b), the same set of neurotransmitters seen for adult MBONs [Aso et al., 2014a] (Supp. Table 3).

EM reconstruction of MBONs and DAN/OAN/MBINs reveals a canonical circuit motif (Fig. 3b, d and Ext. Data Fig. 5) that appears in every compartment, independent of DAN/OAN/MBIN or MBON neurotransmitter (except in the shaft compartment that lacks modulatory input in L1). In this motif, KCs synapse onto MBONs, as previously shown in adult *Drosophila* [Owald and Waddell, 2015; Cohn et al., 2015; Barnstedt et al., 2016; Schürmann, 2016] and bees and locusts [Cassenaer and Laurent, 2012; Menzel, 2012; Schürmann, 2016]. However, we identified two unexpected connection types. The first are numerous KC-to-DAN/OAN/MBIN connections (Fig. 3d, Ext. Data Fig. 5). Second, a sizable fraction of DAN/OAN/MBIN presynaptic sites (which are polyadic) each simultaneously contacts both KCs and MBONs, with generally at least one of the postsynaptic KCs synapsing onto one of the postsynaptic MBONs within less than a micron of the

DAN/OAN/MBIN-KC synapse (Fig. 3c). Thus, DAN/OAN/MBINs synapse both onto the pre- and postsynaptic side of many KC-to-MBON synapses. For comparison, MBONs receive on average 3.44% of their input from individual DAN/OAN/MBINs and 1.3% from an individual KC. If only 5% of the 73 mature KCs are active in response to a given odor, as has been shown in the adult [Honegger et al., 2011], then the MBONs receive on average ca. 4.8% of their input from active KCs, very similar to the % of DAN/OAN/MBIN input.

DAN/OAN/MBINs convey reinforcement signals and are thought to modulate the efficacy of KC-to-MBON connections through volume-release in the vicinity of KC presynaptic terminals [Waddell, 2013; Owald and Waddell, 2015; Cohn et al., 2015; Hige et al., 2015; Owald et al., 2015; Menzel, 2012; Schürmann, 2016] and as expected, we observed DAN/OAN/MBIN axon boutons containing dense-core vesicles (Ext. Data Fig. 7). We also observed dense core vesicles in addition to clear-core vesicles in 1/3 of KCs (Ext. Data Fig. 7), consistent with findings in the adult that many KCs co-release sNPF peptide with acetylcholine [Barnstedt et al., 2016].

Our EM reconstruction also revealed DAN/OAN/MBIN synapses containing clear vesicles (Ext. Data Fig. 7and Fig. 3c) indistinguishable from those that release classical neurotransmitters [Ohyama et al., 2015]. All DAN/OAN/MBIN terminals with clear-core vesicles contained dense core vesicles and the vast majority of dense core vesicles are located within the presynaptic boutons (Ext. Data Fig. 8). This suggests that DAN/OAN/MBINs may have two concurrent modes of action onto KCs and MBONs: activation via synaptic release (of dopamine, octopamine, or fast neurotransmitters) and neuromodulation via volume release. These two modes, coupled with the diverse connection types among KCs, DAN/OAN/MBINs, and MBONs, may provide a powerful and flexible substrate for associative learning.

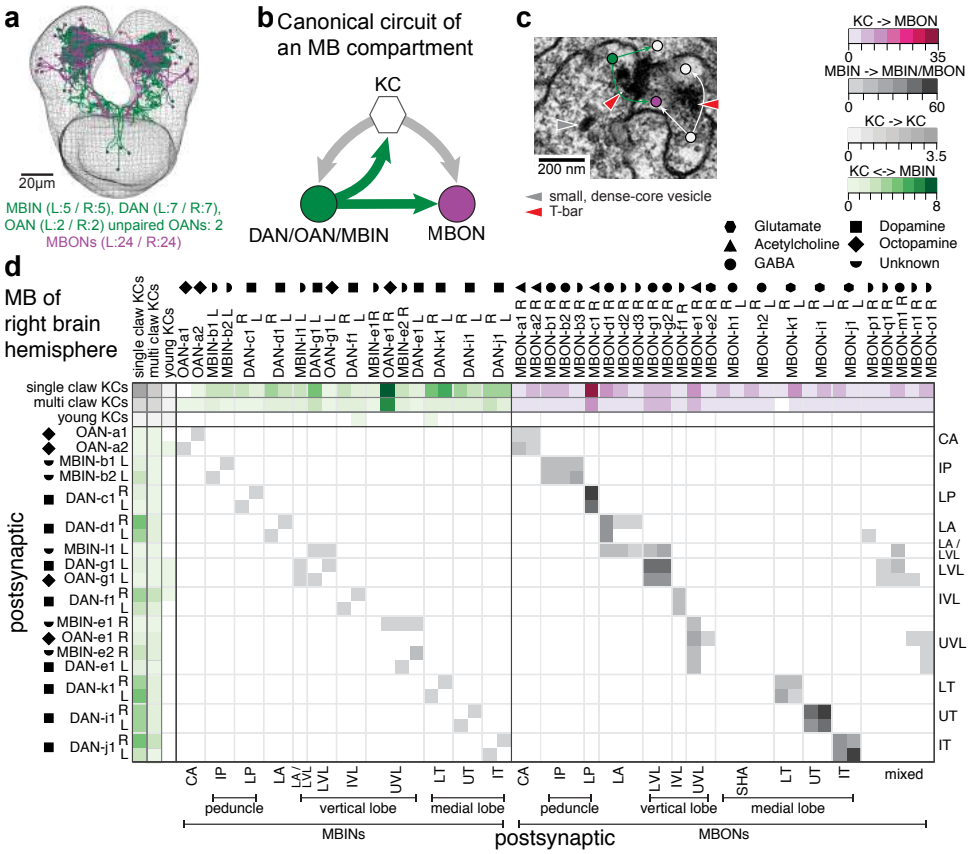

Figure 3: A canonical circuit in every mushroom body compartment.
a EM-reconstructed DAN/OAN/MBIN (*green*) and MBONs (*magenta*).
b Canonical circuit present in every MB compartment, with previously unknown KCs synapses onto DAN/OAN/MBINs, and from these onto MBONs.
c Example of an MBIN presynaptic site (*green dot*) with a KC (*white dot*) and an MBON (*magenta dot*) postsynaptic to it. The same KC is also presynaptic to the MBON in close proximity. Dense-core and clear vesicles are visible in the DAN axon close to a presynaptic site.
d The connectivity matrix between KCs, DAN/OAN/MBINs, and MBONs of the right-hemisphere MB shows the specific, compartment-centric synapses among cells types. Each entry represents the num. synapses from a row to a column (values are averaged for KCs). Note absence of DAN in SHA (develops later in larval life). DAN/OAN/MBINs synapse only onto MBONs innervating their compartment, and axo-axonically onto same-compartment DAN/OAN/MBINs. Note the presence of multi-compartment MBONs in the vertical lobe and LA.

Heterogeneous KC-to-MBON/DAN/OAN/MBIN connections in multiple compartments

Previous studies in adult *Drosophila* have shown that different lobes and compartments within the lobes are involved in forming different types of memories [Waddell, 2013; Aso et al., 2014b; Lin et al., 2014b; Galili et al., 2014; Das et al., 2014; Huetteroth et al., 2015; Owald and Waddell, 2015; Owald et al., 2015; Bouzaiane et al., 2015; Perisse et al., 2016; Aso and Rubin, 2016]. Functional studies in larvae [Gerber et al., 2009; Diegelmann et al., 2013; Rohwedder et al., 2016] also suggest that vertical and medial

lobes may be implicated in distinct types of memory formation (aversive and appetitive, respectively). Our EM study shows that all mature KCs make synaptic connections with MBONs and DAN/OANs in both the vertical and medial MB lobes (Ext. Data Fig. 9a-c, Ext. Data Fig. 10a-c and Supp. Table 4a, b). Furthermore, individual MBONs are innervated by between 40% to almost all of the KCs, with an average of 70% (Ext. Data Fig. 9a). This extensive innervation provides MBONs access to the high-dimensional KC representation and suggests that individual KCs may be involved in the formation and storage of associations involving multiple stimuli and valences, as suggested for the adult [Waddell, 2013; Owald and Waddell, 2015] (but see [Perisse et al., 2013]).
Our EM reconstruction reveals that in the larva, the axon terminals of all DAN/OAN/MBINs overlap with all KCs within a compartment and could potentially connect to all KCs, unlike in the adult [Perisse et al., 2013; Aso et al., 2014a]. Nevertheless, only subsets of KCs synapse onto either the DAN/OAN/MBIN or the MBON, or both, within a given compartment, with a broad distribution in the number of synaptic contacts (Ext. Data Fig. 9d, e, Ext. Data Fig. 10d, e and Supp. Table 4a, b). Estimating connection strength using synapse number, distinct subsets of KCs synapse strongly with DAN/OAN/MBINs and MBONs in distinct compartments (Ext. Data Fig. 9c, Ext. Data Fig. 10c, Supp. Table 4a, b and Supp. Table 1). This could arise from an innately broad distribution of synapse strengths or activity-dependent changes in synapse number. Either way, this heterogeneity implies that distinct MBONs and DAN/OAN/MBINs respond to heterogeneous combinations of active KCs.

Comprehensive profile of MBON inputs

EM reconstruction and synaptic counting provides a comprehensive view of the signals carried by the MBONs (Fig. 4a, b and Supp. Table 2a). In general, MBONs are among the neurons in the L1 larval brain receiving the largest number of inputs, with a median of 497 and a maximum of about 1500 postsynaptic sites. The median for other neurons

reconstructed so far is around 250 in L1 [Ohyama et al., 2015; Berck et al., 2016].

We analyzed the detailed structure of KC-to-MBON connectivity to determine the nature of the sensory signals relayed to MBONs. About 25% of the KC input to MBONs originates in KCs that integrate inputs from non-olfactory PNs (Fig. 4b, c), significantly more than in networks with shuffled PN modalities ($p < 0.05$). This pattern of non-olfactory input is stereotyped: the fraction of non-olfactory input received by homologous MBONs across hemispheres is more similar than across different MBONs in the same hemisphere ($p < 0.002$, Mann-Whitney U Test). These observations, along with the sparse activity of olfactory KCs seen in adult flies [Honegger et al., 2011], suggest that non-olfactory signals may have a large influence on the activity of certain MBONs despite the small number of non-olfactory KCs. To quantify this influence, we compared the total number of synapses made by thermosensory KCs onto the different MBONs to 0.05 times the total number of synapses made by non-thermosensory KCs (Ext. Data Fig. 9f). This ratio quantifies the relative influence of a stimulus that activates thermosensory KCs to a typical odor stimulus that activates 5% of olfactory KCs [Honegger et al., 2011]. The ratio is high for some MBONs (d3, o1 and b3) and stereotyped for homologous MBONs across hemispheres, suggesting that some MBONs may be wired to respond strongly to non-olfactory cues, such as temperature. We also examined whether the olfactory input received by homologous MBONs is stereotyped by computing the correlation between the number of connections they receive from each olfactory PN via KCs. Unlike for non-olfactory input, homologous MBONs across hemispheres receive a less similar pattern of olfactory PN input than different MBONs in the same hemisphere ($p > 0.99$, Mann-Whitney U Test), arguing against stereotypy. Therefore the lack of stereotypy in the olfactory PN-to-KC connectivity and the greater degree of stereotypy in the non-olfactory PN-to-KC connectivity are inherited by the MBONs.

Interestingly, MBONs do not receive their inputs exclusively from KCs, DANs and other

MBONs. We found that some compartments (Fig. 4b) have two kinds of MBONs that differ in the amount of input they receive from non-MB sources. Some MBONs are postsynaptic almost exclusively to MB neurons (over 90%), while some receive 50% or more of their inputs from non-MB neurons on dendritic branches outside the MB compartments (Fig. 4b and Supp. Table 2a). MBONs with significant input from outside the MB typically receive input from other MBONs as well. The convergence of modulatory neurons, of olfactory, thermal and visual KCs, and of "other" non-MB inputs onto some MBONs makes them flexible sites for learning and integration of multisensory and internal state information (via DANs, as suggested by functional studies in the adult [Krashes et al., 2009; Lewis et al., 2015; Lin et al., 2014b; Perisse et al., 2016], and possibly via the "other" new non-MB inputs identified here).

The MBON output network

In adult *Drosophila* MBONs form a multi-layered feedforward network [Aso et al., 2014a; Perisse et al., 2016]. Consistent with this, we found synaptic connections between MBONs in different compartments, on both the ipsi- and contralateral sides, that create a bilaterally symmetric structured feedforward circuit (Fig. 4a, Supp. Table 5). Most inter-lobe connections are mediated by GABAergic (MBON-g1, g2, h1, h2) and Glutamatergic (MBON-i1, j1, k1) MBONs, potentially providing a substrate for lateral inhibition between the lobes. Glutamate has previously been found to be inhibitory in the fly [Liu and Wilson, 2013], but an excitatory effect on some neurons cannot be excluded. Some VL MBONs could also disinhibit (via inhibition of inhibitory ML MBONs), or directly excite, other VL MBONs, potentially providing within-region facilitation.

In addition, there is a hierarchy of interactions across regions of the MB. MBONs of the peduncle and calyx are exclusively at the bottom of the inhibitory hierarchy, receiving inputs from GABAergic MBONs from both the VL and the ML, but not synapsing onto any other MBONs (Fig. 4a). Furthermore, ML may also disinhibit the peduncle MBON-c1

that the VL inhibits (Fig. 4a).

Homo- and hetero-compartment MBON connections to DANs and OANs

The mushroom body connectome further revealed several feedback connections from MBONs onto DAN/OAN/MBIN of the same compartment (Fig. 5a-b). MBON-e2 from the tip compartment of the VL (UVL) synapses onto the dendrites of OAN-e1 outside

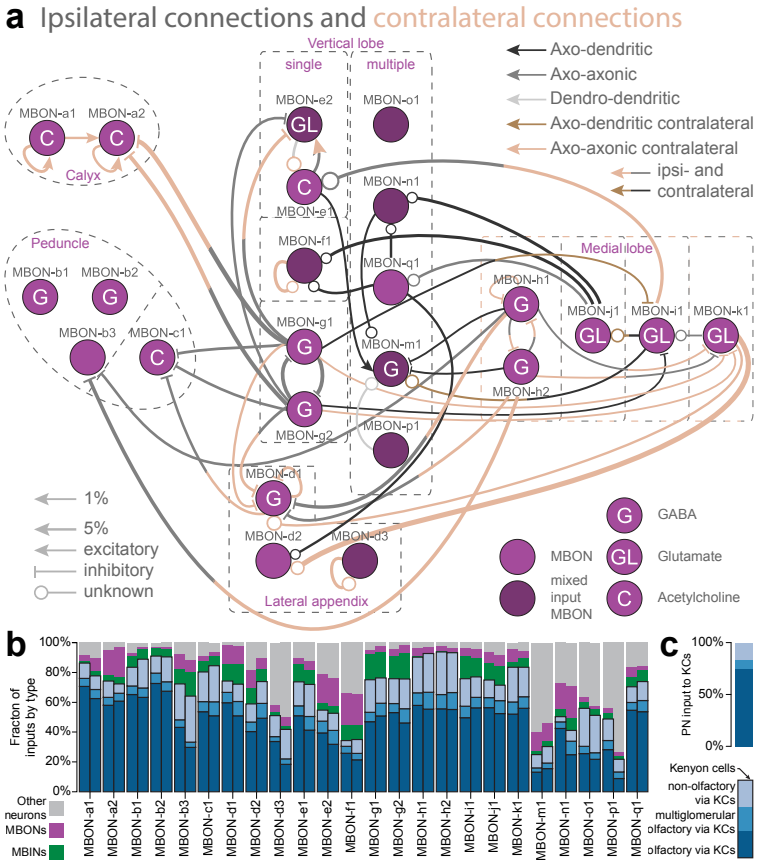

Figure 4: MBON inputs and circuits.
a Ipsi- and contralateral connections between MBONs. MBONs are in the compartments innervated by their dendrites. Most connections among MBONs are axo-axonic, and fewer are axo-dendritic. Few MBONs avoid synapting to others. Most inter-lobe connections are mediated by GABAergic (MBON-g1, g2, h1, h2) and glutamatergic (MBON-i1, j1, k1) MBONs, potentially providing a substrate for lateral inhibition between compartments of opposite valence.
b Fractions of synaptic input onto MBONs by neuron type. Left and right homologous MBONs are shown adjacent. Only vertical lobe and LA MBONs get less than 80% of their input from MB neurons and less than 60% from KCs. Almost all multi-compartment MBONs (MBON-m1, n1, o1 and p1) have a higher fraction of input from non-MB neurons than single-compartment MBONs. The fraction of inputs from PNs to MBONs via KCs is shown within the fraction of KC input (different shades of blue). To determine the fraction of olfactory, multiglomerular olfactory and non-olfactory PN input we took the matrix product of the PN-KC and KC-MBON connections. Most MBONs receive a high fraction of olfactory input via KCs while few MBONs (b3, o1) get nearly half of their inputs via KCs from non-olfactory PNs.
c Percentages of different types of PN input to the KCs. While there are almost equal numbers of olfactory and non-olfactory PNs synapting onto KCs, non-olfactory PNs represent only about 16% of the inputs to KC dendrites.

the MB (bilateral; Fig. 5a and Supp. Fig. 1b). MBON-q1 from IVL/LVL compartments is presynaptic to the axons of the DANs from these two compartments in addition to the MBIN-l1 from the LA compartment (Fig. 5b and Supp. Fig. 1b). An MBON-to-DAN feedback connection was found in the α1 compartment of the adult VL and is implicated in the formation of long-term memory [Ichinose et al., 2015].

Interestingly, we also found hetero-compartment feed-across connections where MBONs that innervate one region of the MB synapse onto DAN/OAN/MBIN innervating other regions (Fig. 5c and Supp. Fig. 1b). The feed-across motifs could play a role during conflicting memory formation [Das et al., 2014; Aso and Rubin, 2016] or during reversal learning and more generally they could enhance the flexibility of modulatory input to the MB.

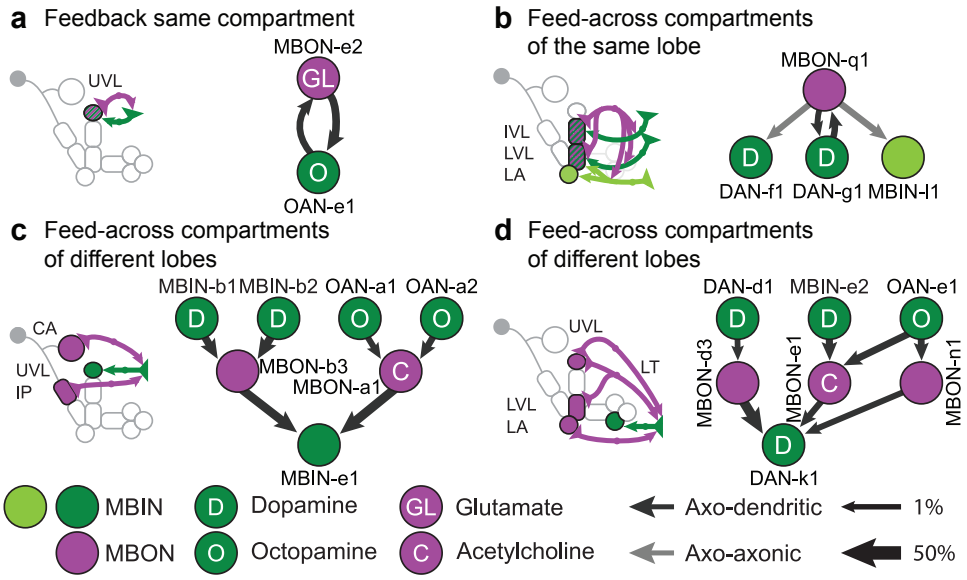

Figure 5: Intra- and inter-compartment feedback: MBONs of one MB compartment synapse onto MBINs of the same or other compartments.
Schematics of connections from output neurons (MBONs) onto input neurons (MBINs) within their own (feedback) or from other compartments (feed-across).
a The output neuron MBON-e2 synapses onto the dendrites of OAN-e1 in its own compartment, UVL.
b Feedback among compartments of the same lobe suggests that the establishment of a memory in a compartment can affect the DANs of adjacent compartments.
c Feed-across motif from proximal MB compartments (calyx and intermediate peduncle) to a distal one (UVL).
d Feed-across motif from the vertical lobe to the medial lobe.

3.4 Discussion

We provide the first complete wiring diagram of a parallel fiber circuit for adaptive behavioral control. Such circuits exist in various forms, for example the cerebellum in vertebrates and the mushroom body in insects. They contribute to multiple aspects of behavioral control including stimulus classification, the formation and retrieval of Pavlovian associations, and memory-based action selection [Heisenberg, 2003; Waddell, 2013; Owald and Waddell, 2015; Schürmann, 2016]. A comprehensive wiring diagram of such a multi-purpose structure is an essential starting point for functionally testing the observed structural connections and for elucidating the circuit implementation of these fundamental brain functions.

Even though individual neurons may change through metamorphosis, many of the basic aspects of the MB architecture are shared between larval and adult *Drosophila* stages and with other insects (see Supp. Table 6, Supp. Table 7) [Heisenberg, 2003; Gerber et al., 2009; Aso et al., 2014a,b; Waddell, 2013; Menzel, 2012; Owald and Waddell, 2015; Bouzaiane et al., 2015; Perisse et al., 2016; Rohwedder et al., 2016; Schürmann, 2016; Takemura et al., 2017]. We therefore expect that the circuit motifs identified here are not unique to the L1 developmental stage, but instead represent a general feature of *Drosophila* and insect MBs.

A canonical circuit in each MB compartment with unexpected motifs

Our EM reconstruction revealed a canonical circuit in each MB compartment that features two unexpected motifs in addition to the previously known DAN/OAN-to-KC and KC-to-MBON connections. First, we were surprised to observe that the number of KC-to-DAN/OAN/MBIN synapses is comparable to the number of KC-to-MBON synapses. As KCs were shown to be cholinergic in adults [Barnstedt et al., 2016], this connection could potentially depolarize DAN/OAN/MBIN axons. Untrained, novel odors

can activate DANs in adult *Drosophila* [Riemensperger et al., 2005; Mao and Davis, 2009] and OANs in bees [Menzel, 2012]). Similar brief short-latency activations of dopamine neurons by novel stimuli are observed in monkeys, too, and are interpreted as salience signals [Schultz, 2015]. Learning could potentially modulate the strength of the KC-to-DAN/OAN/MBIN connection, either weakening it, or strengthening it. The latter scenario could explain the increase in DAN activation by reinforcement-predicting odors observed in adult *Drosophila* [Riemensperger et al., 2005], bees and monkeys [Menzel, 2012; Schultz, 2015].

Another unexpected finding was that DANs synapse directly onto MBONs, rather than only onto KCs. Such a motif could provide a substrate for neuromodulation-gated Hebbian spike-timing dependent plasticity which has so far been observed in locust MB [Cassenaer and Laurent, 2012], even though, in *Drosophila*, dopamine receptors have been shown to be required in KCs for memory formation [Kim et al., 2007].

Single-claw KCs and the dimensionality of the MB representation

In addition to random and bilaterally asymmetric olfactory and structured non-olfactory PN-to-KC connectivity (Ext. Data Fig. 3), our analysis identified single-claw KCs whose number and lack of redundancy are inconsistent with random wiring (Fig. 2). Random wiring has previously been shown to increase the dimension of sensory representations when the number of neurons participating in the representation is large compared to the number of afferent fibers, as in the cerebellum or adult mushroom body [Babadi and Sompolinsky, 2014; Litwin-Kumar et al., 2017]. However, our model shows that when the number of neurons is limited, random wiring alone is inferior to a combination of random and structured connectivity that ensures each input is sampled without redundancy. The presence of single-claw KCs may reflect an implementation of such a strategy. In general, our results are consistent with a developmental program that secures complete and high-dimensional sensory representations by KCs to support stimulus discrimination

at both larval and adult stages.

Mutual inhibition as general motif of the MBON-MBON network

The current study reveals the complete MBON-MBON network at synaptic resolution (Fig. 4a). Previous studies in the larva have shown that odor paired with activation of medial and vertical lobe DANs leads to learned approach [Rohwedder et al., 2016] and avoidance [Gerber et al., 2009; Diegelmann et al., 2013], respectively. Our connectivity analysis reveals that glutamatergic MBONs from the medial lobe laterally connect to MBONs of the vertical lobe. The glutamatergic MBON-to-MBON connections could be inhibitory [Liu and Wilson, 2013], although further studies are needed to confirm this. Furthermore, inhibitory GABAergic MBONs from the vertical lobe laterally connect to MBONs of the medial lobe. An example is the feedforward inhibition of ML MBON-i1 output neuron by the VL GABAergic MBON-g1, -g2 output neurons. A similar motif has been observed in *Drosophila* adult, where aversive learning induces depression of conditioned odor response in the approach-promoting MBON-MVP2 (MBON-11) which in turn causes a disinhibition of conditioned odor responses in the avoidance-promoting MBON-M4/M6 (MBON-03) due to the MBON-MVP2 to MBON-M4/M6 feedforward inhibitory connection [Aso et al., 2014a,b; Hige et al., 2015; Owald et al., 2015; Bouzaiane et al., 2015; Perisse et al., 2016].

Combining the present connectivity analysis of the MBON-MBON network in the larva and previous studies in the adult *Drosophila* [Aso et al., 2014a,b; Owald et al., 2015; Owald and Waddell, 2015; Perisse et al., 2016], the rule seems to be that MBONs encoding opposite learnt valance laterally inhibit each other. Such inhibitory interactions have been proposed as a paradigmatic circuit motif for memory-based action selection [Lorenz, 1973].

3.5 Material and Methods

Circuit mapping and electron microscopy

We reconstructed neurons and annotated synapses in a single, complete central nervous system from a 6-h-old $[iso]$ *Canton S G1 x w*^{1118} *[iso] 5905* larva acquired with serial section transmission EM at a resolution of 3.8 x 3.8 x 50 nm, that was first published in [Ohyama et al., 2015] along with the detailed sample preparation protocol. Briefly, the CNS of 6-h-old female larvae were dissected and fixed in 2% gluteraldehyde 0.1 M sodium cacodylate buffer (pH 7.4) to which an equal volume of 2% OsO_4 in the same buffer was added, and microwaved at 350-W, 375-W and 400-W pulses for 30 sec each, separated by 60-sec pauses, and followed by another round of microwaving but with 1% OsO_4 solution in the same buffer. Then samples were stained en bloc with 1% uranyl acetate in water by microwave at 350 W for 3x3 30 sec with 60-sec pauses. Samples were dehydrated in an ethanol series, then transferred to propylene oxide and infiltrated and embedded with EPON resin. After sectioning the volume with a Leica UC6 ultramicrotome, sections were imaged semi-automatically with Leginon [Suloway et al., 2005] driving an FEI T20 TEM (Hillsboro), and then assembled with TrakEM2 [Cardona et al., 2012] using the elastic method [Saalfeld et al., 2012]. The volume is available at http://openconnecto.me/catmaid/, titled “acardona_0111_8”.

To map the wiring diagram we used the web-based software CATMAID [Saalfeld et al., 2009], updated with a novel suite of neuron skeletonization and analysis tools [Schneider-Mizell et al., 2016], and applied the iterative reconstruction method [Schneider-Mizell et al., 2016]. All annotated synapses in this wiring diagram fulfill the four following criteria of mature synapses [Ohyama et al., 2015; Schneider-Mizell et al., 2016]: (1) There is a clearly visible T-bar or ribbon. (2) There are multiple vesicles immediately adjacent to the T-bar or ribbon. (3) There is a cleft between the presynaptic and the postsynaptic

neurites, visible as a dark-light-dark parallel line. (4) There are postsynaptic densities, visible as black streaks hanging from the postsynaptic membrane.

In this study we validate the reconstructions as previously described [Ohyama et al., 2015; Schneider-Mizell et al., 2016], a method successfully employed in multiple studies [Ohyama et al., 2015; Heckscher et al., 2015; Fushiki et al., 2016; Schneider-Mizell et al., 2016; Zwart et al., 2016; Jovanic et al., 2016; Schlegel et al., 2016]. Briefly, in *Drosophila*, as in other insects, the gross morphology of many neurons is stereotyped and individual neurons are uniquely identifiable based on morphology [Goodman et al., 1981; Bate et al., 1981; Costa et al., 2016]. Furthermore, the nervous system in insects is largely bilaterally symmetric and homologous neurons are reproducibly found on the left and the right side of the animal. We therefore validated MBON, DAN, OAN, MBIN, APL and PN neuron reconstructions by independently reconstructing synaptic partners of homologous neurons on the left and right side of the nervous system. By randomly re-reviewing annotated synapses and terminal arbors in our dataset we estimated the false positive rate of synaptic contact detection to be 0.0167 (1 error per 60 synaptic contacts). Assuming the false positives are uncorrelated, for an n-synapse connection the probability that all n are wrong (and thus that the entire connection is a false positive) occurs at a rate of 0.0167^n. Thus, the probability that a connection is false positive reduces dramatically with the number of synaptic connections contributing to that connection. Even for $n = 2$ synapse connections, the probability that the connection is not true is 0.00028 (once in every 3,586 two-synapse connections) and we call connections with two or more connections 'reliable' connections. See [Ohyama et al., 2015; Schneider-Mizell et al., 2016] for more details.

Identification of PNs

The olfactory PNs from this same EM volume were previously traced and identified [Berck et al., 2016]. To identify the photosensory and thermosensory PNs connected

to KCs, we traced all neurons downstream of 12 photosensory neurons in the left and right brain hemispheres and all neurons downstream of three previously characterized cold sensing neurons , expressed in 11F02-GAL4 line [Klein et al., 2015].

Learning in first instar larvae with a substitution experiment

Learning experiments were performed as described in [Schroll et al., 2006; Rohwedder et al., 2016]. The fly strain *PGMR58E02-GAL4attP2* (Bloomington Stock Center no. 41347) and the *attP2* control strain were crossed to *P20XUAS-IVS-CsChrimson.mVenusattP18* (Bloomington Stock Center no. 55134). Flies were reared at 25℃ in darkness on 4% agarose with a yeast and water paste including retinal in a 0.5 mM final concentration. First instar feeding-stage larvae in groups of 30 individuals were placed on plates filled with 4% agarose and the odor ethyl-acetate (100-times diluted in distilled water) was presented on filter papers located on the lid. Larvae were exposed to constant red light (630nm, power: 350µW/cm2) during this odor presentation for 3 minutes. Subsequently larvae were transferred to a new plate and no odor was presented in the dark for 3 minutes. This paired training cycle was repeated two times. We also performed the unpaired experiment (odor presentation in the dark and red light without odor) with another group of 30 naïve larvae. After a 5-minute test with odor presentation on one side of the lid larvae were counted on the side of the odor, no odor and a 1 cm area in the middle of the plate. Preference and performance indices were calculated as in Rohwedder et al. [2016]. Namely for both the paired and unpaired, the number of larvae on the no-odor side are subtracted from the number of larvae on the odor side, and the result is divided by the total number of larvae on the plate (including those in the middle). The performance index is half of the value for the paired minus the unpaired preference scores.

Random models of PN-to-KC connectivity

Individual PN connection probabilities were computed as the number of KCs contacted divided by the total number of KCs. Probabilities were computed separately for the two hemispheres. To generate the random networks in Fig. 2a, we assumed that PN-to-KC connections were formed independently according to these probabilities. We then iteratively generated KCs until the number of multi-claw KCs matched the number found in the reconstruction. To compare dimensionality and classification performance for random networks with varying degrees of connectivity (Fig. 2c), we scaled the individual PN connection probabilities so that, on average, each KC received between 1 and 10 claws (Fig. 2b, c). In this case, we fixed the total number of KCs (single- and multi-claw) to be equal to the number found in the reconstruction.

To obtain KCs with a specified number of claws (Fig. 2b), PN connections were determined by weighted random sampling using the individual connection probabilities described above. When comparing detailed connectivity statistics to random models, we used this type of sampling to match the KC degree distribution for the random models to that of the data.

We also evaluated how many random multi-claw KCs would be required to ensure coverage of the subset of PNs that are connected to single-claw KCs. We restricted our analysis to these PNs and iteratively added multi-claw KCs, with the distribution of claw counts determined by the reconstructed connectivity, until each PN was connected to at least one KC.

Model of sparse KC responses

We assumed the activity of the ith KC was given by $s_i = [\sum_j J_{ij} x_j - \theta_i]_+$, where $[\cdot]_+$ denotes rectification, J is the matrix of PN-to-KC connections, x_j is the activity of the jth PN, and θ_i is the KC activity threshold. Simulated odor-evoked PN activity was generated by sampling the value of each x_j independently from a rectified unit Gaussian

distribution. The value of θ_i was adjusted so that each KC fired for a fraction $f = 0.05$ of odors. The entries of J were either the synapse counts from the reconstructed data or, for the case of random connectivity, chosen in the manner of the previous section with a weight sampled randomly from the distribution of synaptic contact numbers found in the EM reconstruction.

To assess classification performance (Fig. 2b, c), the KC responses to 8 odors were evaluated (10 odors were used when simulating the adult MB). Odor responses again consisted of rectified unit Gaussian random variables, but corrupted by Gaussian noise with standard deviation 0.2. A maximum-margin classifier was trained to separate the odors into two categories to which they were randomly assigned, and the error rate was assessed when classifying odors with different noise realizations. Dimensionality (Fig. 2f) was assessed by estimating the KC covariance matrix $C_{ij} = \langle (z_i - \langle z_i \rangle)(z_j - \langle z_j \rangle) \rangle$, where z_i is the z-scored activity of neuron i, using 1,000 random simulated odors. We then computed $\dim = (\sum_i \lambda_i)^2 / \sum_i \lambda_i^2$, where $\{\lambda_i\}$ are the eigenvalues of C [Litwin-Kumar et al., 2017].

To implement recurrence, we modified the model so that the activity of the ith KC was given by $s_i(t) = \Theta\left(\sum_j J_{ij} x_j + \sum_k J^{\mathrm{rec}}_{ik} s_k(t-1) - \theta_i\right)$, where J^{rec}_{ik} is a matrix of recurrent KC-to-KC interactions and t is the timestep. J^{rec} is equal to $\alpha_1 J^{\mathrm{KC}\to\mathrm{KC}} + \alpha_2 J^{\mathrm{APL}}$, where $J^{\mathrm{KC}\to\mathrm{KC}}$ was determined by the KC-to-KC synapse counts (either dendro-dendritic only or both dendro-dendritic and axo-axonic) and $J^{\mathrm{APL}}_{ik} \propto c_i^{\mathrm{APL}\to\mathrm{KC}} c_k^{\mathrm{KC}\to\mathrm{APL}}$, with $c_i^{\mathrm{APL}\to\mathrm{KC}}$ representing the number of APL synapses onto the ith KC and $c_k^{\mathrm{KC}\to\mathrm{APL}}$ representing the number of synapses onto APL from the kth KC. J^{APL} was scaled so that the average of its entries equaled that of J. The scalar $\alpha_1 = 0.33$ was chosen so that the strength of KC-to-KC and PN-to-KC connections were comparable, while $\alpha_2 = 0.05$ represents the gain of the APL neuron. A single randomly chosen KC was updated on each timestep, with the number of timesteps equal to 5 times the number of KCs. We also modeled

facilitatory KC-to-KC interactions by assuming KC-to-KC connections only depolarize the postsynaptic neuron when it is already above threshold.

Immunostaining

Third-instar larvae were put on ice and dissected in PBS. For all antibodies brains were fixed in 3.6% formaldehyde (Merck) in PBS for 30 min except anti-dVGlut that required bouin's fixation [DrObysheva et al., 2008]. After several rinses in PBT (PBS with 1% or 3% Triton X-100; Sigma-Aldrich), brains were blocked with 5% normal goat serum (Vector Laboratories) in PBT and incubated for at least 24 hours with primary antibodies at 4℃. Before application of the secondary antibodies for at least 24 hours at 4℃ or for 2 hours at room temperature, brains were washed several times with PBT. After that, brains were again washed with PBT, mounted in Vectashield (Vector Laboratories) and stored at 4℃ in darkness. Images were taken with a Zeiss LSM 710M confocal microscope. The resulting image stacks were projected and analyzed with the image processing software Fiji [Schindelin et al., 2011]. Contrast and brightness adjustment, rotation, and arrangement of images were performed in Photoshop (Adobe Systems).

Antibodies

Brains were stained with the following primary antibodies, polyclonal goat anti-GFP fused with FITC (1:1000, Abcam, ab6662), polyclonal rabbit anti-GFP (1:1000, Molecular Probes, A6455), polyclonal chicken anti-GFP (1:1000, Abcam, ab13970), monoclonal mouse anti-TH (1:500, ImmunoStar, 22941), polyclonal rabbit anti-TDC2 (1:200, CovalAb, pab0822-P), monoclonal mouse anti-ChAT (1:150, Developmental Studies Hybridoma Bank, ChaT4B1), polyclonal rabbit anti-GABA (1:500, Sigma, A2052), and rabbit anti-dVGlut (1:5000; Daniels et al. [2004]) for identifying GFP positive, dopaminergic, octopaminergic, cholinergic, GABAergic, and glutamatergic neurons, respectively. The following secondary antibodies were used, polyclonal goat anti-chicken Alexa Fluor 488 (1:200, Molecular Probes, A11039), polyclonal goat anti-rabbit Alexa Fluor

488 (1:200, Molecular Probes, A11008), polyclonal goat anti-rabbit Alexa Fluor 568 (1:200, Molecular Probes, A11011), polyclonal goat anti-rabbit Cy5 (1:200, Molecular Probes, A10523), polyclonal goat anti-mouse Alexa Fluor 647 (1:200, Molecular Probes, A21235), and polyclonal goat anti-rabbit Alexa Fluor 647 (1:200, Molecular Probes, A21245).

Identifying GAL4 lines that drive expression in MB-related neurons

To identify GAL4 lines (listed in Supp. Table 3) that drive expression in specific MB-related neurons, we performed single-cell FLP-out experiments (for flp-out methodology see [Nern et al., 2015; Ohyama et al., 2015]) of many candidate GAL4 lines (LiTruman2014). We generated high-resolution confocal image stacks of the projection patterns of individual MBONs/DANs/OANs (multiple examples per cell type), which allowed their identification. Most MBONs/DANs/OANs were uniquely identifiable based on the dendritic and axonal projection patterns (which MB compartment they project to and the shape of input or output arbour outside the MB). These were also compared to previously reported single-cell FLP-outs of dopaminergic and octopaminergic neurons in the larva [Selcho et al., 2009; Pauls et al., 2010; Selcho et al., 2014; Slater et al., 2015; Rohwedder et al., 2016]. Some compartments were innervated by an indistinguishable pair of MBONs or MBINs.

Estimating the birth order of KCs

KCs arise from four neuroblasts per hemisphere that divide continuously from the embryonic to the late pupal stage [Ito and Hotta, 1992; Kunz et al., 2012]. The primary neurite of newborn KCs grows through the center of the MB peduncle, pushing existing KCs to the surface of the peduncle [Kurusu et al., 2002] (Ext. Data Fig. 4h). As new cells are added, their somas remain closer to the neuroblast at the surface of the brain and push away existing somas. The point of entry into the lineage bundle of each KC primary neurite remains as a morphological record of the temporal birth order, with

some noise. For every KC, we measured the distance from the point where its primary neurite joins the lineage bundle to a reference point consisting of the point where the neurite of the last KC (potentially the oldest of that lineage) joins the bundle before the bundle enters the neuropil (Fig. 1f) to form the peduncle together with the other three bundles. This measurement revealed that single-claw KCs are born early in MB development, followed by 2-claw KCs, 3-claw KCs and so on (Fig. 1f), with the last-born KCs being immature and expected to develop into multi-claw KCs later in larval life [Lee et al., 1999].

3.6 Acknowledgements

We thank A. Khandelwal, J. Lovick, J. Valdes-Aleman, I. Larderet, V. Hartenstein, A. Fushiki, B. Afonso, P. Schlegel and M. Berck for reconstructing 31% of the raw skeletons and 19% of the raw postsynaptic sites. We thank R. Axel, G. M. Rubin and Y. Aso for their comments on the manuscript. AL-K was supported by NIH grant #F32DC014387. AL-K and LFA were supported by the Simons Collaboration on the Global Brain. LFA was also supported by the Gatsby, Mathers and Kavli Foundations. CEP and YP were partially supported by the XDATA program of the Defense Advanced Research Projects Agency (DARPA) administered through Air Force Research Laboratory contract FA8750-12-2-0303, and the NSF BRAIN Early Concept Grants for Exploratory Research (EAGER) award DBI-1451081. BG and TS thank the Deutsche Forschungsgemeinschaft, CRC 779; Deutsche Forschungsgemeinschaft, GE 1091/4-1; the European Commission, FP7-ICT MINIMAL. We thank the Fly EM Project Team at HHMI Janelia for the gift of the EM volume, the Janelia Visiting Scientist program, the HHMI visa office, and HHMI Janelia for funding.

3.7 Author contributions

K.E., F.L., A.L.-K., B.G., L.F.A., A.T., M.Z. and A.C. conceived the project, analyzed the data and wrote the manuscript.

K.E., F.L., I.A., C.S.-M., T.S. A.T. and A.C. reconstructed neurons.

K.E. performed learning experiments.

A.L.-K. built the models.

J.W.T contributed GAL4 lines and their imagery.

R.D.F. generated EM image data.

A.L.-K., C.S.-M., Y.P. and C.E.P. analysed connectivity patterns.

F.L. and A.H. performed immunostainings.

C.E. generated functional data.

3.8 Supplemental data

Extended Data Figures:

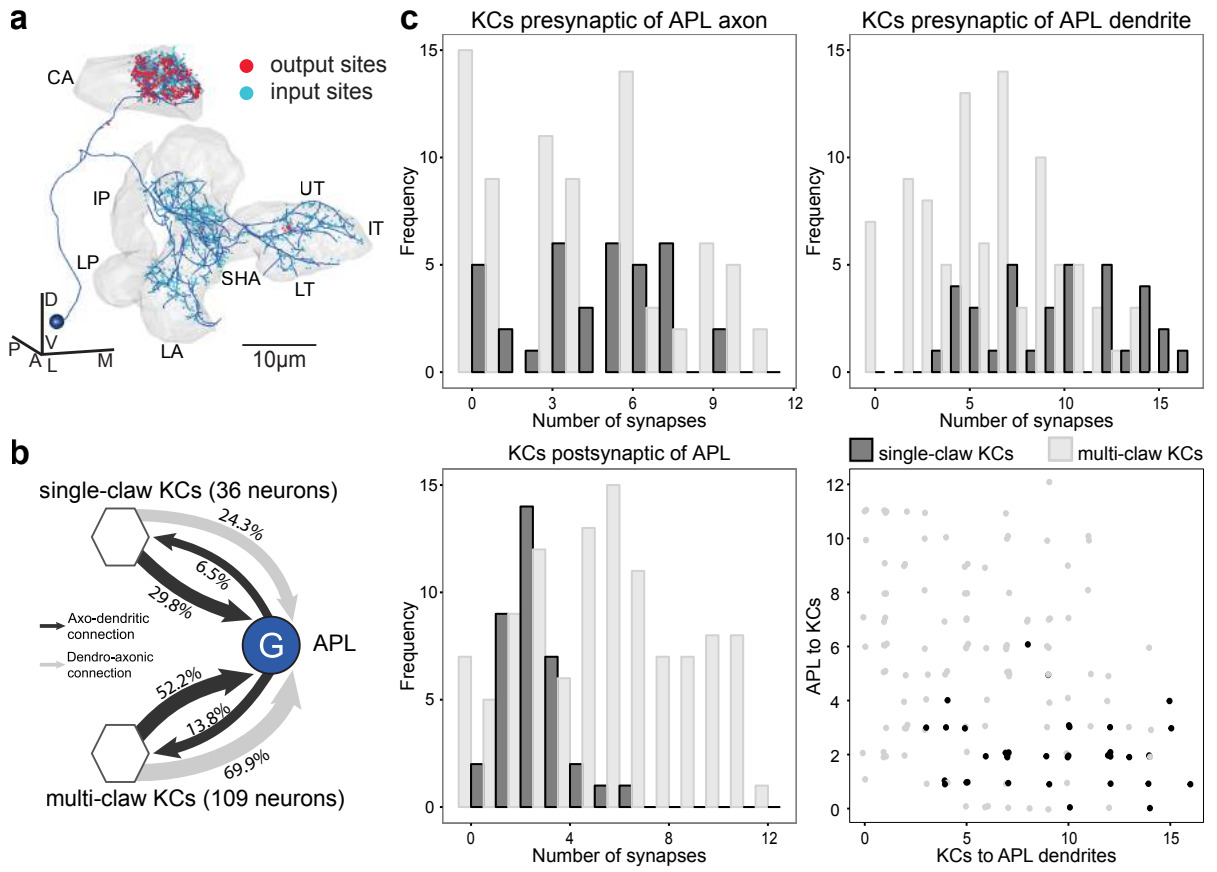

Extended Data Figure 1: Connectivity of the larval APL neuron.
a Morphology of the right hemisphere larval APL neuron. While APL dendrites are postsynaptic to the KCs in LA, LVL, IVL and all medial lobe compartments, its axon is both post- and presynaptic to the MB calyx. Presynaptic sites in *red* and postsynaptic sites in *blue*.
b APL connectivity with KC types. Connections are displayed as fractions of input onto the receiving neurons. APL forms more axo-dendritic connections with multi-claw than with single-claw KCs. All mature KCs connect to APL on its dendrite as well as on its axon.
c Strength of synaptic connections between KCs and the APL neuron for single-claw and multi-claw KCs separately. While single-claw KCs have a higher synapse count connecting to the APL dendrites than multi-claw KCs, both groups of KCs project a similar number of synapses to the APL axon. In the calyx, APL makes more synapses onto multi-claw than onto single-claw KCs. In the lobes, single-claw KCs make more synapses with APL pre- than postsynaptically.

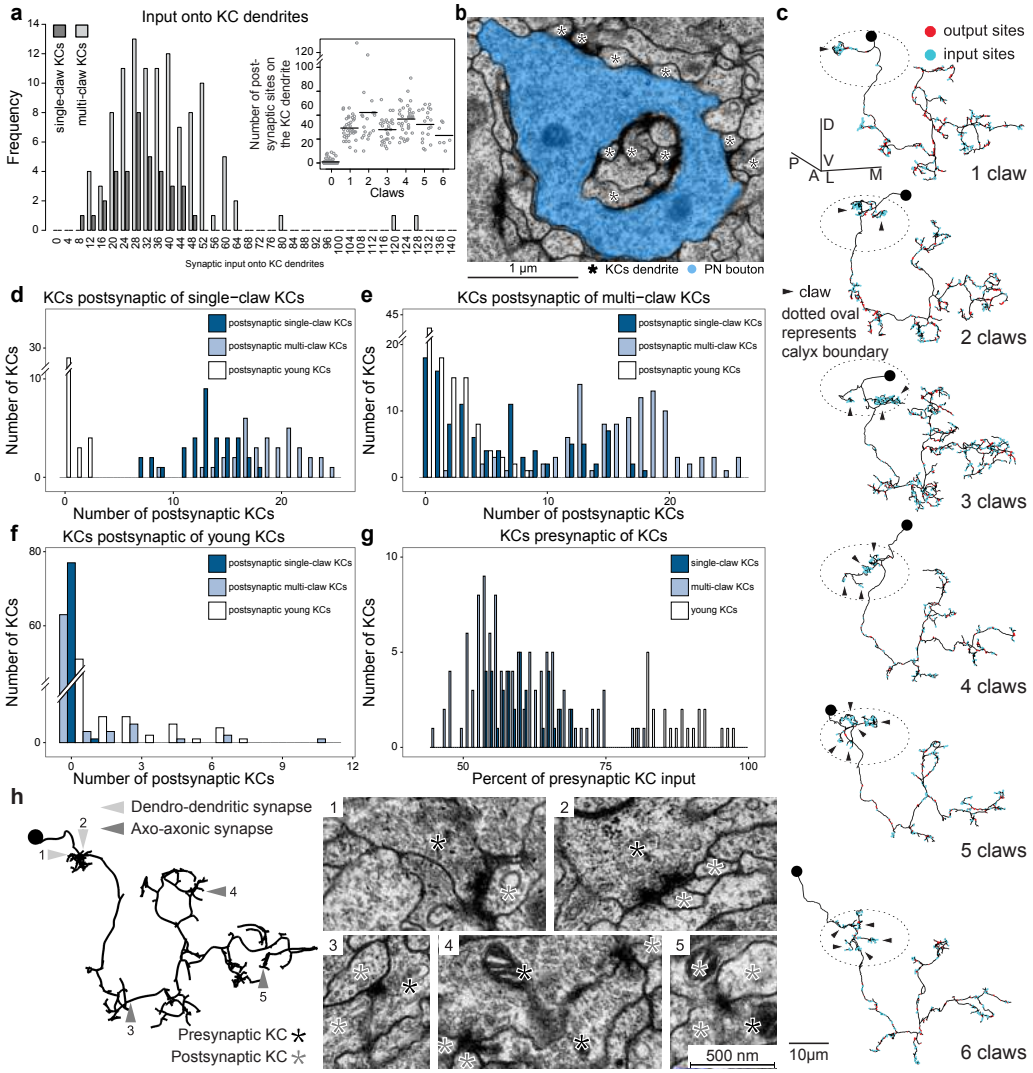

Extended Data Figure 2: Input onto KC dendrites and KC-KC connections.
a Total synaptic input onto KC dendrites from PNs, the APL neuron and calyx MBINs for single- and multi-claw KCs from both hemispheres. *Insert:* Sum of the KC postsynaptic sites in the calyx as a function of the number of claws. Grey circles show individual KCs and black line shows the mean. Young KCs that have no claws or only form short branches in the calyx have few postsynaptic sites. Mature KCs forming one to six claws present a similar total amount of postsynatic sites in the calyx.
b A PN bouton (blue) and its associated KC dendritic arborizations. Stars indicate all dendrites of the single-claw KC for this PN.
c Prototypical examples of KCs according to the structure of their dendrites, traditionally known as “claws”. In first instar, we define each “claw” (indicated by arrows) as a connection from a PN providing at least 10% of the postsynaptic sites of the KC dendritic arbor. This connectivity-based definition generally agrees with the count of physically separate claw-like dendritic branches that wrap around the axon terminals of the PNs. Single-claw KCs have not yet been described in the adult fly or other insects.
d-g Frequency of different numbers of postsynaptic KC-partners of KCs with at least two synapse connections, plotted separately for three different types of KCs.
d Postsynaptic partners of single-claw KCs.
e Postsynaptic partners of multi-claw KCs.
f Postsynaptic partners of young KCs.
g KC input onto KCs as a percent of total KC input. For most KCs more than 50% of their presynaptic partners are other KCs.
h Morphology of an example reconstructed KC (left) and example electron micrographs showing KC-KC synapses (right). Dendro-dendritic connections are in the clayx compartment (1 and 2) and axo-axonic connections are located in the peduncle (3), vertical lobe (4) and medial lobe (5).

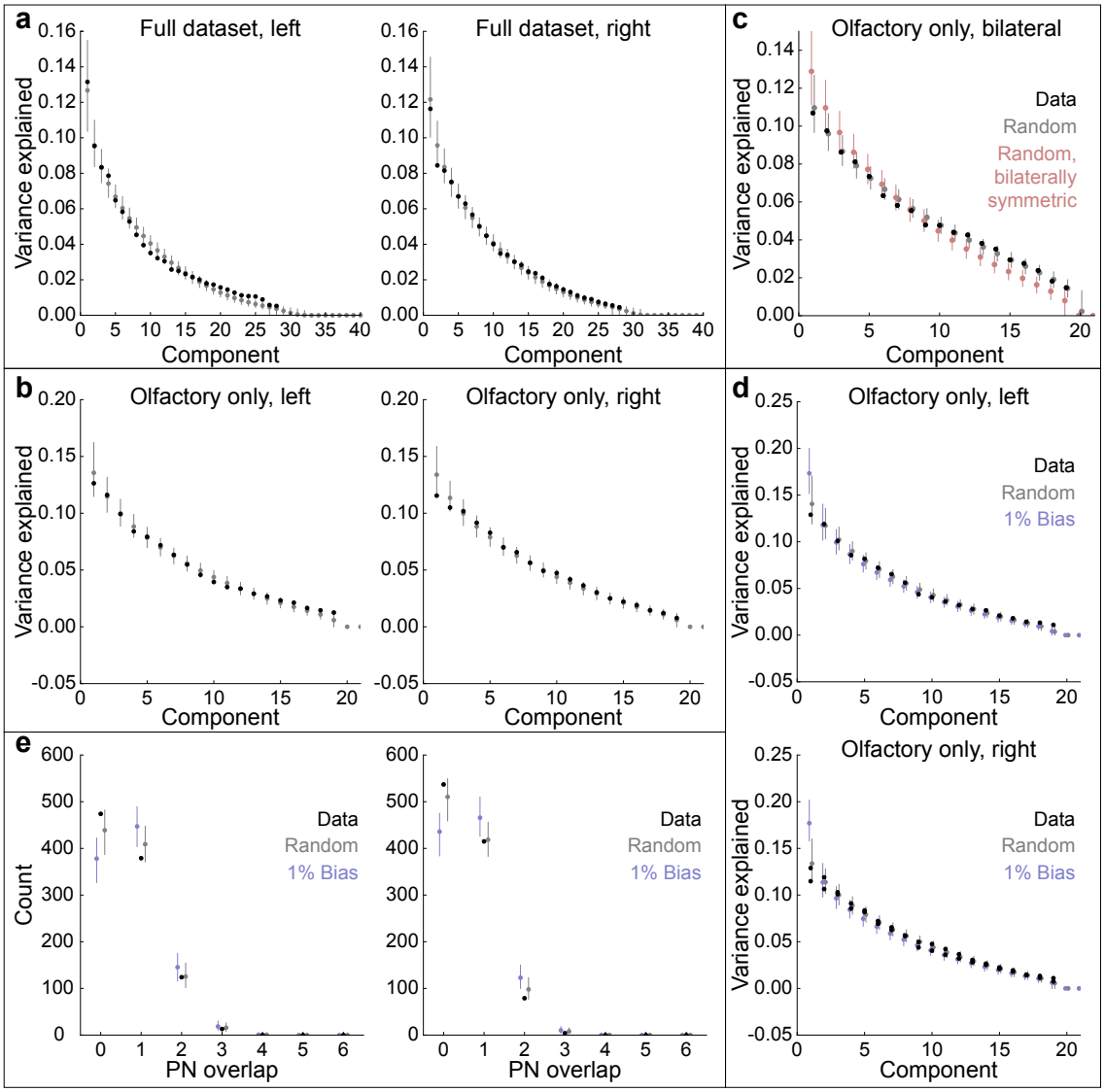

Extended Data Figure 3: Test of structure in PN-to-KC connectivity.
a We performed principal components analysis on the PN-to-KC connectivity matrices for the left and right hemispheres [Caron et al., 2013]. The analysis is restricted to multi-claw KCs. The variance explained by each principal component in descending order is compared to that obtained from random models in which KCs sample PNs according to the individual PN connection probabilities (see Methods). Gray circles and bars denote mean and 95% confidence intervals for the variance explained by each principal component of the random connectivity matrices, while the black circles indicate the values obtained from data. Note a small deviation from the random model, likely due to the non-olfactory PNs.
b Same as a but restricted to connections between olfactory PNs and KCs.
c Same as b but combining the PN-to-KC connectivity for both hemispheres. The data is compared to a random model in which KCs in each hemisphere sample PNs randomly and independently (grey), and to a bilaterally symmetric model in which the connectivity is random but duplicated across the two hemispheres (pink).
d To assess the ability of our method to identify structured connectivity, we also generated connectivity matrices in which a weak bias was added (blue). Networks were generated in which PNs were randomly assigned to one of two groups. For each KC, the probabilities of connecting to PNs belonging to one randomly chosen group were increased by 1%, while the probabilities for the other group were decreased by 1% (the baseline probabilities were on average approximately 5%). This procedure was performed independently for each KC and leads to networks in which KCs preferentially sample certain PNs. The data is inconsistent with this model, illustrating that biases of $\sim 1\%$ connection probability can be identified using our methods.
e As an independent method to identify structure in the PN-to-KC wiring, we considered the distribution of olfactory PN overlaps for all KC pairs, defined as the number of olfactory PNs from which both KCs receive input. This quantity specifically identifies biases in the likelihood of KCs to sample similar inputs. As in b, no such structure was identified.

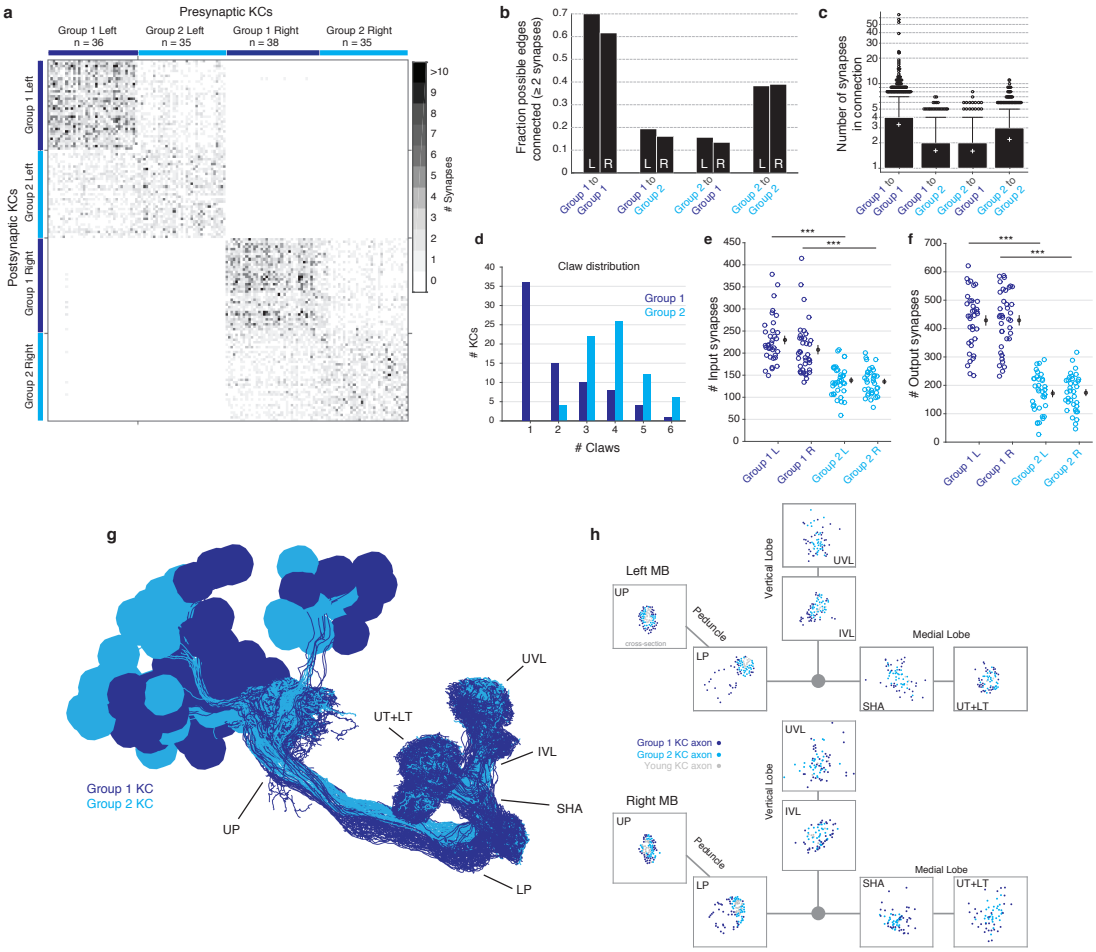

Extended Data Figure 4: KC-KC clustering.
Synaptic connectivity between KCs reveals two communities within the MB.
a Heat map representation of the KC-KC network adjacency matrix, sorted by community structure as discovered by the Louvain method [Blondel et al., 2008], which identifies groups of KCs with more within-group connections than expected by chance. We denote the denser community on each side as "Group 1" and the other community as "Group 2". Number of cells in each group is shown in the column labels.
b The number of observed 2+ synapse connections between pairs of KCs within and between groups in the same side of the body, normalized by the total number of all possible such connections (L: left, R: right).
c Distribution of number of synapses per edge for connections within and between each group. Boxes indicate interquartile interval, whiskers 95th percentile, white cross indicates mean, outliers shown.
d Claw distribution by group (both sides aggregated). Note that all single claw KCs are in Group 1.
e Total number of anatomical input synapses onto Group 1 and Group 2 KCs, including from non-KC sources. Group 1 cells have significantly more inputs than Group 2 cells on each side ($p < 10^{-10}$, t-test with Bonferroni correction).
f Total number of anatomical output synapses from Group 1 and Group 2 KCs, including synapses onto non-KC targets. Group 1 cells have significantly more outputs than Group 2 cells on each side ($p < 10^{-10}$, t-test with Bonferroni correction).
g KC anatomy labeled by group for the right MB. Note that both groups of KCs come from each lineage cluster. Labeled spots indicate locations of cross-section views in h.
h Cross-sections of the two principle axon branches of KCs in the left (above) and right (below) MBs at the locations indicated in g. Orientations of each cross-section are arbitrary.

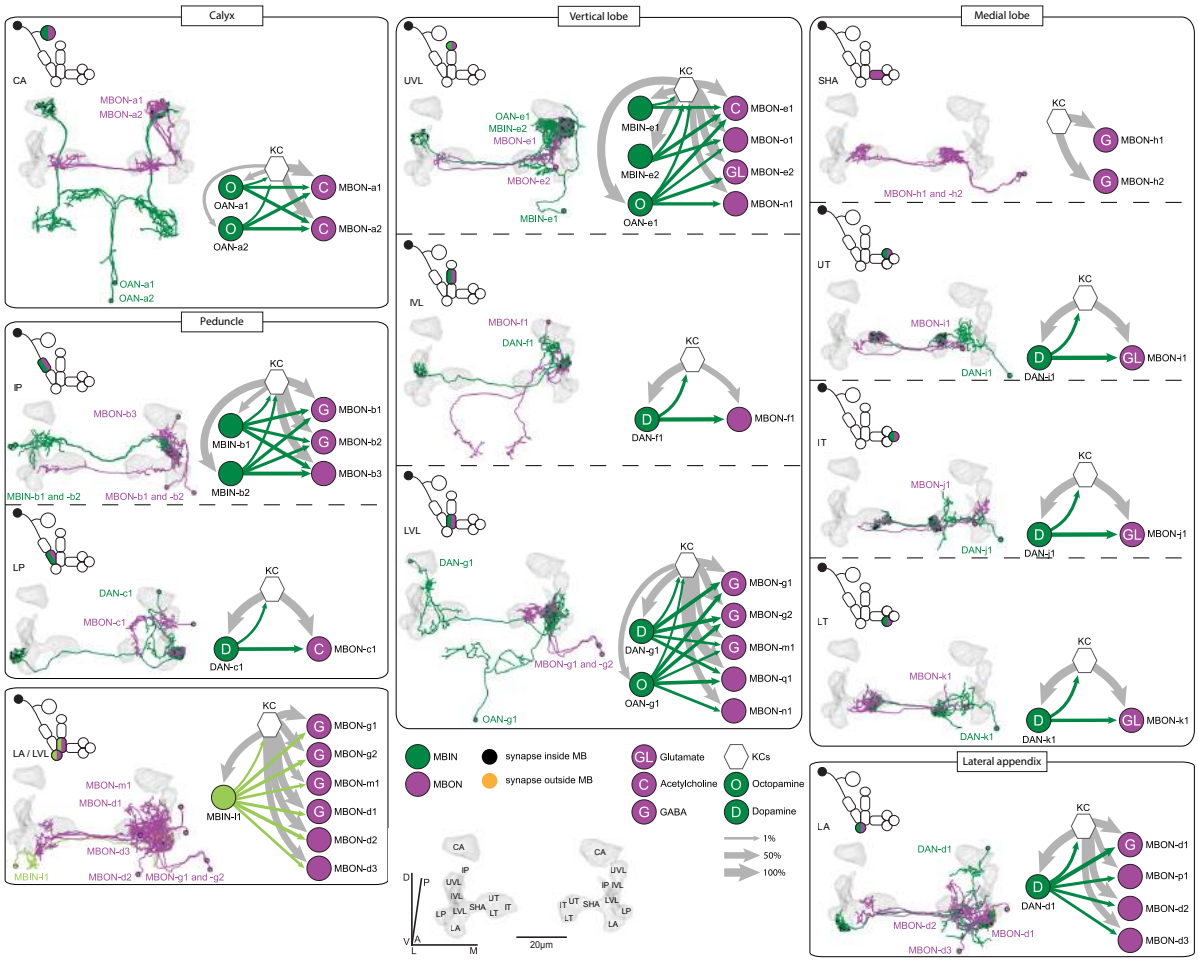

Extended Data Figure 5: Neurons in the canonical circuit in every MB compartment.
Neuronal morphology and connectivity of MBINs and MBONs participating in the canonical circuit motif of each MB compartment (MBINs in green and MBONs in magenta). Neurons connecting to the left hemisphere MB are displayed in anterior view (right hemisphere has the same morphology, data not shown). Locations of MBINs synapsing on MBONs in a given compartment are shown depending on their location (inside the MB neuropil, *black*; outside the MB, *orange*). MBIN axons and MBON dendrites tile the MB into 11 distinct compartments. For each compartment the MBIN and MBON neurons and their connections as a fraction of total input to the receiving neuron are shown on the right. MBONs are diverse in the neurotransmitter that they release (see legend). All compartments present the canonical circuit motif except for SHA, that does not develop its DAN until later in larval life.

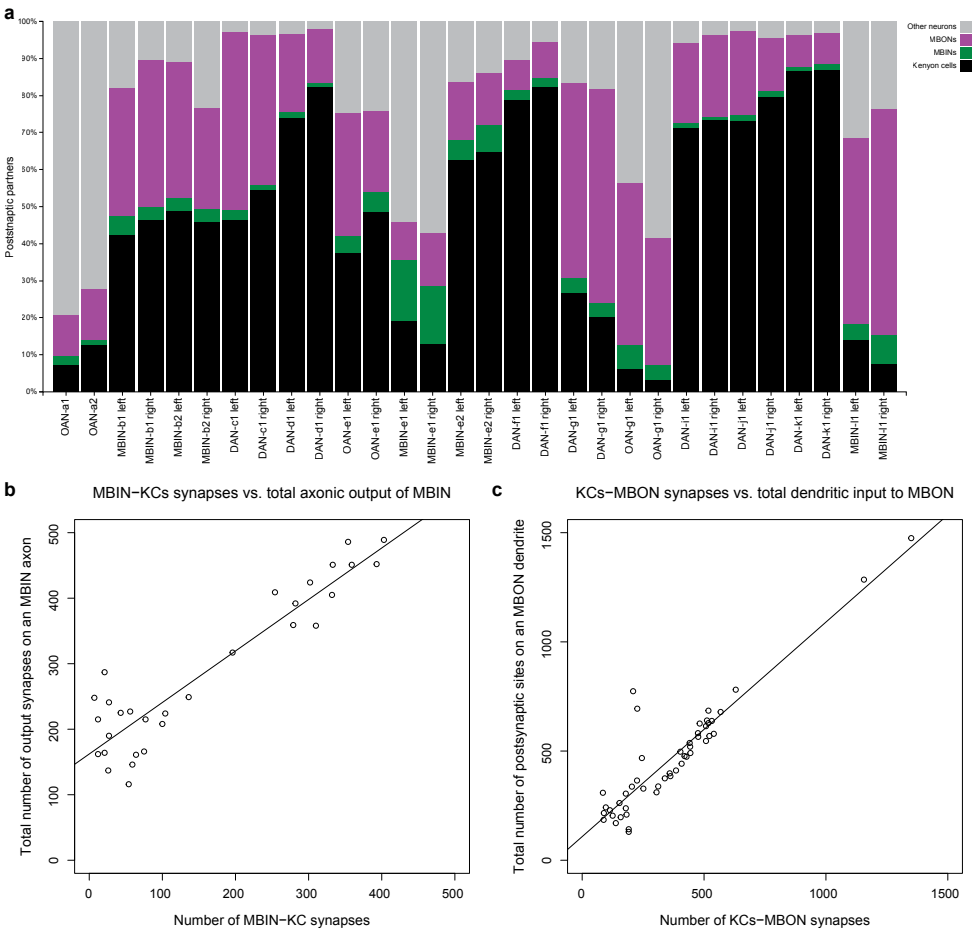

Extended Data Figure 6: Fractions of postsynaptic inputs by cell type.
a Fractions of synaptic output from MBINs onto KCs, other MBINs, MBONs and other neurons. Some MBINs show a high percentage of connections to MB neurons while others connect with less then 50% of their synapses to MB neurons.
b Number of MBIN-KC synapses in relation to the number of total synaptic output from MBIN axons showing a positive correlation between presynaptic sites on the MBIN axon and synapses dedicated to KC population.
c Number of KC-MBON synapses in relation to the number of total synaptic input to MBON dendrites showing a positive correlation between postsynaptic sites on the MBON dendrite and fraction of input from KCs.

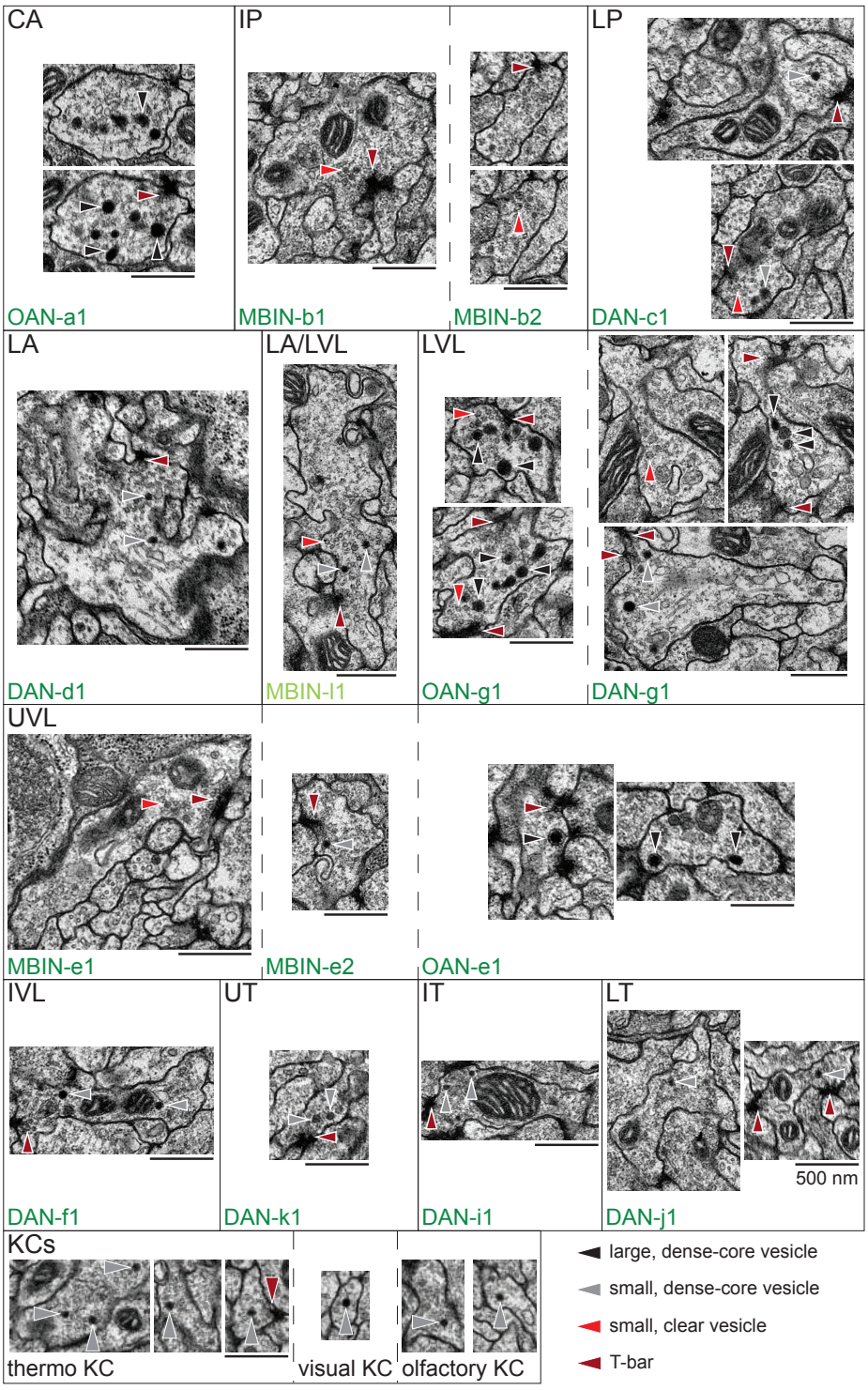

Extended Data Figure 7: MBIN presynaptic vesicle types. Examples of electron micrographs of MBIN presynaptic sites and vesicles. We found three types of vesicles: large dense-core, small dense-core, and small clear vesicles. Octopaminergic and dopaminergic neurons contain small clear vesicles in addition to other vesicle types. While OANs have all the same type of large dense-core vesicles, DANs show a variety of small dense-core vesicles. We found small dense-core vesicles in 1/3 of KCs. Some of these were single-claw, others were multi-claw, some received olfactory and other non-olfactory PN input. The largest number of dense core vesicles was observed in the two thermosensory KCs. Scale bar 500 nm in all panels.

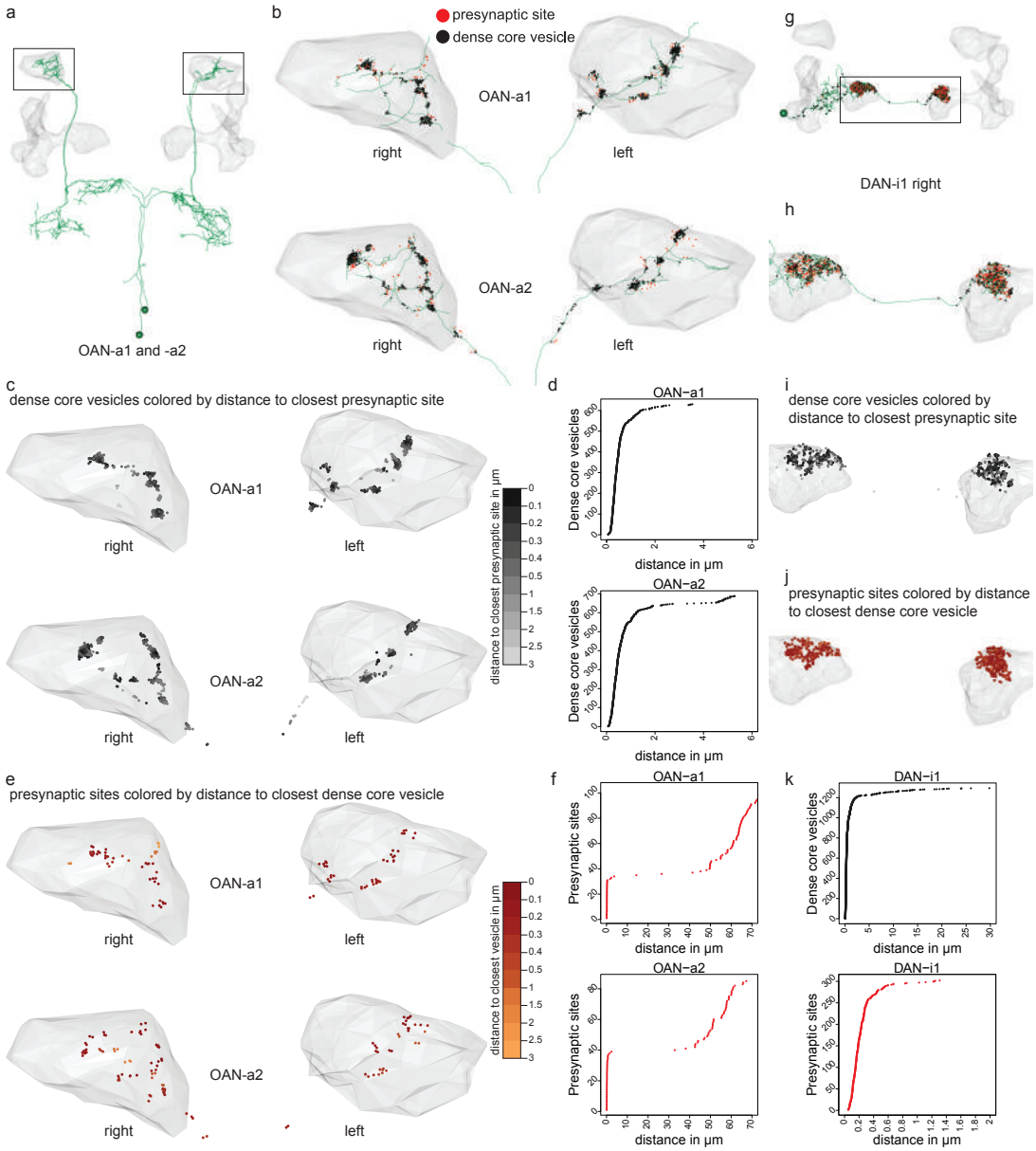

Extended Data Figure 8: Dense core vesicles in OANs and DANs.
a Morphology of OAN-a1 and -a2 innervating the calyx of both MBs.
b Location of presynaptic sites (red) and dense core vesicles (DCV/ black) along the axon of OAN-a1 and -a2.
c DCV color coded by their distance to the closest presynaptic site on the axon of OAN-a1 and -a2.
d Distance (in μm) of DCV to the closest presynaptic site sorted by the value for OAN-a1 and -a2. Most DCV are within 2 μm from a presynaptic site, just a few are further away and appear to be in transit.
e Presynaptic sites color coded by their distance to the closest DCV on the axon of OAN-a1 and -a2.
f Distance (in μm) of presynaptic sites to the closest DCV sorted by the value for OAN-a1 and -a2. Half of the presynaptic sites have a DCV associated within 20 μm. Some presynaptic sites have no close DCV associated and are located in the dendrites of OAN-a1 and a2 (data not shown).
g Morphology of DAN-i1 right innervating the upper toe of the MB medial lobe in both hemispheres with the location of presynaptic sites (red) and dense core vesicles (DCV/ black).
h Zoom in onto the medial lobes from g.
i DCV color coded by their distance to the closest presynaptic site on the axon of DAN-i1 right.
j Presynaptic sites color coded by their distance to the closest DCV on the axon of DAN-i1 right.
k Distance (in μm) of DCV to the closest presynaptic site sorted by the value for DAN-i1 right and left together. Some DCV are further away from presynaptic sites than 10 μm, these DCV are in the dendrites of the DAN (shown in g). And distance (in μm) of presynaptic sites to the closest DCV sorted by the value for DAN-i1 right and left together. Most of the presynaptic sites have a DCV associated within 1 μm.

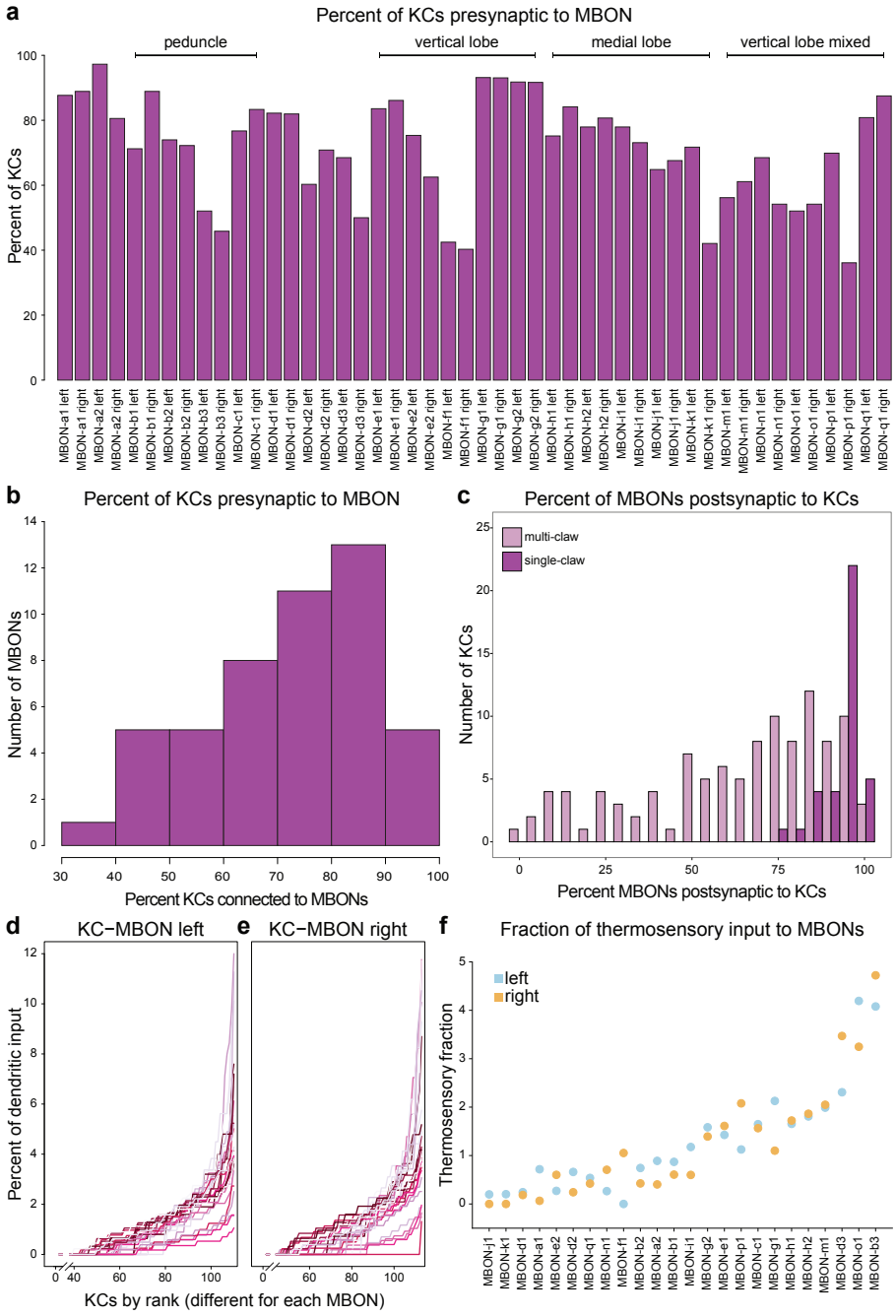

Extended Data Figure 9: KC-to-MBON synaptic connections.

a Percent of mature KCs that are presynaptic to a given MBON.

b Frequency of the percent of KCs presynaptic to MBONs (bin width is 10 percent).

c Frequency of the percentage of MBONs each KC connects to for single-claw and multi-claw KCs separately. All single-claw KCs connect with at least 75% of all MBONs present in their own hemisphere.

d Percent of dendritic MBON inputs from individual KCs in the left brain hemisphere. KCs are ranked by their amount of synapses to the MBON for each MBON separately (each line represents an MBON). Note the rank order of KCs is different for every MBON. Note that a few MBONs receive very strong synaptic input from approximately 20 KCs and less than 3% from the remaining KCs, while most MBONs receive less than 4% of dendritic input from all KCs.

e Same as d, but for the right brain hemisphere.

f Effective strength of thermosensory input to MBONs. The thermosensory fraction is defined as the number of synapses received by an MBON from thermosensory KCs divided by 0.05 times the number of synapses received from all other KCs. The fraction thus represents the relative influence of an input that activates the thermosensory KCs compared to that of a typical stimulus that activates 5% of KCs [Honegger et al., 2011].

Extended Data Figure 10: MBIN-to-KC synaptic connections.
a Percent of mature KCs that are postsynaptic to a given MBIN. On average 68% of KCs in a compartment are postsynaptic to at least one MBIN of that compartment.
b Frequency of the percent of KCs postsynaptic to MBINs (bin width is 10 percent).
c Frequency of the percentage of MBINs presynaptic to each KC for single-claw and multi-claw KCs separately. All single-claw KCs receive synaptic input from at least 50% of all MBINs present in their own hemisphere.
d Percent of axonic outputs from MBINs connecting to individual KCs in the left brain hemisphere. KCs are ranked by their amount of synapses they receive from an MBIN for each MBIN separately (each line represents an MBIN). Note the rank order of KCs is different for every MBIN. Note that a few MBINs connect very strongly to approximately 10 KCs and less than 2% to the remaining KCs, while most MBINs dedicate less than 2% of their axonic output to all KCs.
e Same as d, but for the right brain hemisphere.

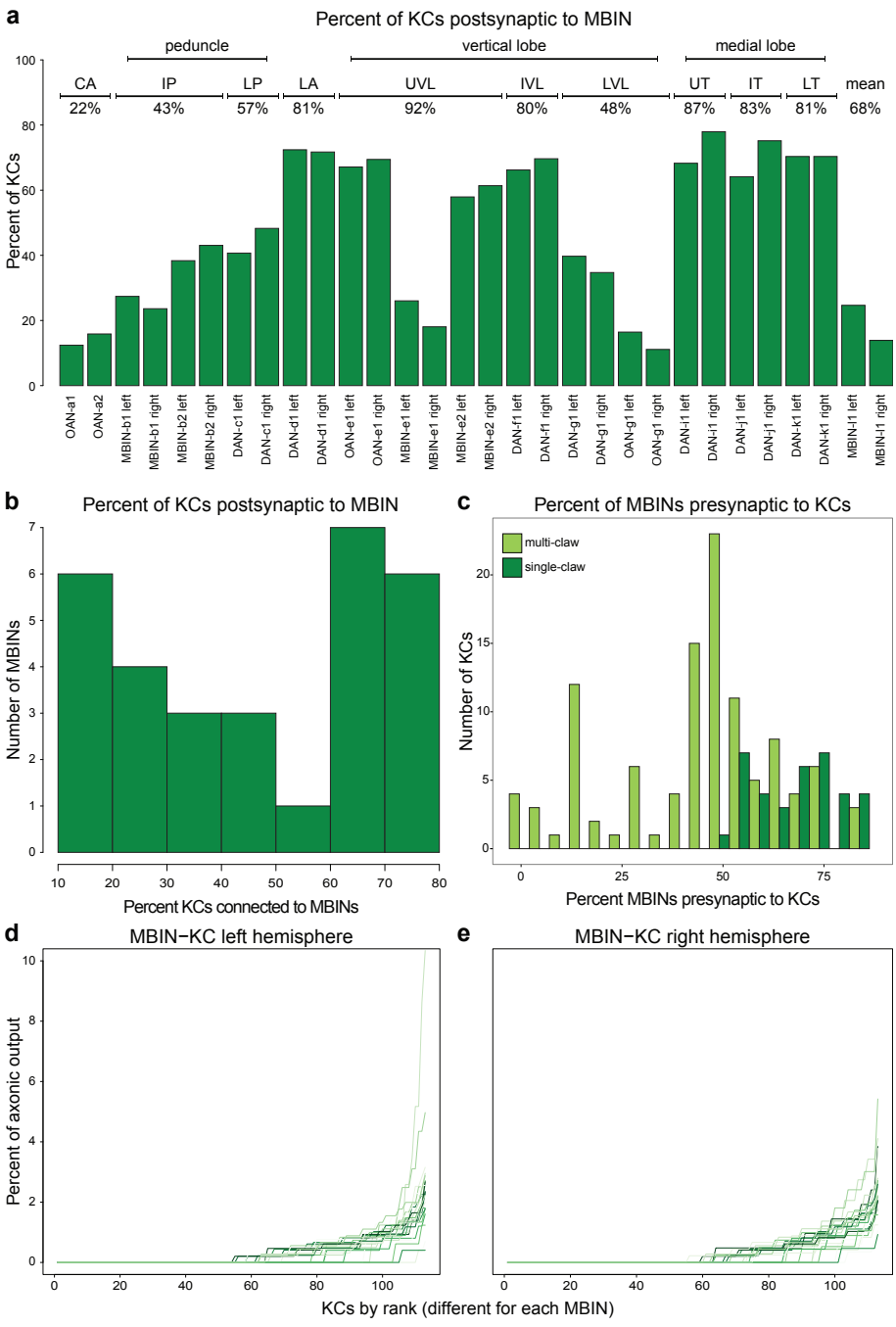

Supplemental Tables:

Supplemental Table 1: Connectivity matrix of the entire MB network.
Number of synapses for each edge in the MB network. Neurons in rows are presynaptic to neurons in columns. PN-PN connections are almost all dendro-dendritic and occur within the antennal lobe. (File found on DVD).

a

MBONs	MBON-a1 left	MBON-a1 right	MBON-a2 left	MBON-a2 right	MBON-b1 left	MBON-b1 right	MBON-b2 left	MBON-b2 right	MBON-b3 left	MBON-b3 right	MBON-c1 left	MBON-c1 right	MBON-d1 left	MBON-d1 right	MBON-d2 left	MBON-d2 right
KCs [#223]	305	319	446	354	360	408	363	385	184	179	1156	1350	420	444	125	251
MBONs [#48]	13	34	99	95	6	3	3	5	26	23	47	38	69	70	25	23
MBINs [#30]	6	16	26	24	35	32	23	24	28	47	105	105	68	83	23	30
others [#585]	30	44	32	22	31	15	12	17	21	35	141	109	9	17	41	37
total input	354	413	603	495	432	458	401	431	259	284	1449	1602	566	614	214	341

MBONs	MBON-d3 left	MBON-d3 right	MBON-e1 left	MBON-e1 right	MBON-e2 left	MBON-e2 right	MBON-f1 left	MBON-f1 right	MBON-g1 left	MBON-g1 right	MBON-g2 left	MBON-g2 right	MBON-h1 left	MBON-h1 right	MBON-h2 left	MBON-h2 right
KCs [#223]	204	115	631	523	158	139	89	100	520	441	477	476	428	527	544	509
MBONs [#48]	17	16	30	40	57	50	60	58	20	21	27	31	28	24	28	12
MBINs [#30]	10	7	103	76	14	13	27	28	121	102	100	110	4	2	4	5
others [#585]	173	143	95	97	66	80	91	96	34	14	30	14	17	17	13	20
total input	404	281	859	736	295	282	267	282	695	578	634	631	477	570	589	546

MBONs	MBON-i1 left	MBON-i1 right	MBON-j1 left	MBON-j1 right	MBON-k1 left	MBON-k1 right	MBON-m1 left	MBON-m1 right	MBON-n1 left	MBON-n1 right	MBON-o1 left	MBON-o1 right	MBON-p1 left	MBON-p1 right	MBON-q1 left	MBON-q1 right
KCs [#223]	519	482	509	417	568	532	210	226	153	88	226	179	245	85	192	194
MBONs [#48]	40	41	54	40	61	37	105	94	55	51	11	5	15	9	18	7
MBINs [#30]	106	79	81	85	26	41	21	28	15	18	19	16	22	11	19	20
others [#585]	25	25	53	52	30	35	544	437	95	69	157	161	239	299	49	43
total input	690	627	697	594	685	645	880	785	318	226	413	361	521	404	278	264

b

MBINs	OAN-a1	OAN-a2	MBIN-b1 left	MBIN-b1 right	MBIN-b2 left	MBIN-b2 right	DAN-c1 left	DAN-c1 right	DAN-d1 left	DAN-d1 right	OAN-e1 left	OAN-e1 right	MBIN-e1 left	MBIN-e1 right	MBIN-e2 left	MBIN-e2 right
KCs [#223]	22	31	61	54	79	75	104	136	333	403	77	100	26	21	196	254
MBINs [# 30]	7	3	7	4	6	6	6	3	7	5	9	11	22	25	17	32
MBONs [#48]	32	34	48	46	57	44	108	101	96	71	68	48	14	23	50	57
others [#810]	224	170	30	10	24	36	6	8	15	10	61	49	75	95	54	66
total output	285	238	146	114	166	161	224	248	451	489	215	208	137	164	317	409

MBINs	DAN-f1 left	DAN-f1 right	DAN-g1 left	DAN-g1 right	OAN-g1 left	OAN-g1 right	DAN-i1 left	DAN-i1 right	DAN-j1 left	DAN-j1 right	DAN-k1 left	DAN-k1 right	MBIN-l1 left	MBIN-l1 right
KCs [#223]	281	333	59	44	13	8	302	356	286	359	311	395	27	12
MBINs [# 30]	9	10	10	9	13	10	5	3	5	6	3	7	8	12
MBONs [#48]	30	39	117	127	93	84	94	108	90	68	31	38	95	97
others [#810]	39	23	41	45	96	146	23	19	11	18	13	12	60	41
total output	359	405	227	225	215	248	424	486	392	451	358	452	190	162

Supplemental Table 2: Presynaptic partners of MBONs and postsynaptic partners of MBINs.
a Number of input synapses from different types of neurons to MBONs.
b Number of output synapses from MBINs to different types of neurons. Square brackets indicate the number of neurons in that group, e.g. "KCs [#223]" means there are 223 neurons of the KC type contributing to the amount of synapses in the corresponding table cells.

MB tile	Cell	Transmitter this study	Transmitter published	Synonym cell name	Reference	Gal4 Lines
Calyx	OAN-a1	n.a.	OA/TA	sVUMmx1	Selcho et al. 2014	
	OAN-a2	n.a.	OA/TA	sVUMmd1	Selcho et al. 2014	
	MBON-a1	ChAT	ChAT	Odd neuron	Slater et al. 2015	R71E06
	MBON-a2	ChAT	ChAT	Odd neuron	Slater et al. 2015	R71E06
intermediate peduncle	MBIN-b1	n.a.				
	MBIN-b2	n.a.				
	MBON-b1	GABA		BL	Pauls et al. 2010	R21D02
	MBON-b2	GABA		BL	Pauls et al. 2010	R21D02
	MBON-b3	n.a.				
lower peduncle	DAN-c1	DA	likely DA	DL1-5	Selcho et al. 2009	R53C05
	MBON-c1	ChAT				R20F01
lateral appendix	DAN-d1	DA	likely DA	DL 1-4	Selcho et al. 2009	MB143B
	MBON-d1	GABA		la type	Pauls et al. 2010	R12C03
	MBON-d2	n.a.				
	MBON-d3	n.a.				
upper vertical lobe	OAN-e1	OA/TA				R75F01
	MBIN-e1	not DA / not OA				R53C05-LexA
	MBIN-e2	not DA / not OA	likely DA	vl 3 type, DL1-1	Pauls et al. 2010, Selcho et al. 2009	BJD114E05
	MBON-e1	ChAT				R74B11
	MBON-e2	GLUT				R53A10
intermediate vertical lobe	DAN-f1	DA	likely DA	vl 2 type, DL 1-2	Pauls et al. 2010, Selcho et al. 2009	MB145B
	MBON-f1	n.a.				
lower vertical lobe	DAN-g1	DA	likely DA	DL 1-3	Selcho et al. 2009	R27G01
	OAN-g1	n.a.	OA/TA	sVPMmx	Selcho et al. 2014	
	MBON-g1	GABA		vl1 type	Pauls et al. 2010	R21D06
	MBON-g2	GABA		vl1 type	Pauls et al. 2010	R21D06
shaft	MBON-h1	GABA/GLUT		APBL	Pauls et al. 2010	R52E12
	MBON-h2	GABA/GLUT		APBL	Pauls et al. 2010	R52E12
upper toe	DAN-i1	DA	DA	pPAM3	Rohwedder et al. 2016	BJD105C04
	MBON-i1	GLUT				R14C08
intermediate toe	DAN-j1	DA	DA	pPAM4	Rohwedder et al. 2016	BJD105C04
	MBON-j1	GLUT				R18D09
lower toe	DAN-k1	DA	DA	ma type, pPAM2	Pauls et al. 2010, Rohwedder et al. 2016	BJD105C04
	MBON-k1	GLUT				R27G01
multiple tiles innervated	MBIN-l1	not DA / not OA				R49C08
	MBON-m1	GABA				R52H01
	MBON-n1	n.a.				
	MBON-o1	n.a.				
	MBON-p1	n.a.				
	MBON-q1	n.a.				
	APL	GABA	GABA	Larval APL	Masuda-Nakagawa et al. 2014	R55D08

Supplemental Table 3: MBINs and MBONs are listed.
The neurotransmitter for each cell is shown for this study and formerly published studies. Known synonyms of cells and their reference publication are indicated.

Supplemental Table 4: MBIN-to-KC and KC-to-MBON connectivity matrices.
a Connectivity matrix from MBINs to KCs. Color-coded by the number of postsynaptic sites on the KC axonic arbor. KCs are ranked by their number of claws.
b Connectivity matrix from KCs to MBONs. Color-coded by the number of postsynaptic sites on the MBON dendritic arbor. KC ranking is the same as in a.

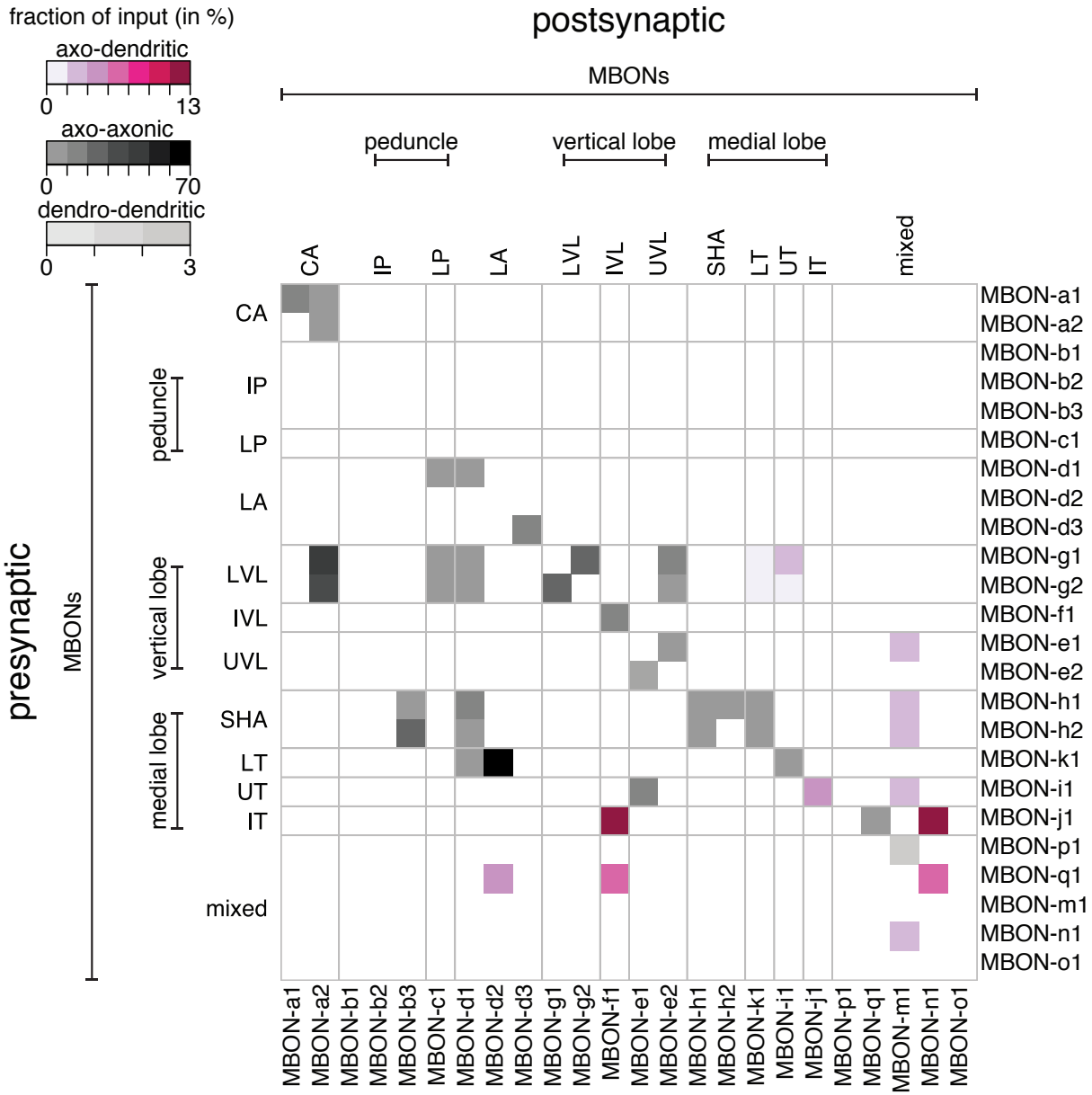

Supplemental Table 5: MBON-MBON connectivity matrix.
Connectivity matrix of MBON interactions color-coded by the type and strength of connections. Axo-dendritic connections are displayed in magenta, axo-axonic in dark grey and dendro-dendritic in light grey. The matrix contains ipsi- and contralateral connections of MBONs. Homologous neurons from the left and right brain hemispheres are fused. Connection strength is shown as percent of inputs received by the postsynaptic neuron from a particular presynaptic neuron.

Common function
The MB is a cerebellum-like structure [Farris, 2011] and essential for olfactory learning and memory in adult [Kaun et al., 2007; Heisenberg et al., 1985; Gerber et al., 2004; Margulies et al., 2005; Davis, 2011] and larva [Honjo and Furukubo-Tokunaga, 2009; Pauls et al., 2010; Michels et al., 2011; Diegelmann et al., 2013; Aceves-Piña and Quinn, 1979] as well as in the honey bee [Menzel, 2001, 2014], comparison of adult and larval MB reviewed in [Gerber and Stocker, 2007; Stocker, 2009].
Common basic neuronal organization:
The MB KCs are derived from the same 4 neuroblast lineages in adult and larva [Ito and Hotta, 1992; Truman and Bate, 1988; Kunz et al., 2012; Thomas et al., 1984; Lee et al., 1999]. KCs have long parallel axons in a bundle forming the peduncle and later bifurcate into the vertical and medial (horizontal) lobes [Armstrong et al., 1998; Kurusu et al., 2002].
The MB is a convergence point for PNs, MBINs, KCs and MBONs in adult and larva, reviewed in [Heisenberg, 2003; Gerber et al., 2009; Strausfeld et al., 2009; Davis, 2011; Owald and Waddell, 2015].
The MB is subdivided in a relatively small number of compartments in adult [Tanaka et al., 2008; Aso et al., 2014a] and larva ([Pauls et al., 2010] and this study).
MB compartments are defined by overlapping innervation of individual MBINs and MBONs in adult [Tanaka et al., 2008; Aso et al., 2014a] and larva ([Pauls et al., 2010] and this study).
A single GABAergic neuron (the APL neuron) innervates most MB compartments in adult [Liu and Davis, 2009] and larva ([Masuda-Nakagawa et al., 2014] and this study).
Common calyx organization:
In calyx, many KCs get olfactory input in adult [Turner et al., 2008; Honegger et al., 2011; Caron et al., 2013] and larva [Python and Stocker, 2002; Ramaekers et al., 2005; Masuda-Nakagawa et al., 2005, 2009; Das et al., 2013; Berck et al., 2016] and some KCs get input from other modalities (including temperature and light) in adult [Bang et al., 2011; Kirkhart and Scott, 2015; Vogt et al., 2016] and larva (revealed by the connectome in this study). KC dendrites wrap around the PN axon boutons by forming ”claw”-like structures [Yasuyama et al., 2002; Leiss et al., 2009].
Multi-claw KCs randomly sample PN inputs in adult [Murthy et al., 2008; Caron et al., 2013] and larva ([Masuda-Nakagawa et al., 2005] and this study).
Calyx receives input of two octopaminergic neurons in adult [Schwaerzel et al., 2003; Busch et al., 2009] and larva ([Selcho et al., 2009, 2014] and this study).
Common global compartment organization:
MBINs are either dopaminergic or octopaminergic in adult [Schwaerzel et al., 2003; Mao and Davis, 2009; Waddell, 2013; Aso et al., 2014a] and larva ([Selcho et al., 2009, 2014] and this study) and have been shown to convey reinforcement signals in bees and locust [Hammer, 1993; Vergoz et al., 2007; Cassenaer and Laurent, 2007] as well as in the adult fly [Aso et al., 2010, 2012; Liu et al., 2012; Burke et al., 2012; Plaçais et al., 2012; Yamagata et al., 2015]. This requires the expression of specific amine receptors in insects [Kim et al., 2007; Qin et al., 2012; Selcho et al., 2009; McQuillan et al., 2012].
There are 21 MBON types in adult [Aso et al., 2014a; Owald and Waddell, 2015] and larva (this study).
MBONs are mainly glutamatergic, cholinergic and GABAergic in adult [Aso et al., 2014a] and larva (shown in this study). Co-activation of KCs and MBINs has been shown to modulate the KC-MBON synapses in flies [Séjourné et al., 2011; Plaçais et al., 2013; Pai et al., 2013] and in bees [Menzel and Manz, 2005].
Common synaptic compartment organization:
The EM connectome in the larva revealed a compartment circuit motif:
KCs not only receive input from DANs but also synapse back onto DANs
DANs synapse onto KCs but also directly onto MBONs
KCs synapse onto MBONs (previously shown in adult *Drosophila* [Ito et al., 1998] and bees [Mauelshagen, 1993]).
Ongoing EM reconstruction of one adult compartment (α-3) confirms the same canonical circuit motif exists in the adult (Gerry Rubin, personal communication).
KC-KC connections
The EM connectome in the larva revealed a high degree of KC-KC interconnectivity: an individual KC receives 59% of its total synaptic input from other KCs. Individual EM sections from peduncle of bees and crickets suggest KC-KC connections [Schürmann, 1971, 1974] and a light-microscopy study in *Drosophila* suggests presynaptic KC sites in calyx [Christiansen et al., 2011]. While total fraction of synaptic input onto individual KCs from other KCs cannot be evaluated in the adult in the absence of a comprehensive EM volume spanning all MB related neurons and a comprehensive reconstruction of the MB, ongoing EM reconstruction of an entire adult a-3 adult compartment confirms the same degree of compartmental axo-axonic KC-KC connectivity (Gerry Rubin, personal communication): an individual KC makes 48% of its total synaptic output in a compartment onto other KCs, in both larva and adult.
Common feedforward and feedback organization:
A light microscopy study in the adult suggests cross-compartment MBON-MBON interactions [Aso et al., 2014a], and a recent functional study shows MBON-MVP2 inhibits MBON-M4/M6 [Perisse et al., 2016]. The EM connectome and antibody labelling in the larva revealed extensive MBON-MBON synaptic connections between different compartments that can implement lateral inhibition.
Light microscopy and functional studies in the adult reveal MBON-DAN feedback connections in some compartments [Aso et al., 2014a; Ichinose et al., 2015]. The EM connectome in the larva revealed MBON-DAN feedback connections in some compartments.

Supplemental Table 6: Common features of larval and adult MB.

1. The number of KCs is larger (2000) in the adult enabling an even greater dimensionality expansion [Ito and Hotta, 1992; Technau and Heisenberg, 1982].

2. There are multiple parallel lobe systems in the adult composed of different KC types [Yang et al., 1995; Tanaka et al., 2008; Perisse et al., 2013; Aso et al., 2014a].

3. Larvae present single-claw KCs ([Ramaekers et al., 2005], and this study), so far not found in the adult.

4. We found no DPM neuron in the larva – a key neuron of the adult circuit [Waddell et al., 2000; Keene et al., 2004, 2006; Yu et al., 2005; Krashes and Waddell, 2008; Haynes et al., 2015].

5. Both larval and adult MB are clearly structured in vertical and horizontal (medial) lobe systems, but the larva has one horizontal (medial) and one vertical lobe, and the adult has three horizontal and two vertical lobes [Lee et al., 1999].

6. In the adult a few compartments are innervated by a much larger number of DANs from the PAM cluster than is the case for any of the larval compartments [Aso et al., 2014a].

Supplemental Table 7: Differences between larval and adult MB.

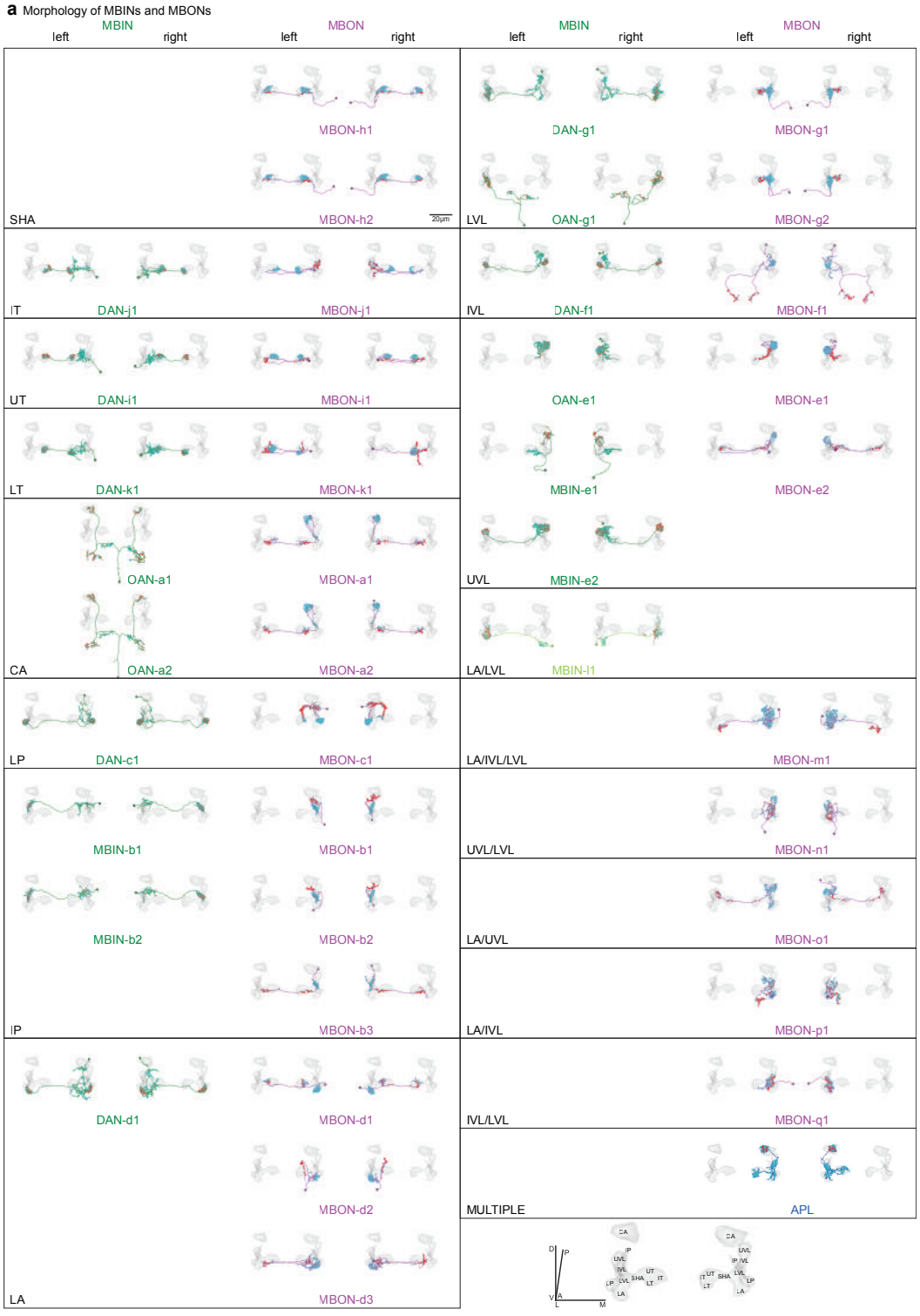
a Morphology of MBINs and MBONs
MBIN
left
right
MBON
left
right
MBIN
left
right
MBON
left
right
MBON-h1
SHA
MBON-h2
20µm
DAN-g1
MBON-g1
LVL
OAN-g1
MBON-g2
IT
DAN-j1
MBON-j1
IVL
DAN-f1
MBON-f1
UT
DAN-i1
MBON-i1
OAN-e1
MBON-e1
LT
DAN-k1
MBON-k1
MBIN-e1
MBON-e2
OAN-a1
MBON-a1
UVL
MBIN-e2
CA
OAN-a2
MBON-a2
LA/LVL
MBIN-l1
LP
DAN-c1
MBON-c1
LA/IVL/LVL
MBON-m1
MBIN-b1
MBON-b1
UVL/LVL
MBON-n1
MBIN-b2
MBON-b2
LA/UVL
MBON-o1
IP
MBON-b3
LA/IVL
MBON-p1
DAN-d1
MBON-d1
IVL/LVL
MBON-q1
MBON-d2
MULTIPLE
APL
LA
MBON-d3

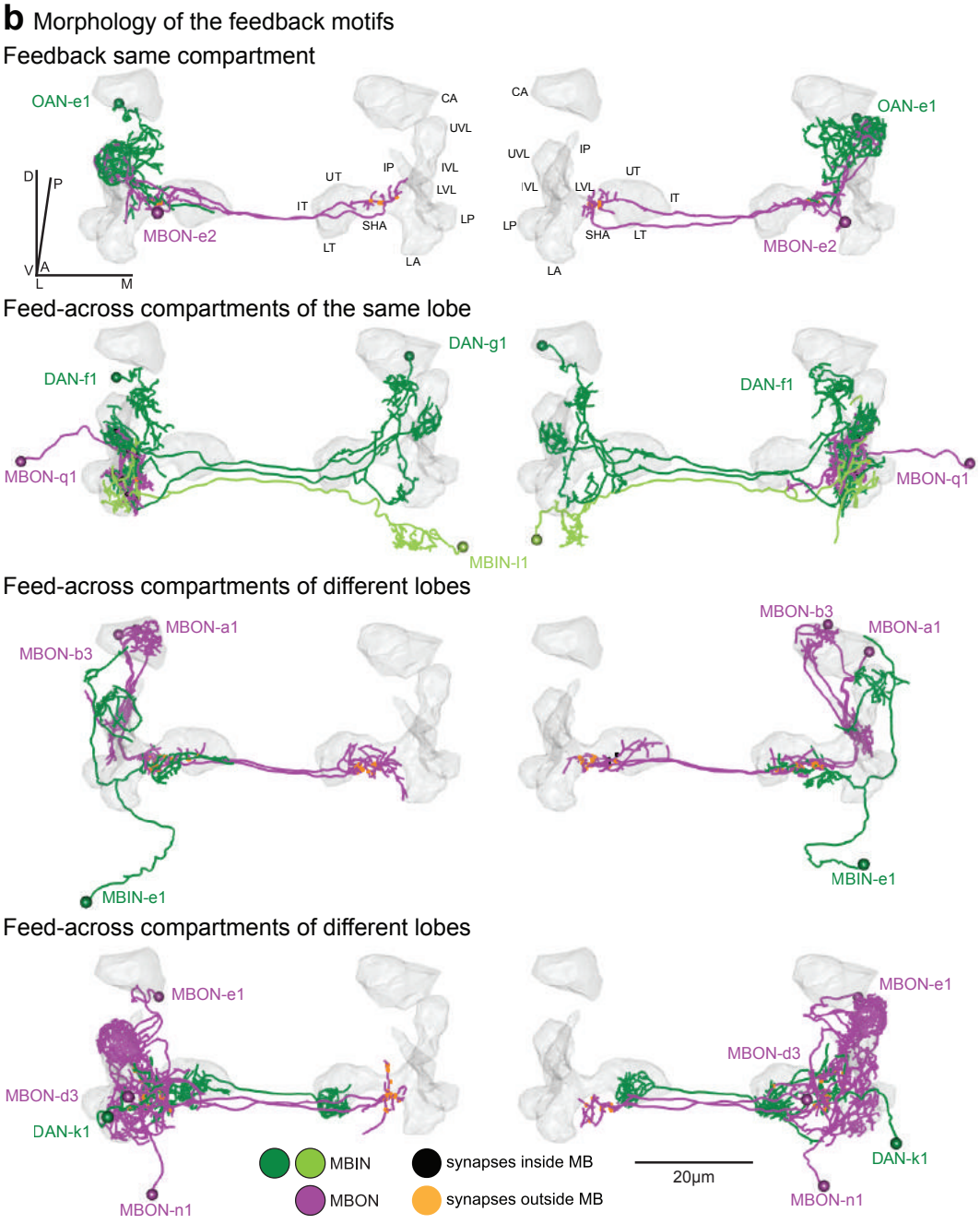

Atlas Figure 1: Morphology of MBINs and MBONs and of their connections in the feedback motifs.
a Neuronal morphology of MBINs and MBONs per MB compartment in anterior view (MBINs in green and MBONs in magenta). Left and right brain hemisphere neurons are displayed separately. The transparent mesh represents the volume of the KC arbors; the legend of compartments is at the bottom right.
b Neuronal morphology of MBINs and MBONs participating in feedback and feed-across motifs (*green*, MBINs; *magenta* MBONs). Neurons connecting to the left and right MB are displayed separately in anterior view. Locations of the feedback and feed-across connections as shown in Figure 5 are shown depending on their location (inside the MB neuropil, black; outside the MB, orange). Feedback and feed-across connections from compartments of different lobes are located outside of the MB neuropil. Feed-across connections of compartments of the same lobe are located inside the MB neuropil.

a Antibody light microscopy analysis for MBINs

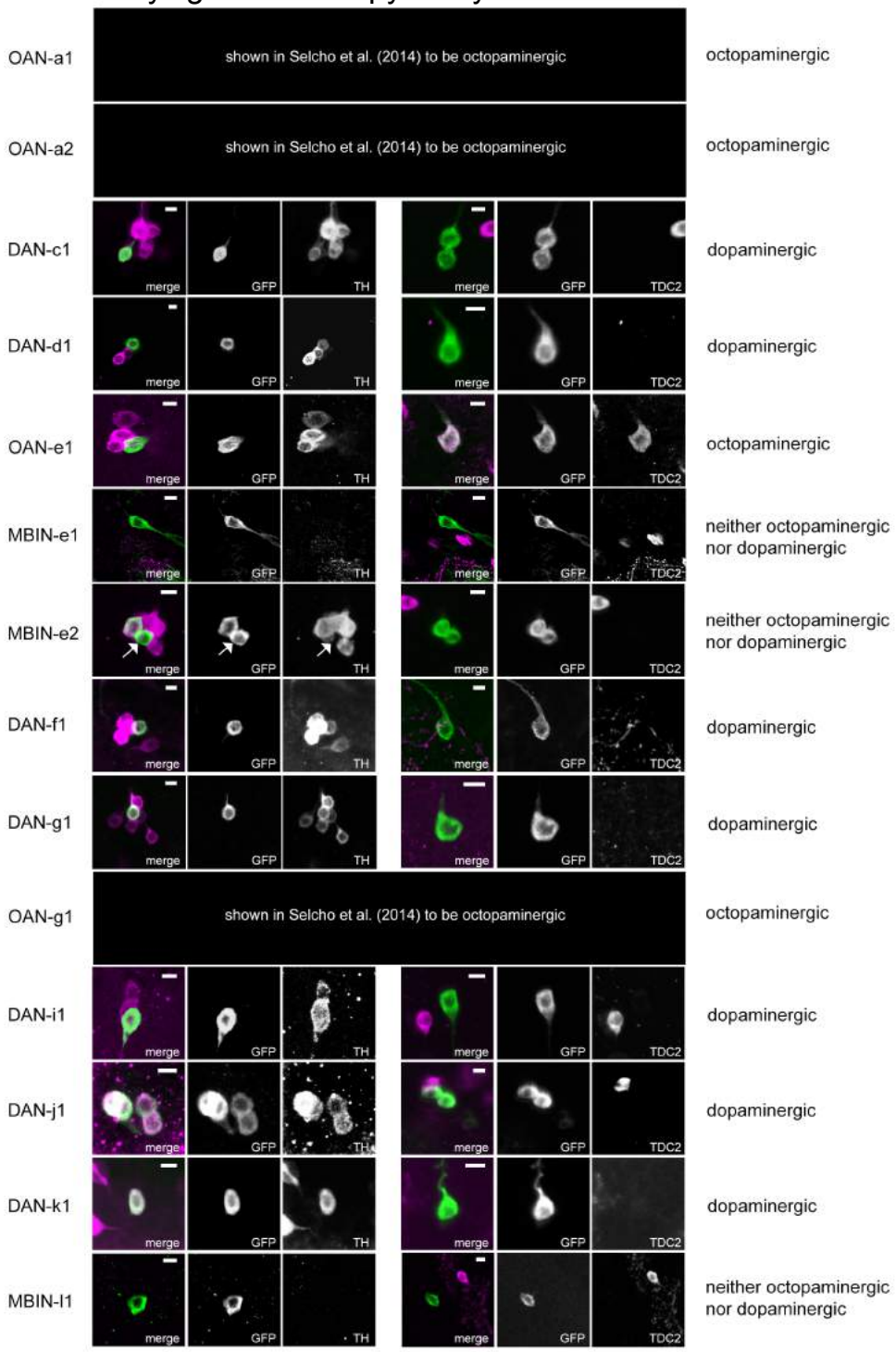

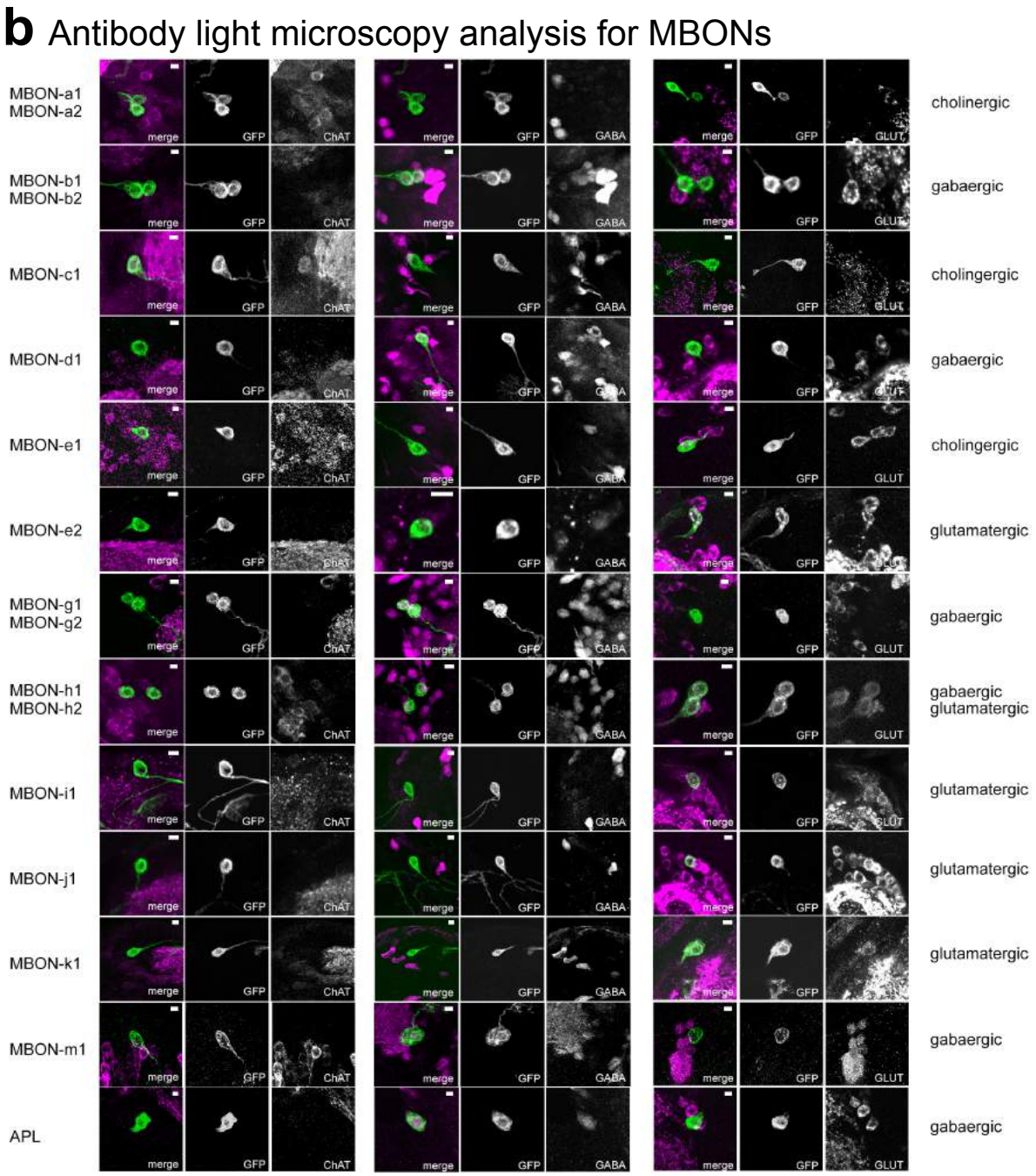

Atlas Figure 2: Antibody light microscopy analysis for mushroom body input and output neurons. *(See next page).*

Atlas Figure 2: *Continues from prior page.*
a Neurotransmitter properties of mushroom body input neuron somata as revealed by selected GAL4 lines. Each row shows from left to right: the name of the individual neuron, a combined anti-GFP (green) and anti-TH (TH: tyrosine hydroxylase; magenta) staining, both antibody stainings separately in black and white, the combined anti-GFP (green) and anti-TDC (TDC: tyrosine decarboxylase) staining, both antibody stainings separately in black and white. Whether a cell is dopaminergic or octopaminergic is listed at the end of each row. For OAN-e1 (OAN: octopaminergic input neuron) we found an overlap of GFP expression and anti-TDC in its soma. In addition, Selcho and coworkers (2014) anatomically described three additional octopaminergic neurons that we cite here and include them in our analysis, renaming them. For DAN-c1, d1, f1, g1, i1, j1 and k1 (DAN: dopaminergic input neuron) we found overlap of GFP expression and anti-TH in their somata. No overlap was detected for MBIN-e1, e2 and l1. Scale bars: 5μm.
b Neurotransmitter properties of mushroom body output neuron somata and the anterior paired lateral (APL) neuron soma as revealed by selected GAL4 lines. Each row shows from left to right: the name of the individual neuron, combined anti-GFP (green) and anti-ChAT (ChAT: choline acetyltransferase; magenta) stainings, both antibody stainings separately in black and white, the combined anti-GFP (green) and anti-GABA (GABA: gamma aminobutyric acid) staining, both antibody stainings separately in black and white, the combined anti-GFP (green) and anti-GLUT (GLUT: vesicular glutamate transporter) staining, both antibody stainings separately in black and white. Whether a cell is cholinergic, GABAergic or glutamatergic is listed at the end of each row. In four cases MBONs show up as pairs of the same type. In all cases the antibody profile of both cells is identical. Thus, we name them individually although we cannot distinguish them; indistinguishable cells have identical connectivity within the MB. For MBON-a1, a2, c1 and e1 (MBON: mushroom body output neuron) we found an overlap of GFP expression and anti-ChAT in their somata. For MBON-b1, b2, d1, g1, g2, h1, h2, m1 and APL we found overlap of GFP expression and anti-GABA in their somata. For MBON-e2, h1, h2, i1, j1 and k1 we found overlap of GFP expression and anti-GLUT in their somata. Scale bars: 5μm.

3.9 References

Aceves-Piña, E. O. and Quinn, W. G. (1979). Learning in normal and mutant *Drosophila* larvae. *Science*, 206(4414):93–96.

Armstrong, J. D., de Belle, J. S., Wang, Z., and Kaiser, K. (1998). Metamorphosis of the mushroom bodies; large-scale rearrangements of the neural substrates for associative learning and memory in *Drosophila*. *Learning & Memory*, 5(1):102–114.

Aso, Y., Hattori, D., Yu, Y., Johnston, R. M., Iyer, N. A., Ngo, T.-T., Dionne, H., Abbott, L., Axel, R., Tanimoto, H., et al. (2014a). The neuronal architecture of the mushroom body provides a logic for associative learning. *Elife*, 3:e04577.

Aso, Y., Herb, A., Ogueta, M., Siwanowicz, I., Templier, T., Friedrich, A. B., Ito, K., Scholz, H., and Tanimoto, H. (2012). Three dopamine pathways induce aversive odor memories with different stability. *PLoS Genet*, 8(7):e1002768.

Aso, Y. and Rubin, G. D. (2016). Parallel dopaminergic neurons write and update memories with cell-type-specific rules. *eLife*.

Aso, Y., Sitaraman, D., Ichinose, T., Kaun, K. R., Vogt, K., Belliart-Guérin, G., Plaçais, P.-Y., Robie, A. A., Yamagata, N., Schnaitmann, C., et al. (2014b). Mushroom body output neurons encode valence and guide memory-based action selection in *Drosophila*. *Elife*, 3:e04580.

Aso, Y., Siwanowicz, I., Bräcker, L., Ito, K., Kitamoto, T., and Tanimoto, H. (2010). Specific dopaminergic neurons for the formation of labile aversive memory. *Current Biology*, 20(16):1445–1451.

Babadi, B. and Sompolinsky, H. (2014). Sparseness and expansion in sensory representations. *Neuron*, 83(5):1213–1226.

Bang, S., Hyun, S., Hong, S.-T., Kang, J., Jeong, K., Park, J.-J., Choe, J., and Chung, J. (2011). Dopamine signalling in mushroom bodies regulates temperature-preference behaviour in *Drosophila*. *PLoS Genet*, 7(3):e1001346.

Barnstedt, O., Owald, D., Felsenberg, J., Brain, R., Moszynski, J.-P., Talbot, C. B., Perrat, P. N., and Waddell, S. (2016). Memory-relevant mushroom body output synapses are cholinergic. *Neuron*, 89(6):1237–1247.

Bate, M., Goodman, C., and Spitzer, N. (1981). Embryonic development of identified neurons: Segment-specific differences in the H cell homologues. *J Neurosci*, 1(1):103–06.

Berck, M. E., Khandelwal, A., Claus, L., Nuñez, L. H., Si, G., Tabone, C. J., Li, F., Truman, J. W., Fetter, R. D., Louis, M., et al. (2016). The wiring diagram of a glomerular olfactory system. *eLife*, page e14859.

Blondel, V. D., Guillaume, J.-L., Lambiotte, R., and Lefebvre, E. (2008). Fast unfolding of communities in large networks. *Journal of statistical mechanics: theory and experiment*, 2008(10):P10008.

Bouzaiane, E., Trannoy, S., Scheunemann, L., Plaçais, P.-Y., and Preat, T. (2015). Two independent mushroom body output circuits retrieve the six discrete components of *Drosophila* aversive memory. *Cell reports*, 11(8):1280–1292.

Burke, C. J., Huetteroth, W., Owald, D., Perisse, E., Krashes, M. J., Das, G., Gohl, D., Silies, M., Certel, S., and Waddell, S. (2012). Layered reward signalling through octopamine and dopamine in *Drosophila*. *Nature*, 492(7429):433–437.

Busch, S., Selcho, M., Ito, K., and Tanimoto, H. (2009). A map of octopaminergic neurons in the *Drosophila* brain. *Journal of Comparative Neurology*, 513(6):643–667.

Cardona, A., Schindelin, S. S. J., Arganda Carreras, I., Preibisch, S., Longair, M., Tomancak, P., Hartenstein, V., and Douglas, R. (2012). TrakEM2 Software for Neural Circuit Reconstruction. *PLoS ONE*, 7(6):e38011.

Caron, S. J., Ruta, V., Abbott, L., and Axel, R. (2013). Random convergence of olfactory inputs in the *Drosophila* mushroom body. *Nature*, 497(7447):113–117.

Cassenaer, S. and Laurent, G. (2007). Hebbian STDP in mushroom bodies facilitates the synchronous flow of olfactory information in locusts. *Nature*, 448(7154):709–713.

Cassenaer, S. and Laurent, G. (2012). Conditional modulation of spike-timing-dependent plasticity for olfactory learning. *Nature*, 482(7383):47–52.

Christiansen, F., Zube, C., Andlauer, T. F., Wichmann, C., Fouquet, W., Owald, D., Mertel, S., Leiss, F., Tavosanis, G., Farca Luna, A. J., Fiala, A., and Sigrist, S. J. (2011). Presynapses in Kenyon cell dendrites in the mushroom body calyx of *Drosophila*. *The Journal of Neuroscience*, 31(26):9696–9707.

Cohn, R., Morantte, I., and Ruta, V. (2015). Coordinated and compartmentalized neuromodulation shapes sensory processing in *Drosophila*. *Cell*, 163(7):1742–1755.

Costa, M., Manton, J. D., Ostrovsky, A. D., Prohaska, S., and Jefferis, G. S. (2016). NBLAST: Rapid, sensitive comparison of neuronal structure and construction of neuron family databases. *Neuron*, 91(2):293–311.

Daniels, R. W., Collins, C. A., Gelfand, M. V., Dant, J., Brooks, E. S., Krantz, D. E., and DiAntonio, A. (2004). Increased expression of the *Drosophila* vesicular glutamate transporter leads to excess glutamate release and a compensatory decrease in quantal content. *The Journal of Neuroscience*, 24(46):10466–10474.

Das, A., Gupta, T., Davla, S., Prieto-Godino, L. L., Diegelmann, S., Reddy, O. V., Raghavan, K. V., Reichert, H., Lovick, J., and Hartenstein, V. (2013). Neuroblast lineage-specific origin of the neurons of the *Drosophila* larval olfactory system. *Developmental biology*, 373(2):322–337.

Das, G., Klappenbach, M., Vrontou, E., Perisse, E., Clark, C. M., Burke, C. J., and Waddell, S. (2014). *Drosophila* learn opposing components of a compound food stimulus. *Current biology*, 24(15):1723–1730.

Davis, R. L. (2011). Traces of *Drosophila* memory. *Neuron*, 70(1):8–19.

Diegelmann, S., Klagges, B., Michels, B., Schleyer, M., and Gerber, B. (2013). Maggot learning and Synapsin function. *Journal of Experimental Biology*, 216(6):939–951.

DrObysheva, D., Ameel, K., Welch, B., Ellison, E., Chaichana, K., Hoang, B., Sharma, S., Neckameyer, W., Srinakevitch, I., Murphy, K. J., et al. (2008). An optimized method for histological detection of dopaminergic neurons in *Drosophila melanogaster*. *Journal of Histochemistry & Cytochemistry*, 56(12):1049–1063.

Farris, S. M. (2011). Are mushroom bodies cerebellum-like structures? *Arthropod structure & development*, 40(4):368–379.

Fushiki, A., Zwart, M. F., Kohsaka, H., Fetter, R. D., Cardona, A., and Nose, A. (2016). A circuit mechanism for the propagation of waves of muscle contraction in *Drosophila*. *eLife*, page 13253.

Galili, D. S., Dylla, K. V., Lüdke, A., Friedrich, A. B., Yamagata, N., Wong, J. Y. H., Ho, C. H., Szyszka, P., and Tanimoto, H. (2014). Converging circuits mediate temperature and shock aversive olfactory conditioning in *Drosophila*. *Current Biology*, 24(15):1712–1722.

Gerber, B. and Stocker, R. F. (2007). The *Drosophila* larva as a model for studying chemosensation and chemosensory learning: a review. *Chemical senses*, 32(1):65–89.

Gerber, B., Stocker, R. F., Tanimura, T., and Thum, A. S. (2009). Smelling, tasting, learning: *Drosophila* as a study case. In *Chemosensory Systems in Mammals, Fishes, and Insects*, pages 187–202. Springer.

Gerber, B., Tanimoto, H., and Heisenberg, M. (2004). An engram found? evaluating the evidence from fruit flies. *Current opinion in neurobiology*, 14(6):737–744.

Goodman, C., Bate, M., and Spitzer, N. (1981). Embryonic development of identified neurons: origin and transformation of the H cell. *J Neurosci*, 1(1):99–102.

Gruntman, E. and Turner, G. C. (2013). Integration of the olfactory code across dendritic claws of single mushroom body neurons. *Nature neuroscience*, 16(12):1821–1829.

Hammer, M. (1993). An identified neuron mediates the unconditioned stimulus in associative olfactory learning in honeybees. *Nature*, 366:59–63.

Haynes, P. R., Christmann, B. L., and Griffith, L. C. (2015). A single pair of neurons links sleep to memory consolidation in *Drosophila melanogaster*. *Elife*, 4:e03868.

Heckscher, E. S., Zarin, A. A., Faumont, S., Clark, M. Q., Manning, L., Fushiki, A., Schneider-Mizell, C. M., Fetter, R. D., Truman, J. W., Zwart, M. F., Landgraf, M., Cardona, A., Lockery, S. R., and Doe, C. Q. (2015). Even-skipped+ interneurons are core components of a sensorimotor circuit that maintains left-right symmetric muscle contraction amplitude. *Neuron*, 88(2):314–329.

Heisenberg, M. (2003). Mushroom body memoir: from maps to models. *Nat Rev Neurosci*, 4:266–75.

Heisenberg, M., Borst, A., Wagner, S., and Byers, D. (1985). *Drosophila* mushroom body mutants are deficient in olfactory learning. *Journal of Neurogenetics*, 2(1):1–30.

Hige, T., Aso, Y., Modi, M. N., Rubin, G. M., and Turner, G. C. (2015). Heterosynaptic plasticity underlies aversive olfactory learning in *Drosophila*. *Neuron*, 88(5):985–998.

Honegger, K. S., Campbell, R. A., and Turner, G. C. (2011). Cellular-resolution population imaging reveals robust sparse coding in the *Drosophila* mushroom body. *The Journal of Neuroscience*, 31(33):11772–11785.

Honjo, K. and Furukubo-Tokunaga, K. (2009). Distinctive neuronal networks and biochemical pathways for appetitive and aversive memory in *Drosophila* larvae. *The Journal of neuroscience*, 29(3):852–862.

Huetteroth, W., Perisse, E., Lin, S., Klappenbach, M., Burke, C., and Waddell, S. (2015). Sweet taste and nutrient value subdivide rewarding dopaminergic neurons in *Drosophila*. *Current Biology*, 25(6):751–758.

Ichinose, T., Aso, Y., Yamagata, N., Abe, A., Rubin, G. M., and Tanimoto, H. (2015). Reward signal in a recurrent circuit drives appetitive long-term memory formation. *eLife*, 4:e10719.

Ito, K. and Hotta, Y. (1992). Proliferation pattern anf postembryonic neuroblasts in the brain of *Drosophila melanogaster*. *Developmental Biology*, 149:134–48.

Ito, K., Suzuki, K., Estes, P., Ramaswami, M., Yamamoto, D., and Strausfeld, N. J. (1998). The organization of extrinsic neurons and their implications in the functional roles of the mushroom bodies in *Drosophila* melanogaster meigen. *Learning & Memory*, 5(1):52–77.

Jovanic, T., Schneider-Mizell, C. M., Shao, M., Masson, J.-B., Denisov, G., Fetter, R. D., Mensh, B. D., Truman, J. W., Cardona, A., and Zlatic, M. (2016). Competitive disinhibition mediates behavioral choice and sequences in *Drosophila*. *Cell*, 167(3):858–870.

Kaun, K. R., Hendel, T., Gerber, B., and Sokolowski, M. B. (2007). Natural variation in *Drosophila* larval reward learning and memory due to a cGMP-dependent protein kinase. *Learning & Memory*, 14(5):342–349.

Keene, A. C., Krashes, M. J., Leung, B., Bernard, J. A., and Waddell, S. (2006). *Drosophila* dorsal paired medial neurons provide a general mechanism for memory consolidation. *Current biology*, 16(15):1524–1530.

Keene, A. C., Stratmann, M., Keller, A., Perrat, P. N., Vosshall, L. B., and Waddell, S. (2004). Diverse odor-conditioned memories require uniquely timed dorsal paired medial neuron output. *Neuron*, 44(3):521–533.

Kim, Y.-C., Lee, H.-G., and Han, K.-A. (2007). D1 dopamine receptor dDA1 is required in the mushroom body neurons for aversive and appetitive learning in *Drosophila*. *The Journal of Neuroscience*, 27(29):7640–7647.

Kirkhart, C. and Scott, K. (2015). Gustatory learning and processing in the *Drosophila* mushroom bodies. *The Journal of Neuroscience*, 35(15):5950–5958.

Klein, M., Afonso, B., Vonner, A. J., Hernandez-Nunez, L., Berck, M., Tabone, C. J., Kane, E. A., Pieribone, V. A., Nitabach, M. N., Cardona, A., Zlatic, M., Sprecher, S. G., Gershow, M., Garrity, P. A., and Samuel, A. D. T. (2015). Sensory determinants of behavioral dynamics in *Drosophila* thermotaxis. *Proceedings of the National Academy of Sciences*, 112(2):E220–E229.

Krashes, M. J., DasGupta, S., Vreede, A., White, B., Armstrong, J. D., and Waddell, S. (2009). A neural circuit mechanism integrating motivational state with memory expression in *Drosophila*. *Cell*, 139(2):416–427.

Krashes, M. J. and Waddell, S. (2008). Rapid consolidation to a radish and protein synthesis-dependent long-term memory after single-session appetitive olfactory conditioning in *Drosophila*. *Journal of Neuroscience*, 28(12):3103–3113.

Kunz, T., Kraft, K. F., Technau, G. M., and Urbach, R. (2012). Origin of *Drosophila* mushroom body neuroblasts and generation of divergent embryonic lineages. *Development*, 139(14):2510–2522.

Kurusu, M., Awasaki, T., Masuda-Nakagawa, L. M., Kawauchi, H., Ito, K., and Furukubo-Tokunaga, K. (2002). Embryonic and larval development of the *Drosophila* mushroom bodies: concentric layer subdivisions and the role of fasciclin II. *Development*, 129(2):409–419.

Lee, T., Lee, A., and Luo, L. (1999). Development of the *Drosophila* mushroom bodies: sequential generation of three distinct types of neurons from a neuroblast. *Development*, 126(18):4065–4076.

Leiss, F., Grohand, C., Butcherand, N. J., Meinertzhagen, I. A., and Tavosanis, G. (2009). Synaptic organization in the adult *Drosophila* mushroom body calyx. *J Comp Neurol*, 517(6):808–24.

Lewis, L. P., Siju, K., Aso, Y., Friedrich, A. B., Bulteel, A. J., Rubin, G. M., and Kadow, I. C. G. (2015). A higher brain circuit for immediate integration of conflicting sensory information in *Drosophila*. *Current biology*, 25(17):2203–2214.

Lin, A. C., Bygrave, A. M., de Calignon, A., Lee, T., and Miesenböck, G. (2014a). Sparse, decorrelated odor coding in the mushroom body enhances learned odor discrimination. *Nature neuroscience*, 17(4):559–568.

Lin, S., Owald, D., Chandra, V., Talbot, C., Huetteroth, W., and Waddell, S. (2014b). Neural correlates of water reward in thirsty *Drosophila*. *Nature neuroscience*, 17(11):1536–1542.

Litwin-Kumar, A., Decker Harris, K., Axel, R., Sompolinsky, H., and Abbott, L. F. (2017). Optimal degrees of synaptic connectivity. *Neuron, in press*.

Liu, C., Plaçais, P.-Y., Yamagata, N., Pfeiffer, B. D., Aso, Y., Friedrich, A. B., Siwanowicz, I., Rubin, G. M., Preat, T., and Tanimoto, H. (2012). A subset of dopamine neurons signals reward for odour memory in *Drosophila*. *Nature*, 488(7412):512–516.

Liu, W. W. and Wilson, R. I. (2013). Glutamate is an inhibitory neurotransmitter in the *Drosophila* olfactory system. *Proceedings of the National Academy of Sciences USA*, 110(25):10294–10299.

Liu, X. and Davis, R. L. (2009). The GABAergic anterior paired lateral neuron suppresses and is suppressed by olfactory learning. *Nature neuroscience*, 12(1):53–59.

Lorenz, K. (1973). Autobiography. In *Les Prix Nobel*. Nobel Foundation, Stockholm.

Luo, S. X., Axel, R., and Abbott, L. (2010). Generating sparse and selective third-order responses in the olfactory system of the fly. *Proceedings of the National Academy of Sciences USA*, 107(23):10713–10718.

Mao, Z. and Davis, R. L. (2009). Eight different types of dopaminergic neurons innervate the *Drosophila* mushroom body neuropil: anatomical and physiological heterogeneity. *Frontiers in neural circuits*, 3:5.

Margulies, C., Tully, T., and Dubnau, J. (2005). Deconstructing memory in *Drosophila*. *Current Biology*, 15(17):R700–R713.

Masuda-Nakagawa, L. M., Gendre, N., O'Kane, C. J., and Stocker, R. F. (2009). Localized olfactory representation in mushroom bodies of *Drosophila* larvae. *Proceedings of the National Academy of Sciences USA*, 106(25):10314–10319.

Masuda-Nakagawa, L. M., Ito, K., Awasaki, T., and O'Kane, C. J. (2014). A single GABAergic neuron mediates feedback of odor-evoked signals in the mushroom body of larval *Drosophila*. *Frontiers in neural circuits*, 8:35.

Masuda-Nakagawa, L. M., Tanaka, N. K., and O'Kane, C. J. (2005). Stereotypic and random patterns of connectivity in the larval mushroom body calyx of *Drosophila*. *Proceedings of the National Academy of Sciences of the United States of America*, 102(52):19027–19032.

Mauelshagen, J. (1993). Neural correlates of olfactory learning paradigms in an identified neuron in the honeybee brain. *Journal of neurophysiology*, 69(2):609–625.

McQuillan, H. J., Nakagawa, S., and Mercer, A. R. (2012). Mushroom bodies of the honeybee brain show cell population-specific plasticity in expression of amine-receptor genes. *Learning & Memory*, 19(4):151–158.

Menzel, R. (2001). Searching for the memory trace in a mini-brain, the honeybee. *Learning & Memory*, 8(2):53–62.

Menzel, R. (2012). The honeybee as a model for understanding the basis of cognition. *Nature Reviews Neuroscience*, 13(11):758–768.

Menzel, R. (2014). The insect mushroom body, an experience-dependent recoding device. *Journal of Physiology-Paris*, 108(2):84–95.

Menzel, R. and Manz, G. (2005). Neural plasticity of mushroom body-extrinsic neurons in the honeybee brain. *Journal of Experimental Biology*, 208(22):4317–4332.

Michels, B., Chen, Y.-c., Saumweber, T., Mishra, D., Tanimoto, H., Schmid, B., Engmann, O., and Gerber, B. (2011). Cellular site and molecular mode of synapsin action in associative learning. *Learning & Memory*, 18(5):332–344.

Murthy, M., Fiete, I., and Laurent, G. (2008). Testing odor response stereotypy in the *Drosophila* mushroom body. *Neuron*, 59(6):1009–1023.

Nern, A., Pfeiffer, B. D., and Rubin, G. M. (2015). Optimized tools for multicolor stochastic labeling reveal diverse stereotyped cell arrangements in the fly visual system. *Proceedings of the National Academy of Sciences USA*, page 201506763.

Ohyama, T., Schneider-Mizell, C. M., Fetter, R. D., Aleman, J. V., Franconville, R., Rivera-Alba, M., Mensh, B. D., Branson, K. M., Simpson, J. H., Truman, J. W., Cardona, A., and Zlatic, M. (2015). A multilevel multimodal circuit enhances action selection in *Drosophila*. *Nature*, 520:633–39.

Owald, D., Felsenberg, J., Talbot, C. B., Das, G., Perisse, E., Huetteroth, W., and Waddell, S. (2015). Activity of defined mushroom body output neurons underlies learned olfactory behavior in *Drosophila*. *Neuron*, 86(2):417–427.

Owald, D. and Waddell, S. (2015). Olfactory learning skews mushroom body output pathways to steer behavioral choice in *Drosophila*. *Current opinion in neurobiology*, 35:178–184.

Pai, T.-P., Chen, C.-C., Lin, H.-H., Chin, A.-L., Lai, J. S.-Y., Lee, P.-T., Tully, T., and Chiang, A.-S. (2013). *Drosophila* ORB protein in two mushroom body output neurons is necessary for long-term memory formation. *Proceedings of the National Academy of Sciences*, 110(19):7898–7903.

Papadopoulou, M., Cassenaer, S., Nowotny, T., and Laurent, G. (2011). Normalization for sparse encoding of odors by a wide-field interneuron. *Science*, 332(6030):721–725.

Pauls, D., Selcho, M., Gendre, N., Stocker, R. F., and Thum, A. S. (2010). *Drosophila* larvae establish appetitive olfactory memories via mushroom body neurons of embryonic origin. *The Journal of Neuroscience*, 30(32):10655–10666.

Perisse, E., Owald, D., Barnstedt, O., Talbot, C. B., Huetteroth, W., and Waddell, S. (2016). Aversive learning and appetitive motivation toggle feed-forward inhibition in the *Drosophila* mushroom body. *Neuron*.

Perisse, E., Yin, Y., Lin, A. C., Lin, S., Huetteroth, W., and Waddell, S. (2013). Different kenyon cell populations drive learned approach and avoidance in *Drosophila*. *Neuron*, 79(5):945–956.

Plaçais, P.-Y., Trannoy, S., Friedrich, A. B., Tanimoto, H., and Preat, T. (2013). Two pairs of mushroom body efferent neurons are required for appetitive long-term memory retrieval in *Drosophila*. *Cell Reports*, 5(3):769–780.

Plaçais, P.-Y., Trannoy, S., Isabel, G., Aso, Y., Siwanowicz, I., Belliart-Guérin, G., Vernier, P., Birman, S., Tanimoto, H., and Preat, T. (2012). Slow oscillations in two pairs of dopaminergic neurons gate long-term memory formation in *Drosophila*. *Nature neuroscience*, 15(4):592–599.

Python, F. and Stocker, R. (2002). Adult-like complexity of the larval antennal lobe of *Dr. melanogaster* despite markedly low numbers of odorant receptor neurons. *Cell Tissue Res*, 445(4):374–87.

Qin, H., Cressy, M., Li, W., Coravos, J. S., Izzi, S. A., and Dubnau, J. (2012). Gamma neurons mediate dopaminergic input during aversive olfactory memory formation in *Drosophila*. *Current Biology*, 22(7):608–614.

Ramaekers, A., Magenat, E., Marin, E., Gendre, N., Jefferis, G., Luo, L., and Stocker, R. (2005). Glomerular maps without cellular redundancy at successive levels of the *Drosophila* larval olfactory circuit. *Current Biology*, 15(11):982–92.

Riemensperger, T., Völler, T., Stock, P., Buchner, E., and Fiala, A. (2005). Punishment prediction by dopaminergic neurons in *Drosophila*. *Current biology*, 15(21):1953–1960.

Rohwedder, A., Wenz, N. L., Stehle, B., Huser, A., Yamagata, N., Zlatic, M., Truman, J. W., Tanimoto, H., Saumweber, T., Gerber, B., and Thum, A. (2016). Four individually identified paired dopamine neurons signal reward in larval *Drosophila*. *Current Biology*.

Saalfeld, S., Cardona, A., Hartenstein, V., and Tomancak, P. (2009). CATMAID: Collaborative Annotation Toolkit for Massive Amounts of Image Data. *Bioinformatics*, 25(19):1984–1986.

Saalfeld, S., Fetter, R., Cardona, A., and Tomancak, P. (2012). Elastic volume reconstruction from series of ultra-thin microscopy sections. *Nature Methods*, 9:717–20.

Schindelin, J., Arganda-Carreras, I., Frise, E., Kaynig, V., Longair, M., Preibisch, S., Saalfeld, S., Schmid, B., Tinevez, J.-Y., White, D., Hartenstein, V., Tomancak, P., and Cardona, A. (2011). Fiji - an open source platform for biological image analysis . *Nature Methods*, 9(7):676–682.

Schlegel, P., Texada, M. J., Miroschnikow, A., Peters, M., Schneider-Mizell, C. M., Lacin, H., Li, F., Fetter, R. D., Truman, J. W., Cardona, A., and Pankratz, M. (2016). Synaptic transmission parallels neuromodulation in a central food-intake circuit. *eLife*, page e16799.

Schneider-Mizell, C. M., Gerhard, S., Longair, M., Kazimiers, T., Li, F., Zwart, M. F., Champion, A., Midgley, F., Fetter, R., Saalfeld, S., et al. (2016). Quantitative neuroanatomy for connectomics in *Drosophila*. *eLife*.

Schroll, C., Riemensperger, T., Bucher, D., Ehmer, J., Völler, T., Erbguth, K., Gerber, B., Hendel, T., Nagel, G., Buchner, E., and Fiala, A. (2006). Light-induced activation of distinct modulatory neurons triggers appetitive or aversive learning in *Drosophila* larvae. *Current Biology*, 16(17):1741–7.

Schultz, W. (2015). Neuronal reward and decision signals: from theories to data. *Physiological Reviews*, 95(3):853–951.

Schürmann, F.-W. (1971). Synaptic contacts of association fibres in the brain of the bee. *Brain Research*, 26(1):169–176.

Schürmann, F.-W. (1974). Bemerkungen zur funktion der corpora pedunculata im gehirn der insekten aus morphologischer sicht. *Experimental Brain Research*, 19(4):406–432.

Schürmann, F.-W. (2016). Fine structure of synaptic sites and circuits in mushroom bodies of insect brains. *Arthropod Structure & Development*.

Schwaerzel, M., Monastirioti, M., Scholz, H., Friggi-Grelin, F., Birman, S., and Heisenberg, M. (2003). Dopamine and octopamine differentiate between aversive and appetitive olfactory memories in *Drosophila*. *The Journal of neuroscience*, 23(33):10495–10502.

Séjourné, J., Plaçais, P.-Y., Aso, Y., Siwanowicz, I., Trannoy, S., Thoma, V., Tedjakumala, S. R., Rubin, G. M., Tchénio, P., Ito, K., Isabel, G., Tanimoto, H., and Preat, T. (2011). Mushroom body efferent neurons responsible for aversive olfactory memory retrieval in *Drosophila*. *Nature neuroscience*, 14(7):903–910.

Selcho, M., Pauls, D., Han, K.-A., Stocker, R. F., and Thum, A. S. (2009). The role of dopamine in *Drosophila* larval classical olfactory conditioning. *PLoS One*, 4(6):e5897.

Selcho, M., Pauls, D., Huser, A., Stocker, R. F., and Thum, A. S. (2014). Characterization of the octopaminergic and tyraminergic neurons in the central brain of *Drosophila* larvae. *Journal of Comparative Neurology*, 522(15):3485–3500.

Slater, G., Levy, P., Chan, K. A., and Larsen, C. (2015). A central neural pathway controlling odor tracking in *Drosophila*. *Journal of Neuroscience*, 35(5):1831–1848.

Stocker, R. F. (2009). The olfactory pathway of adult and larval *Drosophila*. *Annals of the New York Academy of Sciences*, 1170(1):482–486.

Strausfeld, N. J., Sinakevitch, I., Brown, S. M., and Farris, S. M. (2009). Ground plan of the insect mushroom body: functional and evolutionary implications. *Journal of Comparative Neurology*, 513(3):265–291.

Suloway, C., Pulokas, J., Fellmann, D., Cheng, A., Guerra, F., Quispe, Stagg, S., Potter, C., and Carragher, B. (2005). Automated molecular microscopy: the new Leginon system. *Journal of Structural Biology*, 151:41–60.

Takemura, S.-y., Aso, Y., Hige, T., Wong, A., Lu, Z., Xu, C. S., Rivlin, P. K., Hess, H., Zhao, T., Paraq, T., Berg, S., Huang, G., Katz, W., Olbris, D. J., Plaza, S., Umayam, L., Aniceto, R., Chang, L.-A., Lauchie, S., Ogundeyi, O., Ordish, C., Shinomiya, A., Sigmund, C., Takemura, S., Tran, J., Turner, G. C., Rubin, G. M., and Scheffer, L. K. (2017). A connectome of a learning and memory center in the adult *Drosophila* brain. *In preparation*.

Tanaka, N. K., Tanimoto, H., and Ito, K. (2008). Neuronal assemblies of the *Drosophila* mushroom body. *Journal of Comparative Neurology*, 508(5):711–755.

Technau, G. and Heisenberg, M. (1982). Neural reorganization during metamorphosis of the corpora pedunculata in *Drosophila melanogaster*. *Nature*, 295:4.

Thomas, J. B., Bastiani, M. J., Bate, M., and Goodman, C. S. (1984). From grasshopper to *Drosophila*: a common plan for neuronal development. *Nature*.

Truman, J. W. and Bate, M. (1988). Spatial and temporal patterns of neurogenesis in the central nervous system of *Drosophila melanogaster*. *Developmental biology*, 125(1):145–157.

Turner, G. C., Bazhenov, M., and Laurent, G. (2008). Olfactory representations by *Drosophila* mushroom body neurons. *Journal of neurophysiology*, 99(2):734–746.

Vergoz, V., Roussel, E., Sandoz, J.-C., and Giurfa, M. (2007). Aversive learning in honeybees revealed by the olfactory conditioning of the sting extension reflex. *PloS one*, 2(3):e288.

Vogt, K., Aso, Y., Hige, T., Knapek, S., Ichinose, T., Friedrich, A. B., Turner, G. C., Rubin, G. M., and Tanimoto, H. (2016). Direct neural pathways convey distinct visual information to *Drosophila* mushroom bodies. *eLife*, 5:e14009.

Waddell, S. (2013). Reinforcement signalling in *Drosophila*; dopamine does it all after all. *Current opinion in neurobiology*, 23(3):324–329.

Waddell, S., Armstrong, J. D., Kitamoto, T., Kaiser, K., and Quinn, W. G. (2000). The amnesiac gene product is expressed in two neurons in the *Drosophila* brain that are critical for memory. *Cell*, 103(5):805–813.

Yamagata, N., Ichinose, T., Aso, Y., Plaçais, P.-Y., Friedrich, A. B., Sima, R. J., Preat, T., Rubin, G. M., and Tanimoto, H. (2015). Distinct dopamine neurons mediate reward signals for short-and long-term memories. *Proceedings of the National Academy of Sciences*, 112(2):578–583.

Yang, M. Y., Armstrong, J. D., Vilinsky, I., Strausfeld, N. J., and Kaiser, K. (1995). Subdivision of the *Drosophila* mushroom bodies by enhancer-trap expression patterns. *Neuron*, 15(1):45–54.

Yasuyama, K., Meinertzhagen, I. A., and Schürmann, F.-W. (2002). Synaptic organization of the mushroom body calyx in *Drosophila* melanogaster. *Journal of Comparative Neurology*, 445(3):211–226.

Yu, D., Keene, A. C., Srivatsan, A., Waddell, S., and Davis, R. L. (2005). *Drosophila* DPM neurons form a delayed and branch-specific memory trace after olfactory classical conditioning. *Cell*, 123(5):945–957.

Zwart, M. F., Pulver, S. R., Truman, J. W., Fushiki, A., Cardona, A., and Landgraf, M. (2016). Selective inhibition mediates the sequential recruitment of motor pools. *Neuron*, In press.

Chapter II: The Ol$_1$mpiad: Concordance of behavioural faculties of stage 1 and stage 3 *Drosophila* larvae

The Ol$_1$mpiad consortium in alphabetical order: Maria J. Almeida-Carvalho[1], Dimitri Berh[2,3], Andreas Braun[4,5], Yi-chun Chen[6*], Katharina Eichler[7,18], Claire Eschbach[7], Pauline M. J. Fritsch[8], Bertram Gerber[6,9,10*], Nina Hoyer[11], Xiaoyi Jiang[3], Jörg Kleber[6], Christian Klämbt[2], Christian König[12,13], Matthieu Louis[4,14], Birgit Michels[6], Anton Miroschnikow[15], Christen Mirth[1,16], Daisuke Miura[17], Thomas Niewalda[6*], Nils Otto[2], Emmanouil Paisios[6], Michael J. Pankratz[15], Meike Petersen[11], Noel Ramsperger[18], Nadine Randel[7], Benjamin Risse[2,3], Timo Saumweber[6], Philipp Schlegel[15], Michael Schleyer[6], Peter Soba[11], Simon G. Sprecher[8], Teiichi Tanimura[17], Andreas S. Thum[18], Naoko Toshima[6,17], Jim W. Truman[7,19], Ayse Yarali[10,12], Marta Zlatic[7]

[1] Gulbenkian Institute of Science, Oeiras, Portugal
[2] Institute of Neurobiology and Behavioural Biology, University of Münster, Germany
[3] Department of Mathematics and Computer Science, University of Münster, Germany
[4] EMBL/CRG Systems Biology Unit, Centre for Genomic Regulation, Barcelona, Spain
[5] Universitat Pompeu Fabra, Barcelona, Spain
[6] Leibniz Institute for Neurobiology (Genetics), Magdeburg, Germany
[7] Janelia Research Campus, Howard Hughes Medical Institute, USA
[8] Department of Biology, University of Fribourg, Switzerland
[9] Institute of Biology, Otto von Guericke University Magdeburg, Germany
[10] Center for Behavioral Brain Sciences, Otto von Guericke University Magdeburg, Germany
[11] Center for Molecular Neurobiology, University of Hamburg, Germany
[12] Leibniz Institute for Neurobiology (Molecular Systems Biology), Magdeburg, Germany
[13] Institute of Pharmacology and Toxicology, Otto von Guericke University Magdeburg, Germany
[14] Department of Molecular, Cellular, and Developmental Biology, University of California, Santa Barbara, USA
[15] LIMES-Institute, University of Bonn, Germany
[16] School of Biological Sciences, Monash University, Melbourne, Australia
[17] Department of Biology, Kyushu University, Fukuoka, Japan
[18] Department of Biology, University of Konstanz, Germany
[19] Friday Harbor Laboratories, University of Washington, USA
[*] Corresponding authors

Journal of Experimental Biology (2017) 220, 2452-2475

doi: 10.1242/jeb.156646

4.1 Abstract

Mapping brain function to brain structure is a fundamental task for neuroscience. For such an endeavour, the *Drosophila* larva is simple enough to be tractable, yet complex enough to be interesting. It features about 10,000 neurons and is capable of various taxes, kineses, and Pavlovian conditioning. All its neurons are currently being mapped into a light-microscopical atlas, and Gal4 strains are being generated to experimentally access neurons one at a time. In addition, an electron microscopic reconstruction of its nervous system seems within reach. Notably, this EM-based connectome is drafted for a stage 1 larva - because stage 1 larvae are much smaller than stage 3 larvae. However, most behaviour analyses were performed for stage 3 larvae because their larger size makes them easier to handle and observe. It is therefore warranted to either redo the EM reconstruction for a stage 3 larva, or to survey the behavioural faculties of stage 1 larvae. We provide the latter. We probe stage 1 *Drosophila* larvae for free locomotion, feeding, responsiveness to substrate vibration, gentle and nociceptive touch, for burrowing, olfactory and thermotaxis, light avoidance, gustatory choice of various tastants plus odour-taste associative learning, as well as light-electric shock associative learning. Quantitatively stage 1 larvae show lower scores in most tasks, arguably because of their smaller size and lower speed. Qualitatively, however, stage 1 larvae perform strikingly similar to stage 3 in almost all cases. These results bolster confidence in mapping brain structure and behaviour across developmental stages.

4.2 Introduction

Mapping brain function to brain structure is a fundamental task for neuroscience. Focussing on behaviour as the integrated function of the brain, we describe the behavioural

faculties of stage 1 *Drosophila* larvae. This provides a resource for relating behavioural function to the upcoming description of their connectome (e.g. Ohyama et al. [2015]; Berck et al. [2016]; Fushiki et al. [2016]; Jovanic et al. [2016]; Schlegel et al. [2016]; Schneider-Mizell et al. [2016]; Zwart et al. [2016]).

Drosophila is known as a genetic model system. It allows for studying the principles of heredity, development, and brain function. The uncovered genetic and molecular networks are highly conserved, examples including early embryonic development, ion channel and synaptic function (e.g. St Johnston and Nüsslein-Volhard [1992]; Littleton and Ganetzky [2000]). This genetic and molecular similarity defines *Drosophila* as a model for biomedical science.

In the 1970s, also behavioural genetics of *Drosophila* gained momentum. Early study cases explored phototaxis [Benzer, 1967], circadian behaviour [Konopka and Benzer, 1971], and Pavlovian learning [Dudai et al., 1976; Heisenberg et al., 1985; Tully and Quinn, 1985]. The range of experimentally accessible behaviours now includes various further olfactory and gustatory behaviours, courtship, feeding, and aggressive behaviours as well as operant and other learning paradigms (Zhang et al. [2010] and references therein). These studies received a boost by their combination with new methods for transgenesis and transgene expression [Rubin and Spradling, 1982; O'Kane and Gehring, 1987; Brand and Perrimon, 1993]. These and related techniques now allow the comparatively convenient expression of transgenes, in any cell or group of cells, at any time (e.g. Venken et al. [2011]). Thus, *Drosophila* is a powerful model system to understand not 'only' molecular and cellular processes, but also their function in behaviourally meaningful circuitry (e.g. Sivanantharajah and Zhang [2015]) as had been envisioned by Hotta and Benzer [1970]. The elegance of the uncovered minimal biological circuits defines the inspiration of *Drosophila* for engineering, informatics and robotics (e.g. Frye and Dickinson [2004]).

With a slight delay, larval *Drosophila* entered the stage as subjects of behavioural neurogenetics (e.g. Aceves-Piña and Quinn [1979]; Rodrigues [1980]; Heisenberg et al. [1985]), with revived interest since the 1990s [Stocker, 1994; Cobb, 1999; Sokolowski, 2001; Gerber and Stocker, 2007; Gomez-Marin and Louis, 2012; Keene and Sprecher, 2012; Diegelmann et al., 2013]. Larvae possess 10 times fewer neurons than adult flies, but feature fundamental adult-like circuit motifs (for example in the olfactory pathways: Vosshall and Stocker [2007]; Stocker [2008]) as well as fundamental faculties of behaviour - with the obvious exception of reproductive behaviours and flight. Beyond locomotion and feeding, these faculties include various forms of taxes, kineses, and Pavlovian learning. Thus, the larva offers a fortunate balance between being simple enough to be tractable, yet complex enough to be interesting. Indeed, in the foreseeable future the larva's 10,000-neuron nervous system will be mapped into a light-microscopical cell-by-cell atlas [Li et al., 2014], and Gal4 strains can be generated to experimentally access these neurons one at a time. In addition, an electron microscopic reconstruction of the full larval brain and ventral nerve cord, at synaptic resolution, seems within reach (e.g. Ohyama et al. [2015]; Berck et al. [2016]; Fushiki et al. [2016]; Jovanic et al. [2016]; Schneider-Mizell et al. [2016]; Zwart et al. [2016]). These resources will allow mapping behaviour onto circuitry with an unprecedented combination of ease, completeness and precision. Notably, the EM-based connectome is being drafted for a stage 1 larva - because they are considerably smaller than stage 3 larvae and thus are quicker to image using EM techniques. However, the vast majority of published behaviour analyses were performed for stage 3 larvae - as their larger size makes them easier to handle. Although light microscopical observations have not yet ascertained major qualitative discrepancies in the neuroanatomy between stage 1 and stage 3 larvae, it is not trivial to show the utility of the stage 1 connectome for guiding behavioural analyses in stage 3 larvae. This is because not only growth but

also neurogenesis continues across larval stages in at least some brain regions [Ito and Hotta, 1992]. To bolster confidence in connectome-behaviour mappings, it is thus warranted to either redo the EM reconstruction for a stage 3 larva, or to survey the behavioural faculties of stage 1 larvae. We provide the latter.

4.3 Results

We will first present the results of the counting-based assays, followed by the results from the assays based on video-tracking.

Olfactory and gustatory preference

Stage 1 as well as stage 3 larvae show attraction to both odours tested (Fig. 1A, B), in line with what has previously been reported for stage 3 larvae (e.g. Cobb [1999]; Saumweber et al. [2011]). For both odours, it takes slightly longer until this preference becomes significant for stage 1 larvae. The same pattern of results is observed for the preference behaviour for fructose and arabinose (Fig. 2A, B); for sorbitol preference does not reach significant levels in stage 1 larvae during the observation period (Fig. 2C). We note that the early, transient aversiveness of sorbitol in stage 3 larvae is not observed in stage 1 larvae. Preference for various sugars has previously been reported for stage 3 larvae (e.g. Schipanski et al. [2008]; Rohwedder et al. [2012]).

Avoidance of quinine in stage 1 is consistently less than in stage 3 larvae, yet apparently converges towards the same level at the end of the observation period, suggesting that it takes longer for stage 1 larvae until these levels can be reached (Fig. 2D). Avoidance of quinine has previously been reported for stage 3 larvae (e.g. El-Keredy et al. [2012]).

Preference scores for aspartic acid are low, both in stage 1 and stage 3 larvae; indeed only after 16 min does weak attraction to aspartic acid become evident in stage 3 larvae

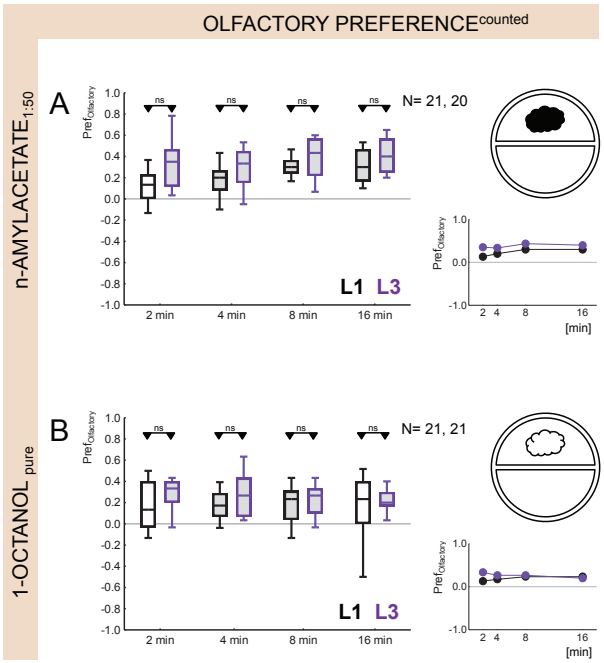

Figure 1: Olfactory preference.
A *n*-amyl acetate. Larvae are allowed to choose between one side of a Petri dish that features a container filled with *n*-amyl acetate as odour (filled cloud), and the other side that does not. An olfactory preference index ($\text{Pref}_{Olfactory}$) is calculated for the distribution of larvae after 2 min, 4 min, 8 min, and 16 min after the experiment has started. Positive values indicate attraction to *n*-amyl acetate, which is statistically significant already after 2 min for stage 3 larvae (L3, magenta-line box plots), while this is the case only after 4 min for stage 1 larvae (L1, black-line box plots). In direct comparisons, attraction of *n*-amyl acetate in L1 is not significantly less than in L3 larvae at any time point. The inset presents the median of the preference indices plotted over time.
B 1-octanol. Same as above, but using 1-octanol (open cloud) as odour. Preference for 1-octanol is statistically uniform in L1 and L3 larvae.
The box plots show the median, 25 % and 75 % quantiles as the box boundaries, and 10 % and 90 % quantiles as whiskers. * and ns refer to Bonferroni-corrected MWU comparisons between groups ($P<0.05/4$); grey shading of the box plots indicates Bonferroni-corrected within-group significance from zero in OSS tests ($P<0.05/4$).
Sample sizes are given within the figure.

(Fig. 2E), an effect that fails to reach significance for stage 1 larvae. Attraction to aspartic acid has previously been reported for stage 3 larvae [Croset et al., 2016], and using an modified assay geometry for both stage 1 and stage 3 larvae [Kudow et al., 2017].

Thus, for the odours and tastants tested up to this point the general result is that these cues have concordant valence for both larval stages but that it takes slightly longer until the same levels of preference are reached for stage 1 as compared to stage 3 larvae. One simple explanation of these results is that stage 1 larvae are smaller and slower in locomotion than stage 3 larvae (see also Fig. S4A). Such slower locomotion cannot, however, account for the results obtained for salt that are presented in the next section. It has previously been reported for stage 3 larvae as well as for adult *Drosophila* that low salt concentrations are moderately attractive, while high concentrations are strongly aversive; at intermediate concentrations both these behavioural tendencies cancel out [Niewalda et al., 2008; Russell et al., 2011]. This inverted U-shaped dose-effect function for salt preference behaviour may be shifted towards the left, i.e. towards higher

sensitivity, in stage 1 larvae: that is, both attraction at low concentrations and avoidance at high concentrations of salt is stronger in stage 1 larvae (Fig. 2F-H). Obviously, slower locomotion in stage 1 larvae works against such stronger attraction/avoidance scores, such that the valence differences for salt between stage 1 and stage 3 larvae may actually be underestimated.

Thus, olfactory and gustatory preference behaviour in stage 1 and stage 3 larvae is essentially equal in valence and strength, excepting the longer time it takes for stage 1 to express these preferences, and excepting the case of salt where a shift towards higher sensitivity may be reckoned with in stage 1 larvae (Fig. S1).

Odour-tastant associative learning

It has been previously reported for stage 3 larvae that repeatedly presenting an odour together with a fructose reward increases preference for the odour in a subsequent test [Scherer et al., 2003; Neuser et al., 2005; Saumweber et al., 2011]. Specifically, in one group of larvae the odour amyl acetate (AM) is presented together with fructose as reward (+) and 1-octanol without reward (AM+/OCT), while a second group of larvae undergoes reciprocal training (AM/OCT+). Then, animals are tested for their choice between AM versus OCT in the absence of the fructose reward. Appetitive associative memory is indicated by a relatively higher preference for AM after AM+/OCT training compared to the reciprocal AM/OCT+ training. This difference in preference is quantified by the associative performance index (PI) such that positive PIs indicate appetitive associative memory (negative PIs would indicate aversive memory). The elevated preference for the reward-associated odour can be grasped as a memory-based search for reward, because it ceases if the sought-for reward is actually present during the test (Gerber and Hendel [2006]; Saumweber et al. [2011]; Schleyer et al. [2011, 2015a,b]; also see Schleyer et al. [2013]).

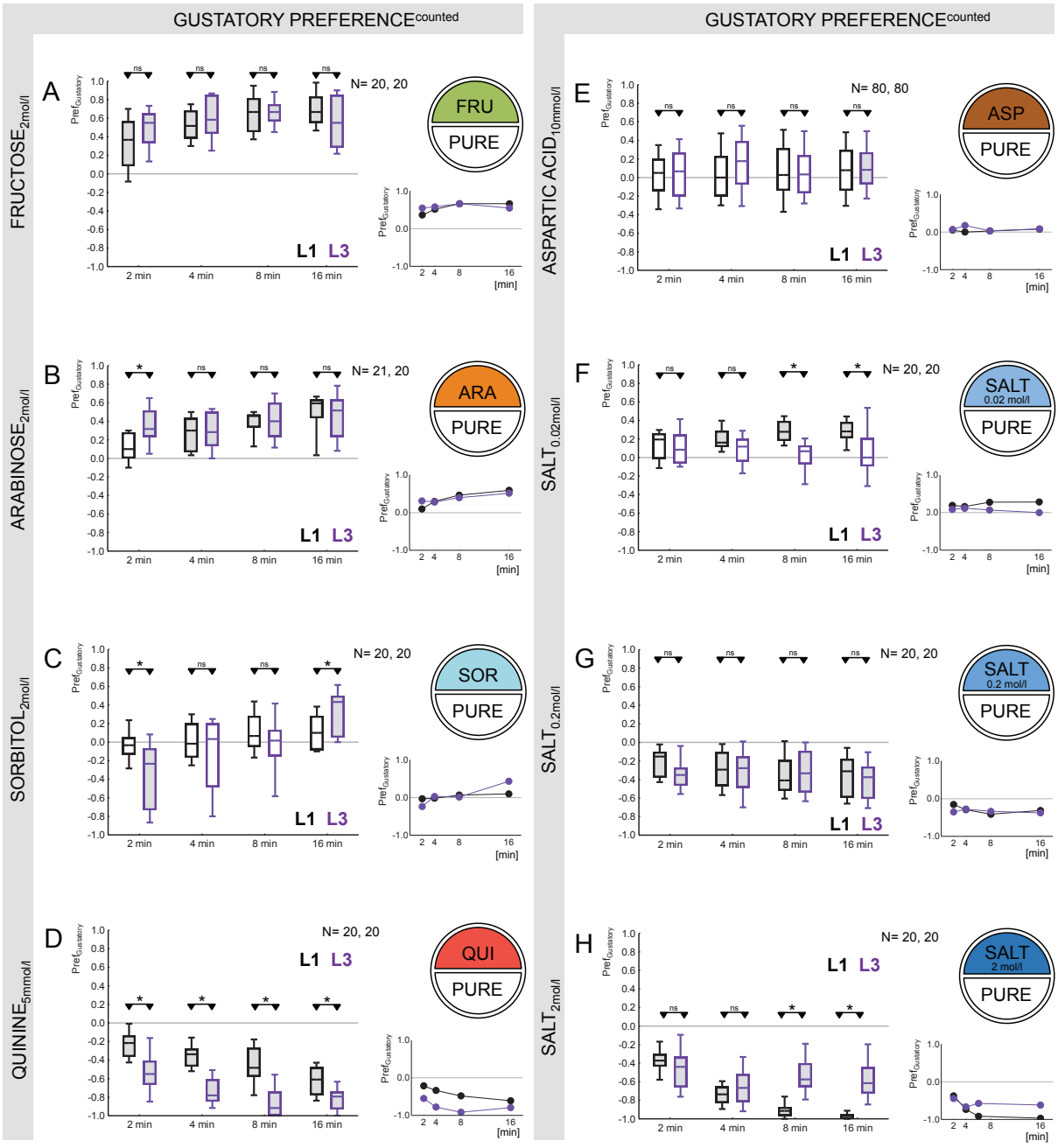

Figure 2: Gustatory preference. *(See next page).*

Figure 2: *Continues from prior page.* **A** Fructose. Larvae are allowed to choose between one side of a Petri dish that contains agarose added with 2 mol/l fructose (FRU; green fill of hemi circle), and pure agarose (PURE) on the other side. A gustatory preference index ($Pref_{Gustatory}$) is calculated for the distribution of the larvae after 2 min, 4 min, 8 min, and 16 min after the experiment has started. Positive values indicate attractiveness of fructose, which is statistically significant already from 2 min on for both stage 1 larvae (L1, black-line box plots) and for stage 3 larvae (L3, magenta-line box plots). Attractiveness of fructose in L1 is not significantly less than in L3 at any time point. The inset presents the median scores plotted over time.
B Arabinose. As above for fructose, but using 2 mol/l arabinose (ARA; orange), and pure agarose (PURE) on the other side. Attraction of arabinose is statistically significant from 4 min on for L1 while this is the case already after 2 min for L3 larvae. Attraction of arabinose in L1 is less than in L3 early on, i.e. after 2 min, but not at the other time points.
C Sorbitol. As above for fructose, but using 2 mol/l sorbitol (SOR; turquoise), and pure agarose (PURE) on the other side. For L1 we find indifference towards sorbitol, at all time points; for L3, we observe slight yet significant avoidance at 2 min and attraction after 16 min. At that latest time point, preference scores in L3 are higher than for L1.
D Quinine. Same as above for fructose, but using 5 mmol/l quinine (QUI, red), and pure agarose (PURE) on the other side. Avoidance of quinine is statistically significant already from 2 min on for L1 as well as for L3 larvae. Avoidance of quinine in L1 is less than in L3 at all time points.
E Aspartic acid. Same as above for fructose, but using 10 mmol/l aspartic acid (ASP, brown), and pure agarose (PURE) on the other side. Attraction to aspartic acid is not statistically significant for any of the time points except for L3 larvae at 16 min. Scores do not differ between L1 and L3, at any time point.
F-H Salt. Same as above for fructose, but using either a low, an intermediate, or a high concentration of salt (NaCl: 0.02 mol/l, 0.2 mol/l, 2 mol/l; blue), and pure agarose (PURE) on the other side. (F) For L1 larvae attraction of the low concentration is statistically significant from 4 min on, while for L3 larvae only tendencies for attraction are observed. At 8 and 16 min, L1 show stronger attraction than L3. (G) For an intermediate concentration of salt, both L1 and L3 larvae show aversion, and do so to the same extent, for all time points. (H) For the high salt concentration, avoidance is statistically significant at all time points for both L1 and L3. At 8 and 16 min, L1 show stronger aversion than L3. It thus seems that the dose-effect function for salt preference in L3, from attraction at very-low to low salt concentrations to aversion at high salt concentrations, is shifted towards the left in L1, i.e. towards a higher sensitivity to salt in L1 than in L3. * and ns refer to Bonferroni-corrected MWU comparisons between groups ($P<0.05/4$); grey shading of the box plots indicates Bonferroni-corrected within-group significance from zero in OSS tests ($P<0.05/4$).
Sample sizes are given within the figure.

As previously reported for stage 3 larvae, odour-fructose training also establishes appetitive memory in stage 1 larvae (Fig. 3A1, left box plot for the associative performance indices and Fig. 3A2, the two left box plots for the underlying preference scores) (also see Pauls et al. [2010]). Notably and also as previously observed for stage 3 larvae, the associative modulation in the preference for the fructose-associated odour is abolished if the test is performed in the presence of the fructose reward (Fig. 3A1, A2, right box plots).

Likewise as previously reported for stage 3 larvae [Schleyer et al., 2015a], odour-aspartic acid training establishes appetitive memory in stage 1 larvae, a memory that can be prevented from behavioural expression by the presence of aspartic acid during the test (Fig. 3B).

To provide a case of taste-punishment learning, we trained stage 1 larvae by presenting one of the odours together with quinine, while the other odour was presented alone. As previously reported for stage 3 larvae [Gerber and Hendel, 2006; Schleyer et al., 2011,

2015a; El-Keredy et al., 2012] no learned behaviour towards the quinine-associated odour is observed (Fig. 3C1, left box plot for the associative performance indices and Fig. 3C2, the two left box plots for the underlying preference scores) - unless quinine is indeed present during the test (Fig. 3C1, right box plot for the associative performance indices and Fig. 3C2, the two right box plots for the underlying preference scores). This arguably is because learned behaviour after odour-punishment training is a form of learned escape that is behaviourally expressed only if the testing situation does indeed require escape. The case of odour-salt associative learning turned out to be special. In stage 3 larvae it was previously found that low concentrations of salt have a rewarding effect, while high concentrations of salt are punishing [Niewalda et al., 2008; Russell et al., 2011]. Using 0.2 mol/l salt as a concentration that was reported to be rewarding in stage 3 larvae we were surprized to observe aversive memory in stage 1 larvae. That is, when tested in the absence of salt, associative performance indices are zero, while negative scores are uncovered when testing is carried out in the presence of salt (Fig. 3D1, D2). As mentioned in the preceding paragraph for quinine, this can be seen as a case of learned escape from the salt-associated odour that is warranted only when the salt to escape from indeed is present. Thus, a salt concentration that is punishing in stage 1 larvae is rewarding in stage 3 (for a confirmation of the latter result under the present conditions: Fig. 3E1, E2). Possibly, the inverted U-shaped dose-effect function for salt as a reinforcer, from rewarding at low to punishing at high concentrations, is shifted towards the left for stage 1 larvae, i.e. towards higher sensitivity. Such an interpretation would also fit the results regarding salt preference behaviour presented in the preceding section. Likely explanations for such a generally increased sensitivity to salt are that the geometry of stage 1 larvae renders them more susceptible to osmotic stress by high salt concentrations in the substrate, and/or that their cuticle is less protective for such osmotic stress. Indeed, salt concentrations high enough to be punishing in stage

3 larvae are lethal for stage 1 (data not shown).

We note that for stage 3 larvae the dose-effect function for the reinforcing effect of salt was reported to be shifted rightward along the concentration axis relative to preference behaviour [Niewalda et al., 2008; Russell et al., 2011]. In other words, a higher salt concentration is needed to be an effective punishment than is required to induce avoidance. This is confirmed within the present study: a salt concentration that stage 3 larvae already avoid in a preference test (0.2 mol/l, Fig. 2G) is not yet punishing to them, but rather still is rewarding (Fig. 3E).

Thus, the faculties for odour-taste associative learning, and the rules for behaviourally expressing the established memories, are strikingly similar for stage 1 larvae when compared to previous reports concerning stage 3 larvae. The exception to this rule is salt, as apparently stage 1 larvae are much more sensitive to salt reinforcement than stage 3.

Odour-DAN activation associative learning

It has previously been reported for stage 3 larvae that repeatedly presenting an odour together with optogenetic activation of the R58E02-Gal4 positive DAN neurons associatively increases preference for the odour in a subsequent test [Rohwedder et al., 2016]. Specifically, in one group of larvae the odour ethyl acetate (EA) is presented paired with red light for optogenetic DAN activation (*), alternated with blank trials (EA*/blank training). A second group of larvae receives unpaired presentations of odour and red light (EA/* training). Then, all animals are tested for their preference for EA. Appetitive associative memory is indicated by a relatively higher preference for EA after paired EA*/blank training compared to unpaired EA/* training. This difference in preference is quantified by the associative performance index (PI) such that positive PIs indicate appetitive associative memory (negative PIs would indicate aversive memory).

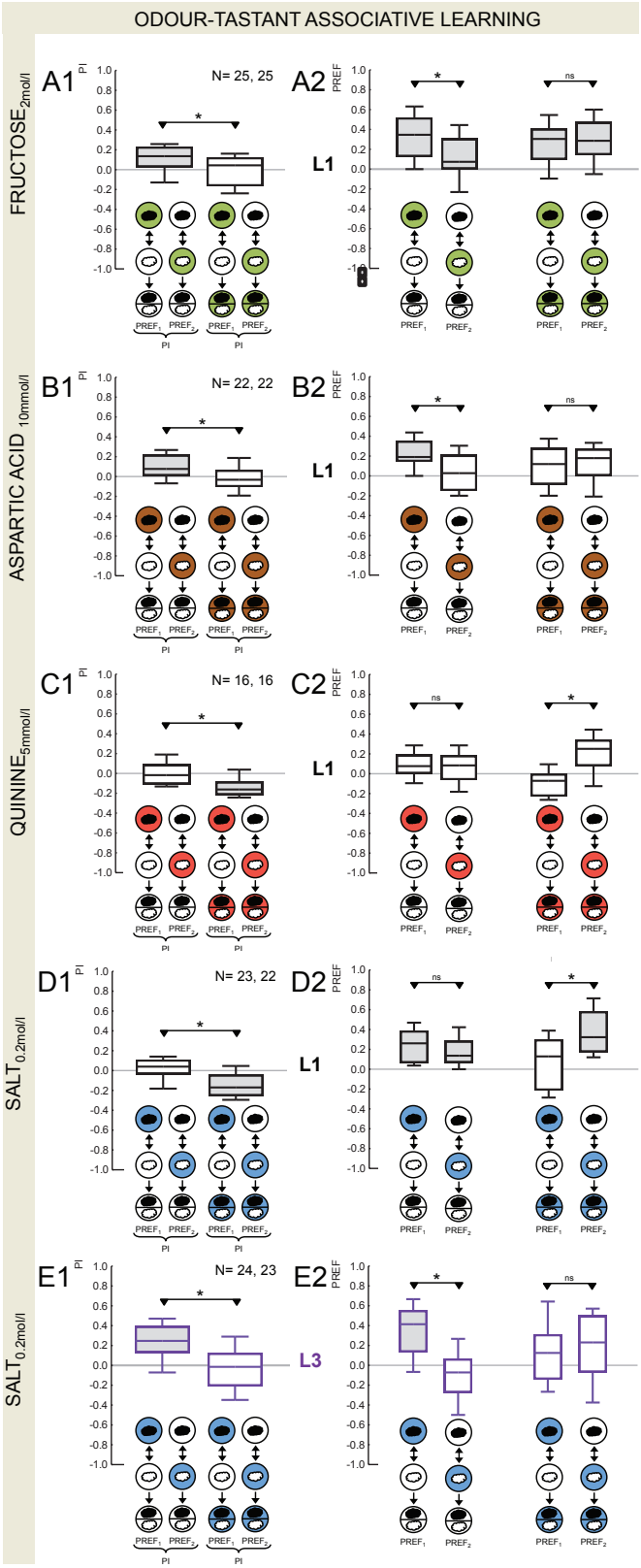

Figure 3: Odour-tastant associative learning.
A Fructose as reward in stage 1 larvae. One set of stage 1 larvae receives one odour (*n*-amyl acetate: black cloud) paired with a fructose reward (green fill of Petri dish), and the other odour (1-octanol: white cloud) with pure agarose (white fill of Petri dish); in a second set of larvae, training is reciprocal (*n*-amyl acetate without and 1-octanol with reward). Testing of the choice between both odours is performed either in the absence of the fructose reward, that is on pure agarose plates (below left box plot in A1), or in the presence of the fructose reward (below right box plot in A1). Appetitive associative memory is indicated by positive Performance Indices (PIs), showing that larvae systematically prefer the previously rewarded over the previously non-rewarded odour (the underlying preference scores (PREF) are presented in A2, such that preference for *n*-amyl acetate yields positive scores). Associative performance indices are significant in the absence, but not in the presence of the fructose reward. This indicates that appetitive associative memory supports learned search behaviour, which is only expressed in the absence of the sought-for fructose reward.
B Aspartic acid as reward in stage 1 larvae. as in (A), yet using 10 mmol/l aspartic acid (brown) as a reward. Appetitive associative memory is indicated by positive PIs. Notably, aspartic acid memory is only expressed in the absence but not in presence of aspartic acid.
C Quinine as punishment in stage 1 larvae. as in (A), yet using 5 mmol/l quinine (red) as a punishment. Aversive associative memory is indicated by negative PIs. Notably, quinine memory is only expressed in the presence but not in absence of quinine, i.e. is a form of learned escape.
D, E Salt as punishment in stage 1, but as reward in stage 3 larvae. as in (A), yet using 0.2 mol/l sodium chloride (blue) in stage 1 larvae (L1; D, black-line box plots) or stage 3 larvae (L3; E, magenta-line box plots). Notably, L1 show aversive memory in the presence but not in absence of this salt concentration, while L3 show appetitive memory in the absence but not the presence of salt. It thus seems that the dose-effect function for salt reinforcement in L3, from rewarding at low salt concentrations to punishing at high salt concentrations [Niewalda et al., 2008; Russell et al., 2011], is shifted towards the left in L1, i.e. towards higher sensitivity. Thus, a salt concentration that is rewarding to L3 already is punishing to L1.
* and ns refer to MWU comparisons between groups (A1-E1: * $P<0.05$; A2-E2: * or ns $P <$or $>0.05/2$); grey shading of the box plots indicates Bonferroni-corrected within-group significance from zero in OSS tests (A1-E1: $P<0.05/2$; A2-E2: $P<0.05/4$).
Sample sizes are given within the figure.

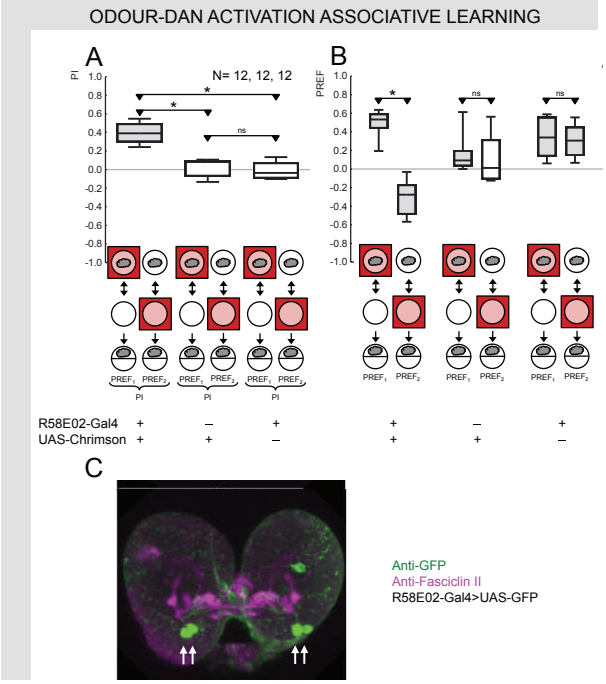

Figure 4: Odour-DAN activation associative learning.
A DAN activation as reward in stage 1 larvae. One set of stage 1 larvae receives odour (ethyl acetate: grey cloud) paired with red light for optogenetic DAN activation (red square around Petri dish), alternated with blank trials (white-filled Petri dish). In a second set of larvae, odour presentation and red light are unpaired. In both groups, this training is followed by a test of odour preference. Appetitive associative memory is indicated by positive Performance Indices (PIs), reflecting that larvae have a systematically higher preference for the odour after paired rather than unpaired training. For the experimental genotype expressing Chrimson in the R58E02-Gal4 DANs, positive PIs are observed, showing that DAN activation is sufficient as an internal reward signal. In the effector and the driver control genotypes, the DANs are not activated and PIs are indistinguishable from chance levels. **B** Preference scores underlying the PIs from (A). * and ns refer to Bonferroni-corrected MWU comparisons between groups (A, B: P $<$or $>$0.05/3); grey shading of the box plots indicates Bonferroni-corrected within-group significance from zero in OSS tests (A: P$<$0.05/3; B: P$<$0.05/6). (C) Anti-GFP visualization in R58E02-Gal4 x UAS-GFP stage 1 larvae (green) (expression from R58E02-Gal4 in stage 3 larvae has recently been described by Rohwedder et al. [2016]). Expression of GFP can be discerned in two pPAM-cluster neuron cell bodies in each hemisphere (arrows) projecting onto the mushroom bodies revealed through anti-Fasciclin II detection (magenta). For a tentative identification of these cells as DAN-i1 and -j1 please refer to the body text; occasionally and as can be seen in the current preparation, an additional cell is observed which does not innervate the mushroom bodies. The scale bar represents 100 µm.
Sample sizes are given within the figure.

The present results show that odour-DAN activation training establishes appetitive memory also in stage 1 larvae (Fig. 4A, for the associative performance indices of the experimental as well as the effector and driver control strains; Fig. 4B for the underlying preference scores). Thus, activation of the R58E02-Gal4 DANs is sufficient as an internal reward signal also in stage 1 larvae. Interestingly the R58E02-Gal4 driver labels three DANs of the pPAM-cluster in stage 3 larvae, respectively innervating the shaft, upper and intermediate toe of the mushroom body medial lobe [Rohwedder et al., 2016]. However, only two such cells are labelled in stage 1 (Fig. 4C, arrows; occasionally, an additional cell is observed which does not innervate the mushroom bodies). Specifically, stage 3 R58E02-Gal4 larvae express in DAN-h1, -i1 and -j1 (Rohwedder et al. [2016]; nomenclature according to Eichler et al. [2017]). Given that Eichler et al. [2017] found that of these DANs only DAN-h1 is not present in a stage 1 whole-brain EM volume,

the two mushroom body-innervating cells labelled in Figure 4C in a stage 1 larva are tentatively identified as DAN-i1 and DAN-j1.

Light/dark-electric shock associative learning

Stage 1 larvae were trained either with pairings of light with electric shock and darkness without shock, or were trained reciprocally with light-alone trials and pairings of darkness with electric shock punishment. This was followed by a test of their light-dark preference (see sketch Fig. 5A). Stage 1 larvae behave regardless of previous training regimen in such a test; that is, performance indices are zero (Fig. 5A, left box plots). Correspondingly, light-dark preference scores are equal between the reciprocally trained groups of stage 1 larvae and indicate avoidance of light (Fig. 5B, left box plots). This result was surprising, given the previously reported ability of stage 3 larvae in a similar paradigm [von Essen et al., 2011]. We therefore ran the current paradigm also for stage 3 larvae and confirmed their ability of light/dark-electroshock learning (Fig. 5A). Indeed, avoidance of light was stronger after the light had been paired with electric shock as compared to the reciprocally trained group of stage 3 larvae (Fig. 5B, middle box plots); no such alteration is seen when the shock is omitted during training, arguing that these differences in light avoidance are associative in character and are unrelated to the difference in the duration of light-dark exposure between reciprocal groups (Fig. 5A, B, right box plots).

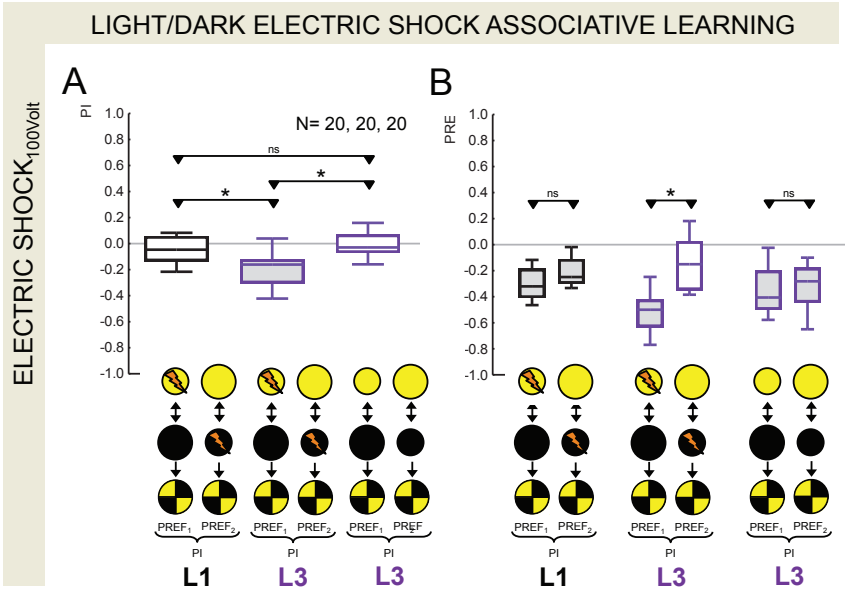

Figure 5: Light/Dark-electric shock associative learning.
One group of larvae receives light exposure (yellow fill of circles) paired with an electroshock punishment (lightning symbol), and darkness (black fill of circles) without electroshock (Light+/Dark training). Circles indicate agarose-filled Petri dishes; the small size of the circles represents a 1 min trial duration, while the large diameter circles indicate a 5 min trial duration. A second group receives Light/Dark+ training. During the test, the preference of the larvae for the lighted quadrants is determined. The performance index (PI) as displayed in (A) quantifies the difference in light preference between both groups, such that negative PIs reflect avoidance of the shock-paired visual condition (the underlying preference scores (PREF) are presented in (B) such that preference for the lighted quadrants yields positive scores). Experiments were performed either with stage 1 larvae (L1, black-line box plots) or stage 3 larvae (L3, magenta-line box plots). Given that total light exposure was not equal between groups (see body text), a control experiment was performed in L3 by subjecting them to training-like handling and light exposure, yet omitting all electroshocks (rightmost condition in A and B). L1 do not show avoidance of the shock-associated visual condition, while L3 do. As shown for L3, differences in light exposure as such are not sufficient to lead to differences in light avoidance, arguing that the negative PIs observed reflect associative memory. * and ns refer to MWU comparisons between groups ($P<0.05/3$); grey shading of the box plots indicates Bonferroni-corrected within-group significance from zero in OSS tests (A: $P<0.05/3$; B: $P<0.05/6$). Sample sizes are given within the figure.

Food intake

Larval feeding behaviour has been measured in different assays (e.g. Bjordal et al. [2014]; Gasque et al. [2013]; Neckameyer [2010]; Schoofs et al. [2014]). In particular for short-term food intake assays, choosing the appropriate duration of the experiment is crucial. We therefore determined food intake in stage 1 larvae at different time points, and compared the changes in food ingested over time to stage 3 larvae (Fig. S2A). We found the time course of food intake across the assay duration to be virtually identical for stage 1 and stage 3 larvae (Fig. S2B). For both stages the largest increase in food uptake occurs between 10 min and 20 min, making 20 min the experimental duration most likely to detect changes in food intake in this assay.

Burrowing

When allowed 60 min to feed, roam around, or burrow into the substrate of a Petri dish containing yeast diet, it takes stage 1 larvae longer to burrow into the substrate than stage 3 larvae. That is, while half of the stage 3 larvae have already burrowed into the substrate after 5 min, this takes about 10 times longer for stage 1 larvae (Fig. S3).

Mechano-nociception and touch

We aimed at exerting a stimulus to stage 1 and stage 3 larvae that is noxious but not damaging. This is not trivial, as the cuticle is softer in stage 1 larvae and therefore noxious stimuli normally used for stage 3 larvae (30-100 mN) frequently cause tissue damage to stage 1 larvae. We therefore calibrated stimulation to a force of 20 mN for stage 1 and 50 mN for stage 3 larvae. Under such conditions of different physical stimulation adjusted to be not physically damaging for either stage, both stage 1 and stage 3 larvae show the previously characterized types of behaviour towards noxious stimuli, namely stop, stop-and-turn, bending, and rolling, and do so at about the same proportions (Fig. 6A). Only rolling, the strongest nociceptive behaviour, is tendencially less likely to occur in stage 1 larvae under the chosen conditions (Fig. 6A, right bars); note that arguably rolling is a noci-defensive, rather than noci-ceptive behaviour.

Upon gentle touch with an eyelash, both stage 1 and stage 3 larvae show the typical behavioural signs of disturbance [Kernan et al., 1994], at about the same proportions. That is, in the large majority of cases animals from both stages show withdrawal of the head followed by turning, or a single backward wave of body peristalsis which then is also followed by turning (Fig. 6B).

To further investigate rolling behaviour, we optogenetically activated the somatosensory Basin interneurons (Fig. 6C) in stage 1 larvae. Crossing the R72F11-GAL4 driver strain with the UAS-Chrimson effector strain and raising larvae in food supplemented with retinal for proper function of the Chrimson protein, we observed rolling behaviour in 95

% of animals in response to light stimulation (Fig. 6D). This fits with what has previously been reported for stage 3 larvae [Ohyama et al., 2015]. No rolling was seen in the genetic control strains, and only very rarely if retinal was omitted from the larval diet. Movie 1 and Movie 2 present examples of optogenetically induced rolling behavior in stage 1 and stage 3 larvae, respectively.

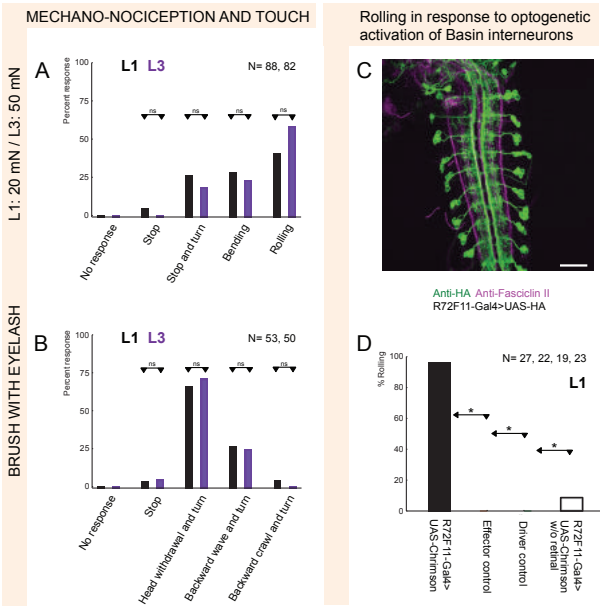

Figure 6: Mechano-nociception and touch.
A Mechano-nociception. Shown are the responses of stage 1 (L1, black bars) and stage 3 larvae (L3, magenta bars) to a mechano-nociceptive stimulus adjusted to be just-not damaging for either stage (L1: 20 mN, L3: 50 mN). Both, L1 and L3 display nociceptive behaviour (Bending, Rolling) as well as non-nociceptive behaviour (Stop, Stop and turn) at the same rates. ns refers to Bonferroni-corrected two-tailed z-tests between L1 and L3 ($P>0.05/4$) (XLSTAT, Statcon, Witzenhausen, Germany).
B Gentle touch. Shown are the responses of stage 1 (L1, black bars) and stage 3 larvae (L3, magenta bars) to an innocuous mechanical stimulus with an eyelash. L1 and L3 larvae exhibit behavioural signs of mild disturbance (Stop, Head withdrawal and turn, Backward wave and turn, Backward crawl and turn) at the same rates. ns refers to Bonferroni-corrected two-tailed z-tests between L1 and L3 ($P>0.05/4$) (XLSTAT, Statcon, Witzenhausen, Germany).
C, D Rolling in response to optogenetic activation of Basin interneurons. Shown in (C) is the anti-HA visualization from a R72H11 x UAS-HA stage 1 larva (green). Expression of HA can be discerned in the Basin interneurons of the ventral nerve cord; longitudinal fibre bundles stained for anti-Fasciclin II (magenta) allow orientation in the preparation. Scale bar: 25 µm. (D) Larvae of the indicated genotypes were stimulated with light and scored for rolling behaviour. Larvae of the experimental genotype expressing Chrimson in the Basin interneurons are likely to show rolling upon light stimulation, while larvae of the genetic controls, or larvae of the experimental genotype raised without retinal (open bar), are not. * refers to $P<0.05/3$ in Bonferroni-corrected two-tailed z-tests between the experimental genotype raised with retinal versus the respective control condition (XLSTAT, Statcon, Witzenhausen, Germany). Sample sizes are given within the figure.

Video-tracking of the response to 'Buzz' mechanosensory disturbance

We measured translational run speed as well as the angular sideways speed of stage 1 and stage 3 larvae, both under baseline conditions and upon presenting a disturbing mechanosensory 'buzz' stimulus [Eschbach et al., 2011; Saumweber et al., 2014]. Under baseline conditions, translational run speed is about 4-fold lower in stage 1 as compared to stage 3 larvae, while angular speed is equal in both stages (Fig. S4A,

B). In other words, stage 1 larvae run slower, but if they move sideways or turn, these lateral movements are of the same speed as in stage 3 larvae. In order to compare the buzz-induced changes in translational run speed and angular speed between stages, we normalized these measures, for each larva, to the ones obtained immediately before the buzz. Such normalized measures of translational run speed and angular speed do not reveal a difference between stage 1 and stage 3 larvae (Fig. S4C, D). Both stages hunch and slow down (i.e. 'startle') for 2-3 s after the buzz; during the first of these seconds they typically implement sideways movements (see also Movie 6 and Movie 7).

Video-tracking of 'free' locomotion

In Figure 7A as well as in Movies 3-5 we show example tracks of locomotion for stage 1 and stage 3 larvae. As previously reported [Otto et al., 2016] larval locomotion alternates between go- and reorientation phases.

Qualitatively, we note that body contractions and the resulting peristalsis during go-phases appear to be less regular in stage 1 than in stage 3 larvae (Fig. 7B, Movie 3). Quantitatively, the frequency of peristaltic contractions during go-phases was by about 20 % higher for stage 1 than for stage 3 larvae (Fig. 7C). As expected from their smaller body size, the absolute speed during go-phases was much slower for stage 1 than for stage 3 larvae (Fig. 7D; see also Fig. S4A). Notably, from a 4-fold difference in absolute speed during go-phases only a minute difference remains when considering speed relative to body length (Fig. 7E).

Stage 1 larvae were much more likely to be observed in a bent body posture than stage 3 larvae (Fig. 7F); for example, stage 1 larvae were found to be bent by 30 °or more in about 30 % of the frames, while for stage 3 larvae this was the case for only 10 % of all frames. Also, turn rate was much higher in stage 1 than in stage 3 larvae (Fig. 7G). In effect, stage 1 larvae gained less relative distance from their site of origin than stage 3 larvae (Fig. 7H). This reduced 'exploration range' in stage 1 larvae, even

when normalized to body length, manifests largely by differences in bending and turning behaviour (Fig. 7F, G), rather than in speed (Fig. 7E).

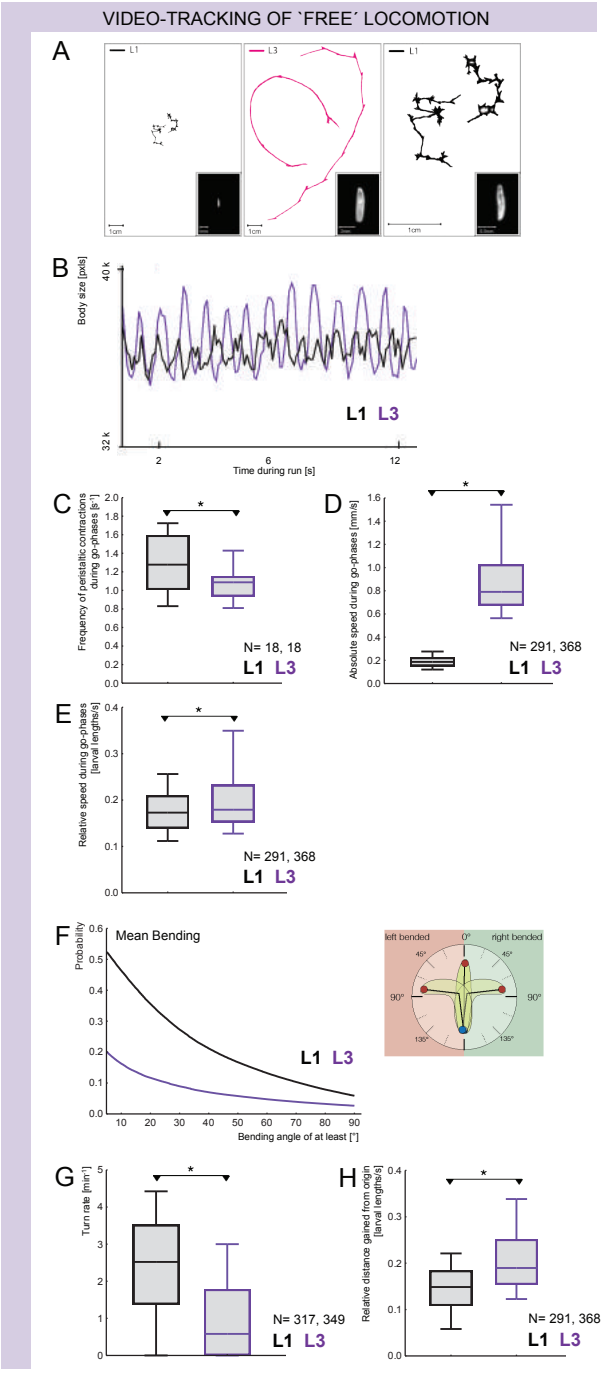

Figure 7: Video-tracking of 'free' locomotion.
A Examples of tracks of individual larvae from FIMTrack. Tracks of two stage 1 larvae (L1, black) and two stage 3 larvae (L3, magenta) under free crawling conditions. Images of stage 1 larvae are scaled to represent them at the same absolute size (L1, left), or at the same relative size (L1, right) as stage 3 larvae (L3, middle).
B-E Characterization of go-phases. (B) Example plots of body size over time indicating peristaltic contractions during a go-phase for stage 1 larvae (L1, black) and stage 3 larvae (L3, magenta). Note the slightly less regular organization of peristalsis in stage 1 compared to stage 3 (see also Movie 3). (C) Frequency of peristaltic contractions during go-phases, derived from the temporal maxima in body size of stage 1 (L1, black-line box plots) and stage 3 (L3, magenta-line box plots). Peristaltic contraction frequency is higher in stage 1 as compared to stage 3. (d, e) Absolute (D) and relative (E) speed during go-phases in stage 1 (L1, black-line box plots) and stage 3 (L3, magenta-line box plots). Absolute speed is much less in stage 1 than in stage 3. This difference is strongly reduced when considering speed relative to body length. * refers to $P<0.05$ in MWU comparisons between L1 and L3.
F-H Characterization of bending, turns and 'exploration range'. (F) Probability distribution of frames with bending angles ≥ 5 ° for stage 1 and stage 3 larvae (L1, black line and L3, magenta line). In stage 1 the likelihood to observe animals in a bent state was higher than in stage 3 for all considered bending angles. (G) Turn rate of stage 1 larvae (L1, black-line box plots) is substantially higher than in stage 3 larvae (L3, magenta-line box plots). (H) The gain in their relative distance to origin is less in stage 1 than in stage 3 larvae. This suggests a smaller 'exploration range' in stage 1 than in stage 3, even when considered relative to body length. * refers to $P<0.05$ in MWU comparisons between L1 and L3.
Sample sizes are given within the figure.

Video-tracking of thermotaxis

Stage 1 larvae as well as stage 3 larvae crawl away from their starting position at the

hot 33 °C isothermal line and reduce their distance to the colder side linearly during the observation period (Fig. 8A, B; Movie 8, Movie 9). While navigating away from the heat, stage 1 and stage 3 larvae show a median bearing of about 62 °and 58 °towards the cold side, respectively (Fig. 8C). In other words, both stage 1 and stage 3 are typically oriented obliquely to the isothermal lines of 29 °C and 18 °C respectively, with stage 1 doing slightly higher-amplitude zig-zagging during go-phases and being oriented towards the 'wrong', hot side slightly more often.

Absolute speed of stage 1 larvae in the heat gradient is about 3-fold lower compared to stage 3 larvae (Fig. 8D); when considering speed normalized to body length, however, stage 1 larvae appear to move faster (Fig. 8E). Indeed, when comparing speed under free crawling conditions versus in the heat gradient, speed is approximately 50 % higher in the heat gradient for stage 1 larvae (Fig. 7D, E versus Fig. 8D, E), while stage 3 larvae do not show higher speed in the heat gradient (Fig. 7D, E versus Fig. 8D, E).

Stage 1 larvae were much more likely to be observed in a bent body posture than stage 3 larvae also in the heat gradient (Fig. 8F); for example, stage 1 larvae were found to be bent by 30 °or more in about 25 % of the frames, while for stage 3 larvae this was the case for only about 7 % of all frames. Also, turn rate was much higher in stage 1 than in stage 3 larvae (Fig. 8G). In effect, stage 1 larvae gained less relative distance from their site of origin than stage 3 larvae (Fig. 8H). While in principle this matches what was observed under free crawling conditions (Fig. 7F-H), we note that the distance to origin that the animals gained per min was massively enhanced during thermotaxis, in particular for stage 1 but also for stage 3 larvae (Fig. 7H versus Fig. 8H).

Thus, within a heat gradient behaviour is obviously oriented for both stage 1 and stage 3 larvae. Stage 1 larvae appear more sensitive to the heat gradient, as the heat-induced modulation of speed and the heat-related gains in distance from origin appear more prominent.

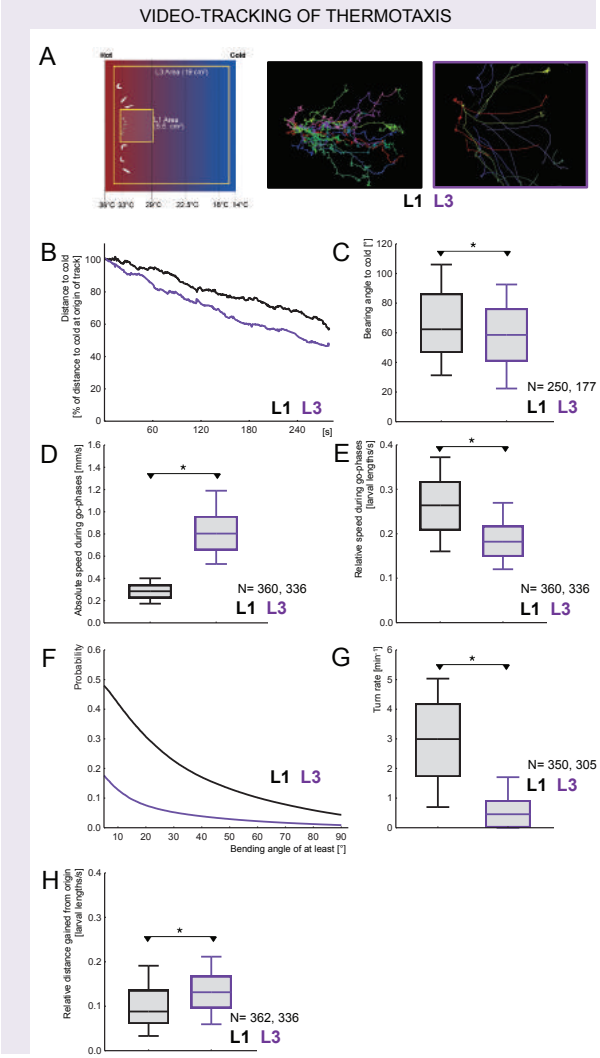

Figure 8: Video-tracking of thermotaxis.
A Sketch of the thermotaxis setup (left). Note that corresponding to the 4-fold differences in body length between stage 1 and stage 3 larvae, the area for stage 3 larvae is 4-fold larger than for stage 1 larvae. The heat gradient is linear; the covered temperatures are aversive for the respective stages within the observation areas delineated for stage 1 and stage 3. The two rightmost panels show screen-shots of the final frames of Movies 8 and 9 with tracks of stage 1 and stage 3 larvae (L1 and L3, respectively). Dimensions were normalized to body length.
B Median distance to the cold side over time, with the distance at the origin of the tracks defined as 100 % distance for both stage 1 larvae (L1, black line) and stage 3 larvae (L3, magenta line).
C-E Characterization of go-phases in a linear heat gradient. (C) Bearing angle to the cold side of stage 1 (L1, black line) and stage 3 (L3, magenta line). Absolute (D) and relative (E) speed during go-phases in stage 1 (L1, black-line box plots) and stage 3 larvae (L3, magenta-line box plots). Absolute speed is much less in stage 1 than in stage 3. This difference is reversed when considering speed relative to body length. * refers to $P<0.05$ in MWU comparisons between L1 and L3.
F-H Characterization of bending, turns and 'exploration range' in a linear heat gradient. (F) Probability distribution of frames with bending angles ≥ 5 ° for stage 1 and stage 3 larvae (L1, black line and L3, magenta line). In stage 1 the likelihood to observe animals in a bent state was higher than in stage 3 for all considered bending angles. (G) Turn rate of stage 1 larvae (L1, black-line box plots) is substantially higher than in stage 3 larvae (L3, magenta-line box plots). (H) The relative distance to origin is less in stage 1 than in stage 3 larvae. This suggests a smaller 'exploration range' in stage 1 than in stage 3, even when considered relative to body length. * refers to $P<0.05$ in MWU comparisons between L1 and L3.
Sample sizes are given within the figure.

Video-tracking of light avoidance

When encountering the dark-light border zone, stage 1 and stage 3 larvae show avoidance behaviour at strikingly different probabilities. That is, 56.7 % of such encounters resulted in retraction for stage 1 larvae (212/ 374 encounters; Fig. S5B and C, Movie 10), while for stage 3 larvae this was observed for only 31.3 % of cases (167/ 534 encounters; Fig. S5B, C, Movie 11). This suggests that stage 1 larvae are more light averse than stage 3 larvae.

Video-tracking of chemotaxis

When located close to an odour source, both stage 1 and stage 3 larvae remained in the vicinity of that odour source, resulting in 'ball-of-wool' trajectories (Fig. 9A, A') not seen in the absence of odour (Fig. 9A"). We described tracks as sequences of runs and turns (Fig. 9B-B"). Mapping these tracks onto the respective reconstructed olfactory experience suggests that turns typically take place after the larvae moved down the odour gradient for some time, and that after a turn they move up the odour gradient (Fig. 9C, C'). In other words, turns reorient the larva up the odour gradient and thus eventually towards the odour source (behaviour in the absence of odour, i.e. in a 'fictive' odour gradient from a 'fictive' odour source located at a corresponding point in the arena, was confirmed to be random in this respect: Fig. 9C"). Indeed, the average olfactory experience during the 15 s preceding a turn consists of negative changes in odour concentration; under such conditions head casts towards the odour entail a large and sudden rise in odour concentration such that this new direction is accepted and a turn is implemented (Fig. 9D, D'). Thus, turning manoeuvres result in a positive change in stimulus intensity in both stage 1 and stage 3 larvae. This was confirmed to not be the case for turns in the no-odour condition relative to a fictive odour source (Fig. 9D"), although turning manoeuvres with similar kinematics do take place under such conditions, too (see below, Fig. 9F"). Specifically, in the presence of an odour source stage 1 larvae turned towards the local odour gradient in 79.4 % of the cases (114 turns towards the odour source of 29 larvae), while in the absence of a real odour source the larvae implemented the expected approximately 50 % of their turns towards a fictive odour source (85 turns towards such fictive odour source of 20 larvae) ($P<0.005$, two tailed t-test, data not shown). Parametrically, and as found in previous work on stage 3 larvae [Gomez-Marin et al., 2011], the probability at which larvae of either stage turned towards the left side was highest whenever the odour gradient was pointing up to their

left (i.e. at bearings values close to 90°: Fig. 9E, E') and lowest whenever the odour gradient was pointing up to their right (i.e. at bearings values close to -90°: Fig. 9E, E'). This was not observed in the absence of odour relative to a fictive odour source (Fig. 9E").

As for the kinematics of the turns, both stage 1 and stage 3 larvae show a reduced forward-speed of centroid movement immediately before a turn (Fig. 9F, F'); as expected from the smaller size of stage 1 larvae, this deceleration was less in stage 1 than in stage 3 larvae. Both stage 1 and stage 3 larvae then initiated a head cast, characterized by a sharp increase of head-speed caused by lateral movement of the head (Fig. 9F, F'). The same kinematics of turning were observed for turns performed in the absence of odour (Fig. 9F").

In addition to the turns analysed above, chemotaxis in stage 3 larvae was reported to involve continuous slight bending of runs toward the local odour gradient a process termed weathervaning [Gomez-Marin and Louis, 2014]. We found that also stage 1 larvae, just like stage 3, bias their runs in this way. Specifically, we observed a correlation between the instantaneous reorientation rate during runs versus the bearing angle between the direction of motion and the direction of the odour source (Fig. 9G, G'); as expected, no such relationship was observed in the absence of odour relative to a fictive odour source (Fig. 9G"). We note a trend in the weathervaning without an odour source, such that the larvae tend to bias their runs towards their right. This may hint at a handedness of larval turning behaviour in stage 1 larvae. Indeed, a weak trend suggesting such right-handedness was previously observed in stage 3 larvae, too (Gomez-Marin and Louis [2014], loc. cit. figure 1D).

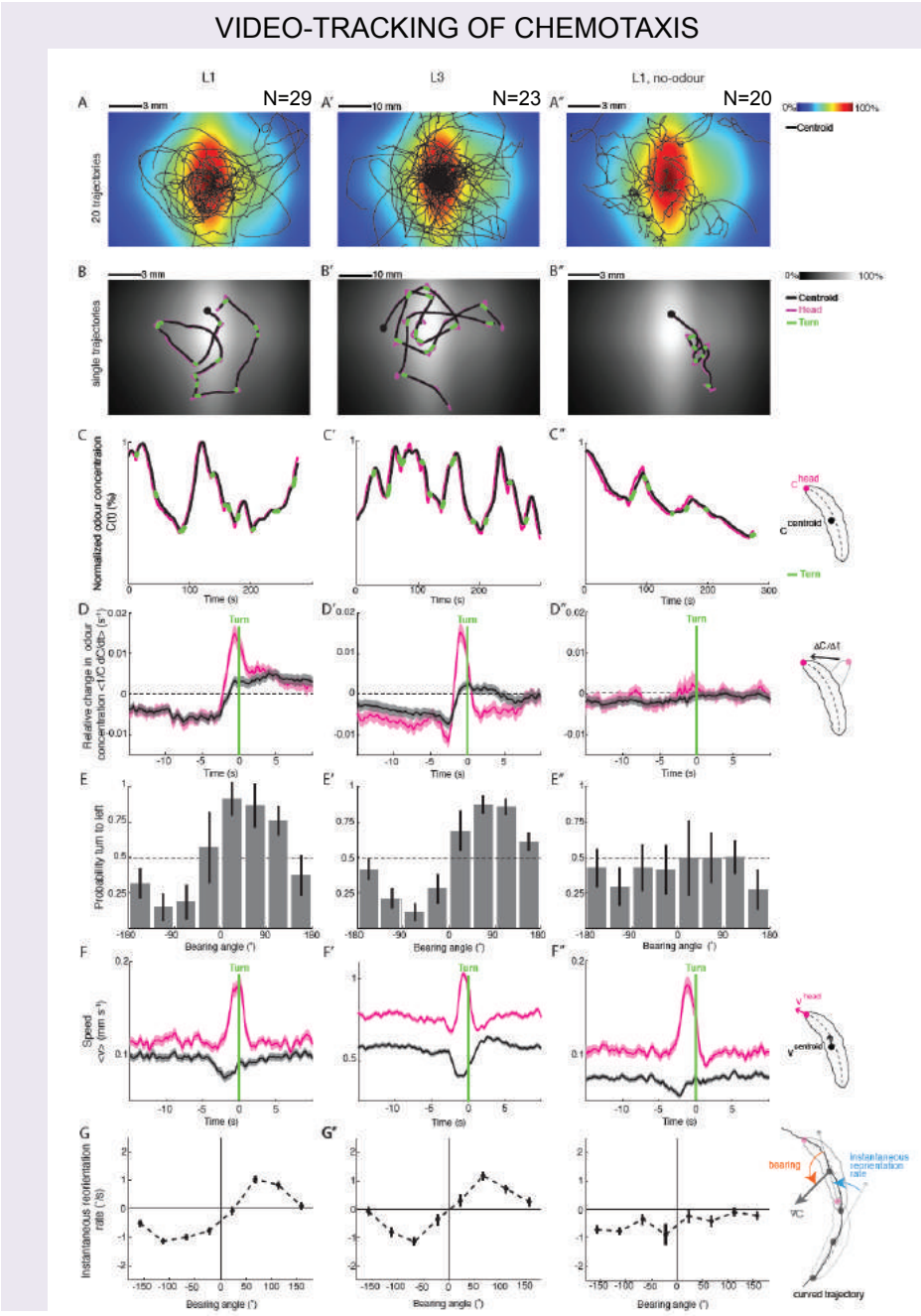

Figure 9: Video-tracking of chemotaxis. *(See next page).*

Figure 9: *Continues from prior page.* **A-A"** Example tracks, based on centroid positions, for stage 1 larvae (A) and stage 3 larvae (a') in a reconstructed odour gradient visualized by the colour scale. (a") shows tracks of stage 1 larvae in the absence of odour, i.e. in this case the colour code indicates a 'fictive' odour landscape.
B-B" Example trajectories of individual larvae in the three experimental conditions. The starting positions are marked with a dot. The trajectory of the centroid is shown in black; the trajectory of the head is shown in magenta. Positions corresponding to turns are marked in green.
C-C" Time courses of concentrations corresponding to the example trajectories shown in (B-B"). Turning manoeuvres are typically implemented after a prolonged period of moving down the odour gradient, both in stage 1 and in stage 3 larvae (C, C'). In the absence of odour, no such relationship is observed relative to a fictive odour source (c").
D-D" Turn-triggered averages of the relative changes in odour concentration at the centroid (black) and at the head (magenta). When moving down-gradient, the beginning of the turning manoeuvre in both stage 1 and stage 3 larvae is associated with a sharp rise in odour concentration at the head, corresponding to a head cast toward the odour source. This entails acceptance of the new direction and completion of the turning manoeuvre (C, C'). Note that turning manoeuvres in the absence of an odour (f") do not show these features relative to a fictive odour source (c").
E-E" Within an odour gradient, turns are more likely to take place towards than away from the odour, in both stage 1 and stage 3 larvae (e, e'). Upon the used convention, for positive bearings left turns reorient the larva up the odour gradient, i.e. effectively towards the odour source. Such turns were most likely for bearing angles around 90°, that is when the larvae were oriented perpendicularly to the odour gradient. For negative bearings, turns towards the right reorient the larvae up the odour gradient; these are most frequent at -90°. In the absence of odour, no such relationship is observed relative to a fictive odour source (e"). Error bars represent an estimate of the standard error calculated based on a bootstrap procedure.
F-F" Turn-triggered averages of head speed (magenta) and centroid speed (black) during turning manoeuvres. Before a turn, centroid speed declines, while head speed increases. This is the case for both stage 1 and stage 3 larvae navigating in an odour gradient (F, F') - and is also true for turning manoeuvres in the absence of odour (f"). Error bars show the confidence interval (5th-95th percentile). Mind the approximately 5-fold higher speed in stage 1 (F, F") than stage 3 larvae (f').
G-G" Trajectories during run periods in an odour gradient are often bent up the odour gradient, i.e. towards the odour source (A, A'). To quantify the underlying behaviour, weathervaning was measured as the relationship between the average instantaneous reorientation rate and the local bearing angle. This shows that both stage 1 and stage 3 larvae bent their runs most strongly toward the odour source when oriented perpendicularly to it, i.e. at bearings of +/- 90°. Error bars show the confidence interval (5th-95th percentile).
Sample sizes are given within the figure.

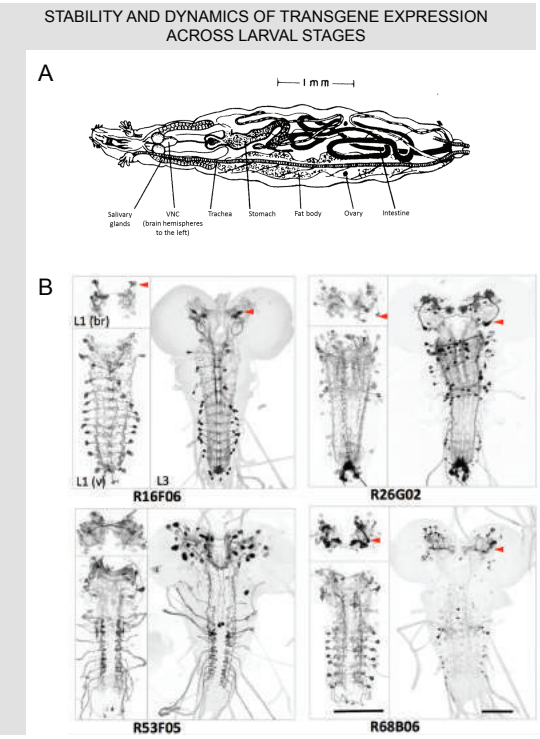

Figure 10: Stability and dynamics of transgene expression across larval stages.
A Schematic overview of the body plan and internal organs of a stage 3 larva (modified from Demerec and Kaufmann [1972]; image courtesy of The Carnegie Institution).
B Confocal projections of stage 1 and stage 3 larval nervous systems (L1 and L3, respectively) for four different driver strains of the Janelia collection [Li et al., 2014]. For L1, separate projections are provided for the brain (br) and the ventral nervous system (v). The chosen strains maintain expression, visualized via anti-GFP staining of brains from crosses of the indicated driver strains with UAS-GFP, in many of the same neurons throughout larval stages. R16F06 shows expression in the AVM011 interneurons of the brain (arrowhead) and in two pairs of segmentally repeated interneurons. R26G02 shows expression in the APL neuron (arrowhead) that innervates the mushroom bodies. R53F05 expresses in a variety of brain interneurons and segmental sensory neurons, and R68B06 in embryonic-born Kenyon cells of the mushroom bodies (arrowhead). In the latter line, expression in the segmental interneurons is largely lost before stage 3 is reached. In other cases, additional expression may be seen in stage 3 (not shown). Indeed, expression patterns often are dynamic across larval stages [Li et al., 2014], such that they must be ascertained on a case-by-case basis. The scale bar represents 100 µm.

4.4 Discussion

In a community-approach featuring 15 types of behavioural experiment, comprising contributions from 37 scientists of 12 labs, we have probed stage 1 *Drosophila* larvae for various behavioural faculties that had previously been described for stage 3 larvae. With few exceptions, our results suggest qualitative concordance of behaviour in stage 1 and stage 3 larvae.

Before going into detail, we would like to stress that this suggestion of concordance is necessarily based on a lack of evidence for qualitative differences in behaviour between stage 1 and stage 3 larvae. This must not be confused with an evidence for the absence of such differences. Indeed future studies using other or refined methods may well uncover qualitative differences in behaviour between stage 1 and stage 3 larvae. Still, the fact that across most of the presently used assays no such differences were uncovered does suggest quite some stability of behavioural organization across larval stages. Is this surprising?

During the 5-7 days between larval hatching and pupariation, larval *Drosophila* increase by well 60-fold in mass (considering approximated body proportions of 1 mm x 0.25 mm x 0.25 mm = 0.0625 mm3 in stage 1 larvae and 4 mm x 1 mm x 1 mm = 4 mm3 in stage 3). If mass increase took place at a 60-fold rate per week in humans and assuming a birth weight of 3.5 kg, parents would face a gargantuan 210 kg baby after the first post-partum week. In other words, finding food and feeding are important to a larva, and shape the organization of its behaviour and body plan. Indeed, the larval nervous system is considerably smaller than its salivary glands (Fig. 10A). The larval nervous system as established upon hatching thus must be immediately 'ready for life' not only in supporting an immediate competitive feeding frenzy, but also to cope with a massively growing body. For the most part, this seems to be accomplished by the

growth of neurons. At only some sites of the brain, such as the antennal lobe body and most drastically the mushroom body [Ito and Hotta, 1992], it has been observed that further neurons continue to be knitted into the circuit and become functional during larval life. Furthermore, in Figure 10B examples of stable as well as dynamic transgene expression across larval stages are presented, speaking to both stability and dynamics of gene regulation as related to the employed driver elements. Based on our present results, and as we think surprisingly, the changes in body size and in the size and number of neurons seem largely inconsequential for larval behaviour - with the only apparent exceptions pertaining to the speed of locomotion, salt- and light-related behaviour. These exceptional cases of discordance are discussed below, in relation to their possible neurogenetic bases (regarding the cases of concordance between stage 1 and stage 3 behaviour, we refer the reader to the references cited in the Introduction and Results sections).

Speed of locomotion

Stage 1 larvae are about 4-fold slower in absolute speed than stage 3 larvae (Fig. S4A, 7D, 9F, F'). Behavioural measures of stage 1 larvae not taking into account their slow speed may therefore yield systematically lower scores. This can be remedied by normalizing the data to speed, by using a scaled-down experimental set up and/ or by using paradigms that allow sufficient time until scores are taken.

We note that maintaining accuracy in behaviour at higher speed in stage 3 larvae demands a better signal to noise ratio in neuronal processing, and that this may be one of the reasons why functionally redundant larval-born neurons are knitted into the embryonic-born circuits (see section *Brain organization* below). The same applies for the larva-to-adult transition.

Salt-related behaviour

Stage 1 larvae appear more sensitive to salt than stage 3, in a way that cannot be

explained by differences in the speed of locomotion. This is the case for innate gustatory preference behaviour towards salt (Fig. 2F, G, Fig. S1) and for the effects of salt as reinforcer (Fig. 3D, E) (also see Niewalda et al. [2008]; Russell et al. [2011]). That is, avoidance of and aversive learning about salt observed for stage 3 larvae is seen earlier during the experiment, is stronger, and/ or is observed already at lower concentrations in stage 1. This higher sensitivity to salt may partially be caused by an unfavourable surface to volume ratio in stage 1, leading to higher sensitivity to desiccation stress. Also, the cuticle of stage 1 larvae is softer than in stage 3. Thus, micro-lesions of the cuticle caused by handling will be more likely and in combination with a possible itching upon salt application will be of more impact for stage 1 than for stage 3 larvae. Furthermore, developmental differences in the expression of salt sensors, and/or in the wiring of salt-sensitive sensory neurons and their downstream circuits may be reckoned with.

Light-related behaviour

The present data suggest that stage 1 larvae are more light averse than stage 3 larvae. That is, in the employed light-annulus assay the likelihood of a retraction response when encountering a dark-light border is almost twice as high for stage 1 as for stage 3 larvae (Fig. S5B, C). Interestingly, the preference scores from a light-dark quadrant assay measured after light-electroshock training are not apparently more negative for stage 1 than for stage 3 larvae (Fig. 5B) [Sawin-McCormack et al., 1995]. This could imply that in the latter type of assay more time needs to be allowed for stage 1 larvae to reveal the full extent of their light avoidance, and/ or of light-electroshock associative memory. In other words, what appears to be an inability to form light-electric shock associations in stage 1 larvae may partially reflect that assay conditions are suboptimal for stage 1, revealing but a weak trend for aversive memory (Fig. 5). Data on the behaviour of stage 1 larvae in a light gradient are not yet available.

Considering that in addition to suboptimal assay conditions there may be 'true' biological reasons for the poor light-electroshock association scores in stage 1, we note that stage 1 larvae are capable of learning with electroshock as punishment if odours are used for association [Aceves-Piña and Quinn, 1979]. This implies that it may be visual processing, rather than electric shock processing, which is not permissive for association formation. In this context it seems relevant that serotonergic neurons innervating the larval optic neuropil start to form extensive ramifications only in late, wandering stage 3 larvae [Mukhopadhyay and Campos, 1995]; this innervation has previously been related to the loss of light avoidance upon the transition from feeding- to wandering-stage 3 [Sawin-McCormack et al., 1995]. Also, the larval mushroom body lacks serotonergic innervation [Blenau and Thamm, 2011; Giang et al., 2011; Huser et al., 2012]; specifically, the serotonergic CSD neuron is present in larvae, yet is innervating the mushroom bodies only after metamorphosis [Huser et al., 2012; Roy et al., 2007]. It is therefore tempting to speculate that alterations in serotonergic signalling may be partially responsible for differences in light aversion and/ or light-electroshock associative learning across larval stages, in particular as pupariation approaches. Changes in serotonergic signalling may also impact other behavioural alterations along the larval-pupal transition, such as changes in geotaxis, aggregation and locomotion.

Brain organization: The mushroom bodies as exceptional case

To date, surprisingly few discrepancies have been revealed between a stage 1 larval nervous system reconstructed at synaptic resolution from the electron microscope versus what was known before from studies based on light microscopy. Arguably the most significant of these discrepancies, in addition to what has been mentioned in the previous section regarding the serotonin system, relates to the mushroom body, a higher-order brain centre of the insects required for learning and memory [Heisenberg, 2003]. That is, the number of mushroom body-intrinsic Kenyon cells (KCs) increases

from about 100 in stage 1 [Eichler et al., 2017] to 800-1200 in stage 3 [Ito and Hotta, 1992]. In no other case have similarly massive increases in neuron number during larval stages been reported. If the added KCs were simply redundant to the already existing ones, one may interpret this as reflecting the need for a better signal to noise ratio in stage 3 larvae because of their higher speed of locomotion. Interestingly, however, a group of about 20 early-born KCs qualitatively differs from the later-born ones in their connectivity to the second-order sensory projection neurons (PNs) that map sensory information onto the KCs. That is, each early-born KC has but one claw, a postsynaptic specialization at which it connects to but one PN. In turn, PNs connect to but one such early-born KC, plus, later on, a random set of about 4-8 later-born KCs. These later-born KCs typically sample 2-6 PNs. Thus, for the earliest set of PN-KC connections a 1:1 connectivity makes sure that all PNs get fairly sampled. Once this is achieved, combinatorial and randomized PN-KC connections are added to fine-tune the sensory representation across the KCs. This implies that mushroom body function in stage 1 larvae is more narrowly constrained by a 1:1 PN-KC connectivity than is the case in stage 3 larvae. As far as associative olfactory learning abilities are concerned, this does not seem to lead to qualitative differences in mnemonic ability between stage 1 and stage 3 (Fig. 3) [Aceves-Piña and Quinn, 1979; Heisenberg et al., 1985; Scherer et al., 2003; Neuser et al., 2005; Niewalda et al., 2008; Gerber and Hendel, 2006; Pauls et al., 2010; El-Keredy et al., 2012; Schleyer et al., 2015a]. Clearly, however, differences in for example the stimulus-specificity of memory, in the ability to detect components from compound stimuli or the ability to discern stimuli from contextual background may be expected.

Taken together, despite massive growth there appears to be a phase of relative stability in brain organization between stage 1 and stage 3 larvae. Clearly, however, profound reorganization then takes place during the pupal stages and into early adulthood [Levine

et al., 1995; Truman, 1996; Consoulas et al., 2000; Tissot and Stocker, 2000]. As discussed above for the visual system as an example, much of this is indeed foreshadowed already at the end of larval life, as larvae develop out of feeding- and into wandering-stage 3 and pupa. These changes in behavioural and brain organization during the larval-pupal transition may warrant a separate survey.

In conclusion, our results show a striking match in the behavioural faculties of stage 1 and stage 3 larvae. Keeping due caveats in mind, it thus appears valid to interpret the behavioural faculties of stage 3 larvae in the context of the electron microscope-based synaptic connectome described for stage 1 - and vice versa.

4.5 Material & Methods

The aim of this study is to test stage 1 *Drosophila* larvae for their behavioural faculties, with a focus on assays that have been routinely used for stage 3 larvae. When designing the present experiments, three general considerations were borne in mind. Firstly, we wanted to employ methods of experimentation, data acquisition and analysis as similar as possible to the ones previously used for stage 3. These methods differ to some extent across assays and laboratories. Secondly, and conflictingly, we aimed at homogeneity of methods across the assays of this survey in order to allow meaningful comparisons across assays. Thirdly, in some cases it did not seem reasonable to use the very same experimental parameters for stage 1 and stage 3 larvae. For example, using the same parameters for nociceptive stimulation as in stage 3 would have been damaging if not lethal for stage 1 larvae. The below thus corresponds to the reasoned judgement of the contributing scientists as what is a reasonable balance between comparability of their respective assay to published work as well as between stages versus comparability

across the assays within this survey.

We first present general aspects of our methods regarding the larvae and statistics used. Then we will present counting-based assays, followed by assays based on video-tracking.

Larvae

We used stage 1 larvae from the Canton-S wild-type strain, aged 30 h (+/- 2 h) after egg laying. Three days before the experiment approximately 350 adult flies were transferred to apple juice agar plates (25 % juice and 1.25 % sucrose in 2.5 % agar solution), and maintained at 25 °C, 60-70 % relative humidity and a 12/ 12 h light/ dark cycle. One day before each experiment flies were allowed to lay eggs for 2 h on a fresh apple juice agar plate, and then removed. After 30 h we collected approximately 30 larvae from the apple juice plates, briefly rinsed them in a droplet of water and started the experiment. In cases when also stage 3 larvae were used, these were aged 5 days (120 h) after egg laying.

Exceptions to the above are mentioned along the description of the behavioural paradigms.

Statistics

Non-parametric statistics were applied throughout. For comparisons to chance levels (i.e. to zero) one-sample sign tests (OSS) were used (provided on www.fon.hum.uva.nl/Service/Statistics.html). For between-group comparisons, Kruskal-Wallis tests (KW) and Mann-Whitney U-tests (MWU) were employed as appropriate (Statistica 12 from StatSoft). We used a Bonferroni correction whenever warranted to maintain an error rate below 5 %. Data are displayed as box plots, where the middle line shows the median, the box boundaries the 25, 75 % quantiles, and the whiskers the 10, 90 % quantiles.

Exceptions to the above are mentioned in the respective figure legends.

Behavioural paradigms

Olfactory preference

We used Petri dishes of 55 mm inner diameter (Sarstedt, Nümbrecht, Germany), filled with freshly boiled 1 % agarose solution. Once solidified, dishes were stored until use at 4 ℃ for up to a week.

We added 10 µl of *n*-amyl acetate (AM, Merck, Darmstadt, Germany; CAS: 628-63-7) into Teflon containers of 5 mm diameter. These containers were then closed by a lid perforated with 5-10 holes, each of approximately 0.5 mm diameter and placed at the edge of the dish. The position of the container was varied (left, right, front, back) to average-out spurious effects of the experimental surround. AM was diluted in paraffin oil (1:50; paraffin oil: CAS: 8012-95-1; Merck, Darmstadt, Germany). Paraffin oil is without apparent behavioural significance as an odour [Saumweber et al., 2011].

We placed 30 larvae to the middle of each Petri dish and closed the lid. At the time point(s) mentioned along the Results section, we scored the number of larvae located either on the AM side, the other side, or a 10 mm-wide 'neutral' middle stripe. We calculated an olfactory preference index ($\text{Pref}_{Olfactory}$) as the difference between the number of larvae on the AM side (#AM) minus the number of larvae on the other side (#) and divided this difference by the total number of larvae on the dish:

(1) $\text{Pref}_{Olfactory}$ = (#AM - #) / #Total

Thus, $\text{Pref}_{Olfactory}$ values were constrained between 1 and -1; positive values indicate preference for and negative values indicate aversion of AM. In a second set of experiments 1-octanol (OCT) (CAS: 111-87-5; Merck, Darmstadt, Germany) was used as odour.

Gustatory preference

We prepared Petri dishes of 55 mm inner diameter (Sarstedt, Nümbrecht, Germany) such that one side was filled with 1 % agarose solution that in addition contained e.g. fructose at a 2 mol/l concentration (FRU) (CAS: 57-48-7, purity 99 %, Sigma-Aldrich, Steinheim, Germany) while the other side was filled with 1 % agarose only (PURE). After preparation, Petri dishes were covered with their lids and left at room temperature until the experiment started later the same day.

The position of the tastant side was varied (left, right) to average-out spurious effects of the experimental surround. We placed approximately 30 (stage 1) or 15 (stage 3) larvae to the middle of these Petri dishes and closed the lid. At the time points mentioned along the Results section, we scored the number of larvae located either on the PURE side, the FRU side, or a 5 mm-wide 'neutral' middle stripe. We calculated a gustatory preference index ($\text{Pref}_{Gustatory}$) as the number of larvae on the fructose side (#FRU) minus the number of larvae on the pure side (#PURE) and divided this difference by the total number of larvae on the dish:

(2) $\text{Pref}_{Gustatory}$ = (#FRU - #PURE) / #Total

Thus, $\text{Pref}_{Gustatory}$ values were constrained between 1 and -1; positive values indicate preference for and negative values indicate aversion of fructose. In addition, experiments were performed as above for fructose, except that either 2 mol/l arabinose (ARA) (CAS: 10323-20-3, purity 99 %, Sigma-Aldrich, Steinheim, Germany), or 2 mol/l sorbitol (SOR) (CAS: 50-70-4, purity 98 %, Sigma-Aldrich, Steinheim, Germany), or 5 mmol/l quinine hemisulfate (QUI) (CAS: 6119-70-6, purity 92 %, Sigma-Aldrich, Seelze, Germany), or 10 mmol/l aspartic acid (ASP) (CAS: 56-84-8, purity $\geq$ 99 %, Sigma-Aldrich, Steinheim, Germany), or sodium chloride (NaCl) (CAS: 7647-14-5, purity $\geq$ 99.5 %, Roth, Karlsruhe, Germany, at the concentrations mentioned along the

Results section) was used.

Odour-tastant associative learning: fructose and aspartic acid

We followed standard methods for a two-odour, reciprocal conditioning paradigm (Scherer et al. [2003]; Neuser et al. [2005]; for detailed protocols see Gerber et al. [2010, 2013]; Apostolopoulou et al. [2013]). Adapted to the small size of stage 1 larvae we used smaller Petri dishes (55 mm diameter) than is standard for stage 3 larvae (90 mm), filled with either only 1 % agarose (PURE), or with 1 % agarose plus fructose (FRU; 2 mol/l) as reward. Olfactory choice performance of larvae was compared after either of two reciprocal training regimen: one set of larvae received *n*-amyl acetate (CAS: 628-63-7; AM; Merck, Germany, diluted 1:50 in paraffin oil) together with fructose as reward (+) and 1-octanol (CAS: 111-87-5; OCT; Sigma-Aldrich, Germany; undiluted) without reward (AM+/OCT; this cycle of 5 min/ 5 min training trials was performed for a total of 3 times). The other set of larvae underwent reciprocal training (AM/OCT+). The sequence of training trials was balanced across repetitions of the experiment (i.e. OCT/AM+ and in the reciprocal case OCT+/AM). Then, animals were tested for their relative preference between AM versus OCT. They were placed to the middle of a Petri dish equipped with AM on the one side and OCT on the other side. After 3 min their numbers (#) were scored as on the AM side, the OCT side, or at the middle, and preference scores calculated as:

(3) PREF = (#AM - #OCT) / #Total

Appetitive associative memory is indicated by a relatively higher preference for AM after AM+/OCT training compared to the reciprocal AM/OCT+ training. These differences in preference were quantified by the associative performance index (PI):

(4) PI = (PREF$_{AM+/OCT}$ - PREF$_{AM/OCT+}$) / 2

Thus, positive PI values indicate appetitive memory and a rewarding effect of the tastant, while negative PI values would indicate aversive memory and a punishing effect of the tastant. In stage 3 larvae it was shown that the preference for the previously rewarded odour is a form of learned search behaviour, such that the location of the odour source during the test informs the animal about the likely location of the reward. Fittingly, such learned search is abolished if the test is performed in the presence of the sought-for reward (Gerber and Hendel [2006]; Saumweber et al. [2011]; Schleyer et al. [2011, 2015a,b]: also see Schleyer et al. [2013]). To determine whether the same organization of behaviour is found in stage 1 larvae, we ran the test after the above training regimen either in the absence or in the presence of fructose throughout the testing Petri dish.

The same type of behavioural paradigm was used for 10 mmol/l aspartic acid (ASP; (CAS: 56-84-8, purity $\geq$ 99 %, Sigma-Aldrich, Steinheim, Germany)) as reinforcer.

Odour-tastant associative learning: quinine and salt

The behavioural paradigm followed the methods as described above for odour-fructose and odour-aspartic acid learning, except that 5 mmol/l quinine (QUI; CAS: 6119-70-6; Sigma-Aldrich, Seelze, Germany) was used as reinforcer. Notably, in stage 3 larvae it was shown that 5 mmol/l quinine is an effective punishment. In particular, the preference for the previously non-punished odour is a form of escape behaviour that is expressed only when the testing situation indeed warrants escape, i.e. if the quinine punishment is present during the test (Gerber and Hendel [2006]; Schleyer et al. [2011, 2015a]; El-Keredy et al. [2012]; also see Schleyer et al. [2013]). To see whether the same organization of behaviour is found in stage 1 larvae, we ran the test after the above

training regimen either in the absence or in the presence of quinine throughout the testing Petri dish.

The same type of behavioural paradigm was used for 0.2 mol/l NaCl (salt; CAS: 7647-14-5; Roth, Karlsruhe, Germany) as reinforcer. Of note, in stage 3 larvae it was shown that low concentrations of salt can be rewarding, while high concentrations of salt can be punishing. Specifically, based on the literature concerning stage 3 larvae 0.2 mol/l salt is expected to be an effective reward, and learned search be abolished if the test is performed in the presence of that reward (Gerber and Hendel [2006]; Niewalda et al. [2008]; Russell et al. [2011]; also see Schleyer et al. [2013]). To see whether this is the case in stage 1 larvae, too, we ran the test after the above training regimen either in the absence or in the presence of salt throughout the testing Petri dish. As our results indicated that, unexpectedly, 0.2 mol/l salt is a punishment to stage 1 larvae, we repeated the experiment for stage 3 larvae as well; the same size of Petri dishes as for stage 1 larvae was used for these experiments.

Odour-DAN activation associative learning

Odour-DAN activation associative learning experiments were performed according to Rohwedder et al. [2016], with the modifications described in Eichler et al. [2017]. Double heterozygous stage 1 larvae of the experimental genotype express Chrimson as effector in dopaminergic neurons (DANs) innervating the mushroom body medial lobe. They were the offspring of a cross of PGMR58E02-GAL4attP2 (henceforth abbreviated as R58E02-Gal4; Liu et al. [2012]; Bloomington stock center no. 41347) and P20XUAS-IVS-CsChrimson.mVenusattP18 (henceforth abbreviated as UAS-Chrimson; Klapoetke et al. [2014]; Bloomington stock center no. 55134). Effector control larvae resulted from a cross of UAS-Chrimson and a strain carrying an empty attP2 landing site [Pfeiffer et al., 2008; Jenett et al., 2012]. Driver control larvae resulted from a cross of R58E02-Gal4 and a strain carrying an empty attP18 landing site [Pfeiffer et al., 2010].

Eggs were incubated at 25 °C in constant darkness on 4 % agarose with a yeast and water paste including retinal at 0.5 mM final concentration. At 40 h after egg-laying, groups of 30 individual stage 1 larvae were placed on plates filled with 4 % agarose. The odour ethyl acetate (EA; CAS: 141-78-6, Sigma-Aldrich, St-Louis, MO, USA, 100-times diluted in distilled water) was presented on filter papers located on the lid. In this situation, the larvae were exposed to constant red light from above (626 nm, 3.5 µW/mm2) (*) for 3 minutes. Subsequent to this EA*-trial, larvae were transferred to a new plate, and were left for 3 min without odour and in darkness (blank). This paired EA*/blank-training cycle was repeated two more times. A second set of larvae underwent reciprocal training with unpaired presentations of odour and red light (EA/*). The sequence of training trials was balanced across repetitions of the experiment (i.e. blank/EA* and in the reciprocal case */EA). Then, animals were tested for their relative preference for EA versus blank. They were placed to the middle of a Petri dish of 90 mm inner diameter equipped with EA on the one side and a blank filter paper on the other side. After 5 min, their numbers (#) were scored as on the EA side, the blank side, or at a 10-mm middle stripe, and preference scores were calculated as:

(5) PREF = (#EA - #blank) / #Total

Appetitive associative memory is indicated by a relatively higher preference for EA after EA*/blank training compared to the reciprocal EA/* training. These differences in preference were quantified by the associative performance index (PI):

(6) PI = ($PREF_{EA*/blank}$ - $PREF_{EA/*}$) / 2

Light/Dark-electric shock associative learning

The behavioural paradigm follows von von Essen et al. [2011], modified into a two-group paradigm. Adapted to the small size of stage 1 larvae we used 55 mm Petri dishes throughout (Greiner Bio-One, Wemmel, Belgium) filled with 1 % agarose (CAS: 3810.4, Roth, Karlsruhe, Germany). Petri dishes were equipped with two copper electrodes located at opposing sides of the Petri dish, through which 100 V shock could be applied (Müter RTT3, 0-270 V AC, 2.5 A, 675 W). For light stimulation, LEDs (OSRAM LED, 80012 White) were used at an intensity of 760 lux.

A cohort of larvae was transferred onto a Petri dish and light was switched on for 1 min (for stage 1 and stage 3 larvae about 45 and 25 animals, respectively, were used per cohort; this ensured that for both stage 1 and stage 3 about 20 animals remain for scoring during the test). During the last 30 s of this light stimulation the larvae were exposed to a continuous electric shock (+). Afterwards the light was switched off and the larvae were left untreated for 5 min (Light+/Dark training). This training cycle was repeated towards a total of 5 times (total duration of light exposure: 5 x 1 min = 5 min: sketch Fig. 5). A second group of larvae underwent Light/Dark+ training (total duration of light exposure: 5 x 5 min = 25 min: sketch Fig. 5). The sequence of training trials was balanced across repetitions of the experiment (i.e. either as above, or Dark/Light+ and Dark+/Light). Then the larvae were tested for their preference between light and dark on a testing Petri dish equipped with a modified lid such that two quarters were covered by black tape. They were placed to the centre of the testing Petri dish and after 5 min their numbers (#) were scored according to their location on a light or dark quadrant:

(7) PREF = (#Light - #Dark) / #Total

Memory is indicated by stronger light avoidance after Light+/Dark training than

after Dark+/Light training. This differences in preference was quantified by the performance index (PI):

(8) PI = ($PREF_{Light+/Dark}$ - $PREF_{Dark+/Light}$) / 2

As mentioned above, the total duration of light exposure was not equal between groups (5 min versus 25 min: sketch Fig. 5). Therefore, in order to test whether such differences in light exposure can in themselves lead to differences in light preference, a control experiment was run (for stage 3 larvae); it featured training-like handling and light exposure for both groups, yet omitted electroshocks.

Food intake

Larvae were raised and staged as described above except that a droplet of yeast paste was added to the apple juice agar plates used for egg laying. Also, the stage 3 larvae used were younger than indicated above, namely 96 +/- 1 h after egg laying. Stage 3 larvae were transferred from agar plates to vials containing standard fly food at 48 h after egg laying.

Larvae were washed and transferred onto apple juice-agar plates (stage 1: 30-40 larvae/plate; stage 3: 5 larvae/plate); these plates contained 0.1 g fluorescent yeast paste (0.3 % fluorescein sodium salt, Sigma Aldrich, order #F6377). Larvae were then left untreated for 5, 10, 20 or 30 min. All experiments were performed at 18 ℃. Afterwards larvae were removed, washed, and transferred onto an adhesive tape wrapped around a glass slide to incapacitate them. For image acquisition a fluorescence binocular (Olympus SZX 12) with mounted camera (F-View U-Tv1, Olympus; Software: CellF 2.8, Olympus) was used. ImageJ was used to calculate fluorescence intensity F of the whole larva by averaging over all pixel values for each individual larva. Fluorescence intensity data of individual larvae from the 10, 20, and 30 min time points were separately

normalized to the mean F of all individuals at time point 5 min for the stage 1 and the stage 3 data, respectively. Such separate normalization for stage 1 and stage 3 larvae is warranted because the size difference between them makes it necessary to adjust image acquisition (zoom) accordingly.

We note that incapacitating the larvae prior to image acquisition by exposure to high ($\sim$ 60 ℃) or low ($<$-20 ℃) temperature turned the larvae opaque, resulting in an impractically diffuse, low-contrast fluorescence signal.

We further note that using yeast coloured with crimson red powder, an assay that we previously used for stage 3 larvae [Schoofs et al., 2014] proved to be impractical in stage 1 as the staining in the gut was too weak (not shown).

Burrowing

For the burrowing assay, 10 larvae (either stage 1 or stage 3) were collected and placed onto the surface of a 60 mm-diameter tissue culture dish filled with yeast diet (180 g/l yeast, Lesaffre SAF-Instant Red #15909, #31105, and #31150, in 0.5 % agar). Larvae were left to forage and the percentage of larvae remaining on the surface of the food was determined at 0, 5, 15, 30 and 60 min.

Mechano-nociception

Strains of *Drosophila*, rearing conditions and staging procedures were as described above except that egg-laying was allowed for 2 h on 60-smm grape juice agar dishes at 25 ℃ and 70 % relative humidity and a 12/12 h light/dark cycle. Stage 3 larvae were staged and grown on yeast paste containing grape juice agar plates and assayed at 96 h +/- 2 h after egg laying.

Mechano-nociception assays were performed as described in Hwang et al. [2007] with some modifications. Stage 1 or stage 3 larvae were placed on a 100 mm, 2 % agar dish overlaid with 1 ml of distilled water to create a thin water-film on the agar surface. Straight-moving larvae were stimulated with a von Frey filament. In order to

be noxious without actually lesioning the larvae, stimulation was calibrated to exert a force of 20 mN for stage 1 and 50 mN for stage 3 larvae. Stimulation consisted of briefly (approximately 1 s) exerting the respective force to the dorso-lateral side of a mid-abdominal larval segment. Each larva was stimulated twice within several seconds. Only the response to the second stimulation was scored according to Hwang et al. [2007] as: No response, Stop, Stop and turn, or Rolling (360 °rotation along the body axis); in addition, Bending was introduced to score for an incomplete nociceptive response (simultaneous convulsive head and tail movements) that did not result in Rolling. In order to compare proportions of larvae displaying each type of behaviour at L1 versus L3 stages, we used two-tailed z-tests.

Touch

Strains of *Drosophila*, rearing conditions and staging procedures were as described in the previous section. Larvae were briefly (approximately 1 s) and gently brushed with an eyelash (kind gift of Assia Hijazi) on the T2 segment, which was identified by the presence of spiracles. Each larva was touched four times and the behaviour was scored according to Kernan et al. [1994] as: No response, Stop, Head withdrawal and turn, Backward wave and turn, Backward crawl and turn. In order to compare proportions of larvae displaying each type of behaviour at L1 versus L3 stages, we used two-tailed z-tests.

Rolling in response to optogenetic activation of Basin interneurons

Experiments on rolling upon Basin interneuron activation were performed using the experimental setup described by Ohyama et al. [2013] and follow the methods from Ohyama et al. [2015], with modifications described below.

Double heterozygous stage 1 larvae of the experimental genotype express Chrimson as effector in Basin interneurons. They were the offspring from the cross of male w[1118];PGMR72F11-Gal4attP2 (henceforth abbreviated as R72F11-Gal4; Ohyama

et al. [2015]; Bloomington stock center no. 39786) and female UAS-Chrimson (Klapoetke et al. [2014]; Bloomington stock center no. 55134), and were tested for rolling behaviour upon light stimulation. To obtain effector control larvae, female UAS-Chrimson flies were crossed to males of a strain carrying an empty attP2 landing site [Pfeiffer et al., 2008; Jenett et al., 2012] and assayed for rolling behaviour; R72F11-Gal4 larvae were used as driver control.

Eggs were incubated at 25 ℃ in constant darkness on standard fly food with retinal at 0.5 mM final concentration. For control experiments without retinal, larvae of the experimental genotype were grown on retinal free food. At 24-30 h after egg laying, individual stage 1 larvae were collected with 15 % sucrose and individually placed on a 4 % agar plate for video tracking as described in Ohyama et al. [2013]; the illumination required for tracking was provided by an infrared light array (850 nm). After a 30-s accommodation period, a red light stimulus (627 nm, 160 µW/mm2) was applied for 15 s. This 30 s / 15 s cycle was repeated 4 more times. If a larva could for technical reasons not be tracked during at least 4 of the stimulations of this protocol, its data was discarded (this happened in less than 10 % of the cases when image contrast was insufficient). From the tracked images, rolling behaviour was scored according to Tracey et al. [2003]. A larva was classified as 'Rolling' if it showed rolling behaviour at least once during the stimulation protocol.

Video-tracking of the response to 'Buzz' mechanosensory disturbance

To measure the locomotor changes by mechanosensory disturbance, we used the 'Buzz' setup described in Eschbach et al. [2011] and Saumweber et al. [2014] with minor changes to accommodate the small size of stage 1 larvae. Specifically, (i) a higher-resolution camera (Basler ace acA2040-90umNIR, Ahrensburg, Germany), ii) a new custom-written software, and (iii) agarose-filled Petri dishes of smaller diameter (90 mm) were used. In brief, either stage 1 or stage 3 larvae were tracked in groups

of about 20 with 10 such groups being assayed. After an accommodation period of 4.8 s, a single mechanosensory disturbance was delivered by a loudspeaker below the Petri dish (duration: 0.2 s, frequency: 100 Hz, defined as 'Buzz'). Following Eschbach et al. [2011] the baseline translational run speed and the baseline angular speed was determined for the 2 s before the Buzz, for each individual larva. Data from these individual larvae during the 4 s after Buzz onset then are expressed normalized to their individual baseline as relative translational run speed and relative angular speed, in 1-s bins. Negative scores thus indicate slowing down and turning less, respectively, while positive scores indicate speeding up and turning more.

Video-tracking of 'free' locomotion

Larvae were staged and maintained as described above, except that neither sugar nor juice were added to the yeast agar plate (5 % agar, food grade, CAS: 9002-18-0, Applichem, Darmstadt, Germany, with 0.125 % acetic acid, Sigma-Aldrich, Hamburg, Germany).

Tracking experiments were performed according to Risse et al. [2013, 2014]. In brief, cohorts of 18 - 22 stage 1 larvae were placed on a 55 mm x 55 mm test arena covered with 0.8 % agar (food grade, CAS: 9002-18-0, Applichem, Darmstadt, Germany). Upon their placement onto this test arena, the larvae were allowed a $\approx$ 2 min period to accommodate themselves until a 5 min window for data acquisition started, at 10 frames per s (Movie 3, top; Movie 4). The minimum track length analysed was 600 frames (1 min). A total of 16 larval cohorts yielded 294 tracks with a median track length of 1199 frames ($\approx$ 2 min).

Locomotion of stage 1 larvae was compared to stage 3 larvae (Movie 3, bottom; Movie 5). Stage 3 larvae are about four times larger than stage 1 (median body length stage 1: 1.29 mm; median body length stage 3: 5.10 mm; based on $>$300 larvae each). To obtain the same resolution in the recordings as for stage 1 larvae (40 pixels per larval

length), stage 3 larvae were filmed on a larger (225 mm x 225 mm) test arena. Also, as stage 3 larvae are quicker in overcoming their initial disorientation upon placement onto the test arena, the 5 min data acquisition window started already after a $\approx$ 1 min accommodation period. From 16 larval cohorts, this yielded 370 tracks with minimum track length of 600 frames (median: 1334 frames $\approx$ 2 min 13 s). These tracks were analysed using FIMTrack (fim.uni-muenster.de) and according to Otto et al. [2016] were classified into 'go' and 'reorientation' phases; data during collisions were not analysed. From the gathered tracks the following parameters were determined (see Risse et al. [2013, 2014], for details):

- frequency of peristaltic contractions during go-phases (based on the temporal distribution of body size);
- absolute speed during go-phases, and speed relative to larval length;
- probability distribution of bending angles across all recorded frames and larvae;
- turn rate (based on those transitions between go and reorientation phases that entailed a change in bearing of at least 30°);
- distance gained from origin, relative to larval length.

Video-tracking of thermotaxis

Larvae were staged and maintained as described in the preceding section.

Measurements of thermotaxis follow Risse et al. [2014]. In brief, a temperature gradient was established ranging from 38 °C to 14 °C in a 225 mm x 225 mm tracking area, with a linear range from 33-18 °C at a gradient of 0.08 °C/mm (Fig. 8A). Reflecting the differences in absolute size and exploration range (Fig. 7), the observation area for stage 3 larvae was a 190 m x 190 mm area within this linear range. For stage 1 larvae the observation area was 55 mm x 55 mm, spanning a 33-29 °C temperature range,

temperatures that are aversive to stage 1 and stage 3 larvae [Garrity et al., 2010].
Groups of 15 - 20 stage 1 or stage 3 larvae were placed along the 33 °C isothermal line. Stage 1 larvae were allowed 2 min to accommodate themselves until a 4 min 40 s window for data acquisition started, at 10 frames per s. The minimum track length analysed was 600 frames (1 min). A total of 15 cohorts of stage 1 larvae yielded 362 such tracks with a median track length of 1398 frames ($\approx$ 2 min 20 s).
Given that stage 3 larvae are quicker in overcoming their initial disorientation upon placement in the tracking area than stage 1 larvae, stage 3 were allowed only a 1 min accommodation period before data acquisition started. This yielded 336 tracks of $>$600 frames with a median track length of 1382 frames ($\approx$ 2 min 18 s).
Tracks were analysed using FIMTrack (fim.uni-muenster.de) and according to Otto et al. [2016] were classified into 'go' and 'reorientation' phases; data during collisions were not analysed. From the gathered tracks the following parameters were determined:

- median distance to the cold side of the observation area over time, with the origin of the respective track defined as 100 % distance (Fig. 8B); for stage 1 larvae the cold side corresponds to the 29 °C isothermal line, for stage 3 larvae it corresponds to the 18 °C isothermal line;
- bearing angle to the cold side during go-phases, taking the median of all frames of a given larva (Fig. 8C); a bearing angle of 0 °implies larvae are headed straight towards the cold side; 180 °implies they are headed straight to the hot side;
- absolute speed, and speed relative to larval length, during go-phases (Fig. 8D, E);
- probability distribution of bending angles across all observed larvae (Fig. 8F);
- turn rate (Fig. 8G), based on those transitions between go-/ reorientation-/ go-phases that entailed a change in bearing between the go-phases of at least

30°;

- distance gained from origin of track, relative to larval length (Fig. 8H).

Video-tracking of light avoidance

Larvae were staged and maintained as described in the preceding section.

The analysis of light avoidance follows Kane et al. [2013] and Risse et al. [2014]. In brief, a dark-light boundary was established using an LCD projector with a programmed light pattern (Fig. S5A). We projected an annulus of light (1450 Lux) onto a dark agar surface (80 Lux). Dimensions were adjusted to the body size of stage 1 and stage 3 larvae, respectively (stage 1: radius of the inner dark area rdark= 7.5 mm, width of light annulus w= 2.5 mm; stage 3: radius of the inner dark area rdark= 42.5 mm, width of light annulus w= 5.5 mm).

We placed 15-20 larvae to the middle of the dark area and allowed the larvae to move for 7 min. The location of the larvae was determined as the location of their centroid. To assess the probability at which the larvae show avoidance behaviour when encountering light, we identified animals that entered the dark-light border zone and then determined the number of animals moving back to the dark area versus those animals not doing so. The dark-light border zone was defined as a zone of one larval length between the dark and light area, of which two thirds are located in the dark and one third in the light area (rin = rdark - 2/3 larval length $\approx$ 6.9 mm for stage 1 and 39 mm for stage 3 larvae; rout = rdark + 1/3 larval length $\approx$ 8.6 mm for stage 1 and 44 mm for stage 3 larvae). The proportion larvae of that showed light avoidance behaviour at L1 versus L3 stages was compared with a two-tailed z-test.

Video-tracking of chemotaxis

Larvae were raised and staged as described above except that only 150-200 flies, of the w1118 genotype, were used for egg-laying. Molasses-apple juice agarose plates

with added yeast paste were used as a substrate. After collecting the larvae, they were briefly transferred onto an agarose Petri dish before testing.

The specifics of the chemotaxis assay and the tracking arena follow Gomez-Marin et al. [2011] (also see Louis et al. [2008a,b]). In brief, the top part of a rectangular plastic lid (Falcon 353958 rectangular plate lid, Corning Inc., USA) was coated with a layer of 3 % agarose (SeaKem, LE Agarose, Lonza, Switzerland) to later serve as the base of the chemotaxis arena. Next, a solution of odour diluted in paraffin oil was pipetted into a single 9 mm-well of a 96-well-plate lid (Falcon 353071 lid for 96 well plates, Corning Inc., USA). For stage 3 larvae, 10 µl of ethyl butyrate (CAS: 105-54-4, Fluka) (30 mM dilution in paraffin oil; CAS: 8012-95-1, Sigma Aldrich) were pipetted to one of the centrally located 9 mm-wells. To adjust for the smaller size of stage 1 larvae, we used a custom-made well with only 3 mm diameter and reduced the volume of odour solution to 3 µl. We note that without these adjustments, and using Canton-Special larvae, poor chemotactic performance was observed in preliminary experiments with stage 1 larvae (not shown). The lid with the odour droplet was flipped over and placed onto the first lid, creating a closed behavioural arena with the odour-source well-plate lid at the top and the lid with the agarose surface at the bottom. The arena remained closed for approximately 15 s, allowing an odour gradient to establish. Then, the top lid was briefly opened and a single larva was introduced into the centre of the bottom, agarose-coated lid. Tracking then lasted for a maximum of 5 min and automatically ceased as soon as a larva left the field of view. The arena was illuminated from above by a flat light pad (Slimlite Lightbox, Kaiser). We obtained and analysed 29 tracks for stage 1 larvae and 23 tracks for stage 3 larvae (Fig. 9A, A'). Reference measurements of locomotion of stage 1 larvae were also performed in the absence of odour (Fig. 9A"). Corresponding reference measurements in stage 3 larvae were presented before [Gomez-Marin et al., 2011]. In this non-odour condition, data was analysed relative to a 'fictive' odour located

at the same position as in the odour cases (rightmost column of panels in Fig. 9). Behaviour was recorded at 5 frames s^{-1} with a video camera below the setup. Tracking and image processing were performed with the SOS-track software [Gomez-Marin et al., 2012; Gomez-Marin and Louis, 2012, 2014]. The positions of head, tail, centroid and midpoint were extracted from every frame to calculate the kinematic variables of interest. Tracks were decomposed into runs and turns by the threshold rule of Gomez-Marin et al. [2011]; loc. cit. figure 2B) (Fig. 9B-B"); specifically, we set the threshold to identify the onset of a turning manoeuvre for stage 1 larvae to a reorientation speed of 9 $°s^{-1}$ and to 12 $°s^{-1}$ for stage 3 larvae. To compare behaviour between stage 1 and stage 3 larvae an odour gradient reconstructed for the stage 3 case Gomez-Marin et al. [2011] was normalized and scaled by a factor of 3 to reflect the smaller diameter of the odour source used for the stage 1 case. Conclusions regarding chemotaxis of stage 1 larvae remained unaltered if the original gradient was used for the analyses. That is, the scaling factor merely acts as a proxy for slight shape changes of the gradient in the set-up used for stage 1 larvae. Next, tracks were mapped onto the respective odour gradient to reconstruct the sensory experience of the larvae as it moved about the arena (Fig. 9C-C"). This way the turn-triggered-averages of the locally experienced odour concentration and the speed of the larvae before and after turns could be computed (Fig. 9D-D", F-F"). We calculated the probability of turning towards the left depending on the orientation of larvae towards the odour source (bearing). Upon the used convention, left turns reorient the larva towards the odour source when the bearing is larger than 0°; for bearings smaller than 0°, right turns reorient the larva towards the odour source. We relied on a bootstrap strategy to estimate a confidence interval in these turn probabilities calculated on the full dataset (Fig. 9E-E"); the standard error was calculated as described in Martinez and Martinez [2012]. To see whether the curvature of a track is correlated with the direction to the odour source, weathervaning was quantified as described in

Gomez-Marin and Louis [2014] through the instantaneous orientation rate separated across the bearing angle towards the odour source (Fig. 9G-G"); error bars represent the confidence interval (95 %) and were calculated by bootstrapping.

Immunohistology

Immunohistology related to odour-DAN activation associative learning

Males from the R58E02-Gal4 strain (Liu et al. [2012]; Bloomington stock center no. 41347) were crossed to females homozygous for pJFRC2-10XUAS-IVS-mCD8::GFP (henceforth abbreviated as UAS-GFP; Pfeiffer et al. [2010]; Bloomington stock center no. 32186). Larval tissues were dissected in phosphate buffered saline (PBS) added with 10 % normal goat serum and fixed for 30 min in 4 % paraformaldehyde at room temperature. After multiple rinses in PBS with 1 % Triton X-100 (PBS-TX), tissues were mounted on poly-lysine (CAS: 25988-63-0, Sigma-Aldrich, St-Louis MO, USA) coated coverslips, pre-blocked with 10 % normal goat serum in PBS-TX for 30 minutes, and incubated in rabbit anti-GFP IgG (1:1000; Abcam, ab290, Atlanta GA, USA) and mouse 1d4 anti-Fasciclin II (1:50; Developmental Studies Hybridoma Bank, Iowa City, IA, USA) in PBS-TX for 2 days at 4 ℃. After multiple rinses in PBS-TX, tissues were incubated for 2 days at 4 ℃ with Alexa Fluor 488 goat anti-rabbit and Alexa Fluor 633 goat anti-mouse IgG (1:500; Invitrogen, A-11008 and A-21052, respectively, Carlsbad CA, USA). Nervous systems were then washed three times in PBS-TX and mounted in antifade mountant (ProLong gold, Molecular probes, Eugene OR, USA). Immunolabeled nervous systems were imaged on a Zeiss 710 confocal microscope using their 40 x oil immersion objective (N.A. 1.4). Images of brains were assembled from a 2 x 1 array of tiled stacks, and with each stack scanned as an 8-bit image with a resolution of 512 x 512 and a Z-step interval of 1 µm.

Immunohistology related to rolling behaviour in response to optogenetic activation of Basin interneurons

Males from the R72F11-Gal4 strain (Bloomington stock center no. 39786) were crossed to females of the strain 10xUAS-HA;CyO/Sp;MKRS/TM6 (henceforth abbreviated as UAS-HA; Nern et al. [2015]). Brains were removed from stage 1 larvae and fixed in phosphate buffered saline (PBS) added with 10 % normal goat serum for 30 min in 4 % paraformaldehyde, at room temperature. After multiple rinses in PBS with 1 % Triton X-100 (PBS-TX), tissues were mounted on poly-lysine (CAS: 25988-63-0, Sigma-Aldrich, St-Louis MO, USA) coated coverslips, pre-blocked with 10 % normal goat serum in PBS-TX for 30 min, and incubated in rabbit anti-HA IgG (1:500; Cell Signaling Technology, C29F4 Danvers MA, USA) and mouse 1d4 anti-Fasciclin II (1:50; Developmental Studies Hybridoma Bank, Iowa City, IA, USA) in PBS-TX for 2 days at 4 ℃. After multiple rinses in PBS-TX, tissues were incubated for 2 days at 4 ℃ with Alexa Fluor 488 goat anti-rabbit and Alexa Fluor 633 goat anti-mouse IgG (1:500; Invitrogen, A-11008 and A-21052, respectively, Carlsbad CA, USA). Nervous systems were then washed three times in PBS-TX and mounted in antifade mountant (ProLong gold, Molecular probes, Eugene OR, USA). Immunolabeled nervous systems were imaged on a Zeiss 710 confocal microscope using a 63 x oil immersion objective.

Immunohistology related to stability and dynamics of transgene expression across larval stages

Males from the indicated GAL4 strains (Li et al. [2014]; R16F06-GAL4, R26G02-GAL4, R53F05-GAL4, R68B06-GAL4; Bloomington stock center no.s 48734, 48065, 50440, 39458) were crossed to females homozygous for P10XUAS-IVS-mCD8::GFPattP40 (Pfeiffer et al. [2010]; Bloomington stock center no. 32186). Larval tissues were dissected in phosphate buffered saline (PBS) and fixed for 1 hr in 4 % formaldehyde in PBS at room temperature. After multiple rinses in PBS with 1 % Triton X-100 (PBS-TX),

tissues were mounted on poly-lysine (CAS: 25988-63-0, Sigma, St. Louis, MO, USA) coated coverslips, pre-blocked with 3 % normal donkey serum in PBS-TX for 1 hr, and incubated in the following primary antibodies: rabbit anti-GFP IgG (1:1000; Invitrogen A11122), mouse anti-Neuroglian (1:50; BP104, Developmental Studies Hybridoma Bank, Iowa City, IA, USA), and rat anti-N-cadherin (1:50; DN-Ex #8, Developmental Studies Hybridoma Bank, Iowa City, IA, USA) in PBS-TX for 2 days at 4 ℃. After multiple rinses in PBS-TX, tissues were incubated for 2 days at 4 ℃ with the following secondary antibodies, all at 1:500 dilution and obtained from Jackson ImmunoResearch (West Grove, PA, USA): AlexaFluor 488 conjugated donkey anti-rabbit (#711-545-152), AlexaFluor 594 donkey anti-mouse IgG (#715-585-151), and AlexaFluor 647 donkey anti-rat IgG (#712-605-153). Nervous systems were then washed two to three times in PBS-TX, dehydrated through a graded ethanol series, cleared in xylene, and mounted in DPX (Sigma, St. Louis, MO, USA). Immunolabeled nervous systems were imaged on a Zeiss 510 confocal microscope using their 40 x oil immersion objective (N.A. 1.3). Images of each nervous system were assembled from a 2 x 3 array of tiled stacks, with each stack scanned as an 8-bit image with a resolution of 512 x 512 and a Z-step interval of 2 µm.

All experiments and analyses comply with applicable ethical regulations and law.

The data underlying the presented figures and used for statistical analyses are documented in Supplemental Table 1.

Assuming effect sizes were equal or moderately less in stage 1 relative to data published for stage 3 larvae, sample sizes were chosen to be equal or moderately higher relative to previously published sample sizes for stage 3.

4.6 Acknowledgements

We thank J. Herrmann for help with the FIM set-up (Münster), H. Reim, C. Tauber, J. Saumweber and B. Kracht for laboratory assistance (Magdeburg), Aljoscha Nern and Gerald Rubin (Janelia) for kindly providing the UAS-HA stock, and R. Glasgow, Zaragoza, Spain, for language editing.

Funding:

The Gulbenkian/ Melbourne group was supported by the Fundação para a Ciência e a Tecnologia (FCT) (post-doctoral fellowship to MJAC: SFRH/BPD/75993/2011; exploratory grant to MJAC and CKM: EXPL/BEX-BID/0497/2013).

The Münster group was supported by the Cluster of Excellence Cells in Motion (CiM) and the CiM International Max Planck research school (CiM-IMPRS).

The Barcelona group was supported by the Spanish Ministry of Economy and Competitiveness, 'Centro de Excelencia Severo Ochoa 2013-2017' (SEV-2012-0208), the CERCA Programme/Generalitat de Catalunya, the 'la Caixa' International PhD Programme, and the Spanish Ministry of Science and Innovation (BFU2011-26208).

The LIN-GoLM group received support from the Wissenschaftsgemeinschaft Gottfried Wilhelm Leibniz (WGL), the State of Sachsen-Anhalt, the Center for Behavioral Brain Sciences Magdeburg (CBBS), and the Otto von Guericke Universität Magdeburg (OvGU), as well as from the Deutsche Forschungsgemeinschaft (DFG) (CRC 779 Motivated behaviour: B11; GE1091/4-1), and the European Commission (FP7-ICT project Miniature Insect Model for Active Learning MINIMAL).

The Janelia group received support from the Howard Hughes Medical Institute (HHMI).

The Fribourg group was supported by a starter grant from the European Research Council (ERC-2012-StG 309832-PhotoNaviNet) and the Swiss National Science

Foundation (31003A_169993). The Hamburg group was supported by the Deutsche Forschungsgemeinschaft (DFG) (SPP 1926, Next generation optogenetics), and the Landesforschungsförderung Hamburg (LFF-FV27). The LIN-MolSysBiol group received support from the Wissenschaftsgemeinschaft Gottfried Wilhelm Leibniz (WGL), the State of Sachsen-Anhalt, the Center for Behavioral Brain Sciences Magdeburg (CBBS), and from the Deutsche Forschungsgemeinschaft (DFG) (CRC 779 Motivated behaviour: B15; YA272/2-1).

The Bonn group was supported by the Deutsche Forschungsgemeinschaft (DFG) (PA 787/7-1) and Cluster of Excellence ImmunoSensation.

The Konstanz group was supported by Deutsche Forschungsgemeinschaft (TH1584/1-1, TH1584/3-1), the Baden-Württemberg Stiftung, and the Zukunftskolleg of the University of Konstanz.

4.7 Author contributions

Developed the concepts or approach: BG, CKl, MP, AT.

Performed experiments and/or data analysis: Gulbenkian/ Melbourne: MJAC; Münster: BR, DB, NO, XJ; Barcelona: AB; LIN-GoLM: BM, EP, JK, MS, TN, TS, YcC; Janelia: CE, KE, NR; Fribourg: PF; Hamburg: MP, NH, PS; Magdeburg, PharmTox: CKö; LIN-MolSysBiol: AY; Bonn: AM, PS; Kyushu: DM, NT; Konstanz: NR; Washington: JT.

Prepared or edited the manuscript and figures: BG, TN, YcC, with input from all authors.

4.8 Supplemental information

Supplemental tables:

Supplemental Table 1: The table presents the data underlying the displayed figures and reported statistics.

Supplementary tables can be found on the accompanying DVD.

Supplemental figures:

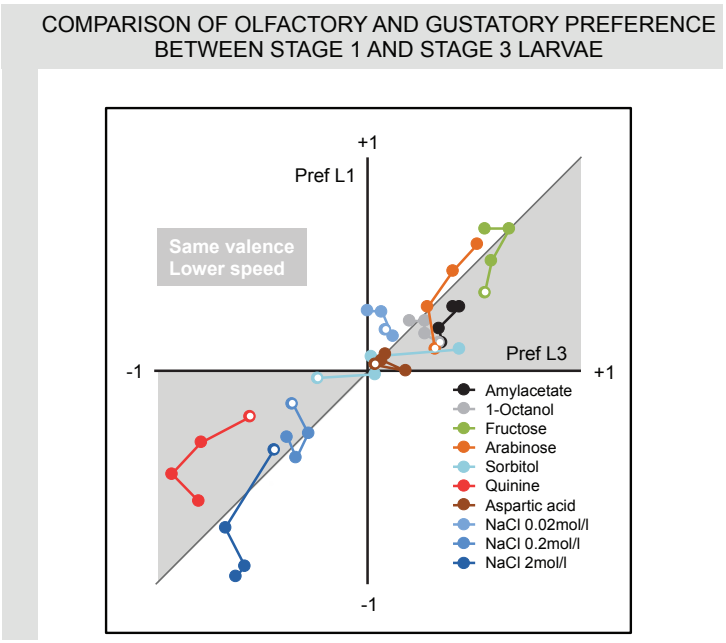

Supplemental Figure 1: Comparison of olfactory and gustatory preference between stage 1 and stage 3 larvae. Plot of the median olfactory and gustatory preference scores of stage 1 larvae (L1) and stage 3 larvae (L3) taken from Figure 1 and Figure 2. If both valence and speed were equal between L1 and L3, data would fall onto the diagonal. If valence were qualitatively the same, yet e.g. speed were reduced in L1, preference scores should have the same sign yet be consistently closer to zero in L1 than in L3 such that data points would fall into the grey shaded areas. This is observed for all tested odours and tastants, excepting low-salt and high-salt. In these two exceptional cases, L1 show significantly stronger attraction and stronger avoidance, respectively, than L3. Obviously, these effects cannot be accounted for by lower speed of locomotion in L1 (see Fig. S4, Fig. 7). The white dot represents the respectively first time point of measurement.

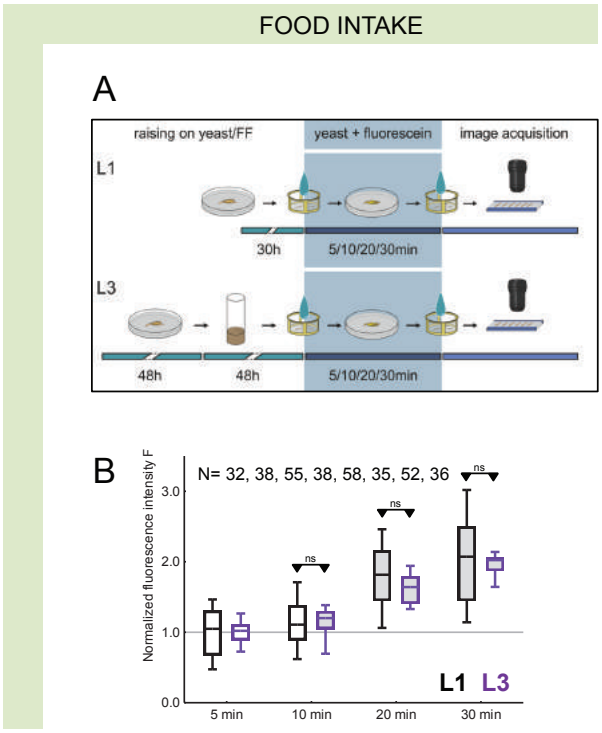

Supplemental Figure 2: Food intake.
A Sketch of the food intake assay. Stage 1 and stage 3 larvae were allowed to feed from yeast paste supplemented with fluorescein (blue shading). After 5, 10, 20, and 30 min fluorescence was measured.
B Time course of food intake. Shown is the fluorescence intensity F for stage 1 larva (L1, black-line box plots) or stage 3 larvae (L3, magenta-line box plots), separately normalized to fluorescence after 5 min (grey baseline against further increases are judged; therefore data at the 5 min time point are not statistically compared). For both stages a steep increase in food intake is seen between 10 min and 20 min; the time course of food intake appears indistinguishable between L1 and L3. ns refers to MWU comparisons between groups ($P<0.05/3$); grey shading of the box plots indicates Bonferroni-corrected within-group significance from zero in OSS tests ($P<0.05/3$). Data at time point 5 min are not statistically compared, because scores at this time point were defined to be 1, as described in the Materials & Methods section.
Sample sizes are given within the figure.

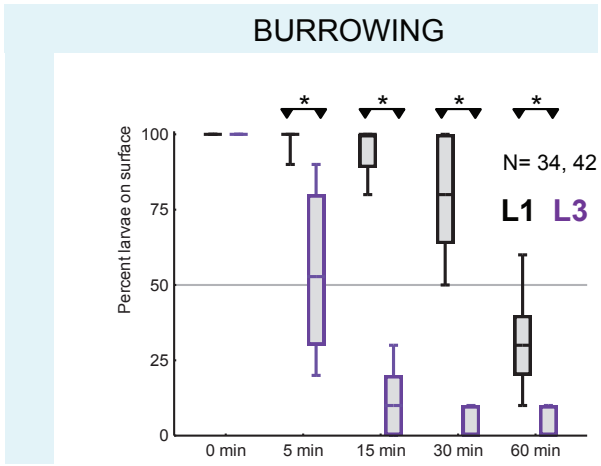

Supplemental Figure 3: Burrowing.
Groups of 10 larvae (either stage 1 larvae, L1, black-line box plots, or stage 3 larvae, L3, magenta-line box plots) were placed onto a yeast-diet substrate and the percentage of larvae visible on the surface was determined at 0, 5, 15, 30, and 60 min. L1 are significantly slower in burrowing into the substrate than L3. * refers to Bonferroni-corrected MWU comparisons between L1 and L3 ($P<0.05/4$). Data at time point 0 min are not statistically compared, because per the experimental procedures all larvae were located on the surface.
Sample sizes are given within the figure.

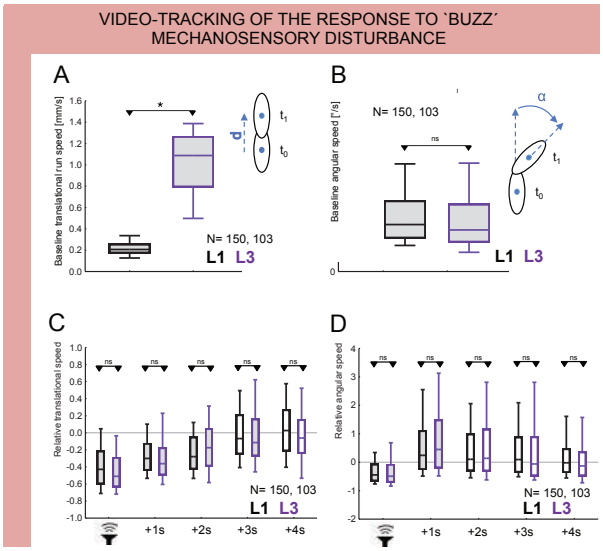

Supplemental Figure 4: Video-tracking of the response to a 'Buzz' mechanosensory disturbance.
A, B Baseline translational run speed and baseline angular speed. Shown are baseline translational run speed (mm/s) and baseline angular speed (°/s) of stage 1 larvae (L1, black-line box plots) or stage 3 larvae (L3, magenta-line box plots) during a 2-s time window before the Buzz. L1 have about 5-fold lower baseline translational run speed than L3. Baseline angular speed is not different between L1 and L3.
* and ns refer to MWU comparisons between L1 and L3 (P<or >0.05).
C, D Relative translational run speed and relative angular speed during and after the 'Buzz'. (C) Shows run speed, for each individual larva normalized to the 2 s before the 0.2-s/100-Hz Buzz mechanical disturbance was delivered. Data are separated in 1-s bins for the 4 s after Buzz onset. (D) Shows the same as in (C), for angular speed. Both L1 and L3 show startle behaviour, in that they hunch and slow down, and then turn.
* and ns refer to Bonferroni-corrected MWU comparisons between L1 and L3 (P<or >0.05/5); grey shading of the box plots indicates Bonferroni-corrected within-group significance from zero in OSS tests (P<0.05/5).
Sample sizes are given within the figure.

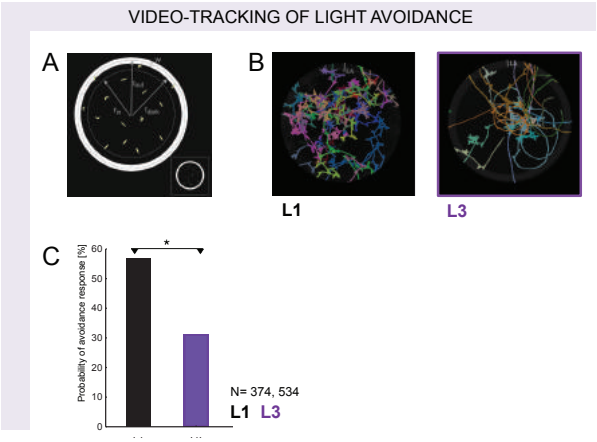

Supplemental Figure 5: Video-tracking of light avoidance.
A Sketch of the light avoidance setup, consisting of an inner dark area (according to the radius r_{dark}), an annulus of light (of width w), and the indicated dark-light border zone (according to r_{in} and r_{out}). Dimensions were adjusted according to the differences in body length between stage 1 and stage 3 larvae (L1 and L3, respectively) (see Methods section); the inset shows the set-up used for stage 1 larvae for comparison.
B Screen-shots of the final frames of Movies 10 and 11 with tracks of stage 1 and stage 3 larvae (L1 and L3, respectively). Dimensions were normalized to body length. The width of the light annulus is indicated (LA).
C Percentage of larvae showing avoidance behaviour at the dark-light border zone. This is the case more often for stage 1 than for stage 3 (L1 and L3, respectively), suggesting stage 1 is more light averse than stage 3. * refers to a two-tailed z-test between L1 and L3 (P<0.05) (XLSTAT, Statcon, Witzenhausen, Germany).
Sample sizes are given within the figure.

Supplemental movies:

Movie 1: Example of rolling behaviour in response to optogenetic activation of Basin interneurons in a stage 1 larva

Tracked rolling behaviour of an individual stage 1 larva expressing Chrimson in the Basin interneurons (R72F11-Gal4 x UAS-Chrimson) upon light stimulation starting at 4 s. Frame rate: 26 frames/s.

Movie 2: Example of rolling behaviour in response to optogenetic activation of Basin interneurons in a stage 3 larva

Tracked rolling behaviour of an individual stage 3 larva expressing Chrimson in the Basin interneurons (R72F11-Gal4 x UAS-Chrimson) upon light stimulation starting at 4 s. Frame rate: 26 frames/s.

Movie 3: Example go-phases of individual stage 1 and stage 3 larvae

Examples of go-phases (125 frames, 12.5 s) of a stage 1 larva (top) and a stage 3 larva (bottom) using the FIM tracking system. Note that the peristaltic pattern in the stage 1 larva is less regular than in stage 3.

Movie 4: Free locomotion of a group of stage 1 larvae

A group of stage 1 larvae moving freely in the 55 mm x 55 mm test arena for 7 min (5-fold time-lapse) recorded with FIM and analysed with FIMTrack [Risse et al., 2013, 2014]. Trajectories are blended in after 25 s. The larvae alternate between brief go and reorientation phases; most of the phase transitions lead to changes in bearing $>$30 °which we defined as turns (Fig. 7G). When compared to stage 3 larvae (Movie 5), the relatively smaller 'exploration range' in stage 1 larvae (Fig. 7H) manifests largely by differences in bending and turning behaviour (Fig. 7F, G), rather than in speed (Fig. 7E).

Movie 5: Free locomotion of a group of stage 3 larvae

Stage 3 larvae moving freely in the 225 mm x 225 mm test arena for 5.3 min (5-fold

time-lapse) recorded with FIM and analysed with FIMTrack [Risse et al., 2013, 2014]. Trajectories are blended in after 15 s. Similar to stage 1 larvae, also stage 3 larvae alternate between go- and reorientation phases, however relatively fewer of the phase transitions lead to changes in bearing >30 ° which we defined as turns (Fig. 7G). Together with differences in bending behaviour (Fig. 7F), this results in a larger exploration range in stage 3 than in stage 1 larvae, even when normalized to body length (Fig. 7H).

Movie 6: 'Buzz' response of stage 1 larvae

Examples of stage 1 larval behaviour before, during, and after presentation of three consecutive Buzzes (only behaviour in response to the first Buzz was analysed in Figure S4). The white dot in the lower right panel indicates the presentation of the Buzz. Note that the animals startle in response to the Buzz, i.e. hunch and slow down, and then turn.

Movie 7: 'Buzz' response of stage 3 larvae

Examples of stage 3 larval behaviour before, during, and after presentation of three consecutive Buzzes (only behaviour in response to the first Buzz was analysed in Figure S4). The white dot in the lower right panel indicates the presentation of the Buzz. Note that the animals startle in response to the Buzz, i.e. hunch and slow down, and then turn.

Movie 8: Thermotaxis of a group of stage 1 larvae

Stage 1 larvae moving in a 55 mm x 55 mm arena as described for Movie 4. Larval behaviour is observed within a linear 0.08 °C/mm heat gradient between 33 °C and 29 °C for 7 min (5-fold time-lapse). Larvae are placed at about 33 °C. Tracks are blended in after 23 s.

Movie 9: Thermotaxis of a group of stage 3 larvae

Stage 3 larvae moving in a 225 mm x 225 mm arena as described for Movie 5. Larval

behaviour is observed within a linear 0.08 °C/mm heat gradient between 33 °C and 18 °C for 5 min (5-fold time-lapse). Larvae are placed at about 33 °C. Tracks are blended in after 15 s.

Movie 10: Light avoidance of a group of stage 1 larvae

Stage 1 larvae moving in a central dark area surrounded by a light annulus of the indicated width (w) for 7 min (5 fold time-lapse). From 26 s onwards, r_{in} and r_{out} and larval trajectories are blended in (Fig. S5 A). The flags are set to define r_{in} and r_{out}. Trajectories are boldened after 73 s. Light avoidance is measured in the dark-light border zone (r_{out} - r_{in}).

Movie 11: Light avoidance of a group of stage 3 larvae

Stage 3 larvae moving in a central dark area surrounded by a light annulus of the indicated width (w) for 7 min (5 fold time-lapse). From 26 s onwards, r_{in} and r_{out} and larval trajectories are blended in (Fig. S5 A). The flags are set to define r_{in} and r_{out}. Trajectories are boldened after 73 s. Light avoidance is measured in the dark-light border zone (r_{out} - r_{in}).

Movies can be found on the accompanying DVD.

4.9 References

Aceves-Piña, E. O. and Quinn, W. G. (1979). Learning in normal and mutant drosophila larvae. *Science*, 206(4414):93–96.

Apostolopoulou, A. A., Widmann, A., Rohwedder, A., Pfitzenmaier, J. E., and Thum, A. S. (2013). Appetitive associative olfactory learning in drosophila larvae. *JoVE (Journal of Visualized Experiments)*, (72):e4334–e4334.

Benzer, S. (1967). Behavioral mutants of drosophila isolated by countercurrent distribution. *Proceedings of the National Academy of Sciences*, 58(3):1112–1119.

Berck, M. E., Khandelwal, A., Claus, L., Hernandez-Nunez, L., Si, G., Tabone, C. J., Li, F., Truman, J. W., Fetter, R. D., Louis, M., et al. (2016). The wiring diagram of a glomerular olfactory system. *Elife*, 5:e14859.

Bjordal, M., Arquier, N., Kniazeff, J., Pin, J. P., and Léopold, P. (2014). Sensing of amino acids in a dopaminergic circuitry promotes rejection of an incomplete diet in drosophila. *Cell*, 156(3):510–521.

Blenau, W. and Thamm, M. (2011). Distribution of serotonin (5-ht) and its receptors in the insect brain with focus on the mushroom bodies. lessons from drosophila melanogaster and apis mellifera. *Arthropod structure & development*, 40(5):381–394.

Brand, A. H. and Perrimon, N. (1993). Targeted gene expression as a means of altering cell fates and generating dominant phenotypes. *development*, 118(2):401–415.

Cobb, M. (1999). What and how do maggots smell? *Biological reviews*, 74(4):425–459.

Consoulas, C., Duch, C., Bayline, R. J., and Levine, R. B. (2000). Behavioral transformations during metamorphosis: remodeling of neural and motor systems. *Brain research bulletin*, 53(5):571–583.

Croset, V., Schleyer, M., Arguello, J. R., Gerber, B., and Benton, R. (2016). A molecular and neuronal basis for amino acid sensing in the drosophila larva. *Scientific Reports*, 6.

Demerec, M. and Kaufmann, B. P. (1972). *Drosophila guide: introduction to the genetics and cytology of Drosophila melanogaster*. Carnegie Institution of Washington Washington, DC.

Diegelmann, S., Klagges, B., Michels, B., Schleyer, M., and Gerber, B. (2013). Maggot learning and synapsin function. *Journal of Experimental Biology*, 216(6):939–951.

Dudai, Y., Jan, Y.-N., Byers, D., Quinn, W. G., and Benzer, S. (1976). dunce, a mutant of drosophila deficient in learning. *Proceedings of the National Academy of Sciences*, 73(5):1684–1688.

Eichler, K., Li, F., Litwin-Kumar, A., Park, Y., Andrade, I., Schneider-Mizell, C. M., Saumweber, T., Huser, A., Eschbach, C., Gerber, B., Fetter, R. D., Truman, J. W., Priebe, C., Abbott, L. F., Thum, A., Zlatic, M., and Cardona, A. (2017). The complete connectome of the mushroom body of a drosophila larva. *Nature*, In press.

El-Keredy, A., Schleyer, M., König, C., Ekim, A., and Gerber, B. (2012). Behavioural analyses of quinine processing in choice, feeding and learning of larval drosophila. *PloS one*, 7(7):e40525.

Eschbach, C., Cano, C., Haberkern, H., Schraut, K., Guan, C., Triphan, T., and Gerber, B. (2011). Associative learning between odorants and mechanosensory punishment in larval drosophila. *Journal of Experimental Biology*, 214(23):3897–3905.

Frye, M. A. and Dickinson, M. H. (2004). Closing the loop between neurobiology and flight behavior in drosophila. *Current opinion in neurobiology*, 14(6):729–736.

Fushiki, A., Zwart, M. F., Kohsaka, H., Fetter, R. D., Cardona, A., and Nose, A. (2016). A circuit mechanism for the propagation of waves of muscle contraction in drosophila. *Elife*, 5:e13253.

Garrity, P. A., Goodman, M. B., Samuel, A. D., and Sengupta, P. (2010). Running hot and cold: behavioral strategies, neural circuits, and the molecular machinery for thermotaxis in c. elegans and drosophila. *Genes & development*, 24(21):2365–2382.

Gasque, G., Conway, S., Huang, J., Rao, Y., and Vosshall, L. B. (2013). Small molecule drug screening in drosophila identifies the 5ht2a receptor as a feeding modulation target. *Scientific reports*, 3:srep02120.

Gerber, B., Biernacki, R., and Thum, J. (2010). Odour—sugar learning in larval drosophila. In Zhang, B., Freemann, M. R., and Waddell, S., editors, *Drosophila Neurobiology Methods: A Laboratory Manual*, page 443–55. Cold Spring Harbor: CSHL Press.

Gerber, B., Biernacki, R., and Thum, J. (2013). Odor–taste learning assays in drosophila larvae. *Cold Spring Harbor Protocols*, 2013(3):213–23.

Gerber, B. and Hendel, T. (2006). Outcome expectations drive learned behaviour in larval drosophila. *Proceedings of the Royal Society of London B: Biological Sciences*, 273(1604):2965–2968.

Gerber, B. and Stocker, R. F. (2007). The drosophila larva as a model for studying chemosensation and chemosensory learning: a review. *Chemical senses*, 32(1):65–89.

Giang, T., Rauchfuss, S., Ogueta, M., and Scholz, H. (2011). The serotonin transporter expression in drosophila melanogaster. *Journal of neurogenetics*, 25(1-2):17–26.

Gomez-Marin, A. and Louis, M. (2012). Active sensation during orientation behavior in the drosophila larva: more sense than luck. *Current opinion in neurobiology*, 22(2):208–215.

Gomez-Marin, A. and Louis, M. (2014). Multilevel control of run orientation in drosophila larval chemotaxis. *Frontiers in behavioral neuroscience*, 8:38.

Gomez-Marin, A., Partoune, N., Stephens, G. J., and Louis, M. (2012). Automated tracking of animal posture and movement during exploration and sensory orientation behaviors. *PloS one*, 7(8):e41642.

Gomez-Marin, A., Stephens, G. J., and Louis, M. (2011). Active sampling and decision making in drosophila chemotaxis. *Nature communications*, 2:441.

Heisenberg, M. (2003). Mushroom body memoir: from maps to models. *Nature Reviews Neuroscience*, 4(4):266–275.

Heisenberg, M., Borst, A., Wagner, S., and Byers, D. (1985). Drosophila mushroom body mutants are deficient in olfactory learning: Research papers. *Journal of neurogenetics*, 2(1):1–30.

Hotta, Y. and Benzer, S. (1970). Genetic dissection of the drosophila nervous system by means of mosaics. *Proceedings of the National Academy of Sciences*, 67(3):1156–1163.

Huser, A., Rohwedder, A., Apostolopoulou, A. A., Widmann, A., Pfitzenmaier, J. E., Maiolo, E. M., Selcho, M., Pauls, D., von Essen, A., Gupta, T., et al. (2012). The serotonergic central nervous system of the drosophila larva: anatomy and behavioral function. *PLoS One*, 7(10):e47518.

Hwang, R. Y., Zhong, L., Xu, Y., Johnson, T., Zhang, F., Deisseroth, K., and Tracey, W. D. (2007). Nociceptive neurons protect drosophila larvae from parasitoid wasps. *Current Biology*, 17(24):2105–2116.

Ito, K. and Hotta, Y. (1992). Proliferation pattern of postembryonic neuroblasts in the brain of drosophila melanogaster. *Developmental biology*, 149(1):134–148.

Jenett, A., Rubin, G. M., Ngo, T.-T., Shepherd, D., Murphy, C., Dionne, H., Pfeiffer, B. D., Cavallaro, A., Hall, D., Jeter, J., et al. (2012). A gal4-driver line resource for drosophila neurobiology. *Cell reports*, 2(4):991–1001.

Jovanic, T., Schneider-Mizell, C. M., Shao, M., Masson, J.-B., Denisov, G., Fetter, R. D., Mensh, B. D., Truman, J. W., Cardona, A., and Zlatic, M. (2016). Competitive disinhibition mediates behavioral choice and sequences in drosophila. *Cell*, 167(3):858–870.

Kane, E. A., Gershow, M., Afonso, B., Larderet, I., Klein, M., Carter, A. R., De Bivort, B. L., Sprecher, S. G., and Samuel, A. D. (2013). Sensorimotor structure of drosophila larva phototaxis. *Proceedings of the National Academy of Sciences*, 110(40):E3868–E3877.

Keene, A. C. and Sprecher, S. G. (2012). Seeing the light: photobehavior in fruit fly larvae. *Trends in neurosciences*, 35(2):104–110.

Kernan, M., Cowan, D., and Zuker, C. (1994). Genetic dissection of mechanosensory transduction: mechanoreception-defective mutations of drosophila. *Neuron*, 12(6):1195–1206.

Klapoetke, N. C., Murata, Y., Kim, S. S., Pulver, S. R., Birdsey-Benson, A., Cho, Y. K., Morimoto, T. K., Chuong, A. S., Carpenter, E. J., Tian, Z., et al. (2014). Independent optical excitation of distinct neural populations. *Nature methods*, 11(3):338–346.

Konopka, R. J. and Benzer, S. (1971). Clock mutants of drosophila melanogaster. *Proceedings of the National Academy of Sciences*, 68(9):2112–2116.

Kudow, N., Miura, D., Schleyer, M., Toshima, N., Gerber, B., and Tanimura, T. (2017). Preference for and learning of amino acids in larval drosophila. *Biology Open*, 6(3):365–369.

Levine, R. B., Morton, D. B., and Restifo, L. L. (1995). Remodeling of the insect nervous system. *Current opinion in neurobiology*, 5(1):28–35.

Li, H.-H., Kroll, J. R., Lennox, S. M., Ogundeyi, O., Jeter, J., Depasquale, G., and Truman, J. W. (2014). A gal4 driver resource for developmental and behavioral studies on the larval cns of drosophila. *Cell Reports*, 8(3):897–908.

Littleton, J. T. and Ganetzky, B. (2000). Ion channels and synaptic organization: analysis of the drosophila genome. *Neuron*, 26(1):35–43.

Liu, C., Plaçais, P.-Y., Yamagata, N., Pfeiffer, B. D., Aso, Y., Friedrich, A. B., Siwanowicz, I., Rubin, G. M., Preat, T., and Tanimoto, H. (2012). A subset of dopamine neurons signals reward for odour memory in drosophila. *Nature*, 488(7412):512–516.

Louis, M., Huber, T., Benton, R., Sakmar, T. P., and Vosshall, L. B. (2008a). Bilateral olfactory sensory input enhances chemotaxis behavior. *Nature neuroscience*, 11(2):187–199.

Louis, M., Piccinotti, S., and Vosshall, L. B. (2008b). High-resolution measurement of odor-driven behavior in drosophila larvae. *JoVE (Journal of Visualized Experiments)*, (11):e638–e638.

Martinez, W. L. and Martinez, A. R. (2012). *Computational statistics handbook with MATLAB*, volume 22. CRC press.

Mukhopadhyay, M. and Campos, A. R. (1995). The larval optic nerve is required for the development of an identified serotonergic arborization in drosophila melanogaster. *Developmental biology*, 169(2):629–643.

Neckameyer, W. S. (2010). A trophic role for serotonin in the development of a simple feeding circuit. *Developmental neuroscience*, 32(3):217–237.

Nern, A., Pfeiffer, B. D., and Rubin, G. M. (2015). Optimized tools for multicolor stochastic labeling reveal diverse stereotyped cell arrangements in the fly visual system. *Proceedings of the National Academy of Sciences*, 112(22):E2967–E2976.

Neuser, K., Husse, J., Stock, P., and Gerber, B. (2005). Appetitive olfactory learning in drosophila larvae: effects of repetition, reward strength, age, gender, assay type and memory span. *Animal behaviour*, 69(4):891–898.

Niewalda, T., Singhal, N., Fiala, A., Saumweber, T., Wegener, S., and Gerber, B. (2008). Salt processing in larval drosophila: choice, feeding, and learning shift from appetitive to aversive in a concentration-dependent way. *Chemical senses*, 33(8):685–692.

Ohyama, T., Jovanic, T., Denisov, G., Dang, T. C., Hoffmann, D., Kerr, R. A., and Zlatic, M. (2013). High-throughput analysis of stimulus-evoked behaviors in drosophila larva reveals multiple modality-specific escape strategies. *PLoS One*, 8(8):e71706.

Ohyama, T., Schneider-Mizell, C. M., Fetter, R. D., Aleman, J. V., Franconville, R., Rivera-Alba, M., Mensh, B. D., Branson, K. M., Simpson, J. H., Truman, J. W., et al. (2015). A multilevel multimodal circuit enhances action selection in drosophila. *Nature*, 520(7549):633–639.

O'Kane, C. J. and Gehring, W. J. (1987). Detection in situ of genomic regulatory elements in drosophila. *Proceedings of the National Academy of Sciences*, 84(24):9123–9127.

Otto, N., Risse, B., Berh, D., Bittern, J., Jiang, X., and Klämbt, C. (2016). Interactions among drosophila larvae before and during collision. *Scientific Reports*, 6.

Pauls, D., Selcho, M., Gendre, N., Stocker, R. F., and Thum, A. S. (2010). Drosophila larvae establish appetitive olfactory memories via mushroom body neurons of embryonic origin. *Journal of Neuroscience*, 30(32):10655–10666.

Pfeiffer, B. D., Jenett, A., Hammonds, A. S., Ngo, T.-T. B., Misra, S., Murphy, C., Scully, A., Carlson, J. W., Wan, K. H., Laverty, T. R., et al. (2008). Tools for neuroanatomy and neurogenetics in drosophila. *Proceedings of the National Academy of Sciences*, 105(28):9715–9720.

Pfeiffer, B. D., Ngo, T.-T. B., Hibbard, K. L., Murphy, C., Jenett, A., Truman, J. W., and Rubin, G. M. (2010). Refinement of tools for targeted gene expression in drosophila. *Genetics*, 186(2):735–755.

Risse, B., Otto, N., Berh, D., Jiang, X., and Klämbt, C. (2014). Fim imaging and fimtrack: Two new tools allowing high-throughput and cost effective locomotion analysis. *JoVE (Journal of Visualized Experiments)*, (94):e52207–e52207.

Risse, B., Thomas, S., Otto, N., Löpmeier, T., Valkov, D., Jiang, X., and Klämbt, C. (2013). Fim, a novel ftir-based imaging method for high throughput locomotion analysis. *PloS one*, 8(1):e53963.

Rodrigues, V. (1980). Olfactory behavior of drosophila melanogaster. In *Development and neurobiology of Drosophila*, pages 361–371. Springer.

Rohwedder, A., Pfitzenmaier, J. E., Ramsperger, N., Apostolopoulou, A. A., Widmann, A., and Thum, A. S. (2012). Nutritional value–dependent and nutritional value–independent effects on drosophila melanogaster larval behavior. *Chemical senses*.

Rohwedder, A., Wenz, N. L., Stehle, B., Huser, A., Yamagata, N., Zlatic, M., Truman, J. W., Tanimoto, H., Saumweber, T., Gerber, B., et al. (2016). Four individually identified paired dopamine neurons signal reward in larval drosophila. *Current Biology*, 26(5):661–669.

Roy, B., Singh, A. P., Shetty, C., Chaudhary, V., North, A., Landgraf, M., Vijayraghavan, K., and Rodrigues, V. (2007). Metamorphosis of an identified serotonergic neuron in the drosophila olfactory system. *Neural Development*, 2(1):20.

Rubin, G. M. and Spradling, A. C. (1982). Genetic transformation of drosophila with transposable element vectors. *Science*, 218(4570):348–353.

Russell, C., Wessnitzer, J., Young, J. M., Armstrong, J. D., and Webb, B. (2011). Dietary salt levels affect salt preference and learning in larval drosophila. *PloS one*, 6(6):e20100.

Saumweber, T., Cano, C., Klessen, J., Eichler, K., Fendt, M., and Gerber, B. (2014). Immediate and punitive impact of mechanosensory disturbance on olfactory behaviour of larval drosophila. *Biology open*, page BIO20149183.

Saumweber, T., Weyhersmüller, A., Hallermann, S., Diegelmann, S., Michels, B., Bucher, D., Funk, N., Reisch, D., Krohne, G., Wegener, S., et al. (2011). Behavioral and synaptic plasticity are impaired upon lack of the synaptic protein sap47. *Journal of Neuroscience*, 31(9):3508–3518.

Sawin-McCormack, E. P., Sokolowski, M. B., and Campos, A. R. (1995). Characterization and genetic analysis of drosophila melanogaster photobehavior during larval development. *Journal of neurogenetics*, 10(2):119–135.

Scherer, S., Stocker, R. F., and Gerber, B. (2003). Olfactory learning in individually assayed drosophila larvae. *Learning & Memory*, 10(3):217–225.

Schipanski, A., Yarali, A., Niewalda, T., and Gerber, B. (2008). Behavioral analyses of sugar processing in choice, feeding, and learning in larval drosophila. *Chemical senses*, 33(6):563–573.

Schlegel, P., Texada, M. J., Miroschnikow, A., Schoofs, A., Hückesfeld, S., Peters, M., Schneider-Mizell, C. M., Lacin, H., Li, F., Fetter, R. D., et al. (2016). Synaptic transmission parallels neuromodulation in a central food-intake circuit. *eLife*, 5:e16799.

Schleyer, M., Diegelmann, S., Michels, B., Saumweber, T., and Gerber, B. (2013). 'decision making' in larval drosophila. In Menzel, R. and Benjamin, P., editors, *Invertebrate learning and memory*. Elsevier.

Schleyer, M., Miura, D., Tanimura, T., and Gerber, B. (2015a). Learning the specific quality of taste reinforcement in larval drosophila. *Elife*, 4:e04711.

Schleyer, M., Reid, S. F., Pamir, E., Saumweber, T., Paisios, E., Davies, A., Gerber, B., and Louis, M. (2015b). The impact of odor–reward memory on chemotaxis in larval drosophila. *Learning & Memory*, 22(5):267–277.

Schleyer, M., Saumweber, T., Nahrendorf, W., Fischer, B., von Alpen, D., Pauls, D., Thum, A., and Gerber, B. (2011). A behavior-based circuit model of how outcome expectations organize learned behavior in larval drosophila. *Learning & Memory*, 18(10):639–653.

Schneider-Mizell, C. M., Gerhard, S., Longair, M., Kazimiers, T., Li, F., Zwart, M. F., Champion, A., Midgley, F. M., Fetter, R. D., Saalfeld, S., et al. (2016). Quantitative neuroanatomy for connectomics in drosophila. *Elife*, 5:e12059.

Schoofs, A., Hückesfeld, S., Schlegel, P., Miroschnikow, A., Peters, M., Zeymer, M., Spieß, R., Chiang, A.-S., and Pankratz, M. J. (2014). Selection of motor programs for suppressing food intake and inducing locomotion in the drosophila brain. *PLoS Biol*, 12(6):e1001893.

Sivanantharajah, L. and Zhang, B. (2015). Current techniques for high-resolution mapping of behavioral circuits in drosophila. *Journal of Comparative Physiology A*, 201(9):895–909.

Sokolowski, M. B. (2001). Drosophila: genetics meets behaviour. *Nature Reviews Genetics*, 2(11):879–890.

St Johnston, D. and Nüsslein-Volhard, C. (1992). The origin of pattern and polarity in the drosophila embryo. *Cell*, 68(2):201–219.

Stocker, R. F. (1994). The organization of the chemosensory system in drosophila melanogaster: a rewiew. *Cell and tissue research*, 275(1):3–26.

Stocker, R. F. (2008). Design of the larval chemosensory system. In *Brain Development in Drosophila melanogaster*, pages 69–81. Springer.

Tissot, M. and Stocker, R. F. (2000). Metamorphosis in drosophila and other insects: the fate of neurons throughout the stages. *Progress in neurobiology*, 62(1):89–111.

Tracey, W. D., Wilson, R. I., Laurent, G., and Benzer, S. (2003). painless, a drosophila gene essential for nociception. *Cell*, 113(2):261–273.

Truman, J. W. (1996). Metamorphosis of the insect nervous system. In Gilbert, L. I., Tata, J. R., and Atkinson, B. G., editors, *Metamorphosis: postembryonic reprogramming of gene expression in amphibian and insect cells*, pages 283–320. Academic Press.

Tully, T. and Quinn, W. G. (1985). Classical conditioning and retention in normal and mutant drosophila melanogaster. *Journal of Comparative Physiology A*, 157(2):263–277.

Venken, K. J., Simpson, J. H., and Bellen, H. J. (2011). Genetic manipulation of genes and cells in the nervous system of the fruit fly. *Neuron*, 72(2):202–230.

von Essen, A. M., Pauls, D., Thum, A. S., and Sprecher, S. G. (2011). Capacity of visual classical conditioning in drosophila larvae. *Behavioral neuroscience*, 125(6):921.

Vosshall, L. B. and Stocker, R. F. (2007). Molecular architecture of smell and taste in drosophila. *Annu. Rev. Neurosci.*, 30:505–533.

Zhang, B., Freeman, M. R., and Waddell, S. (2010). *Drosophila Neurobiology: A Laboratory Manual*. Cold Spring Harbor Laboratory Press.

Zwart, M. F., Pulver, S. R., Truman, J. W., Fushiki, A., Fetter, R. D., Cardona, A., and Landgraf, M. (2016). Selective inhibition mediates the sequential recruitment of motor pools. *Neuron*, 91(3):615–628.

Chapter III: Immediate and punitive impact of mechanosensory disturbance on olfactory behaviour of larval *Drosophila*

Timo Saumweber[1,2,#], Carmen Cano[3,*], Juliane Klessen[2], Katharina Eichler[3,‡], Marcus Fendt[4,5], Bertram Gerber[2,3,5,6,#]

[1] Institut für Biologie, Universität Leipzig, Tierphysiologie, 04103 Leipzig, Germany.
[2] Abteilung Genetik von Lernen und Gedächtnis, Leibniz Institut für Neurobiologie (LIN), 39118 Magdeburg, Germany.
[3] Institut für Biologie, Universität Leipzig, Genetik, 04103 Leipzig, Germany.
[4] Institut für Pharmakologie und Toxikologie, Medizinische Fakultät, Otto-von-Guericke-Universität Magdeburg, 39120 Magdeburg, Germany.
[5] Center for Behavioral Brain Science (CBBS), 39016 Magdeburg, Germany.
[6] Institut für Biologie, Otto von Guericke Universität Magdeburg, Verhaltensgenetik, 39106 Magdeburg, Germany.
[*] Present address: Institut für Psychologie, Universität Bonn, 53111 Bonn, Germany.
[‡] Present address: Institut für Biologie, Universität Konstanz, 78457 Konstanz, Germany.
[#] Correspondence

Biology Open (2014) 3, 1005-1010

doi: 10.1242/bio.20149183

5.1 Abstract

The ability to respond to and to learn about mechanosensory disturbance is widespread among animals. Using *Drosophila* larvae, we describe how the frequency of mechanosensory disturbance ('buzz') affects three aspects of behaviour: free locomotion, innate olfactory preference, and potency as a punishment. We report that (i) during 2-3 seconds after buzz onset the larvae slowed down and then turned, arguably to escape this situation; this was seen for buzz frequencies of 10, 100, and 1000 Hz, (ii) innate olfactory preference was reduced when tested in the presence of the buzz; this effect was strongest for the 100 Hz frequency, (iii) after odour-buzz associative training, we observed escape from the buzz-associated odour; this effect was apparent for 10 and 100, but not for 1000 Hz. We discuss the multiple behavioural effects of mechanosensation and stress that the immediate effects on locomotion and the impact as punishment differ in their frequency-dependence. Similar dissociations between immediate, reflexive behavioural effects and reinforcement potency were previously reported for sweet, salty and bitter tastants. It should be interesting to see how these features map onto the organization of sensory, ascending pathways.

5.2 Introduction

Drosophila larvae have but 10,000 neurons, yet display a relatively rich behavioural repertoire (Vogelstein et al. [2014]; for reviews, see Cobb [1999]; Diegelmann et al. [2013]; Gerber and Stocker [2007]; Schleyer et al. [2013]): they are not only able to feed, smell and taste, to sense visual, tactile and noxious stimuli, temperature and vibration, but also use these kinds of sensory information for learning. Larvae form associative memories between an odour and rewards such as fructose [Scherer et al., 2003] or low

salt concentrations [Niewalda et al., 2008], whereas high salt concentrations or bitter substances as well as electric shocks can be used as punishment [Aceves-Piña and Quinn, 1979; El-Keredy et al., 2012; Niewalda et al., 2008]. We focus on the behavioural impact of mechanical disturbance ('buzzes'). In particular our experiments concern (i) the impact of buzzes on locomotion and on (ii) innate olfactory behaviour, as well as (iii) their potency as punishment [Eschbach et al., 2011].

Locomotion in larval *Drosophila* is studied mostly in Petri dish arenas covered with an agarose substrate. Their behaviour consists of runs, accomplished by peristaltic waves of muscular contraction that propagate from back to front (e.g. Gomez-Marin and Louis [2014]). Runs feature low-amplitude side movements ($<$20 degrees/s) of the first 1-3 segments, called head weathervaning. Weathervaning can support slightly curved runs and does not entail a break of the peristaltic wave [Gomez-Marin and Louis, 2014]. Peristaltic runs can be interrupted to accommodate reorientation events. Upon such an interruption the larvae typically show more pronounced side movements of their head ($\sim$60 degrees/s). Dependent on when the peristaltic wave is re-initiated during these movements, the body is pushed forward in this new orientation. The mechanosensory chordotonal organs and the brain hemispheres are apparently dispensable for these locomotor patterns, arguing they are produced by circuitry in the ventral nerve cord; however, brain and mechanosensory input are required for the integration of these locomotor patterns into adaptive, biologically meaningful behaviour [Berni et al., 2012; Caldwell et al., 2003; Ohyama et al., 2013; Wu et al., 2011].

Interestingly in the current context, the presentation of a buzz can both interrupt peristaltic running [Eschbach et al., 2011; Ohyama et al., 2013; Zhang et al., 2013] and serve as punishment in an associative olfactory learning experiment [Eschbach et al., 2011] (both these effects may under natural conditions help larvae to avoid predatory wasps [Zhang et al., 2013]). In these experiments an odour A is presented with a buzz,

but another odour X is presented without a buzz. After such training, the preference between both odours is tipped to the disadvantage of the previously punished odour (Fig. 1). In accordance with what has been found for other types of aversive olfactory learning in the larva [Apostolopoulou et al., 2014a,b; El-Keredy et al., 2012; Gerber and Hendel, 2006; Niewalda et al., 2008; Schleyer et al., 2011; Schroll et al., 2006; Selcho et al., 2009], such learned behaviour can best be understood as an escape strategy. Consider that you will not run out of a movie theatre upon seeing the emergency exit sign, but only when there is an emergency to escape from. Likewise, the larvae do not show conditioned escape during the test unless the punishment is present and escape indeed is warranted (for buzz as punishment [Eschbach et al., 2011]). In other words, the smell of the previously punished odour does not itself trigger escape, but gives direction to an escape which is otherwise triggered - namely by the buzz.
The current study aims to further our understanding of the behavioural impact of buzz-mechanosensation in larval *Drosophila*. We parametrically describe the potency of buzzes of various frequency (10, 100, 1000 Hz) as punishment, as well as their impact on free locomotion and olfactory preference behaviour.

5.3 Results

Buzz as punishment

Drosophila larvae were trained such that one odour, namely either *n*-amyl acetate or 1-octanol (AM, OCT), was associated with a buzz as punishment (-). Then, the larvae were offered a choice between AM and OCT (Fig. 1A,B). Preference scores as displayed in Fig. 1C (left) were defined such that positive scores indicate a choice of AM while negative scores indicate a choice of OCT. We used ‘standard’ 0.2 s-duration buzzes at a frequency of 100 Hz [Eschbach et al., 2011]. Preference scores were shifted

towards OCT after AM-/OCT training as compared to AM/OCT- training (Fig. 1C, left). Correspondingly, the associative performance index, which measures the difference in preference, was significantly negative (Fig. 1C, right). Increasing buzz duration by a factor of ten, i.e. from 0.2 s to 2 s, did not increase this associative effect (Fig. 1D; for the underlying preference scores, see supplementary material Fig. S1), suggesting that the punitive effect of the buzz might be largely exerted by its onset [Zhang et al., 2013]. Next, we asked whether the frequency of buzz punishment has an influence on associative scores (Fig. 2B; supplementary material Fig. S2B). Buzzes of 10 Hz and 100 Hz support significantly negative associative performance indices, whereas 1000 Hz buzzes did not. A relatively low frequency of 10 Hz supported the same level of associative effect as the standard 100 Hz buzz, while the scores using 1000 Hz buzzes were less relative to the 100 Hz buzz.

We were surprised to observe that the 1000 Hz buzz did not support a punitive effect. As mentioned in the Introduction, both for bad-taste and for the buzz as punishment, learned behaviour is part of an escape process and is expressed only in the presence of the punishment. Therefore the lack of associative effect of a 1000 Hz buzz may either be because no odour-buzz memory is established, or because the 1000 Hz buzz during testing does not allow the behavioural expression of an otherwise intact odour-buzz memory. Given that the standard buzz of 100 Hz was effective as punishment (middle plot in Fig. 2B), we trained larvae with such a standard 100 Hz buzz, but tested them in the presence of a 1000 Hz buzz. It turned out that associative scores were intact (Fig. 2C; supplementary material Fig. S2C). This argues that a 1000 Hz buzz is permissive for learned escape. In turn, as the standard 100 Hz buzz was also permissive for learned escape (middle plot in Fig. 2B), we trained larvae with a 1000 Hz buzz, but tested them in the presence of the standard 100 Hz buzz. In such an experiment, associative scores were zero (Fig. 2D; supplementary material Fig. S2D).

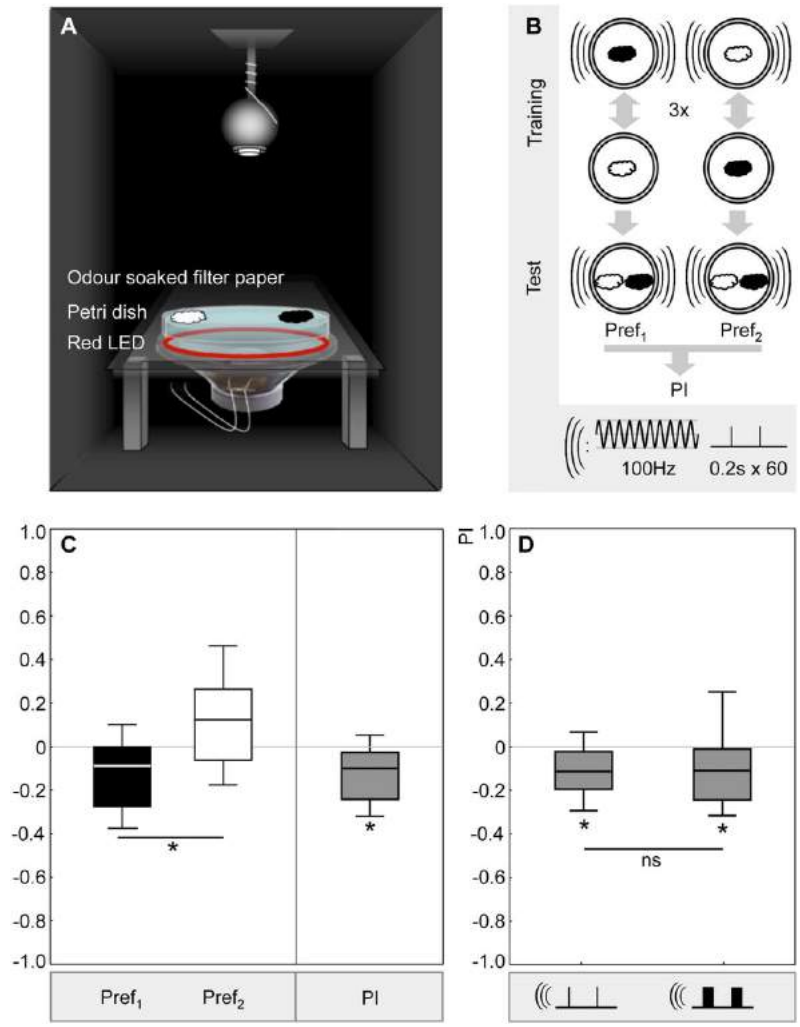

Figure 1: Buzz as punishment.
A Experimental set-up: In a sound- and light-isolated box, a Petri dish was placed on top of a speaker delivering vibration as a mechanosensory punishment ('buzz'). The dish was illuminated with a ring of red LEDs. Odours, represented as clouds, were applied using odour-soaked filter papers fixed to the lid of the dish. Larvae were allowed to crawl over the dish while one odour was presented together with the buzz, alternated with another odour being presented without the buzz (not shown). During testing a choice situation was created by placing different odours on either side, as shown. Larval behaviour was recorded with a digital camera mounted above the Petri dish.
B Experimental design: during training, larvae either received a first trial with buzz punishment during the presentation of *n*-amyl acetate (filled cloud) and a second trial with the presentation of 1-octanol (open cloud) without the buzz. In a second group, larvae were trained reciprocally. These training cycles were repeated two more times. During the test, the larvae faced a choice between both odours. Preference scores were calculated on the basis of the number of larvae on either side; then, the associative performance (PI) was determined as the difference in preferences between the reciprocally trained groups, such that negative PIs indicate aversive memory. Please note that during testing the buzz was presented (see Introduction for rationale). The sequence of trial types was varied across repetitions of the experiment, making sure that in half of the cases *n*-amyl acetate or 1-octanol were first within training cycles, counterbalanced with buzz presentation during the first or second trial. During a punished trial, a 100 Hz buzz was presented every 5th second for a duration of 0.2 s, unless specified otherwise.
C, D Results: to the left of panel C, odour preferences from the reciprocally trained groups are shown. $Pref_1$ indicates the preference for *n*-amyl acetate when *n*-amyl acetate had been punished whereas $Pref_2$ indicates the preference for *n*-amyl acetate for the reciprocally trained group in which 1-octanol had been punished. Data are presented as box-whisker plots, such that the middle line represents the median, the box the lower and the upper quartile, and the whiskers the 90 and 10 percentiles. * indicates a MWU-test of $P<0.05$; U=506; N=50, 50. To the right of panel C, the associative $Pref_1$ performance indices are presented; in this case * indicates significance from zero, that is an OSS-test of $P<0.05$; N=50.
D Increasing buzz duration from 0.2 s (left) to 2.0 s (right) did not affect associative performance scores (ns: MWU-test of P=0.65; U=643; N=49, 29; * OSS-tests of $P<0.05/2$; sample sizes as above).

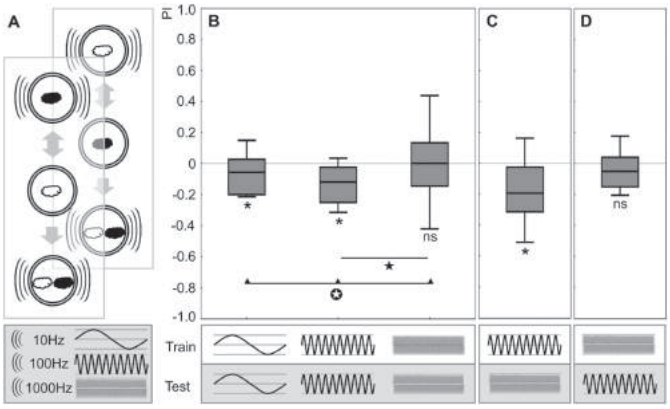

Figure 2: Buzz as punishment: frequency-dependence.
A Sketch of the experimental design using buzz frequencies of 10 Hz, 100 Hz and 1000 Hz. Presenting the buzz during the test is required, because conditioned avoidance is not behaviourally expressed if there is no 'reason' to escape (see Introduction for rationale).
B Associative performance indices when using buzzes at the indicated frequencies. Associative performance is observed for 10 Hz and 100 Hz, but not for 1000 Hz buzzes. * and ns refer to $P<0.05/3$ and $P>0.05/3$ (OSS-tests), respectively; Embedded Image refers to $P<0.05/2$ (MWU-test, $P<0.05/2$; $U=327.0$), Embedded Image refers to $P<0.05$ (KW-test: $P<0.05$; $H=7.71$; $df=2$). From left to right, sample size is N=32, 38, 28.
C, D Associative performance indices when using buzzes differing in frequency between training and test. Odour-buzz memory, if established using a 100 Hz buzz, can be behaviourally expressed at 1000 Hz (C). In turn, 1000 Hz buzzes cannot function as punishment (D). * and ns indicate $P<0.05$ and $P>0.05$, respectively (OSS-tests) (N=50, 43).

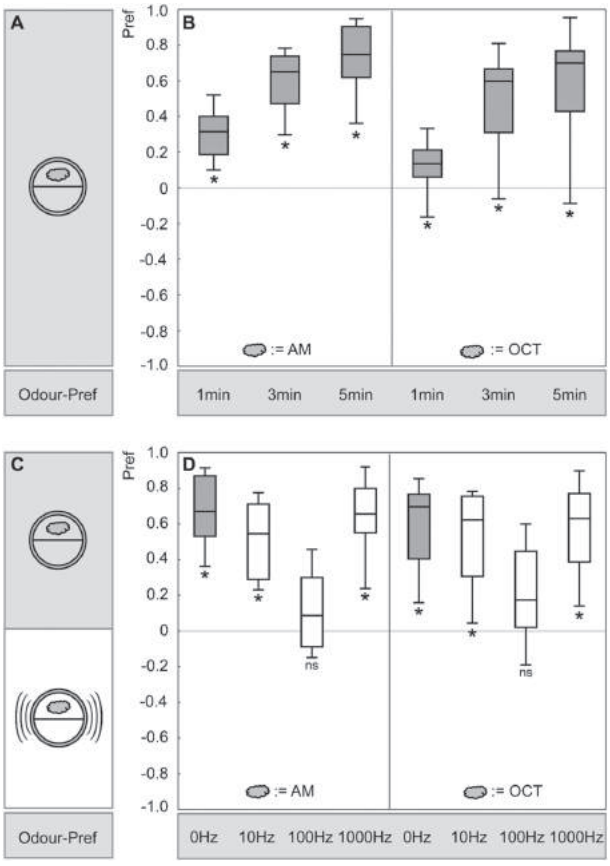

Figure 3: Buzz as modulator of olfactory preference.
A, B Time course of olfactory preference. Larvae were offered the choice between an odour side and a blank side of a Petri dish. Preference was scored after 1 min, 3 min, and 5 min, using either *n*-amyl acetate (AM) or 1-octanol (OCT) as odours. For both odours, choice behaviour reached a steady state after 5 min; therefore these 5-min scores are displayed in panels C and D. * indicates significance from zero (OSS-tests, $P<0.05/3$) (N=24 for AM and N=23 for OCT preferences).
C, D Modulation of innate olfactory preference behaviour by the buzz. Odour preferences, for AM or for OCT, are displayed, either assayed without the buzz, or assayed in the presence of the buzz at the indicated frequency. Buzzes of 100 Hz abolish innate olfactory behaviour. * and ns refer to $P<0.05/4$ and $P>0.05/4$, respectively (OSS-tests) (N=24, 19, 19, 18; N=23, 19, 18, 18).

This argues that a 1000 Hz buzz does not support the establishment of an aversive memory to begin with.

We conclude that buzzes of 10 as well as of 100 Hz are effective as punishment, whereas buzzes of 1000 Hz are not.

Of note, the fact that 100 Hz buzzes induce aversive memory for concomitantly presented odours means that these odours are effectively processed towards the larvae's 'memory centre' during training. Also, 100 Hz buzzes allow for the retrieval of such olfactory memories, arguing that also during testing odours can be effectively processed towards and from this 'memory centre'. Thus, the associative aspects of odour processing remain intact in the presence of a 100 Hz buzz.

Buzz as modulator of innate olfactory behaviour

We offered the larvae a choice between an odour side (either AM or OCT) versus a blank side of a Petri dish and recorded their preference - and did so either in the presence or in the absence of a buzz (Fig. 3A,C). Given that it takes 3-5 min for the larvae to distribute themselves between both sides of the Petri dish (Fig. 3B), we chose to focus on the data at 5 min. This was done for either 10, 100, or 1000 Hz buzzes. In the presence of 10 Hz and 1000 Hz buzzes the larvae behaved the same as larvae tested without a buzz; to our surprise, however, in the presence of 100 Hz buzzes innate odour preference was strongly decreased, for both the odours employed (Fig. 3D).

We conclude that 100 Hz buzzes, but not 10 or 1000 Hz buzzes, strongly modulate innate olfactory behaviour - while, as mentioned above, associative aspects of olfactory processing remain unaffected in the presence of a 100 Hz buzz.

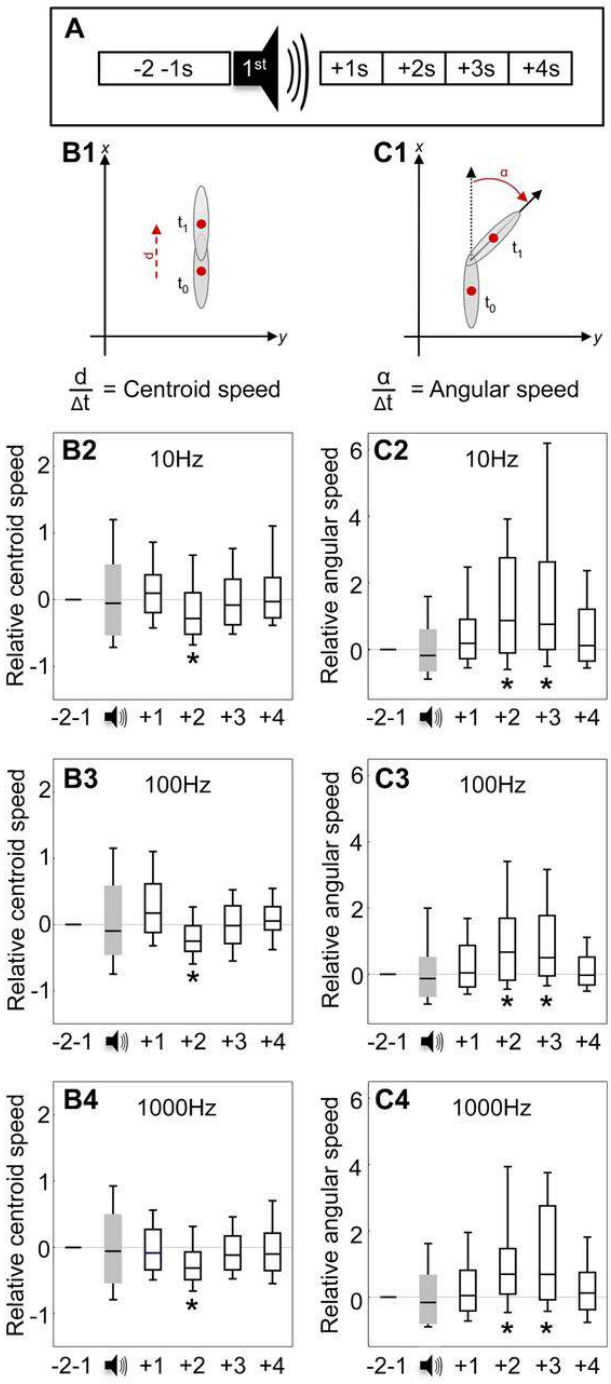

Figure 4: Buzz as modulator of locomotion.
Larval locomotion was assayed 2 s before, during, and 4 s after buzz onset (A). Analysed parameters were centroid speed (B) and angular speed (C), displayed for the four 1-s time windows normalized to the 2 s before buzz onset, using buzzes of the indicated frequency. At all buzz frequencies, larvae slow down (@ 2 s), and turn (@ 2-3 s). * indicates $P<0.05/5$ (OSS-tests) (N=88, 82, 84 for 10, 100 and 1000 Hz, respectively).

Buzz as modulator of locomotion

We monitored locomotion of individual larvae and quantified their innate behaviour with respect to buzzes of 10, 100, or 1000 Hz. We present speed and turning propensity upon the very first (Fig. 4), the 10th (supplementary material Fig. S3) and the 60th buzz

within a 5 min period (supplementary material Fig. S4). We normalized data to the 2 s before the onset of the respective buzz as baseline. In keeping with Eschbach et al. [Eschbach et al., 2011], the larvae 'startled', that is they briefly slowed down and then turned in response to a 100 Hz buzz (Fig. 4B3,C3). The speed dropped below baseline at second 2, yet returned to baseline while turning was still in progress, until at second 3 to 4 after the buzz the new direction was assumed. The same qualitative pattern of results was found for 10 Hz and 1000 Hz buzzes (Fig. 4B2,C2,B4,C4). These results were surprisingly stable over dozens of repetitions of the buzz (for the 10th and 60th buzz, see supplementary material Fig. S3, Fig. S4).

We conclude that innate behaviour towards buzzes is a rather repetition-stable behaviour consisting of sequential slowing-down and turning, and that this behaviour does not depend on the frequency of the buzzes, at least not across 10, 100, and 1000 Hz.

5.4 Discussion

We demonstrate that mechanical disturbances (buzzes) impact immediate behaviour and are effective as punishment - and that buzzes of different frequency differ in impact across the types of behaviour assayed: 10 Hz buzzes function as punishment, do not modulate innate olfactory behaviour, and induce startle. Buzzes of 100 Hz also serve as punishment, do reduce innate olfactory preference and elicit startle. Lastly, 1000 Hz buzzes cannot serve as punishment, do not modulate innate chemotaxis, and do make larvae startle. How can these differences in frequency-dependence be understood?

For sugars, salt, and quinine, mismatches have been reported between the dose-effect functions of immediate and reinforcing effects [El-Keredy et al., 2012; Niewalda et al., 2008; Russell et al., 2011; Schipanski et al., 2008]. For example, figure 5 in El-Keredy et al. found that the suppressing effect of quinine on feeding is shifted by about one

order of magnitude towards higher concentrations as compared to the punishing effect of quinine [El-Keredy et al., 2012]. The authors suggested that different sensory neurons differing in dose-effect function and differentially hooked up to feeding behaviour versus reinforcement signalling are responsible for these effects. This was confirmed by Apostolopoulou et al.: ablating Gr33a-Gal4 positive gustatory sensory neurons reduces feeding-suppression by quinine, but leaves punishment processing unaffected [Apostolopoulou et al., 2014b].

A buzz interrupts peristaltic running and induces a brief hunch, followed by large-amplitude sideways movements of the head and ensuing peristaltic runs into a new direction [Bharadwaj et al., 2013; Ohyama et al., 2013; Wu et al., 2011; Zhang et al., 2013] (Fig. 4). This sequential pattern of behaviour is reminiscent of startle in mammals (supplementary material Fig. S5): upon a sudden and intense visual, tactile or acoustic stimulus, mammals interrupt current behaviour, close their eyes, flatten their ears, bend their spine and limbs and stiffen their neck (these behaviours are typically measured as 'startle'). In a second phase, the eyes are widely opened, the ears pricked, and, while the spine and body parts remain bent, the head is rotated sideways [Landis and Hunt, 1939; Strauss, 1929; Gerber et al., 2014; Koch, 1999; Yeomans and Frankland, 1995]. As in larvae, these behaviours seem to initially protect the subject, followed by attempts at threat localization, reorientation, and preparation for a fight or flight decision.

Regarding the neurogenetics of sensing mild mechanical disturbance like buzzes, the precise targeting of chordotonal neurons within the central nervous system is required [Wu et al., 2011]. Further, these chordotonal neurons are necessary for modulating head casts, crawling and hunching with respect to vibration and gentle touch [Caldwell et al., 2003; Fushiki et al., 2013; Ohyama et al., 2013; Wu et al., 2011]. Within these chordotonal neurons, the natural sounds of wasps and yellow jackets as well as pure tones of 500 Hz are sensed by NOMPC, NANCHUNG, and INACTIVE channels [Zhang

et al., 2013]. In terms of sufficiency, optogenetic activation of chordotonal neurons evokes aspects of startle behaviour [Ohyama et al., 2013]. Thus, activity in the chordotonal neurons seems largely necessary and sufficient for larval startle behaviour. Extracellular recordings of chordotonal neurons and Ca^{2+} imaging fit these conclusions in showing an optimum function with a peak at about 500 Hz [Zhang et al., 2013]. Stimuli with 10, 100 or 1000 Hz, as used in the current study and in Eschbach et al., would, according to Zhang et al., induce only very moderate activity [Eschbach et al., 2011; Zhang et al., 2013]. When summed up across all chordotonal neurons across all body segments, however, even such moderate activity may be sufficient for startle (Fig. 4).
To summarize, the different frequency-dependencies of how buzzes affect locomotion, innate olfactory preference, and their potency as a punishment, parametrically dissociate these three types of behavioural effects. It should be fascinating to map these dissociations, which likewise have been found for the taste system, onto the emerging behaviour-connectome relationships of the larva [Cardona et al., 2010, 2012].

5.5 Material and Methods

Larvae

Third-instar feeding stage larvae of the Canton S strain were used, raised on standard food in groups of about 200, under standard conditions (25℃, 60-70 % relative humidity, 12/12 light/dark cycle).

Set up and stimuli

The experimental setup follows Eschbach et al. and Eschbach [Eschbach et al., 2011; Eschbach, 2011] (Fig. 1A). It consists of a 50x50x75 cm wooden box covered on the inside by silencing foam. A speaker (MC GEE 201847, CON Elektronik, Greussenheim, Germany, impedance 8 Ω, diameter 16 cm, acoustic pressure: 89.2 dBW-1 power 150

W r.m.s.) was fixed at the bottom, such that a 145 mm diameter Petri dish (Sarstedt, Nuembrecht, Germany) could be placed on top. An opaque inner ring made of Perspex and an outer ring fitted with 30 LEDs (624 nm, Conrad Electronics, Hirschau, Germany) surrounded the Petri dish. The Petri dish was covered with a thin layer of agarose (1 %; electrophoresis grade; Roth, Karlsruhe, Germany) on the eve of the experiment. The speaker was operated via a PC using a custom-written LabVIEW program. A camera (Logitech Webcam Pro 9000, frame rate 30 s^{-1}, Logitech, Munich, Germany) could be fixed above the plate and connected to a PC for offline analysis.

1-octanol (OCT, CAS: 111-87-5, purity: 99 %) and *n*-amyl acetate (AM, CAS: 628-63-7, purity 98 %, diluted 1:50 in paraffin oil, CAS: 8012-95-1) (all Merck, Darmstadt, Germany) were used as odorants. Filter papers (7 mm^2) were loaded with 10 µl of AM or OCT and fixed to the Petri dish cover (50 mm from both the midline and the rim).

Buzz as punishment

Behaviour is compared between reciprocally trained larvae. One set of larvae experienced AM with punishment (-) and OCT without punishment (AM-/OCT), while the other larvae were trained reciprocally (OCT-/AM) (Fig. 1B). For the test, the relative preference between the two odours was measured, allowing us to calculate an associative performance index as the difference in preference between the reciprocally trained larvae. In the next section, we present our 'standard' protocol; parametric variations are mentioned in the course of the Results.

Two filter papers were fixed to the Petri dish lid, both loaded with 10 µl of the same odour (e.g. AM) and the lid was put on the Petri dish. Then, 50 larvae were collected from their rearing vials, washed and transferred to the Petri dish. For punishment, 60 disturbances were applied at a frequency of 100 Hz ('buzzes' in the following), each lasting 0.2 s and presented evenly spaced in time for 5 min. The larvae were then transferred to a fresh Petri dish and OCT was presented, without the buzz (AM-/OCT). This cycle was

repeated two more times (in half of the cases larvae were punished during the 1st, 3rd and 5th trial, while otherwise they were punished in the 2nd, 4th and 6th trial).
For testing, larvae were transferred to a Petri dish equipped with AM on one side and OCT on the other. After 5 min, we counted the number of larvae in the middle (0.5 cm wide stripe), on the AM side and on the OCT side. A preference index is calculated as:

(1) $PREF_1$ = (@AM - @OCT)/TOTAL

Likewise, a preference index $PREF_2$ was determined for larvae of the reciprocally trained group (AM/OCT-). The performance index PI was defined as the difference in preference between the reciprocally trained groups:

(2) PI = ($PREF_1$ - $PREF_2$)/2

Positive scores thus indicate appetitive memory, while negative scores indicate aversive memory, that is a punitive effect of the buzz. Testing was performed in the presence of the buzz (see Introduction for rationale).

Buzz as modulator of olfactory preference

Two 7-mm^2 filter papers were fixed to the Petri dish lid, one of which was loaded with odour (10 µl of either AM or OCT) while the other one was left blank. A group of 50 larvae was collected and transferred to the middle of an agarose-filled Petri dish. The Petri dish was then placed into the assay box described above. After 1, 3 and 5 min we determined the number of larvae on either the odour side or the blank side or the middle stripe, allowing us to calculate a preference score as:

(3) PREF = (@ODOUR - @BLANK)/TOTAL

This experiment was performed either as described, or in the presence of the buzz.

Buzz as modulator of locomotion

We determined two key parameters of the behaviour towards the buzz, namely changes in speed and changes in turning propensity. Single larvae were observed for 5 min, moving over an agarose-filled Petri dish. During this time, buzzes of 0.2 s duration were presented, evenly spaced in time, and data were recorded for offline analyses. For the first buzz as well as for the 10th and the 60th buzz, we determined speed (mm/s; 1 voxel = 0.33 mm) and turning propensity (°/s) (for details, see Eschbach et al. [2011]; Eschbach [2011]). Baseline speed and turning propensity were determined for the 2 s before the buzz; data were then scored for the 1st, 2nd, 3rd and 4th second after onset of the buzz. Data are presented normalized to baseline: negative scores thus indicate slowing down and turning less, respectively, while positive scores indicate speeding up and turning more.

All three experiments were performed using buzzes at frequencies of 100 Hz, as in Eschbach et al. [Eschbach et al., 2011], as well as buzzes of one order of magnitude lower and higher frequency (10 Hz, 1000 Hz). All experiments comply with applicable law and regulations.

Statistics

Statistical analyses were non-parametric throughout and performed with Statistica on a PC (Statsoft 7.0, Tulsa, USA). To compare across multiple groups, we used Kruskal-Wallis tests (KW); Mann-Whitney U-tests (MWU) were used for pairwise comparisons. To test for differences from chance level we used One-Sample Sign-tests (OSS). In cases of multiple comparisons, we applied a Bonferroni correction by dividing 0.05 by the number of comparisons made (presented as $P<0.05/3$ in cases of e.g. three comparisons); this ensures a within-experiment error rate below 5 %. Results of statistical analyses are

presented in the figure legends. Data are presented as box-whisker plots (middle line: median; box: lower and upper quartile; whiskers: 90th and 10th percentile).

List of abbreviations

AM: *n*-amyl acetate; OCT: octanol; TRP: transient receptor potential; NOMPC: No mechanoreceptor potential C; NAN: nanchung; IAV: inactive.

5.6 Acknowledgements

We thank Claire Eschbach and Hannah Haberkern for introducing us to the paradigm, Silvia Petter, Holger Reim and Roswitha Jungnickel for technical assistance, and Rupert Glasgow, Bert Klagges, Christian König, Birgit Michels, Michael Schleyer for discussion and comments. We are particularly grateful to Klaus Schildberger for his extended, generous support and hospitality in his Department.

Funding:

This study received institutional support from the Leibniz Institut für Neurobiologie (LIN) Magdeburg, the Wissenschaftsgemeinschaft Gottfried Wilhelm Leibniz (WGL), and the Universities of Leipzig and Magdeburg. This study was supported by grants from the Bundesministerium für Bildung und Forschung (BMBF Bernstein Network Insect inspired robotics to B.G.), the Deutsche Forschungsgemeinschaft (CRC 779 to B.G. as well as M.F.), and the European Commission (FP7-ICT project Miniature Insect Model for Active Learning [MINIMAL] to B.G.).

5.7 Author contributions

Developed the concept and designed the experiments: T.S., C.C., B.G.

Performed the experiments: T.S., C.C., J.K., K.E., M.F.

Analysed the data: T.S., C.C.

Prepared and edited the manuscript before submission: T.S., M.F., B.G.

5.8 Supplemental data

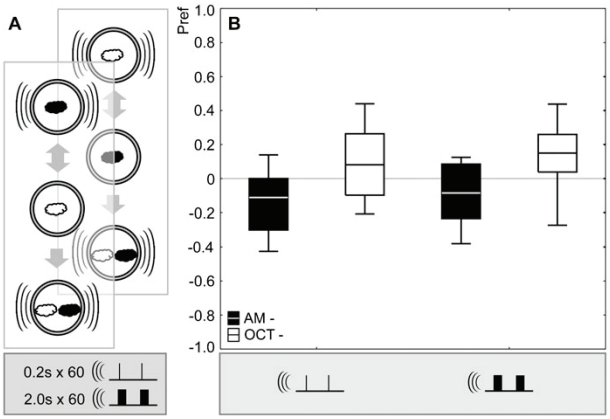

Supplemental Figure 1: Buzz as punishment.
A Experimental design.
B Plotted are the preference scores of reciprocally trained groups of larvae from the experiment displayed in Fig. 1D. The filled box plots indicate AM preference when AM was punished during training (AM-) whereas the open box plots indicate the AM preference for the reciprocally trained group (OCT-).

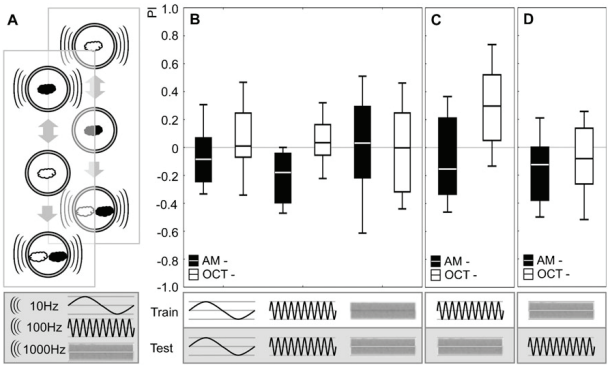

Supplemental Figure 2: Buzz as punishment: frequency-dependence. A Experimental design.
B-D Plotted are the preference scores of reciprocally trained groups of larvae from the experiment displayed in Fig. 2. Other details as in supplementary material Fig. S1.

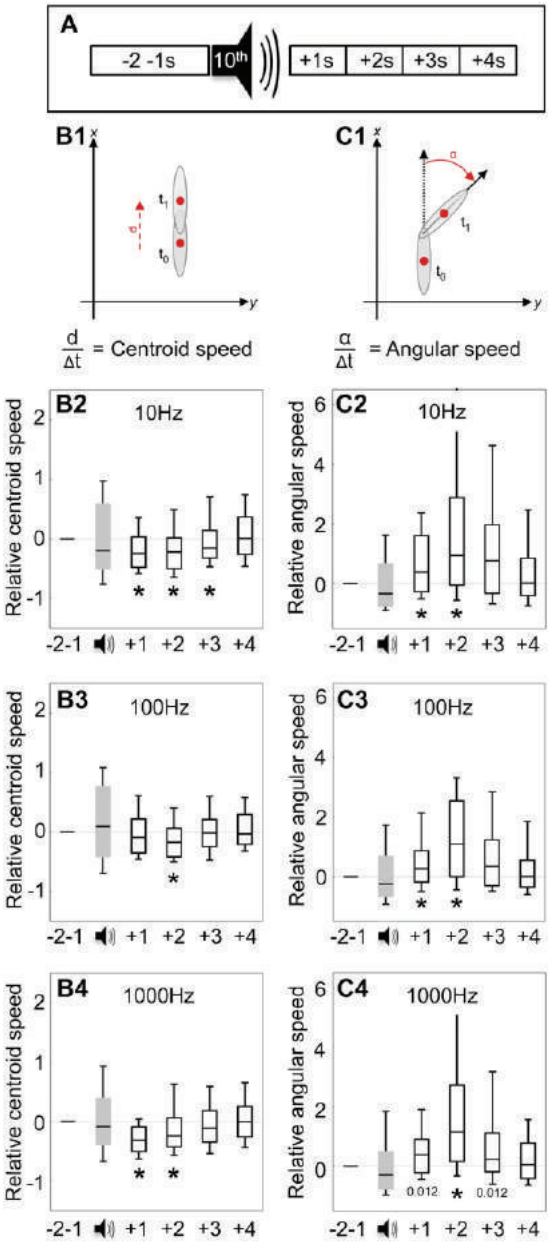

Supplemental Figure 3: Buzz as modulator of locomotion after 10th buzz. Same as Fig. 4, for the 10th buzz.

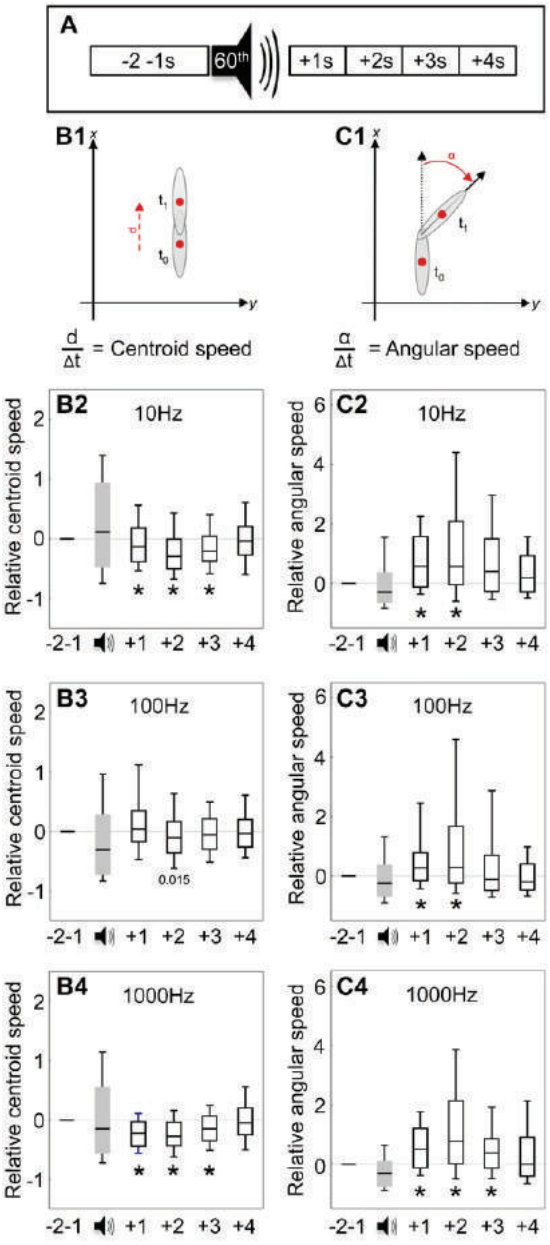

Supplemental Figure 4: Buzz as modulator of locomotion after 60th buzz. Same as Fig. 4 and supplementary material Fig. S3, for the 60th buzz.

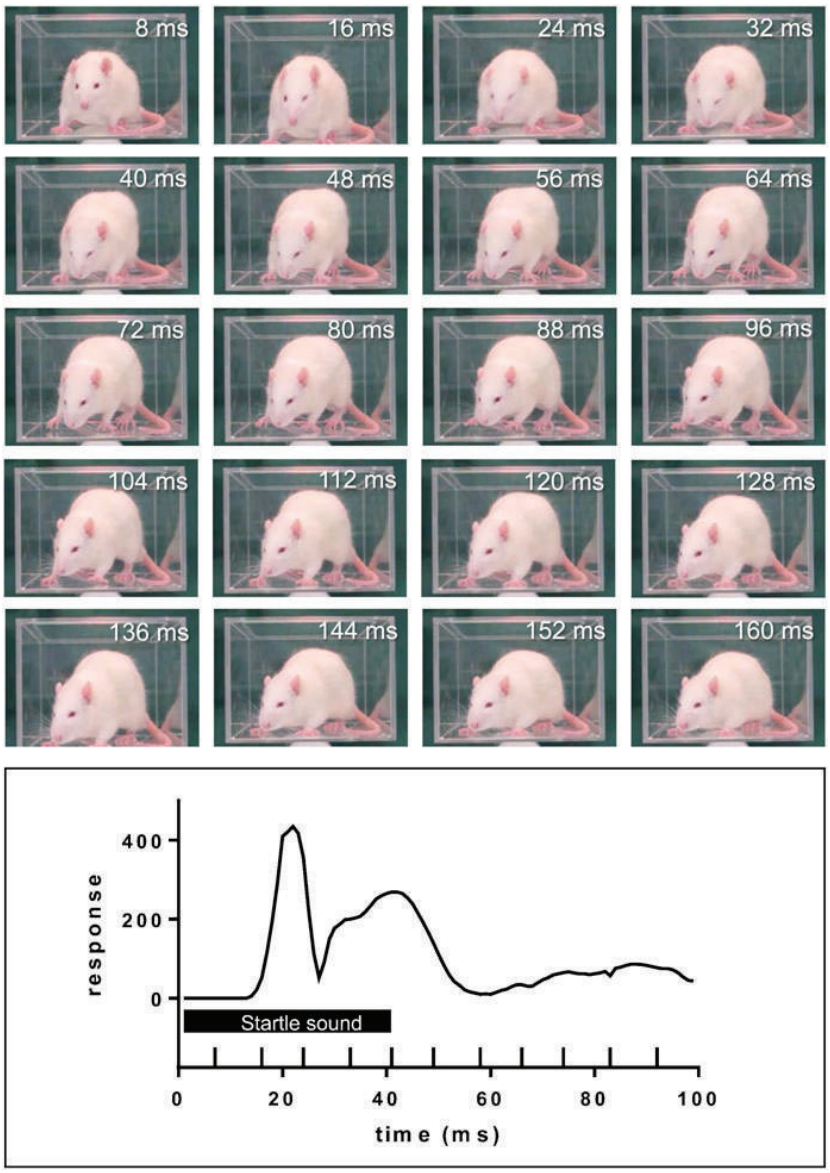

Supplemental Figure 5: Acoustic startle of a rat. A startle system (SR-LAB, San Diego Instruments, San Diego, CA) was used that contained a small custom-made enclosure made of a transparent Plexiglas cylinder (12612612 cm). Movements of the animals were detected by motion-sensitive transducers mounted underneath. The output signal of the transducers was digitized (sampling rate: 1 kHz) and stored on a PC. The acoustic startle probe (40 ms, 120 dB SPL white noise) was generated by high-frequency loudspeakers mounted in the centre of the ceiling of the test chambers. A male Sprague-Dawley rat was exposed to a startle stimulus of 40 ms duration. The startle response was videotaped by a digital camera (Canon, Powershot SX50) in the slow-motion mode. The figures show that startle behaviour is biphasic [Koch, 1999; Yeomans and Frankland, 1995]. The first phase is protective, in particular for the sense organs and the dorsal surface of the neck: the eyes are closed (ca. 16-40 ms), the ears are flattened, the neck is stiffened and the body bent (from ca. 24 ms on), and the legs are straightened (ca. 48 ms). The second phase serves to locate the threat and to prepare a fight or flight decision: the eyes are opened (from ca. 40 ms on), ears pricked (from ca. 96 ms on), and legs lifted. The sketch below indicates a timeline for the presentation of the startle sound (bar) and for the first frames of the picture series shown above. The curve is the voltage output (mV) of the piezoelectric element measuring the startle response.

5.9 References

Aceves-Piña, E. O. and Quinn, W. G. (1979). Learning in normal and mutant drosophila larvae. *Science*, 206(4414):93–96.

Apostolopoulou, A. A., Hersperger, F., Mazija, L., Widmann, A., Wüst, A., and Thum, A. S. (2014a). Composition of agarose substrate affects behavioral output of drosophila larvae. *Frontiers in behavioral neuroscience*, 8:11.

Apostolopoulou, A. A., Mazija, L., Wüst, A., and Thum, A. S. (2014b). The neuronal and molecular basis of quinine-dependent bitter taste signaling in drosophila larvae. *Frontiers in behavioral neuroscience*, 8:6.

Berni, J., Pulver, S. R., Griffith, L. C., and Bate, M. (2012). Autonomous circuitry for substrate exploration in freely moving drosophila larvae. *Current Biology*, 22(20):1861–1870.

Bharadwaj, R., Roy, M., Ohyama, T., Sivan-Loukianova, E., Delannoy, M., Lloyd, T. E., Zlatic, M., Eberl, D. F., and Kolodkin, A. L. (2013). Cbl-associated protein regulates assembly and function of two tension-sensing structures in drosophila. *Development*, 140(3):627–638.

Caldwell, J. C., Miller, M. M., Wing, S., Soll, D. R., and Eberl, D. F. (2003). Dynamic analysis of larval locomotion in drosophila chordotonal organ mutants. *Proceedings of the National Academy of Sciences*, 100(26):16053–16058.

Cardona, A., Saalfeld, S., Preibisch, S., Schmid, B., Cheng, A., Pulokas, J., Tomancak, P., and Hartenstein, V. (2010). An integrated micro-and macroarchitectural analysis of the drosophila brain by computer-assisted serial section electron microscopy. *PLoS Biol*, 8(10):e1000502.

Cardona, A., Saalfeld, S., Schindelin, J., Arganda-Carreras, I., Preibisch, S., Longair, M., Tomancak, P., Hartenstein, V., and Douglas, R. J. (2012). Trakem2 software for neural circuit reconstruction. *PloS one*, 7(6):e38011.

Cobb, M. (1999). What and how do maggots smell? *Biological reviews*, 74(4):425–459.

Diegelmann, S., Klagges, B., Michels, B., Schleyer, M., and Gerber, B. (2013). Maggot learning and synapsin function. *Journal of Experimental Biology*, 216(6):939–951.

El-Keredy, A., Schleyer, M., König, C., Ekim, A., and Gerber, B. (2012). Behavioural analyses of quinine processing in choice, feeding and learning of larval drosophila. *PloS one*, 7(7):e40525.

Eschbach, C. (2011). Classical and operant learning in the larvae of drosophila melanogaster.

Eschbach, C., Cano, C., Haberkern, H., Schraut, K., Guan, C., Triphan, T., and Gerber, B. (2011). Associative learning between odorants and mechanosensory punishment in larval drosophila. *Journal of Experimental Biology*, 214(23):3897–3905.

Fushiki, A., Kohsaka, H., and Nose, A. (2013). Role of sensory experience in functional development of drosophila motor circuits. *PloS one*, 8(4):e62199.

Gerber, B. and Hendel, T. (2006). Outcome expectations drive learned behaviour in larval drosophila. *Proceedings of the Royal Society of London B: Biological Sciences*, 273(1604):2965–2968.

Gerber, B. and Stocker, R. F. (2007). The drosophila larva as a model for studying chemosensation and chemosensory learning: a review. *Chemical senses*, 32(1):65–89.

Gerber, B., Yarali, A., Diegelmann, S., Wotjak, C. T., Pauli, P., and Fendt, M. (2014). Pain-relief learning in flies, rats, and man: basic research and applied perspectives. *Learning & Memory*, 21(4):232–252.

Gomez-Marin, A. and Louis, M. (2014). Multilevel control of run orientation in drosophila larval chemotaxis. *Frontiers in behavioral neuroscience*, 8:38.

Koch, M. (1999). The neurobiology of startle. *Progress in neurobiology*, 59(2):107–128.

Landis, C. and Hunt, W. (1939). *The startle pattern*. New York, Farrar and Rinehart.

Niewalda, T., Singhal, N., Fiala, A., Saumweber, T., Wegener, S., and Gerber, B. (2008). Salt processing in larval drosophila: choice, feeding, and learning shift from appetitive to aversive in a concentration-dependent way. *Chemical senses*, 33(8):685–692.

Ohyama, T., Jovanic, T., Denisov, G., Dang, T. C., Hoffmann, D., Kerr, R. A., and Zlatic, M. (2013). High-throughput analysis of stimulus-evoked behaviors in drosophila larva reveals multiple modality-specific escape strategies. *PLoS One*, 8(8):e71706.

Russell, C., Wessnitzer, J., Young, J. M., Armstrong, J. D., and Webb, B. (2011). Dietary salt levels affect salt preference and learning in larval drosophila. *PloS one*, 6(6):e20100.

Scherer, S., Stocker, R. F., and Gerber, B. (2003). Olfactory learning in individually assayed drosophila larvae. *Learning & Memory*, 10(3):217–225.

Schipanski, A., Yarali, A., Niewalda, T., and Gerber, B. (2008). Behavioral analyses of sugar processing in choice, feeding, and learning in larval drosophila. *Chemical senses*, 33(6):563–573.

Schleyer, M., Diegelmann, S., Michels, B., Saumweber, T., and Gerber, B. (2013). *Invertebrate Learning and Memory: Chapter 5.Decision Making in Larval Drosophila*, volume 22. Elsevier Inc. Chapters.

Schleyer, M., Saumweber, T., Nahrendorf, W., Fischer, B., von Alpen, D., Pauls, D., Thum, A., and Gerber, B. (2011). A behavior-based circuit model of how outcome expectations organize learned behavior in larval drosophila. *Learning & Memory*, 18(10):639–653.

Schroll, C., Riemensperger, T., Bucher, D., Ehmer, J., Völler, T., Erbguth, K., Gerber, B., Hendel, T., Nagel, G., Buchner, E., et al. (2006). Light-induced activation of distinct modulatory neurons triggers appetitive or aversive learning in drosophila larvae. *Current biology*, 16(17):1741–1747.

Selcho, M., Pauls, D., Han, K.-A., Stocker, R. F., and Thum, A. S. (2009). The role of dopamine in drosophila larval classical olfactory conditioning. *PLoS One*, 4(6):e5897.

Strauss, H. (1929). *Das zusammenschrecken: Experimentell-Kinematographische Studie zur Physiologie und Pathophysiologie der Reaktivbewegungen*. PhD thesis.

Vogelstein, J. T., Park, Y., Ohyama, T., Kerr, R. A., Truman, J. W., Priebe, C. E., and Zlatic, M. (2014). Discovery of brainwide neural-behavioral maps via multiscale unsupervised structure learning. *Science*, 344(6182):386–392.

Wu, Z., Sweeney, L. B., Ayoob, J. C., Chak, K., Andreone, B. J., Ohyama, T., Kerr, R., Luo, L., Zlatic, M., and Kolodkin, A. L. (2011). A combinatorial semaphorin code instructs the initial steps of sensory circuit assembly in the drosophila cns. *Neuron*, 70(2):281–298.

Yeomans, J. S. and Frankland, P. W. (1995). The acoustic startle reflex: neurons and connections. *Brain research reviews*, 21(3):301–314.

Zhang, W., Yan, Z., Jan, L. Y., and Jan, Y. N. (2013). Sound response mediated by the trp channels nompc, nanchung, and inactive in chordotonal organs of drosophila larvae. *Proceedings of the National Academy of Sciences*, 110(33):13612–13617.

Chapter IV: Functional architecture of reward learning in mushroom body extrinsic neurons of larval *Drosophila*

Timo Saumweber[1=], Astrid Rohwedder[2=], Michael Schleyer[1], Katharina Eichler[2], Yi-chun Chen[1], Yoshinori Aso[3], Albert Cardona[3], Claire Eschbach[3], Oliver Kobler[4], Marta Zlatic[3], James W. Truman3[=], Andreas S. Thum[2,5=#], Bertram Gerber[1,6,7=#]

[1] Leibniz Institute for Neurobiology (LIN), Department of Genetics, Brenneckestr. 6, 39118 Magdeburg, Germany.
[2] University of Konstanz, Institute for Biology, Universitätsstraße 10, 78464 Konstanz, Germany.
[3] HHMI Janelia Research Campus, Helix Drive 19700, Ashburn, VA 20147, USA.
[4] Leibniz Institute for Neurobiology (LIN), Special Lab Electron and Laserscanning Microscopy and Combinatorial Neuro Imaging Core Facility, Brenneckestr. 6, 39118 Magdeburg, Germany.
[5] Zukunftskolleg, University of Konstanz, Universitätsstraße 10, 78464 Konstanz, Germany.
[6] Center for Behavioral Brain Sciences (CBBS), Magdeburg, Germany.
[7] Otto von Guericke University Magdeburg, Institute for Biology, Universitätsplatz 2, 39106 Magdeburg, Germany.
[=] Equal contributors, [#] Correspondence

In Press: Nature Communications

(manuscript number NCOMMS-17-06962)

6.1 Abstract

Brains adaptively integrate present sensory input, past experience, and options for future action. The insect mushroom body is a paradigmatic brain structure bringing about such integration. We study these processes at single-cell resolution, focusing on the behavioral architecture of the mushroom body input and output neurons (MBINs and MBONs), and the mushroom body intrinsic APL neuron. Our results reveal the identity and morphology of close to all of these 44 neurons in stage 3 *Drosophila* larvae. A combined silencing and optogenetic activation approach uncovers a sparse and specific function of MBINs, MBONs and the APL neuron across three behavioral tasks, namely innate olfactory preference, innate gustatory preference, and associative learning between odor and taste reward. This comprehensive structure-function analysis of the MBIN-MBON-APL network thus provides a cellular-resolution study case of how brains organize behavior.

6.2 Introduction

The insect mushroom body is a paradigmatic case of a central-brain structure bringing about the triadic integration of present sensory input, past experience, and options for future behavior (reviews include Heisenberg [2003]; Strausfeld et al. [2009]; Farris [2011]; Guven-Ozkan and Davis [2014]; Menzel [2014]; Owald and Waddell [2015]; Gerber and Aso [2017]). We use larval *Drosophila* to systematically study these processes at single-cell resolution. Our focus is on the behavioral architecture of the mushroom body input and output neurons, and their role in the association of odor with taste reward as a biologically meaningful learning process. Combined with the complete synaptic connectome of the larval mushroom body [Eichler et al., 2017], this provides

an unprecedentedly detailed picture of how a central brain structure is functionally organized.

The larval olfactory system, recently described at synaptic resolution [Berck et al., 2016], is organized like the one of adult *Drosophila* and other insects, yet at much reduced cell numbers (Figure 1a and b) (reviews include Stocker [1994]; Cobb [1999]; Gerber and Stocker [2007]; Vosshall and Stocker [2007]; Gerber et al. [2009]; Hansson and Stensmyr [2011]; Martin et al. [2011]; Diegelmann et al. [2013]; Galizia [2014]). Its 21 olfactory sensory neurons, typically expressing a general co-receptor and one type of odorant receptor each, define the range of odors detectable for the larva. Each olfactory sensory neuron targets but one glomerulus in the antennal lobe. The 21 antennal lobe glomeruli are laterally connected by 14 interneurons [Thum et al., 2011; Berck et al., 2016]. A set of 21 uni- and 13 multiglomerular second-order olfactory projection neurons, plus 2 ventral unpaired median neurons, connect the antennal lobe with third-order olfactory neurons in the lateral horn and the mushroom body. Depending on the odorant receptors expressed and the connectivity within this system, olfactory stimuli can thus be coded combinatorially across these ascending pathways (see Gupta and Stopfer [2014] for the capacity of temporal coding). The lateral horn is largely sufficient for innate olfactory behavior, while learned olfactory behavior requires the mushroom body loop [Heimbeck et al., 2001; Honjo and Furukubo-Tokunaga, 2009; Pauls et al., 2010; Michels et al., 2011]. The ascending olfactory pathways remain mostly ipsilateral (exceptions in Berck et al. [2016]), are bilaterally symmetrical, and are largely stereotyped. Exceptions to stereotypy are some variable antennal lobe interneurons and the random connection between olfactory projection neurons and most of the $\sim$100 embryonic-born and the $\sim$700 larval-born mushroom body intrinsic Kenyon cells (KCs) [Ito and Hotta, 1992; Masuda-Nakagawa et al., 2005; Thum et al., 2011; Berck et al., 2016; Eichler et al., 2017]. The high input resistance of the KCs and a gain

control mechanism by distributive GABAergic inhibition results in a sparse combinatorial code across the mushroom body [Turner et al., 2008; Masuda-Nakagawa et al., 2014; Eichler et al., 2017]. This architecture of the insect olfactory system resembles that of mammals [Davis, 2004].

Despite significant advances [Colomb et al., 2007; Kwon et al., 2011; Mishra et al., 2013; Apostolopoulou et al., 2014; Stewart et al., 2015; Apostolopoulou et al., 2016; Choi et al., 2016; Croset et al., 2016; Hückesfeld et al., 2016; Kim et al., 2016; Schlegel et al., 2016; Van Giesen et al., 2016], the taste system of the larva is relatively less well understood. The $\sim$80 larval gustatory sensory neurons are located in three external cephalic organs and four pharyngeal sense organs. However, a comprehensive picture of taste coding and of how it proceeds towards the brain is but emerging [Gerber and Stocker, 2007; Cobb et al., 2008; Gerber et al., 2009; Apostolopoulou et al., 2015; Freeman and Dahanukar, 2015]. What is clear is that gustatory sensory neurons project to the subesophageal zone; this includes neurons defined by Gr43a-Gal4 expression that are reportedly necessary for proper fructose preference [Mishra et al., 2013]. From the subesophageal zone, taste information is passed on towards motor control for steering innate gustatory behavior, and towards the central brain including the mushroom body to confer valenced internal reinforcement signals across the KCs. Indeed, dopaminergic and/ or octopaminergic/ tyraminergic interneurons (DANs and OANs, respectively) ascending towards the mushroom bodies are necessary and sufficient for reward signaling in insects [Hammer, 1993; Hammer and Menzel, 1998; Schwaerzel et al., 2003; Schroll et al., 2006; Unoki et al., 2006; Claridge-Chang et al., 2009; Selcho et al., 2009; Aso et al., 2010, 2012; Burke et al., 2012; Liu et al., 2012; Selcho et al., 2014; Yamagata et al., 2015]. Specifically, optogenetic activation of OANs in larval *Drosophila* is sufficient as an internal reward signal [Schroll et al., 2006; Honda et al., 2014], as is the case for the pPAM-subset of DANs [Rohwedder et al., 2016]. A

different set of DANs, in turn, is sufficient as an internal punishment signal [Schroll et al., 2006]. Fittingly, a knock-down of the DopR1 dopamine receptor in the KCs impairs both appetitive and aversive learning (Selcho et al. [2009]; in adult *Drosophila*: Kim et al. [2007]; Qin et al. [2012]). Thus during training an odor-specific subset of KCs is activated via the projection neurons and at the same time most if not all KCs can receive aminergic internal valence signals. As has been shown in adult *Drosophila*, coincident input by odor and by the aminergic valence signal is detected within the odor-activated KCs [Tomchik and Davis, 2009; Gervasi et al., 2010] (also see Vasmer et al. [2014]) allowing their output to be modified; in this way the level of activity in the mushroom body output neurons (MBONs) will reflect learned odor valence upon a subsequent encounter with the odor [Séjourné et al., 2011; Pai et al., 2013; Plaçais et al., 2013; Aso et al., 2014b; Bouzaiane et al., 2015; Cohn et al., 2015; Owald et al., 2015; Hige et al., 2015; Perisse et al., 2016]. Learned valence signals from the MBONs can then add up with innate valence signals from the projection neurons to jointly instruct adaptive behavior in both larvae and adults (Figure 1b) (Schleyer et al. [2015b]; Wystrach et al. [2016]; Paisios et al. [2017]; for adult *Drosophila*: Aso et al. [2014b]). In the case of the larva, turning probability is increased when they are heading away from a previously reward-associated odor as compared to when they are heading towards it. Furthermore, turns have a higher probability to be directed towards the previously reward-associated odor, rather than away from it, while run speed is not associatively modulated [Schleyer et al., 2015b; Paisios et al., 2017]. Thus, the mushroom bodies are a paradigmatic central-brain structure in that they integrate present sensory input (olfactory projection neurons, DANs, and OANs) and past experience with these inputs (the modified KC-to-MBON presynaptic terminals) to provide value-based instruction for future behavior (via the MBONs). In effect the mushroom bodies thus can be regarded as a ‘watershed’ along a sensory-motor continuum, reformatting a coding space that is concerned with

what is and what was the case, into a coding space that is concerned with what should be done.

For both larval and adult *Drosophila* it seems fair to say that despite the clarity of this working hypothesis, the exact division of labor between individual DANs remains to be elucidated (discussion in Das et al. [2016]). This must be revealed, however, to understand how separate memories for distinct kinds of reward can be established (e.g. fructose versus amino acids, Schleyer et al. [2015a]). Likewise, the way in which MBONs organize learned behavior is only recently beginning to be understood in adults [Séjourné et al., 2011; Pai et al., 2013; Plaçais et al., 2013; Aso et al., 2014a,b; Bouzaiane et al., 2015; Owald et al., 2015; Hige et al., 2015; Perisse et al., 2016] and remains clouded in the case of larvae. Here, we systematically address these issues at the single-cell level, in the larva.

6.3 Results

We selected 877 Gal4 driver strains with expression in the central nervous system of stage 3 *Drosophila* larvae (Li et al. [2014], http://flweb.janelia.org/cgi-bin/flew.cgi) and inspected them for coverage of mushroom body extrinsic neurons (MBEs). Systematic multi-color flp-out [Li et al., 2014; Nern et al., 2015] revealed the identity and morphology of 11 mushroom body compartments and 44 individual MBE neurons (Figure 1c-e, Table 1-3). This flp-out approach in addition allowed establishing a collection of 102 Gal4 strains that include MBE neurons in their expression pattern for functional analysis and for narrowing down expression patterns by intersectional strategies [Luan et al., 2006; Pfeiffer et al., 2010] (Table 4). A recent electron microscope reconstruction of a stage 1 larval brain uncovered 3 MBE neurons that have not yet been found in stage 3 larvae; in turn and of particular significance for stage 3 larval behavior, we identified 6 MBE

neurons that are present in stage 3 larvae but are not present in the electron microscope reconstruction of the stage 1 larva (Figure S1 and Figure S2) [Eichler et al., 2017]. These differences suggest that our stage 3 MBE neuron atlas is about 95 % complete, and that functional MBE neurons are incorporated into the system as the larvae grow and mature. Fitting the generally very high level of concordance in MBE morphology across stages (Figure S1 and Figure S2), however, behavioral faculties of stage 1 larvae qualitatively match those of stage 3 larvae across multiple assays, including the odor preference, taste preference and odor-taste associative learning assays employed in the present analysis [The Ol_1mpiad Consortium et al., 2017].

Most MBE neurons are present as one cell per hemisphere, with mirror-image symmetry of the cells at the left and right side of the brain ('pairs'). Exceptions are the OAN-a1 and OAN-a2 neurons with unpaired cell bodies located at the midline in the maxillary and mandibular segment, respectively (Figure S3); both these cells have bilaterally symmetrical morphology. In five cases MBE neurons are present as double pairs, i.e. with two cells per hemisphere (Figure S3, Table 1).

The axonic and dendritic arbors of the MBE neurons define 11 non-overlapping compartments of the mushroom body, and cover these compartments in completion (Figure 1c-e, Figure S4). The majority of MBE neurons innervate a single compartment per hemisphere (38/44) and often the same compartment on the contralateral side (14/38) (Figure 1e). These neurons we call single-compartment MBE neurons (sMBE). Those 6 MBEs that innervate multiple compartments are called multiple-compartment MBE neurons (mMBE).

The innervation by the MBE neurons intersects the axonal projections of the KCs. Thus, within each compartment the MBE neurons can relate to the coding space encompassed across the KCs. In most cases the morphology of the MBE neurons allowed us to distinguish regions rich in presynaptic boutons from regions dominated by spine-like

postsynaptic structures; electron microscopy verified these interpretations [Eichler et al., 2017]. The MBE neurons were accordingly classified as MBE input or MBE output neurons (MBINs or MBONs). Compartments are in register for MBINs and MBONs (Figure 1e). The APL neuron is the only MBE that almost exclusively communicates within the mushroom body and is therefore labeled as MBIN/MBON neuron (structure and function of this neuron will be discussed in more detail below).

All MBINs, excepting OAN-e1, provide inter-hemispheric crosstalk; the same is observed for about half of the MBONs (12/21 sMBON neurons, 3/4 mMBON neurons) (Table 1). This is striking, as little inter-hemispheric integration is otherwise seen along the olfactory ascending pathways [Berck et al., 2016], or the KCs [Kunz et al., 2012; Eichler et al., 2017]. We note that all MBINs, excepting MBIN-m1, were classified as single-compartment type, while the MBONs feature 4 MBEs classified as multiple-compartment type. This suggests that the mushroom body output coding space may be relatively more integrated across compartments than mushroom body input.

For a pre-screen of the function of the MBE neurons, we crossed the mentioned collection of 102 MBE-covering Gal4 driver strains to *UAS-shi*^{ts} (Table 2 and Table 3) (4 MBE neurons were not covered for practical reasons). At restrictive temperature, and thus under acute block of synaptic output, the offspring was assayed in an odor-fructose reward association task. Larvae received the odor *n*-amylacetate (AM) and a fructose reward (FRU) either in a paired manner or, in independent groups of animals, in an unpaired way. Then, animals from both groups were tested for their preference for the odor. From the difference in preference between the paired-trained versus the unpaired-trained groups an associative performance index (PI) was calculated (see Methods section for details).

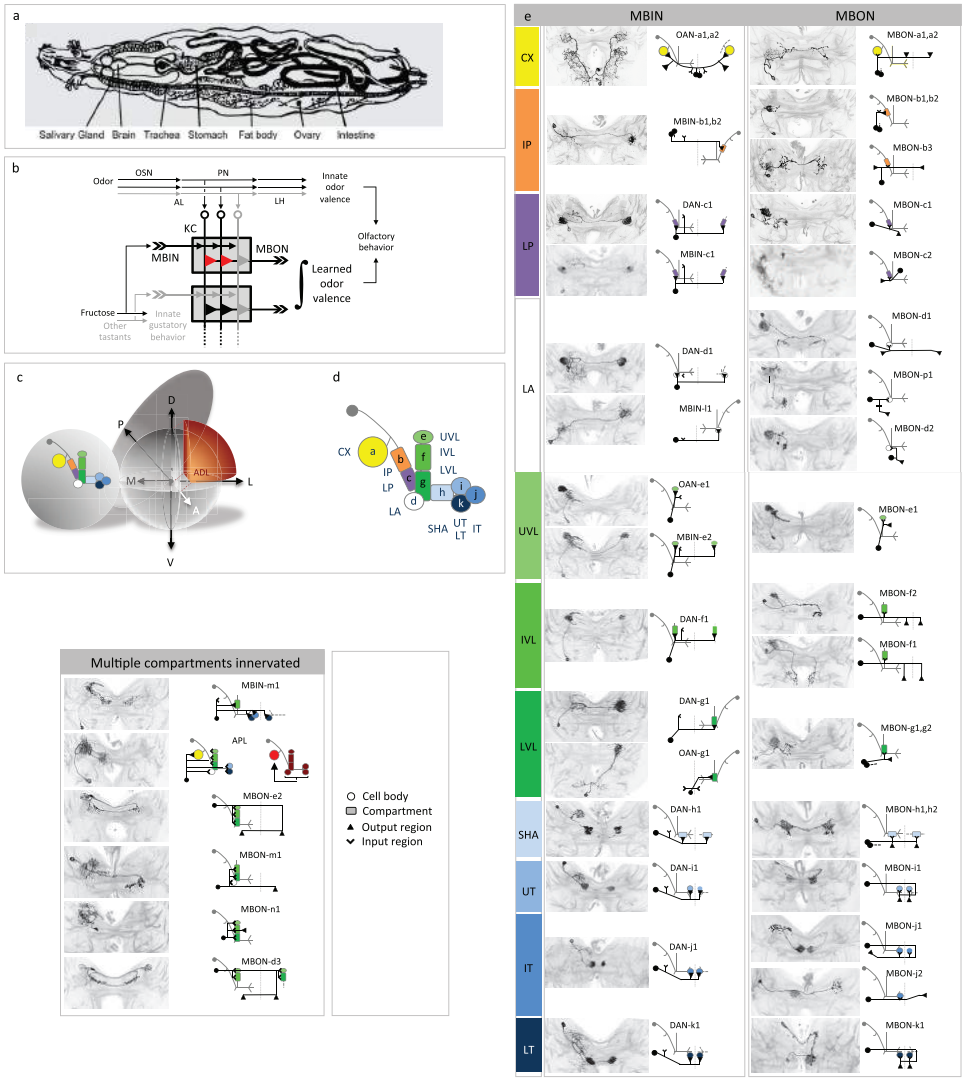

Figure 1: Atlas of the MBE neurons.
a Body plan of stage 3 *Drosophila* larvae (modified from Demerec and Kaufmann [1965]); 'Brain' refers to the ventral nerve cord plus the two brain hemispheres towards the left. Also see Movies 1-5.
b Simplified diagram of the olfactory and gustatory pathways, and of the organization of innate and learned olfactory, as well as of innate gustatory behavior in the larva (for details, see text). AL: antennal lobe, KC: Kenyon cells of the mushroom body, LH: lateral horn, MBIN: mushroom body input neurons, MBON: mushroom body output neurons, OSN: olfactory sensory neurons, PN: olfactory projection neurons. The red triangles indicate KC output synapses that are modulated by the joint presentation of odor and fructose; grey and black synapses indicate silent and active synapses, respectively. The grey boxes indicate mushroom body compartments. Note that learned odor valence can be based on integration across multiple compartments. The within-AL circuitry and the APL neuron are not displayed.
c Schematic of the location and orientation of the mushroom body within the larval nervous system. The mushroom body is only shown in one hemisphere. A: anterior, D: dorsal, P: posterior, L: lateral, M: medial, V: ventral.
d Organization of the larval mushroom body in 11 compartments. CX: calyx; IP and LP: intermediate and lower peduncle; LA: lateral appendix; UVL, IVL and LVL: upper, intermediate, and lower vertical lobe; SHA, UT, IT, LT: shaft as well as upper, intermediate and lower toe of the medial lobe. Single-letter synonyms of compartment names are given as 'a-k'; these letters are used to indicate compartment-innervation by the MBEs in (e).
e Identification of the MBE neurons by compartment innervation, input and output regions, and cell body location. The MBE of only one hemisphere is shown (for the unpaired OAN-a1 and OAN-a2 neurons, the cell bodies are located near the midline). For MBE pairs, the second neuron of the pair is indicated by its cell body and stippled primary neurite. Innervations by ascending sensory interneurons, such as the olfactory projection neurons, are not included. Anatomical panels show z-projections of those parts of the larval brain that include the MBEs. MBEs are visible based on antibody staining against the flp-out effectors; anti-neuroglian staining in grey reveals the local brain structure. Note that the nomenclature for the MBIN-l1 and MBON-p1 neuron is based on their compartment-innervation in the stage 1 larva (Figure S1a and b). For more details, see Table 1 and Eichler et al. [2017].

Combining the data from all those strains that cover a given MBE neuron, and considering the recent report by Rohwedder et al. [2016], this pre-screen identified the MBEs innervating the medial lobe compartments, the lower vertical lobe compartment, and the APL neuron as candidates for being required in odor-fructose association (Figure S5). Next, we generated a collection of 12 split-Gal4 driver strains expressing reliably, strongly, and specifically in 13 MBEs (Table 4) (in 3 cases, drivers were specific for the respective double pair). These driver strains were crossed to *UAS-Kir2.1::GFP* to silence neuronal activity by an immuno-histologically detectable transgene; expression of *Kir2.1::GFP* was confirmed in all cases (not shown). The larvae were then assayed for i) odor-fructose reward association, as well as for innate responsiveness towards the to-be-associated stimuli, namely for ii) odor preference and for iii) fructose preference (Figure 2). Our results show a sparse and specific role of MBEs in these tasks. That is, in 3 cases impairments specifically concerned the odor-fructose association task, but not odor preference and not fructose preference (DAN-h1, MBON-j2, MBON-g1,g2: Figure 2a, g, and j, Figure S6a, g, and j) (regarding the APL neuron see below). In 1 case an impairment in the preference for odor as well as for fructose was found, and no impairment of odor-fructose association (DAN-k1: Figure 2c, Figure S6c, Figure S7a and b). We further note as a special case that while silencing DAN-g1 impaired neither of these three tasks (Figure 2i), this was found to make olfactory behavior more susceptible to non-associative effects of odor-only as well as of fructose-only exposure (Figure S8). In the remaining 5 cases, no phenotype in any of the three tasks was observed (MBON-h1,h2, MBON-k1, DAN-i1, MBON-i1, MBON-j1: Figure 2b, d, e, f, and h, Figure S6b, d, e, f, and h). The fact that if impairments were observed, these impairments were partial suggests a fair degree of redundancy in brain organization for the studied behavioral tasks. In turn and maybe more importantly, we did not observe any case of impairment in all tasks. Together, these results show sparseness and specificity in

the requirement of MBE neurons for odor-fructose association, odor preference, and fructose preference (Figure 2l).

The MBIN found to be required for the odor-fructose association task was DAN-h1 (Figure 2a). This resolves the question whether any one of the four pPAM neurons delivering dopaminergic reward signals towards the mushroom body medial lobe is individually necessary for proper performance in this task [Rohwedder et al., 2016]. We next asked whether in turn individual pPAM neurons are sufficient for mediating an internal reward signal, as this likewise had remained unresolved. Towards this end, instead of presenting a real fructose reward we used *ChR2-XXL* to optogenetically activate DAN-h1, DAN-k1, or DAN-i1 as an internal reward signal (attempts to generate a suitable driver strain for DAN-j1 have failed). We found that activation of DAN-h1 as well as activation of DAN-i1 is sufficient as an internal reward signal, while activation of DAN-k1 remained without such effect (Figure 3a-d, Figure S9; using Chrimson as an optogenetic effector revealed that the rewarding effect of activating DAN-i1 is apparently stronger than for DAN-h1: Figure S10). Corresponding to what was previously reported for fructose as a real reward [Schleyer et al., 2015b; Paisios et al., 2017] the memories established by optogenetic activation of DAN-h1 as well as of DAN-i1 behaviorally express in terms of associative modulations of both turn rate and turning direction (Figure S11).

Thus, activation of either DAN-h1 or of DAN-i1 is sufficient to mediate an internal reward signal (Figure 3a-d), while only DAN-h1 activity evidently participates mediating the rewarding effect of real fructose (Figure 2a and e). This prompted the question whether activity in DAN-i1 is required for mediating other rewards, while for those other rewards DAN-h1 may be dispensable. Indeed, silencing DAN-h1 specifically impaired learning about a fructose reward, but not learning about low-salt or aspartic acid rewards (Figure 3e, Figure S12). In turn, silencing DAN-i1 did not impair learning about fructose,

low-salt, or aspartic acid reward (Figure 3f, Figure S12), and also did not affect learning about arabinose or sorbitol reward (Figure S13). This suggests that different 'matters of concern' to a larva are classified into at least partially separate internal rewarding pathways reaching the mushroom body by different dopaminergic neurons. To some extent, therefore, the coding across the dopaminergic MBINs features characteristics of a labeled-line code. Does such separation of processing channels carry through to mushroom body output?

This does not appear to be the case. That is, task requirement does not match by compartment (Figure 2l): The only MBIN found to be required for proper performance in the odor-fructose association task innervates the medial lobe shaft (DAN-h1: Figure 2a) - but silencing the MBONs from this compartment does not impair performance (MBON-h1,h2: Figure 2b, Figure S14). Rather, silencing MBONs from two other compartments causes impairments in odor-fructose association scores (MBON-j2 from the intermediate toe: Figure 2g; MBON-g1,g2 from the lower vertical lobe: Figure 2j).

Likewise, silencing the MBIN to the lower toe impairs both odor and fructose preference (DAN-k1: Figure 2c, Figure S7a and b), while silencing its output neuron does not (MBON-k1: Figure 2d, Figure S7c and d).

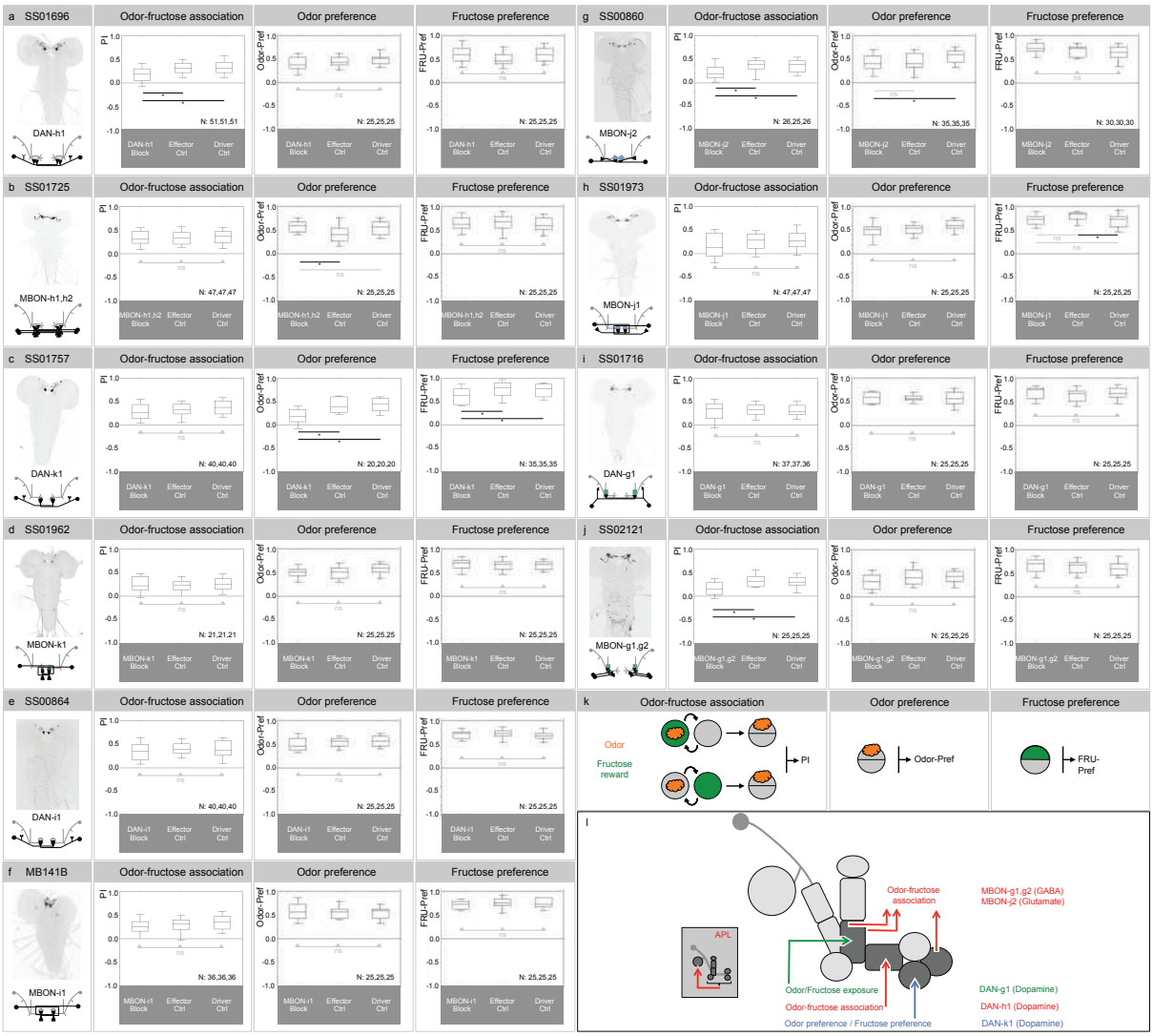

Figure 2: Selective and sparse necessity of MBE neurons for odor-fructose reward association, odor-preference and fructose-preference.

a-j Expression pattern of the indicated split-Gal4 strain and schematic overview of the covered MBE (leftmost column), associative performance indices for odor-fructose reward associative memory (second column), and preference scores of experimentally naïve larvae for the odor (third column) as well as for fructose (rightmost column). Experimental larvae are heterozygous for the indicated split-Gal4 drivers and for *UAS-Kir2.1::GFP*, leading to silencing of the respective MBE (MBE Block). Control larvae are heterozygous for only the *UAS-Kir2.1::GFP* effector (Effector Ctrl), or for only the split-Gal4 drivers (Driver Ctrl). Box plots show the median as the middle line, and 25/75 % and 10/90 % quantiles as box boundaries and whiskers, respectively. Sample sizes are indicated within the figure. At plain horizontal lines * refers to $P>0.05/2$ and ns to $P>0.05/2$ in Mann-Whitney U-tests; at horizontal lines with arrowheads, ns refers to $P>0.05$ in Kruskal-Wallis tests. The preference scores underlying the associative performance indices in the leftmost panels can be found in Figure S6. Expression patterns of split-Gal4 drivers covering the respective MBE are visible based on anti-GFP staining (black); the central nervous system is visible based on background fluorescence (grey).

k From left to right the panel shows schematics of the odor-fructose reward association paradigm, and of the paradigms to measure odor preference or fructose preference, respectively, in experimentally naïve animals. The orange cloud indicates *n*-amylacetate as the odor, the green circle indicates the fructose reward. In half of the cases the sequence of training trials was as indicated in the leftmost display, while for the other half it was reverse (not shown).

l Summary of the necessity experiments. Arrows represent MBE neurons for which activity is required for full performance in the indicated behavioral task. Note that for odor-fructose association the target compartment of the required MBIN (DAN-h1) is different from the compartment of origin of both the required MBONs (MBON-g1,g2 and MBON-j2). Across-compartment communication can arguably be mediated by i.a. the activity of the APL neuron (inset; Figure 1c and Figure 4). For more detail regarding the effect of blocking DAN-g1 on olfactory behavior after non-associative odor and non-associative fructose exposure, see Figure S8. References regarding the indicated transmitters can be found in Table 1.

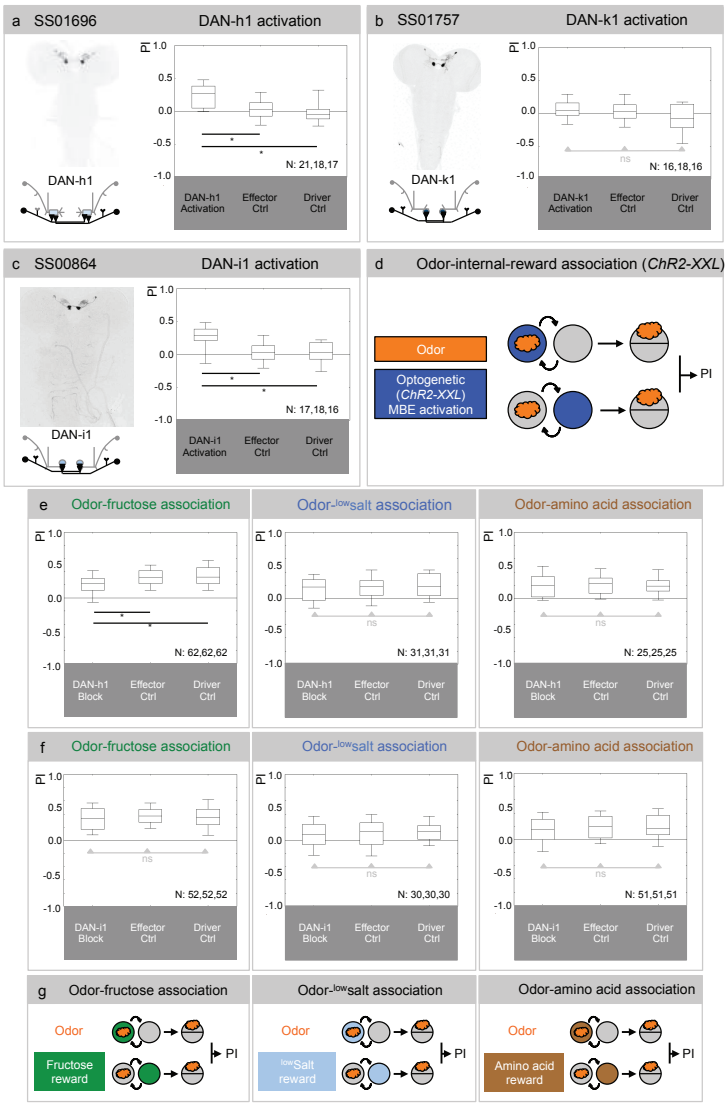

Figure 3: Sufficiency of DAN-h1 and of DAN-i1 as internal reward signal.
a-c Larvae are trained for association of odor with optogenetic activation of dopaminergic MBE input neurons as internal reward. The panels show the expression pattern of the indicated split-Gal4 strain and a schematic of the covered MBE, plus the associative performance indices after odor-internal-reward training. Experimental larvae are heterozygous for the split-Gal4 drivers as well as *UAS-ChR2-XXL* (DAN Activation). Control larvae are heterozygous for only the *UAS-ChR2-XXL* effector (Effector Ctrl), or only the indicated split-Gal4 drivers (Driver Ctrl). Activation of DAN-h1 (a) and activation of DAN-i1 (c) is sufficient as reward, while activation of DAN-k1 is not (b). Other details as in Figure 2. The preference scores underlying the associative performance indices can be found in Figure S9.
d Schematic of the odor-internal-reward association paradigm. The blue color indicates optogenetic activation of the respectively covered MBE neuron. Other details as in Figure 2.
e,f Silencing of DAN-h1 by means of *Kir2.1::GFP* expression leads to an impairment in odor-fructose association (left) (this data includes those odor-fructose association data shown in Figure 2a), but not in odor-^{low}salt (middle) and not in odor-amino acid association (right). Silencing DAN-i1 does not impair association of odor with either of these three rewards (f; odor-fructose association data include those shown in Figure 2e). Likewise, odor-arabinose association as well as odor-sorbitol association are unaffected by silencing of DAN-i1 (Figure S13). Other details as in Figure 2. The preference scores underlying the associative performance indices can be found in Figure S12.
g From left to right, schematic of the odor-fructose, odor-^{low}salt, and odor-amino acid association paradigm are shown. The green, light blue, and brown circles indicate the fructose, odor-^{low}salt, and amino acid reward, respectively. Other details as in Figure 2.

Taken together, our results suggest that within-mushroom body and between-compartment crosstalk takes place during the organization of behavior. How could such crosstalk come about?

At least four circuit motifs of the larval mushroom body matrix could provide such crosstalk. First, four mMBONs integrate inputs from multiple compartments (MBON-e2, MBON-m1, MBON-n1, and MBON-d3: Figure 1e), and in the case of MBON-d3 also across hemispheres. Second, KC-KC synapses provide direct lateral connections [Eichler et al., 2017]. Third, MBON-MBON synapses establish an intricate network of mushroom body efferent circuitry [Eichler et al., 2017]. Fourth, the GABA-ergic APL neuron integrates input from nearly half of the compartments and provides inhibition towards the calyx where the signal is distributed across the KCs (Figure 4a-d). Indeed a connectivity analysis of the APL neuron at the electron microscope revealed that very few KCs are either exclusively presynaptic or exclusively postsynaptic to it, and that for a given KC_x the number of KC_x-APL synapses is unrelated to the number of APL-KC_x synapses; rather, APL establishes a distributive KC_x-APL-KC_y loop (Figure 4b and c; Eichler et al. [2017]). Thus, via the APL neuron most KCs receive inhibition proportional to an integrated read-out of activity in all KCs; in turn, the APL neuron samples most of if not the complete olfactory input that the olfactory projection neurons deliver towards the KCs, plus a sizeable non-olfactory input (Figure 4c and d; Eichler et al. [2017]). Thus, across those KCs receiving olfactory input, GABA-ergic signaling via the APL neuron can contribute to the sparsening of odor-evoked activity; such sparse activity allows for a specific combinatorial coding of odors in the mushroom body. A modulation of this sparseness could tweak the set point between generalization and discrimination of odors, which indeed can be adjusted in a task-dependent way (Mishra et al. [2010]; Barth et al. [2014]; but also see Campbell et al. [2013]; Chen and Gerber [2014]). It can also contribute to negotiate the balance of activity across KCs

activated by different sensory modalities, potentially aiding a task-dependent separation of stimulus foreground from contextual background. Taken together, there is ample substrate for integration of odor-related activity, plus activity related to non-olfactory input, across compartments. In effect it appears that a code in the MBINs that operates with at least some characteristics of a labeled-line code is 're-formatted' into a relatively more integrated, combinatorial code across the network of the MBONs. For the APL neuron as an example we looked into the behavioral significance of such integration. Across-compartment integration via the GABA-ergic APL neuron is required for proper odor-fructose association, as shown by the impairment in this task upon blocking APL; this requirement is specific, as both odor preference and fructose preference remain unchanged (Figure 4e and f, Figure S6l). Thus, without the possibility to maintain a sparse activity pattern across the KCs, and without an ability to separate olfactory stimulus foreground from non-olfactory, contextual background, the larvae are apparently unable to properly perform in the present association task. In turn, optogenetically driving GABA-ergic signaling from the APL neuron should effectively silence the KCs; fittingly, under such conditions odor-fructose association is impaired, either when such GABA-ergic activation is exerted during the training phase only, or only during testing (Figure 4g-j, Figure S15). Again, this effect is specific, as driving the APL neuron neither affects odor preference, nor fructose preference (Figure 4k-n).

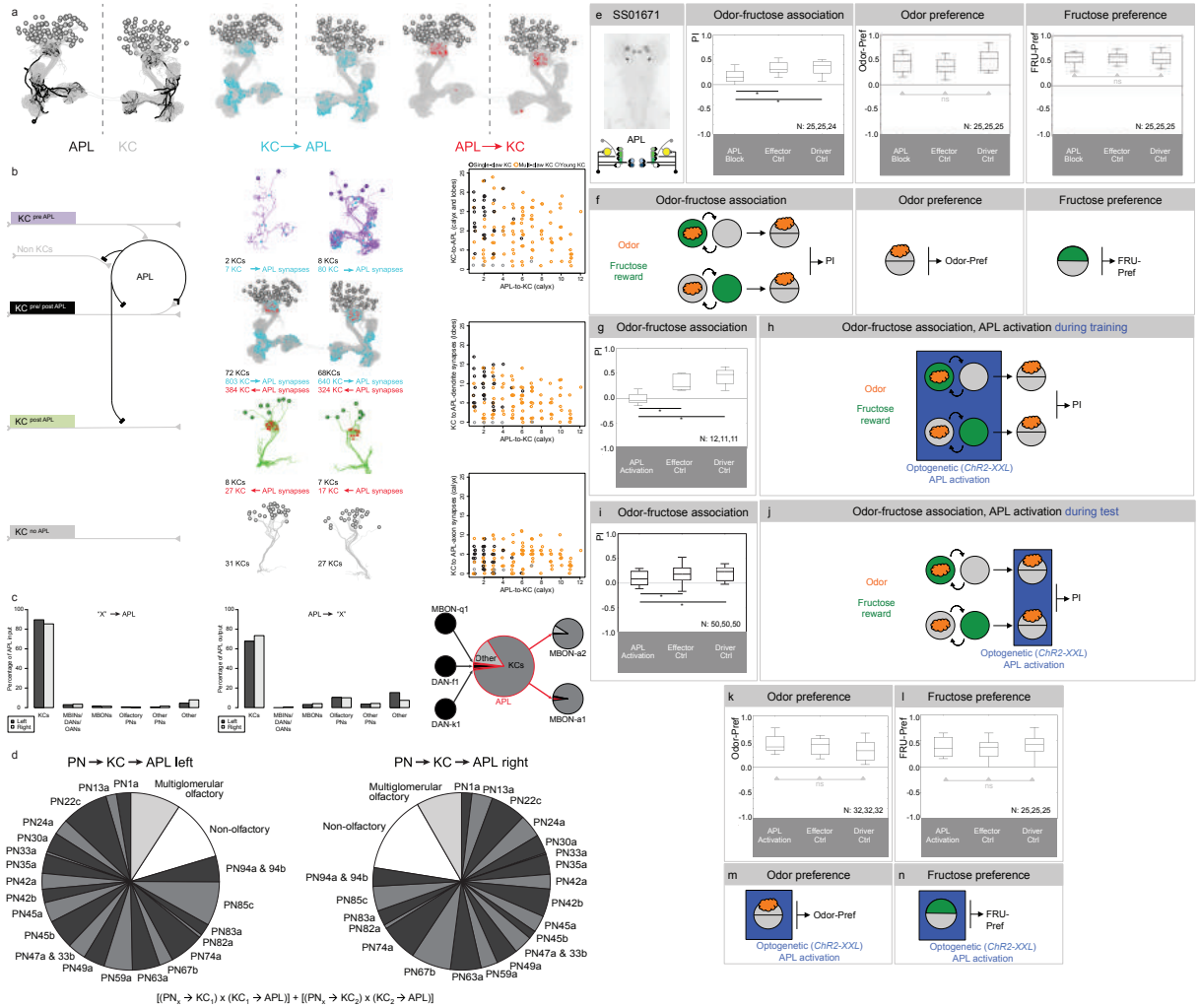

Figure 4: Structure, connectivity and behavioral function of the APL neuron.

a-c The larval APL neuron provides distributive inhibition within the mushroom body, and is embedded into the DAN-MBON network. (a) Electron microscopy reconstruction of the APL neuron relative to the mushroom body Kenyon cells (KCs) in both brain hemispheres (left panel). Sites of KC-to-APL synapses are marked in blue (middle panel), sites of APL-to-KC synapses in red (right panel). Inter-hemispheric connections are from aberrantly developed 'freak' KCs and do not correspond to the so-called ni-cells identified by Kunz et al. [2012]; these were found in the electron microscopy reconstruction but are not shown here.

b Classification of KCs as either being only presynaptic, as both pre- and postsynaptic, as only postsynaptic or as unconnected to the APL neuron (left panel). The anatomy of these KC classes is shown in the middle panel, including their number and the number and the site of KC-to-APL synapses (blue) and APL-to-KC synapses (red). KCs without any synapse with the APL neuron are apparently lacking proper dendrites and axons, and therefore are classified as young and likely immature. The panels to the right show for each KC the number of APL-to-KC synapses versus respectively the number of all KC-to-APL synapses (top), the number of KC to APL-dendrite synapses (middle), and the number of KC to APL-axon synapses (bottom). The type of KC (single-claw, multi-claw and young KC) is color-coded. The lack of correlation implies that inhibition through the APL neuron is distributive, i.e. with but random levels of KC_{α}-APL-KC_{α} feedback.

c Fraction of the APL neurons' presynaptic partners as percent of the total amount of synaptic input to APL (top left), and fraction of APLs' postsynaptic partners as percent of the total amount of synaptic output from APL (top right). Data is shown for the left (black) and right brain hemisphere (grey) separately. KCs contribute more than two thirds of the inputs to the APL neuron, which in turn dedicates about two thirds of its output to KCs. The bottom panel shows the connectivity of the APL neuron with DANs and MBONs. APL receives input from one vertical lobe DAN (DAN-f1) and one medial lobe DAN (DAN-k1) as well as from a vertical lobe MBON (MBON-q1, which was only found in stage 1 larvae: Figure S1 and Figure S2). The APL neuron delivers output to both calyx MBONs (MBON-a1 and MBON-a2). Indicated connections are axo-dendritic and shown as fractions of inputs onto the receiving neuron.

d The APL neuron samples the complete information delivered to the KC via projection neurons (PNs). To determine the total input that the APL neuron receives from KCs that in turn receive their input from uniglomerular olfactory PNs (black and dark grey), multiglomerular olfactory PNs (light grey) and non-olfactory PNs (white), we calculated the matrix product of the respective PN-to-KC connections and the KC-to-APL connections. *(See next page).*

Figure 4: *Continues from prior page.*
e Silencing the APL neuron impairs odor-fructose association, but neither odor preference nor fructose preference. Expression pattern of the split-Gal4 strain covering the APL neuron and schematic of its innervation of the mushroom body (left column), associative performance indices for odor-fructose reward associative memory (second column), and preference scores of experimentally naï larvae for the odor (third column) as well as for fructose (right column). Experimental larvae are heterozygous for the split-Gal4 driver and for *UAS-Kir2.1::GFP* (APL-Block). Control larvae are heterozygous for only the *UAS-Kir2.1::GFP* effector (Effector Ctrl), or for only the split-Gal4 driver (Driver Ctrl). Other details as in Figure 2. The preference scores underlying the associative performance indices can be found in Figure S6.
f From left to right the panel shows schematics of the used behavioral paradigms; further details as in Figure 2.
g Optogenetic activation of the APL neuron during only training abolishes odor-fructose association. Experimental larvae are heterozygous for the split-Gal4 driver as well as *UAS-ChR2-XXL* (APL-Activation). Control larvae are heterozygous for only the *UAS-ChR2-XXL* effector (Effector Ctrl), or for only the split-Gal4 drivers (Driver Ctrl). Other details as in Figure 2 and Figure 3a-d. The preference scores underlying the associative performance indices can be found in Figure S15.
h Schematic of the behavioral paradigm. Blue shading indicates optogenetic stimulation. Other details as in Figure 2.
i, j As in (g, h), showing that activation of the APL neuron during only the test reduces odor-fructose association scores.
k, n) As in (I, j) showing that activation of the APL neuron in experimentally naï animals does neither affect odor preference nor fructose preference.

6.4 Discussion

The present study reveals the identity and morphology of close to all neurons of the MBIN-MBON-APL network of stage 3 *Drosophila* larvae, and provides a survey of their function in innate olfactory behavior, innate gustatory behavior, and odor-taste associative learning. It further provides a collection of split-Gal4 drivers for specifically manipulating a subset of these neurons.

The MBIN-MBON-APL network across larval stages

A stage 3 larva shares characters with its earlier self as a stage 1 larva and its later self as an adult fly [Hartenstein et al., 2008; Ito et al., 2013; Yu et al., 2013]. Across the larval stages body length and speed of locomotion increase about 4-fold. Still, the behavioral faculties of stage 1 larvae are qualitatively concordant with stage 3 [The Ol$_1$mpiad Consortium et al., 2017]. Fittingly, the number and morphology of their MBINs, MBONs, and of the APL neuron are very similar (Figure S1, Figure S2) [Eichler et al., 2017] - with at least two relevant exceptions. Firstly, the DAN-h1 neuron is absent in stage 1 (Figure S1) [Eichler et al., 2017]. Despite this lack of DAN-h1, stage 1 larvae are capable of odor-fructose association [Pauls et al., 2010; The Ol$_1$mpiad Consortium

et al., 2017]. This is in line with our observation in stage 3 larvae that silencing DAN-h1 but partially impairs odor-fructose association (Figure 2a, Figure 3e). The same partial redundancy is revealed for the second case, the output neuron from the intermediate toe of the medial lobe, MBON-j2 (Figure 2g, Figure S1) [Pauls et al., 2010; The Ol_1mpiad Consortium et al., 2017; Eichler et al., 2017].

The MBIN-MBON-APL network across metamorphosis

The general organization of the MBIN-MBON-APL network in stage 3 larvae is also similar to the one in adult *Drosophila*. There are typically 1-2 MBONs per compartment, and also for the OANs and for the DANs of the PPL-cluster there are typically 1-2 neurons per compartment [Tanaka et al., 2008; Aso et al., 2014a]. However, at least three differences in the MBIN-MBON-APL network between larvae and adult *Drosophila* are notable. Firstly, the number of PAM-cluster DANs increases to up to 20 (sic) per cell type and compartment in adult *Drosophila* [Aso et al., 2014a]. PAM-DANs preferentially innervate the medial lobes and are responsible for reward-learning in both larval and adult *Drosophila* [Burke et al., 2012; Liu et al., 2012; Yamagata et al., 2015; Rohwedder et al., 2016]. An increase in the number of PAM-DANs thus suggests a better signal-to-noise ratio for reward processing in adult *Drosophila*. Differences in the sensitivity to reward between PAM-DANs would broaden the dynamic range across which reward strength can be mapped in adult *Drosophila*. Higher-resolution and broad-range mapping of memory strength to reward strength is relevant when memory formation and/ or memory-based decisions need to be quick, as e.g. during fast walking or flight. Qualitative differences in the reward inputs the PAM-DANs receive would additionally allow for more nuanced processing of reward kind in adult *Drosophila*. Together, this may be critical to keep track of rewards that are more variable in time and space, or that are ‘of adult kind’ such as sexual rewards. By contrast, the representation of punishment, for the most part mediated by PPL-DANs (Schroll et al. [2006]; Selcho

et al. [2009]; adult *Drosophila*: Schwaerzel et al. [2003]; Claridge-Chang et al. [2009]; Aso et al. [2010, 2012]; Hige et al. [2015]) does not differ in numbers between larvae and adults. Secondly, neither our inspection of the driver lines of the Janelia collection, nor our extensive flp-out analysis, nor the electron microscope reconstruction of the MBIN-MBON-APL network of stage 1 larvae [Eichler et al., 2017] revealed a larval DPM neuron [Waddell et al., 2000]. Also, none of the driver strains known to cover the DPM neuron in adult *Drosophila* includes a larval DPM neuron (Thum, unpublished). In adult *Drosophila*, the DPM neuron innervates the ipsilateral MB and ramifies throughout the MB but excludes the calyx. It was reported that the DPM neuron produces the amnesiac neuropeptide [Waddell et al., 2000], serotonin [Lee et al., 2011], and GABA [Haynes et al., 2015]. Fitting the absence of the DPM neuron in the larva there is no detectable immunoreactivity against serotonin in its MB (Blenau and Thamm [2011]; Huser et al. [2012]; the serotonergic CSD neuron does not innervate the larval MBs: Roy et al. [2007]). Thus, either the functions of the DPM neuron and of MB-innervating serotonergic neurons are exerted by neurons other than DPM in the larva (e.g. to support memory consolidation: Waddell et al. [2000]; Keene et al. [2004]; Yu et al. [2005]; Lee et al. [2011]), or these functions are conferred by relatively far-range serotonergic volume transmission towards the MBs [Silva et al., 2014], or these functions are not implemented in the larva altogether as is the case for the modulation of sexual behavior, of legged locomotion, and of flight. Thirdly, in the larva KC-APL synapses are present in MB calyx and lobes, but APL-KC synapses are restricted to the calyx (Figure 4a and b). Thus, in addition to a local calyx KC-APL-KC network, the APL neuron establishes an apparent lobe-calyx feedback connection in larvae, reminiscent of the PCT neurons in the bee [Grünewald, 1999a]. No such polarity is apparent in adult *Drosophila*, as KC-APL and APL-KC synapses are intermingled in both calyx and lobes [Liu and Davis, 2009; Pitman et al., 2011; Wu et al., 2011; Lin et al., 2014a]. Furthermore in the case of

the larva, the APL neuron innervates only 7 of 11 MB compartments (Figure 1e, Figure 4a), while the APL neuron innervates all MB compartments in adult *Drosophila* [Liu and Davis, 2009; Pitman et al., 2011; Wu et al., 2011; Lin et al., 2014a]. Differences in function between the larval and the adult APL neuron are to be expected also because the DPM neuron, anatomically and functionally entangled with APL in adult *Drosophila* [Pitman et al., 2011; Wu et al., 2011], is absent in the larva (previous paragraph). Of note, despite these differences in structure and likely also in function, the larval APL neuron does persist through metamorphosis (Figure S16).

DANs and reward-specific memory

Larvae form associative memories between odor and taste reward that can be specific not only for the odor [Chen et al., 2011; Chen and Gerber, 2014] but also for the reward [Schleyer et al., 2015a]. That is, after odor-fructose reward training learned odor attraction is abolished if the test is carried out in the presence of fructose [Gerber and Hendel, 2006; Schleyer et al., 2011, 2015a,b] (innate olfactory behavior is not likewise affected). This is adaptive because tracking down the learned odor in search for a reward is pointless if the sought-for reward is actually present. Indeed, learned search for fructose is abolished in the presence of fructose, but not in the presence of an equally strong aspartic acid reward, and vice versa [Schleyer et al., 2015a]. Thus, memories from odor-fructose and from odor-aspartic acid training can be established and retrieved independently of each other. Fittingly, we found that activity in DAN-h1 is required for proper odor-fructose association but is dispensable for odor-aspartic acid association (Figure 3e). As will be discussed in more detail in the following section, this suggests that a division of labor between DANs contributes to the taste-reward specificity of associative memory in the larva for fructose (and alike rewards) versus aspartic acid (and alike rewards). Indeed, a similar picture may be emerging for adult *Drosophila*, too (Burke et al. [2012]; Lin et al. [2014b]; for a critical discussion Schleyer

et al. [2015a]). Once it becomes possible to study defined subsets of DANs in mammals one can test for similar breaches of the reward-general, common-currency hypothesis of DAN function [Lak et al., 2014]. Of note, behavioral analyses suggest a co-existence of reward-general and reward-specific memories in the larva (Schleyer et al. [2015a]; regarding humans Howard et al. [2015]).

Sparseness and specificity

We report a sparse and specific requirement of MBE activity in behavior organization. For each of the behavioral tasks we looked at, it is only in few MBEs that silencing activity had a measureable effect - and in turn for each of the MBEs we looked, the requirement for their activity was task-specific (Figure 2l). For example, silencing DAN-h1 left odor preference and fructose preference intact (Figure 2a) but selectively impaired odor-fructose and not odor-aspartic acid association, and not the association of odor with low-concentration salt as reward (Figure 2a, Figure 3e). This suggests that rewards are processed by a non-redundant, labeled-line code that maintains information about reward kind. However, in this as in all other cases of impairment by silencing MBEs, the impairment we observed was partial. This is suggestive of a robust, partially redundant combinatorial code. If so, this code is apparently so sparse that single MBINs nevertheless make a behaviorally meaningful, measurable contribution to the processing of specific rewards. Consistent with the activity of individual DANs being meaningful to the larvae, memories established by presenting odor with optogenetic activation of DAN-h1 or DAN-i1 show the same locomotor 'footprint' as odor-fructose memories (Figure S11). The MB compartments would thus allow a larva to form and retrieve memories of specific 'matters of concern' [Heisenberg, 2003; Gerber et al., 2009], according to the activation profile of its MBINs. Interestingly, the DANs innervating the medial and the vertical lobe compartments are primarily concerned with rewards and punishments, respectively [Schroll et al., 2006; Rohwedder et al., 2016]. In a drastically simplified

number game, this implies that a minimum of 4 and a maximum of 15 types of reward-memories and 3-7 punishment-memories can be formed in the larval MB (corresponding to a labeled-line versus a combinatorial coding across the 4 and 3 compartments of the medial and vertical lobes, respectively). Also for the MBONs the impairments upon silencing them were sparse, selective, and partial (Figure 2l). Strikingly, the impairments in odor-fructose association did not match by compartment to the ones observed for silencing the respective MBINs. Thus, although the physiological effects of MBIN-KC coincidence can remain local to the MBINs' target compartment (as shown in adult *Drosophila*: Hige et al. [2015]), the organization of learned behavior apparently involves across-compartment integration, e.g. via the mMBONs, KC-KC as well as MBON-MBON synapses, and/ or via the APL neuron. A reasonable working hypothesis thus is that the ultimate read-out of the MBON network provides a learned-valence signal integrated across large aspects if not the complete MB and reflecting the various associative memories evoked by a given situation. Summed with the innate valence of the stimuli comprising that situation, approach or avoidance will result (Schleyer et al. [2015b]; Wystrach et al. [2016]; Paisios et al. [2017]; for adult *Drosophila*: Aso et al. [2014b]). Thus, within the MB relatively high-dimensional representations of predictive stimuli (across the KCs), and of reinforcement (across the MBINs) are 'reformatted' to provide a rather low-dimensional output to instruct behavior. In other words, it is downstream of the MBON network, and not at the level of the MBINs, that the larval brain operates by a common currency 'behavioral valence' signal.

Function(s) of the APL neuron

The APL neuron collects input from and distributes inhibitory GABA-ergic output across the KCs (Figure 4a-d) (Masuda-Nakagawa et al. [2014]; adult *Drosophila*: Liu and Davis [2009]; Pitman et al. [2011]; Wu et al. [2011]; Lin et al. [2014a]). Thus, the level of activity in a given KC will be scaled to the level of activity across KCs. Innate preference

for odor and for fructose are not affected by altering APL neuron function (Figure 4e, k-n). We will therefore discuss how such distributive inhibition may impact olfactory learning in our paradigm. When encountering an odor, a subset of KCs will be activated. Further KCs may be activated by tonic contextual input. Together these inputs can drive the APL neuron (Masuda-Nakagawa et al. [2014]; adult *Drosophila*: Liu and Davis [2009]; Lin et al. [2014a]; for corresponding findings in bees: Grünewald [1999b]; Filla and Menzel [2015]). Distributive GABAergic inhibition through APL will reduce activity for strongly activated KCs, and silence weakly active KCs. In effect the strongest, most salient input will dominate the KC activity pattern. When at the same time a reward such as fructose is presented, it will be this most salient input that preferentially enters into association. Thus, in our paradigm the salient, phasic olfactory 'foreground' rather than tonic, non-olfactory contextual 'background' will be associated with fructose. If this process is experimentally manipulated, the formation, consolidation, and/ or retrieval of associations will be affected (Figure 4e-j). These effects may depend on the level of APL activity in a complex way. That is, reducing APL activity may level-out processing of foreground versus background stimuli. This will favor learning of contextual background, such that olfactory foreground associations will be of relatively less impact. In turn, mildly increasing APL activity may reduce contextual background learning, making olfactory foreground associations more impactful. Strongly driving APL, however, may silence the KCs and prevent background and foreground learning altogether. Such a scenario can explain why both strongly reducing and strongly driving APL reduces performance in the one-odor, non-discriminatory paradigm of the present study (Figure 4e, g, and i). It may also help integrating otherwise disparate experimental results regarding APL function in discrimination tasks in adults [Liu and Davis, 2009; Pitman et al., 2011; Ren et al., 2012; Wu et al., 2012, 2013].

APL neuron and the 'blocking' effect

In adult *Drosophila* odor-electric shock training entails an odor-specific and associative weakening of odor-evoked activity in the APL neuron (Liu and Davis [2009]; for corresponding findings in bees: Grünewald [1999b]). This corresponds to the synaptic depression often observed after associative learning at the KC-MBON synapse in adult *Drosophila* (Séjourné et al. [2011]; Hige et al. [2015]; Owald et al. [2015]; Perisse et al. [2016]; bee: Menzel [2014]; but also see [Plaçais et al., 2013; Bouzaiane et al., 2015; Cohn et al., 2015]). If this happened in larvae as well, the proximity of the KC-MBON synapses to the KC-APL synapses (Figure S17) [Eichler et al., 2017] suggests that local learning-induced molecular alterations at KC presynaptic sites may affect the KC-APL synapses, too. In the simplest case, a strengthening of the memory trace may correspond to more severe depression of both the KC-MBON and the KC-APL synapses. Less activity in the APL neuron evoked by a trained odor A, relative to a control odor B, will lift inhibition of the KCs. This will favor the processing of stimuli added during later phases of the experiment. That is, it will open a window of facilitated processing of a novel stimulus X that is trained in compound with a stimulus A that already is predictive of reward (such a three-phase train A+, train AX+, test X experiment is called 'blocking': Kamin [1969]). Thus, in addition to predicted reinforcement often being less effectively processed than unpredicted reinforcement and leading to reduced learning about stimulus X (bees: Menzel [2001]; rabbits: Kim et al. [1998]; monkeys: Waelti et al. [2001]) the above scenario implies that stimulus X can be more effectively processed when presented together with the previously-trained stimulus A, leading to better learning of stimulus X. Dependent on the relative impact of these two processes and dependent on whether the KC-APL synapse is depressed (as in the sketched scenario) or whether it is potentiated, learning about stimulus X thus can be blocked, facilitated, or remain at baseline levels. Thus a distributive inhibition circuit as established by the APL neuron

provides the system with a degree of freedom to enhance learning about additional and redundant predictive cues such as X, or to prevent the establishment of such redundant memories. This is of conceptual importance because it means that the system can flexibly rely on either contiguity or contingency for associative memory formation. This may help understanding otherwise contradictory experimental results (adult *Drosophila*: Brembs and Heisenberg [2001]; Young et al. [2011]; bees: Smith and Cobey [1994]; Funayama et al. [1995]; Gerber and Smith [1998]; Gerber and Ullrich [1999]; Hosler and Smith [2000]; Guerrieri et al. [2005]; Filla and Menzel [2015]; mammals: Kamin [1969], as well as e.g. Kim et al. [1998]; Waelti et al. [2001]; Maes et al. [2016]). It may also integrate intensely debated, competing theoretical approaches to learning and memory that are based on variations in processing of predicting stimuli versus variations in processing of reinforcement [Kamin, 1969; Rescorla and Wagner, 1972; Mackintosh, 1974; Pearce and Hall, 1980; Sutton et al., 1981; Wagner, 1981; Miller and Matzel, 1988; Holland, 1993, 1997; Schultz et al., 1997; Fanselow, 1998; Kim et al., 1998; Steinberg et al., 2013; Maes et al., 2016].

6.5 Material and Methods

All experiments used third-instar feeding-stage, 5 day-old *Drosophila melanogaster* larvae, raised and treated under standard conditions (25 °C temperature, 65-70 % humidity, 12/12 light-dark cycle, standard food), unless stated otherwise. Larvae were chosen at random from their food vials. Behavioral experiments were performed under adjustable temperature and humidity conditions using a custom-built set-up (blueprints are available upon request). For the pre-screen larvae were pre-incubated in a water bath for 5 min at 36 °C to ensure synaptic transmission is blocked when using *shibire*^{ts} as the effector (see below). Training and test were then performed at restrictive, yet

slightly lower temperature (32 °C).

Statistical analyses used two-tailed, non-parametric tests throughout (Statistica 12.0, StatSoft software, Hamburg, Germany) (multiple-group comparison with Kruskal-Wallis tests, in case of significance followed by pairwise comparisons with Mann-Whitney U-tests); statistical assumptions for these tests were met. Bonferroni corrections were used to maintain the error of multiple pairwise comparisons below 5 %. Sample sizes were based on previous reports of chemosensory behavior and learning with moderate to weak effect sizes (e.g. Schroll et al. [2006]; Michels et al. [2011]; Saumweber et al. [2011a,b]). All behavioral experiments were run in parallel for the respective experimental group and genetic controls. Experimenters were blind to the specific genotypes.

Data availability

Relevant data can be obtained from the authors.

Odor-fructose reward association: Pre-screen

A standard odor-fructose reward associative learning paradigm was used (Scherer et al. [2003]; Neuser et al. [2005]; Saumweber et al. [2011a]; Apostolopoulou et al. [2013]; Gerber et al. [2013]; Michels et al. [2017]; Figure 2k), adapted to facilitate the pre-screen. These experiments were performed at HHMI Janelia Research Campus. Groups of 30 larvae each were free to move in 90 mm-diameter plastic Petri dishes filled with either plain 2.5 % agar (CAS: 9002-18-0; Fisher BioReagent, Fair Lawn, NJ, USA) or, during rewarded trials, agar with 2 mol/l fructose as a reward (+: CAS: 57-48-7; Fisher Scientific, Pittsburgh, PA, USA). Whenever an odor was to be presented, 10 µl *n*-amylacetate (AM: CAS: 628-63-7, diluted 1:50 in mineral oil: CAS: 8012-95-1; both Avantor Performance Materials, Center Valley, PA, USA) were pipetted on 5 x 5 mm filter papers taped to the lid of the Petri dish. When no odor was to be presented, a blank filter paper was used.

In the paired group, odor and reward were presented together throughout a given 2.5 min trial (AM+), while the unpaired group received odor and reward during separate 2.5 min trials (AM/+). To equate unpaired and paired group for handling and total training duration, sham trials were alternately performed for the paired group during which neither odor nor reward were presented (AM+/blank). In half of the cases, the sequence of training trials was reverse (blank/AM+ and +/AM, respectively). After three training cycles, preference for AM was assayed by placing the larvae to the middle of a fresh plain-agar Petri dish that featured AM on one side and a blank on the other side. After 3 min the number of larvae on either side was determined, and the preference for the odor AM in the paired and unpaired groups calculated:

(1) Odor-Pref = (Number on AM side - Number on blank side) / Total number

From the difference in preference between the paired-trained and unpaired-trained groups the performance index was calculated:

(2) PI = (Odor-Pref $_{Paired}$ - Odor-Pref $_{Unpaired}$) / 2

PI scores thus are bound between (-1; 1), with positive scores indicating appetitive and negative scores aversive memory.

Odor-fructose reward association: Screen

For the validation of candidates from the pre-screen with more specific drivers we wanted to be able to directly observe the effector expression and opted for *UAS-Kir2.1::GFP* as the effector. These experiments, and the ones mentioned below, were performed

at the LIN Magdeburg in the way described above except that i) training and test for these experiments were run at 25 °C because the *Kir2.1*$_{GFP}$ effector does not require heat induction; ii) 1 % agarose (NEEO Ultra-Quality; CAS: 9012-36-6; Roth, Karlsruhe, Germany) was used instead of agar; iii) fresh Petri dishes were used for each training trial; iv) odors were applied using custom made Teflon containers with perforated lids to allow evaporation of odor (AM; CAS: 628-63-7; Merck Millipore, Darmstadt, Germany, diluted 1:20 in paraffin oil, CAS: 8042-47-5; PanReac AppliChem, Darmstadt, Germany).

Odor-^{low} *salt, odor-aspartic acid, odor-arabinose, and odor-sorbitol reward association*

The experiments for odor-^{low}salt, odor-aspartic acid, odor-arabinose, and odor-sorbitol reward association were performed as detailed for odor-fructose association in the previous section, except that 0.4 mol/l NaCl (salt; CAS: 7647-14-5; Roth, Karlsruhe, Germany), 10 mmol/l aspartic acid (ASP; CAS: 56-84-8, Sigma-Aldrich Chemie GmbH, Munich, Germany), 2 mol/l arabinose (ARA; CAS: 10323-20-3; Sigma-Aldrich Chemie GmH, Munich, Germany), and 2 mol/l sorbitol (SOR; CAS: 50-70-4; Roth, Karlsruhe, Germany) were used, respectively.

Innate odor preference

Groups of 30 experimentally naïve larvae were placed to the middle of a Petri dish that featured the odor on one side and a blank on the other side. After 3 min the number of larvae on either side was determined, and the preference for AM was calculated according to equation (1).

Innate fructose, aspartic acid, and low-salt preference

Split Petri dishes were prepared by filling one half with 1 % agarose (blank), and the other half with agarose plus 2 M fructose (FRU). We collected 30 larvae, placed them in the middle of these dishes and after 3 minutes scored their numbers on either side, or on a 10 mm middle zone. The preference for fructose was calculated as:

(3) FRU-Pref = (Number on FRU side - Number on blank side) / Total number

Thus, positive values indicate a preference for, and negative values an avoidance of fructose.

Low-salt and aspartic acid preferences were determined in the same way, except that 0.4 mol/l NaCl and 10 mmol/l aspartic acid were used, respectively.

Genotypes and transgenes: Pre-screen

For the pre-screen we used the double-heterozygous offspring from crosses of Gal4 strains from the Janelia collection (Jenett et al. [2012]; Li et al. [2014]; available from the Bloomington Stock Centre or the Vienna *Drosophila* Resources Center; Table 2 and Table 3) to drive a temperature-sensitive dynamin transgene from the *UAS-shi^{ts}* effector (Kitamoto [2001], Bloomington Stock Centre no. 44222). In the Gal4-expressing cells, this allows to acutely disable synaptic output in a temperature-dependent way. The used Gal4 strains feature insertions of a given enhancer fragment combined to the Gal4 gene as driver construct; these driver constructs were inserted to an attp2 landing site [Pfeiffer et al., 2008]. Therefore a strain carrying this attp2 landing site but no Gal4 construct (”empty”) was crossed to *UAS-shi^{ts}* to obtain baseline, control memory scores for the pre-screen (Ctrl). Note that the same Gal4 construct (respectively combined with a different enhancer fragment) likewise inserted at the attp2 site is used in all strains to drive the *UAS-shi^{ts}* construct. Thus, adverse effects of the attp2 site, the Gal4 construct, or of a leakiness of the *UAS-shi^{ts}* construct would have affected all screened strains, and thus cannot account for differences in memory scores between them.

Genotypes and transgenes: Screen

For validation of candidate cells from the pre-screen a collection of 12 split-Gal4 intersec-

tion strains was generated (Table 4). These express either the transcription activation domain (p65ADZp) or the DNA binding domain (ZpGAL4DBD) of GAL4, each under the control of one of the selected enhancer fragments [Pfeiffer et al., 2010]. Landing sites for the p65ADZp and the ZpGAL4DBD construct were attp40 and attP2, respectively. Upon combining the p65ADZp- and ZpGAL4DBD-strains by classical genetics, a functional Gal4 protein is thus expressed in only the intersection of both strains [Luan et al., 2006; Pfeiffer et al., 2010]. We confirmed specificity by crossing the split-Gal4 drivers to UAS-GFP from Pfeiffer et al. [2010] (Bloomington Stock Centre no. 32185 and 32186) or *UAS-Kir2.1::GFP* (*5xUAS-DCSP-eGFPKir2.1* at VK00005 as landing site; available upon request) and inspecting expression under a Zeiss LSM 510 and/ or a Leica DM 6000 CS confocal microscope.

Split-Gal4 strains with confirmed expression pattern were crossed to *UAS-Kir2.1::GFP* as effector, an inward rectifying potassium channel that silences expressing neurons by preventing them from spiking [Baines et al., 2001]. The advantage of this effector relative to *UAS-shi^{ts}* is that the expression pattern and therefore the manipulated cells can be directly verified via the GFP tag. For the single-cell analyses we were aiming for, this advantage appeared to outweigh the disadvantage of being constitutive in effect. As driver controls the split-Gal4 strains were crossed to that wild-type strain (CSMH, available upon request) that had been used as genetic background for the *UAS-Kir2.1::GFP* strain (Driver Ctrl). As an effector control, a strain homozygous for both the attP40 and attP2 landing sites, yet without a Gal4 domain inserted (”empty”), was crossed to *UAS-Kir2.1::GFP* (Effector Ctrl).

Genotypes and methods for optophysiology

The indicated driver strains were crossed to *UAS-ChR2-XXL* as effector (Dawydow et al. [2014]; Bloomington Stock Centre no. 58374). Double heterozygous progeny was used for activation; larvae heterozygous for either the Gal4 or the effector were

used as genetic controls. Optogenetic experiments were performed in a dark custom-built box equipped for illumination from a blue LED light table (wavelength: 470 nm; intensity: 12 µW/mm2). For the learning experiments, one group of larvae received the odor presentation during blue light illumination alternated with blank trials without odor and without illumination (AM+/blank), whereas a reciprocally trained group of larvae received the odor unpaired with light stimulation (AM/+). All other aspects of the learning task were performed as described for odor-fructose learning. The same type of experiment was also performed using *UAS-Chrimson* as effector (Klapoetke et al. [2014]; Bloomington Stock Centre no. 55134); in this case 630 nm red light at an intensity of 350 µW/mm2 was used, and the odor for training was ethyl acetate (CAS: 141-78-6; Sigma-Aldrich Chemie GmbH, Munich, Germany) diluted in distilled water at a concentration of 10-4.

Immunohistochemistry

877 Gal4 driver strains preselected for expression in the central nervous system of stage 3 *Drosophila* larvae (Li et al. [2014], http://flweb.janelia.org/cgi-bin/flew.cgi) were screened for coverage of MBE neurons. Anatomical screening was further refined by systematic multi-color flp-out analysis of all 877 Gal4 driver lines (Li et al. [2014]; Nern et al. [2015], Figure 1, Figure S2, Table 1, 2 and 3). In addition, expression patterns of split-Gal4 strains (Figure 2, Figure 3, and Figure 4; Figure S8, Figure S10, Figure S13, Figure S14, and Figure S18) were anatomically verified. Specifically, larval brains of the indicated genotypes were dissected in phosphate buffered saline (PBS) and fixed for 1 h in 4 % paraformaldehyde at room temperature. After multiple rinses in PBS with 1 % Triton X-100 (PBT) and incubation in 3 % normal donkey serum in PBT (2 h at room temperature), samples were incubated over 2 nights at 4 ℃ with the indicated primary antibodies. After multiple rinses in PBT, brains were incubated 2 days at 4 ℃ with the indicated secondary antibodies. For mounting brains were

rinsed multiple times in PBT, transferred on a poly-L-lysine (PLL) coated cover glass, dehydrated through a graded ethanol series, cleared in xylene, and embedded in DPX (Sigma). Detailed information including step-by-step protocol and movies can be found on the HHMI Janelia Research Campus website (https://www.janelia.org/project-team/flylight/protocols). Immunolabeled larval nervous systems were imaged on a Zeiss 510 confocal microscope.

To verify *UAS-Kir2.1::GFP* effector gene expression a different protocol was applied, modified after [Selcho et al., 2009]. Larval brains of the indicated genotypes were dissected in Ringer solution. Brains were fixed in 4 % formaldehyde (Merck, Darmstadt) in PBS for 25 min. After several washes with PBT (PBS with 3 % Triton-X 100, Sigma-Aldrich, St. Louis, MO), brains were blocked with 5 % normal goat serum (Jackson Immunoresearch Laboratories, West Grove, PA) in PBS for 2 h and then incubated for 1 day with the indicated primary antibodies at 4 °C. After several washes with PBS, the indicated secondary antibodies were applied for 1 day at 4 °C. Finally, brains were again washed with PBS and mounted in Vectashield (Vector Laboratories).

Antibodies

To visualize the expression patterns of split-Gal4 strains mouse anti-neuroglian (1:50; BP-104; Developmental Studies Hybridoma Bank), rat anti-N-cadherin (1:50; DN-Ex #8; Developmental Studies Hybridoma Bank), and rabbit anti-GFP (1:1.000; Life Technologies A11122) were used as primary antibodies. Alexa Fluor 568 Donkey anti-mouse IgG (1:500; Life Technologies A10037), Alexa Fluor 647 Donkey anti-rat IgG (1:500; Jackson Immuno Research 712-605-153), and FITC conjugated Donkey anti-rabbit (1:500; Jackson Immuno Research 711-095-152) were used as secondary antibodies. To visualize the morphology of individual neurons the multi-color flp-out [Nern et al., 2015] technique was applied. Primary antibodies include mouse anti-neuroglian (1:50; BP-104; Developmental Studies Hybridoma Bank), rabbit anti-HA Tag (1:500; Cell

Signal Technologies 3724S) and rat anti-FLAG Tag (DYKDDDDK Epitope Tag) (1:500; Novus Biologicals NBP1-06712). Secondary antibodies were Alexa Fluor 488 donkey anti-mouse IgG (1:500; Life Technologies A10037), DyLight 549 goat anti-rabbit (1:800; Rockland Antibodies and Assays 611-142-002) and Alexa Fluor 594 donkey anti-rat IgG (1:500; Jackson Immuno Research 712-585-150). In addition the protocol included a post-secondary antibody wash using PBT, blocking using normal mouse serum (1:20 in PBT) and additional incubation with Alexa Fluor 647 mouse anti-V5 Tag (1:200; AbD Serotec MCA1360A647) overnight at 4 ℃. To verify *UAS-Kir2.1::GFP* effector gene expression rabbit anti-GFP (1:1000; Invitrogen A11122) and mouse anti-FASII (1:50; DSHB) were used as primary antibodies, and Alexa Fluor 488 goat anti-rabbit (1:200; Invitrogen A11034) and Cy3 donkey anti-mouse (1:200; Jackson Immunoresearch Laboratories 715-165-150) as secondary antibodies.

Electron-microscopy

We took advantage of the electron microscopy reconstruction of the MB intrinsic neurons, the Kenyon cells, and all their pre- and postsynaptic partners of a 6 h-old stage 1 larva from Eichler et al. [2017]. Images were taken at a 3.8 x 3.8 x 50 nm resolution. Reconstructions were made in a modified version of the web-based software CATMAID [Saalfeld et al., 2009] and with an iterative reconstruction method [Schneider-Mizell et al., 2016]. More detail is available with Eichler et al. [2017].

6.6 Acknowledgements

Institutional support: HHMI Janelia Research Campus, HHMI Janelia Visiting Scientist Program, Leibniz Institut für Neurobiologie (LIN) Magdeburg, Wissenschaftsgemeinschaft Gottfried Wilhelm Leibniz (WGL), Universities of Magdeburg, Leipzig, and Konstanz, and Center of Behavioral and Brain Sciences (CBBS), Magdeburg.

Project funding: Deutsche Forschungsgemeinschaft (CRC 779 and GE1091/4-1 to BG; TH1584/1-1 and TH1584/3-1 to AST), Zukunftskolleg of the University of Konstanz (to AST), Elite Program of the Baden-Württemberg Stiftung (to AST), and European Commission (FP7-ICT Miniature Insect Model for Active Learning [MINIMAL], to BG).
Comments and discussion: Members of our labs, as well as Ayse Yarali (LIN) and Gerald Rubin (Janelia).
Reagents and help: Alison Howard, Jui-Chun Kao (Janelia); the FlyLight team (Janelia); Juliane Saumweber, Thomas Niewalda, Emmanouil Paisios, Ulrich Thomas, Werner Zuschratter (LIN); the workshop team at the LIN.

6.7 Author contributions

T.S.: Conceived of study, coordinated and contributed behavioral experiments, analyzed behavioral, light and electron microscope data, designed figures, wrote manuscript
A.R.: Conceived of study, contributed behavioral and light microscopy data and analysis, contributed to writing of manuscript
M.S.: Contributed experiments and analysis for Figure 4, Figure S8 and Figure S11, contributed to writing of manuscript
K.E.: Contributed electron microscopy data and analysis, contributed to experiments for Figure S5, contributed to writing of manuscript
Yc.C.: Contributed experiments and analysis for Figure 3, contributed to writing of manuscript
Y.A.: Contributed to design and analysis of split-Gal4 strains, contributed to Table 1, contributed to writing of manuscript
A.C.: Contributed electron microscopy data and analysis, contributed to writing of manuscript

C.E.: Contributed experiments and analysis for Figure S10, contributed to writing of manuscript

O.K.: Contributed movies 1-5 and related text

M.Z.: Conceived of study, co-coordinated design of split-Gal4 strains, contributed to writing of manuscript

J.W.T.: Conceived of study, contributed and coordinated light microscopy analyses, co-coordinated design of split-Gal4 strains, contributed to writing of manuscript

A.T.: Conceived of study, analyzed data, designed figures, wrote manuscript

B.G.: Conceived of and coordinated study, analyzed data, designed figures, wrote manuscript

6.8 Supplemental data

Supplemental tables:

MB compartment	Cell	MBE class	Cell body location	Major presynaptic terminals @ (bold: MB compartment)	Major postsynaptic region(s) @ (bold: MB compartment)	Interhemispheric cross talk? (with MB-to-MB connection?)	Lineage	Transmitter	Synonym cell name	Reference
CX*	OAN-a1	sMBIN	SEZ maxillary segment	AL (c + i), CX (c + i), CPL (c + i)	SEZ (both hemispheres)	Yes (No)	Not determined	OA/TA	sVUMmx1	Selcho et al. 2014
	OAN-a2	sMBIN	SEZ mandibular segment	AL (c + i), CX (c + i), CPL (c + i)	SEZ (both hemispheres)	Yes (No)	Not determined	OA/TA	sVUMmd1	Selcho et al. 2014
	MBON-a1	sMBON	PDM	CPM (c + i), CPI (c + i)	**CX (i)**	Yes (No)	CPv2/3	ChAT	odd	Slater et al. 2015
	MBON-a2	sMBON	PDM	CPM (c + i), CPI (c + i)	**CX (i)**	Yes (No)	CPv2/3	ChAT	odd	Slater et al. 2015
IP	MBIN-b1	sMBIN	ADL	**IP (c)**	CPL (i), CPM (i), BPM (i)	Yes (No)	DPLd			
	MBIN-b2	sMBIN	ADL	**IP (c)**	CPL (i), CPM (i), BPM (i)	Yes (No)	DPLd			
	MBON-b1	sMBON	PVL	CPL (i), CPI (i)	**IP (i)**	No (No)	BLV a3/4	GABA	BL	Pauls et al. 2010, Eichler et al. 2017
	MBON-b2	sMBON	PVL	CPL (i), CPI (i)	**IP (i)**	No (No)	BLV a3/4	GABA	BL	Pauls et al. 2010, Eichler et al. 2017
	MBON-b3***	sMBON	PVL	CPL (i), CPM (c + i), CPI (c + i)	**IP (i)**	Yes (No)	CPv2/3			
LP	DAN-c1	sMBIN	PVL	**LP (c + i)**	DP (i), DA (i)	Yes (Yes)	CPd2/3	DA	DL1-5	Selcho et al. 2009, Eichler et al. 2017
	MBIN-c1***	sMBIN	PVL	**LP (c + i)**	DP (i), DA (i)	Yes (Yes)	CPd2/3			
	MBON-c1	sMBON	PDL	CPL (i), BPM (i), CPM (i)	**LP (i)**	No (No)	BLDc	ChAT		Eichler et al. 2017
	MBON-c2	sMBON	PDM	SEZ (i), TG (i)	**LP (i)**, BPL (i); BPM (i)	No (No)	DPM l1	DA	DM1	Selcho et al. 2009
LA	DAN-d1	sMBIN	PVL	**LA (c + i)**	DP (i), BC (i), CPM (i)	Yes (Yes)	CPd2/3	DA	DL 1-4	Selcho et al. 2009, Eichler et al. 2017
	MBIN-l1	sMBIN	PVL	**LA (c)**	BC (i)	Yes (No)	BLV a3/4			
	MBON-d1	sMBON	ADL	CPM (c + i)	**LA (i)**	Yes (No)	DAL CM-1/2	GABA	la type	Pauls et al. 2010, Eichler et al. 2017
	MBON-p1	sMBON	ADL	BPM (i)	**LA (i)**, CPI (i), DP (i), DA (i)	No (No)	DAL CM-1/2			
	MBON-d2***	sMBON	AVM	CPM (i)	**LA (i)**	No (No)	BAmd2			
UVL	OAN-e1	sMBIN	PVL	**UVL (i)**	DA (i), DP (i)	No (No)	CPd2/3	OA		Eichler et al. 2017
	MBIN-e2	sMBIN	PVL	**UVL (c + i)**	DA (i), DP (i)	Yes (Yes)	CPd2/3	DA?	vl 3 type, DL1-1	Pauls et al. 2010, Selcho et al. 2009 - but see also Eichler et al. 2017
	MBON-e1	sMBON	PVL	DA (i), DP (i)	**UVL (i)**	No (No)	CPd2/3	ChAT		Eichler et al. 2017
IVL	DAN-f1	sMBIN	PVL	**IVL (c + i)**	DA (i), DP (i), CPL (i)	Yes (Yes)	CPd2/3	DA	vl 2 type, DL 1-2	Pauls et al. 2010, Selcho et al. 2009, Eichler et al. 2017
	MBON-f2	sMBON	ADL	BC (c + i)	**IVL (i)**	Yes (No)	DAL cl2			
	MBON-f1***	sMBON	PVL	SEZ (c + i)	**IVL (i)**, DA (i), DP (i), CPL (i)	Yes (No)	CPd			
LVL	DAN-g1	sMBIN	PVL	**LVL** (c), CA (c), CPI (c)	DA (i), BC (i), DP (i)	Yes (No)	CPd2/3	DA	DL 1-3	Selcho et al. 2009, Eichler et al. 2017
	OAN-g1	sMBIN	SEZ maxillary segment	**IVL** (c), DA (c), DP (c), CPL (c)	SEZ (c + i)	Yes (No)	Not determined	OA/TA	sVPMmx	Selcho et al. 2014
	MBON-g1	sMBON	AVL	CPM (i)	**LVL (i)**	No (No)	DAL-V 2/3	GABA	vl1 type	Pauls et al. 2010, Eichler et al. 2017
	MBON-g2	sMBON	AVL	CPM (i)	**LVL (i)**	No (No)	DAL-V 2/3	GABA	vl1 type	Pauls et al. 2010, Eichler et al. 2017
SHA	DAN-h1	sMBIN	ADL	**SHA (c + i)**	DA (i), DP (i)	Yes (Yes)	DAL CM-1/2	DA	pPAM1	Rohwedder et al. 2016
	MBON-h1	sMBON	AVL	CPM (c + i)	**SHA (c + i)**	Yes (Yes)	DAL-V 2/3	GABA/GLUT	APBL	Pauls et al. 2010, Eichler et al. 2017
	MBON-h2	sMBON	AVL	CPM (c + i)	**SHA (c + i)**	Yes (Yes)	DAL-V 2/3	GABA/GLUT	APBL	Pauls et al. 2010, Eichler et al. 2017
UT	DAN-i1	sMBIN	ADL	**UT (c + i)**	DA (i), DP (i)	Yes (Yes)	DAL CM-1/2	DA	pPAM3	Rohwedder et al. 2016, Eichler et al. 2017
	MBON-i1	sMBON	ADM	DA (c + i), CPM (c + i)	**UT (c + i)**	Yes (Yes)	DAM-d1	GLUT		Eichler et al. 2017
IT	DAN-j1	sMBIN	ADL	**IT (c+ i)**	DA (i), DP (i)	Yes (Yes)	DAL CM-1/2	DA	pPAM4	Rohwedder et al. 2016, Eichler et al. 2017
	MBON-j1	sMBON	ADM	DA (i), DP (i), CPL (i)	**IT (c + i)**	Yes (Yes)	DAM-d1	GLUT		Eichler et al. 2017
	MBON-j2	sMBON	ADL	DA (c), DP (c), CPL (c)	**IT (i)**	Yes (No)	DAL CM-1/2	GLUT		This study, Figure S18
LT	DAN-k1	sMBIN	ADL	**LT (c + i)**	DA (i), DP (i), BC (i)	Yes (Yes)	DAL CM-1/2	DA	ma type, pPAM2	Pauls et al. 2010, Rohwedder et al. 2016, Eichler et al. 2017
	MBON-k1	sMBON	ADM	DA (c + i)	**LT (c + i)**	Yes (Yes)	DAM-d1	GLUT		Eichler et al. 2017
MI	MBIN-m1	mMBIN	PVL	**ML***** (c + i), IVL**	DA (i)	Yes (Yes)	CPd2/3			
	APL	mMBIN/MBON	AVL	**CX (i)**	**UT (i), LT (i), UVL (i), IVL (i), LVL (i), LA (i),** DA (i)	No (No)	BLV a3/4	GABA	Larval APL	Masuda-Nakagawa et al. 2014, Eichler et al. 2017
	MBON-e2	mMBON	ADM	CPM (c + i), CPI (c + i)	**UVL (i), IVL (i), LVL (i),**	Yes (No)	DAM-d1	GLUT		Eichler et al. 2017
	MBON-m1	mMBON	ADL	BC (c), BPM (c)	**IVL (i), LVL (i), LA (i),** DA (i)	Yes (No)	DAL CM-1/2	GABA		Eichler et al. 2017
	MBON-n1	mMBON	AVM	DA (i), BC (i)	**UVL (i), IVL (i), LVL (i),** DA (i), DP (i), BC (i)	No (No)	BA md1			
	MBON-d3	mMBON	ADM	CPI (c + i), CPM (c + i)	**UVL (c + i), IVL (c + i)**	Yes (Yes)	DAM-d1			

MB compartments and MBE class

CX	Calyx
IP	Intermediate peduncle
LP	Lower peduncle (spur**)
LA	Lateral appendix
UVL	Upper vertical lobe
IVL	Intermediate vertical lobe
LVL	Lower vertical lobe
SHA	Shaft of medial lobe
UT	Upper toe of medial lobe
IT	Intermediate toe of medial lobe
LT	Lower toe of medial lobe
ML	Medial lobe
VL	Vertical lobe
sMBE	MBE with single-compartment innervation
mMBE	MBE with multiple-compartment innervation

Orientation for cell body location

A: anterior
P: posterior
V: ventral
D: dorsal
L: lateral
M: medial

Neuropils/nervous system compartments

AL	antennal lobe (BA****)
SEZ	subesophageal zone (sbg****)
CPM	centroposterior medial compartment
CPI	centroposterior intermediate compartment
CPL	centroposterior lateral compartment
BA	basoanterior compartment
BPM	basoposterior medial compartment
DA	dorsoanterior compartment
DP	dorsoposterior compartment
BC	basocentral compartment
CA	centroanterior compartment
CPI	centroposterior intermediate compartment
TG	thoracic ganglion
BPL	basoposterior lateral compartment
i	ipsilateral projection, relative to cell body location
c	contralateral projection, relative to cell body location

*Ascending sensory interneurons, such as the olfactory PNs, are not included
**Synonym according to Selcho et al. 2009
***Not included in behavioral screen
****Synonym according to Younossi-Hartenstein et al. 2003
*****Innervated compartments within ML cannot be clearly discerned

Supplemental Table 1: Defining features of mushroom body extrinsic neurons (MBEs).

MBE neuron…	… covered in driver strain(s)
OAN-a1	R34A11
OAN-a2	R34A11
MBON-a1	R28A09, R36G04, R37D06, R47C08, R52E12, R64F07, R93G12
MBON-a2	R28A09, R36G04, R37D06, R47C08, R52E12, R64F07, R93G12
MBIN-b1	R14B11, R64E03, R78G08
MBIN-b2	R14B11, R64E03, R78G08
MBON-b1	R12C03, R20H11, R21D02, R22A08, R27F02, R86A06
MBON-b2	R12C03, R20H11, R21D02, R22A08, R27F02, R86A06
MBON-b3	R30E10*, VT17749*
DAN-c1	R30E11, R30G04, R64E03, R76C04, R95H02
MBIN-c1	R64E03, R72G06*
MBON-c1	R20F01, R74B11, R92H01, R94E06
MBON-c2	R12C11
DAN-d1	R21D02, R22A08, R22H04, R30E08, R30F04, R38E08, R64E03, R76C04, R78E04
MBIN-l1	R12C03, R20B12, R20C09, R21A06, R47C08, R47H03, R48D11, R48F09, R52H01, R58F03, R95A11
MBON-d1	R14B11, R20F01, R37G09, R49C08, R84D07
MBON-p1	R15D04, R17B02
MBON-d2	R54A09*, R87G02*, R89B06*, VT32899*
OAN-e1	R24A12, R28A12, R46F09*, R49D11*, R52G03, R64E03, R75F01*
MBIN-e2	R12C03, R14E06, R64E03, R72B05
MBON-e1	R74B11
DAN-f1	R10B07, R21D02, R37D06, R64E03, R76F05, R95H02
MBON-f2	R10B07, R36B06, R42F08, R64A11
MBON-f1	R48E11*
DAN-g1	R10D02, R14E06, R21D02, R27F02, R30E11, R64E03
OAN-g1	R30D03
MBON-g1	R11F03, R21D06, R21D08, R23B09, R48G01, R67E07, R94E06
MBON-g2	R11F03, R21D06, R21D08, R23B09, R48G01, R67E07, R94E06
DAN-h1	R26G04, R30G08, R58E02, R64E03, R64H06, R76F05, R95H02
MBON-h1	R11C10, R11F03, R22B05, R28A10, R28F06, R32D04, R50A04, R67B01, R67E07, R74A06
MBON-h2	R11C10, R11F03, R22B05, R28A10, R28F06, R32D04, R50A04, R67B01, R67E07, R74A06
DAN-i1	R21D02, R30G08, R31C03, R48F09, R49C08, R56H09, R58E02, R64E03, R64H06, R76F05, R95H02
MBON-i1	R14C08, R15F05, R20C05, R20H11, R21C08, R21D02, R21D07, R28A12, R46E11, R53G11, R59C07, R64E01, R65A05, R65E10, R74A06
DAN-j1	R49C08, R58E02, R64E03, R64H06, R76F05
MBON-j1	R11F03, R12C11, R20H11, R21C08, R23B09, R33D07, R46E11, R74C01
MBON-j2	R24E12, R36B06, R54H12, R89G07
DAN-k1	R20H11, R21D02, R27A11, R30G08, R48F09, R64E03, R64H06, R71D01, R76F05
MBON-k1	R20H11, R21D02, R65A05, R74A06
MBIN-m1	R76F05
APL	R20H11, R21D02, R26G02, R55D08
MBON-e2	R12C11, R28A12, R43A02, R65A05
MBON-m1	R20B12, R24D12, R52H01
MBON-n1	R22B05, R29E04, R83G11
MBON-d3	R11F03, R12C11

*Not included in behavioral screen

Supplemental Table 2: Matrix of which Gal4 driver strain(s) include(s) which MBE neuron.

Driver strain…	Stock Number	… covering MBE neuron(s)	Driver strain…	Stock Number	… covering MBE neuron(s)
R10B07	48244	DAN-f1, MBON-f2	R43A02	41256	MBON-e2
R10D02	48437	DAN-g1	R46E11	50272	MBON-j1, MBON-i1
R11C10	48450	MBON-h1,h2	R46F09*	50275	OAN-e1
R11F03	48464	MBON-j1, MBON-h1,h2, MBON-g1,g2, MBON-d3	R47C08	50298	MBIN-l1, MBON-a1,a2
R12C03	45024	MBIN-l1, MBON-b1,b2, MBIN-e2	R47H03	50331	MBIN-l1
R12C11	48497	MBON-j1, MBON-e2, MBON-c2, MBON-d3	R48D11	50365	MBIN-l1
R14B11	49255	MBIN-b1,b2, MBON-d1	R48E11*	50372	MBON-f1
R14C08	48606	MBON-i1	R48F09	50377	DAN-k1, DAN-i1, MBIN-l1
R14E06	48643	DAN-g1, MBIN-e2	R48G01	50381	MBON-g1,g2
R15D04	n.a.	MBON-p1	R49C08	50418	DAN-i1, DAN-j1, MBON-d1
R15F05	48699	MBON-i1	R49D11*	38684	OAN-e1
R17B02	48754	MBON-p1	R50A04	38720	MBON-h1,h2
R20B12	48880	MBIN-l1, MBON-m1	R52E12	38837	MBON-a1,a2
R20C05	48883	MBON-i1	R52G03	38842	OAN-e1
R20C09	48886	MBIN-l1	R52H01	47638	MBIN-l1, MBON-m1
R20F01	48610	MBON-c1, MBON-d1	R53G11	50449	MBON-i1
R20H11	48918	DAN-k1, MBON-j1, MBON-i1, MBON-k1, MBON-b1,b2, APL	R54A09*	50460	MBON-d2
R21A06	n.a.	MBIN-l1	R54H12	48205	MBON-j2
R21C08	48935	MBON-j1, MBON-i1	R55D08	39115	APL
R21D02	48939	DAN-k1, DAN-i1, DAN-f1, DAN-g1, DAN-d1, MBON-i1, MBON-k1,MBON-b1,b2, APL	R56H09	39166	DAN-i1
R21D06	48942	MBON-g1,g2	R58E02	41347	DAN-h1, DAN-i1, DAN-j1
R21D07	48943	MBON-i1	R58F03	39187	MBIN-l1
R21D08	48944	MBON-g1,g2	R59C07	48217	MBON-i1
R22A08	47902	DAN-d1, MBON-b1,b2	R64A11	39289	MBON-f2
R22B05	49300	MBON-h1,h2, MBON-n1	R64E01	48230	MBON-i1
R22H04	n.a.	DAN-d1	R64E03	41351	DAN-h1, DAN-k1, DAN-i1, DAN-j1, DAN-f1, DAN-g1, DAN-c1, MBIN-c1, DAN-d1, OAN-e1, MBIN-b1,b2, MBIN-e2
R23B09	49018	MBON-j1, MBON-g1,g2	R64F07	39311	MBON-a1,a2
R24A12	49061	OAN-e1	R64H06	49608	DAN-h1, DAN-k1, DAN-i1, DAN-j1
R24D12	49080	MBON-m1	R65A05	39329	MBON-i1, MBON-k1, MBON-e2
R24E12	49084	MBON-j2	R65E10	39359	MBON-i1
R26G02	48065	APL	R67B01	39961	MBON-h1,h2
R26G04	n.a.	DAN-h1	R67E07	39444	MBON-h1,h2, MBON-g1,g2
R27A11	47908	DAN-k1	R71D01	39579	DAN-k1
R27F02	48072	DAN-g1, MBON-b1,b2	R72B05	39611	MBIN-e2
R28A09	49445	MBON-a1,a2	R72G06*	39792	MBIN-c1
R28A10	48074	MBON-h1,h2	R74A06	47398	MBON-i1, MBON-k1, MBON-h1,h2
R28A12	47909	MBON-i1, OAN-e1, MBON-e2	R74B11	41301	MBON-e1, MBON-c1
R28F06	48083	MBON-h1,h2	R74C01	39845	MBON-j1
R29E04	49486	MBON-n1	R75F01*	41304	OAN-e1
R30D03	49532	OAN-g1	R76C04	48621	DAN-c1, DAN-d1
R30E08	48099	DAN-d1	R76F05	41305	DAN-h1, DAN-k1, DAN-i1, DAN-j1, DAN-f1, MBIN-m1
R30E10*	49638	MBON-b3	R78E04	39997	DAN-d1
R30E11	48100	DAN-g1, DAN-c1	R78G08	n.a.	MBIN-b1,b2
R30F04	48614	DAN-d1	R83G11	46764	MBON-n1
R30G04	n.a.	DAN-c1	R84D07	40391	MBON-d1
R30G08	48101	DAN-h1, DAN-k1, DAN-i1	R86A06	n.a.	MBON-b1,b2
R31C03	48103	DAN-i1	R87G02*	40500	MBON-d2
R32D04	49711	MBON-h1,h2	R89B06*	40543	MBON-d2
R33D07	49893	MBON-j1	R89G07	41365	MBON-j2
R34A11	49767	OAN-a1,b	R92H01	40631	MBON-c1
R36B06	49929	MBON-j2, MBON-f2	R93G12	40667	MBON-a1,a2
R36G04	49940	MBON-a1,a2	R94E06	40687	MBON-g1,g2, MBON-c1
R37D06	47921	DAN-f1, MBON-a1,a2	R95A11	48834	MBIN-l1
R37G09	49538	MBON-d1	R95H02	40716	DAN-h1, DAN-i1, DAN-f1, DAN-c1
R38E08	50008	DAN-d1	VT17749*	200702**	MBON-b3
R42F08	50164	MBON-f2	VT32899*	203529 **	MBON-d2

* Not included in behavioral screen
** Available from Vienna Drosophila Resource Center
n.a. No longer available from Bloomington Stock Centre

Supplemental Table 3: Matrix of which MBE neuron(s) are included in which Gal4 driver strain(s).

MBE	Classification*	ADsource strain_DBDsource strain	Strain
DAN-g1	AA	R14E06_R27G01	GMR_SS01716
MBON-g1, g2	AA	R21D06_R23B09	GMR_SS02121
DAN-h1	AAA	R76F05_R95H02	GMR_SS01696
MBON-h1, h2	AAA	R20A02_R28A10	GMR_SS01725
MBON-h1, h2	AAA	R20A02_R28A10	GMR_SS00928
DAN-i1	AAA	R13D05_R36B06	GMR_SS00864
MBON-i1	AAA	R15B01_R14C08	GMR_MB141B
MBON-j1	AAA	VT057469_R18D09	GMR_SS01973
MBON-j2	AAA	R89G07_R24E12	GMR_SS00860
DAN-k1	AAA	R48F09_R27A11	GMR_SS01757
MBON-k1	AAA	VT033301_R27G01	GMR_SS01962
APL	AAA	R21D02_R55D08	GMR_SS01671

*A: High Expression strength, reliability, specificity

Supplemental Table 4: List of split-Gal4 intersection strains, their source strains, and the MBE neuron(s) covered.

Supplemental movies:

Movie 1: Body and nervous system of a 3^{rd} instar *Drosophila* larva.

Movie 2: 3D view of the body and nervous system of a 3^{rd} instar *Drosophila* larva, with zoom on motor neuron terminals. Structure is visible based on autofluorescence.

Movie 3: Schematic body plan (top; from Demerec and Kaufmann, 1940) and indication of orientation using a 3D print of a larva (bottom), followed by a series of optical sections from ventral to dorsal, and back. Structure is visible based on autofluorescence.

Movie 4: Indication of orientation using a 3D print of a larva, followed by a series of optical sections from anterior to posterior, and back. Structure is visible based on autofluorescence.

Movie 5: Indication of orientation using a 3D print of a larva, followed by a series of optical sections from left to right, and back. Structure is visible based on autofluorescence.

Movies can be found on the accompanying DVD.

Supplemental figures:

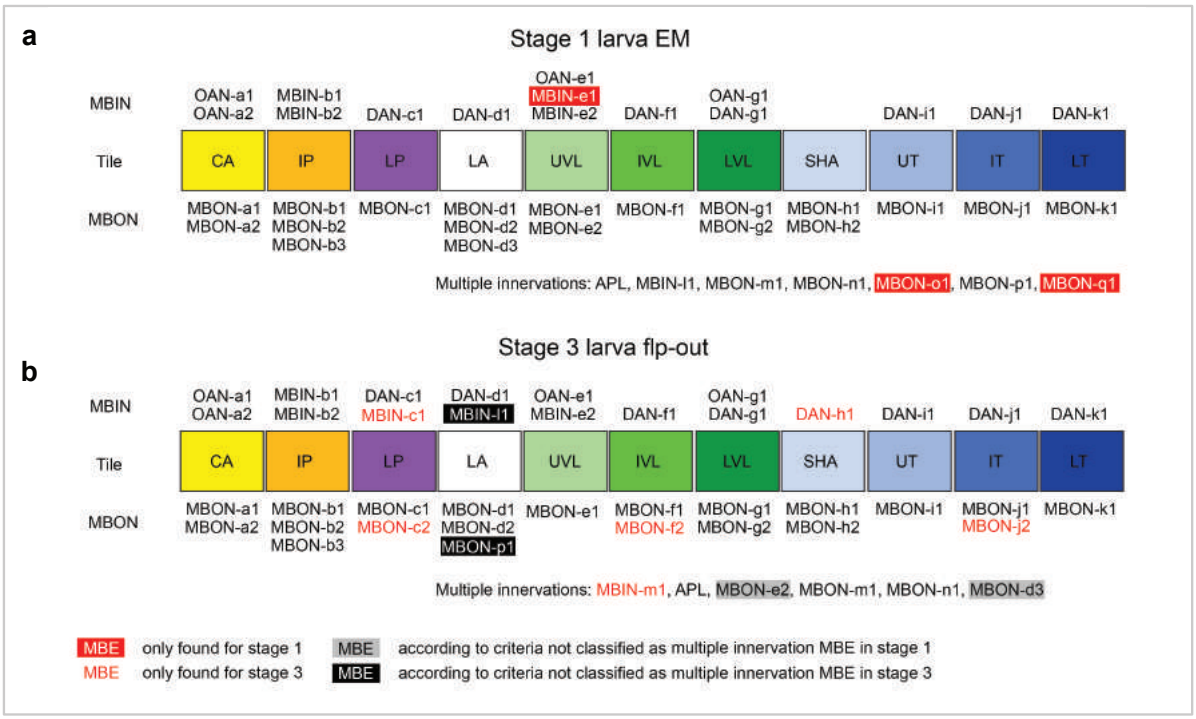

Supplemental Figure 1: Schematic organization of MBE neurons identified in stage 1 and stage 3 larvae.
For both developmental stages (stage 1 in a; stage 3 in b) the compartmental organization of mushroom body extrinsic neurons (MBEs) is presented. Mushroom body input neurons (MBINs) and mushroom body output neurons (MBONs) are listed above and under each tile. MBEs that innervate multiple tiles are shown at the bottom. For stage 1 this is based on the electron microscopy reconstructions of Eichler et al. [2017], for stage 3 on light microscopy brain scans of flp-out experiments. Throughout development 11 tiles can be recognized: calyx (CA); intermediate (IP) and lower peduncle (LP); lateral appendix (LA); upper (UVL), intermediate (IVL) and lower vertical lobe (LVL); the shaft (SHA), lower (LT), intermediate (IT) and upper toe (UT). While overall there is a remarkable consensus in the compartmental architecture, three MBEs were specifically found for stage 1 (MBIN-e1, MBON-o1 and MBON-q1; highlighted by red boxes) and six MBEs seem to be particular at stage 3 (MBIN-c1, DAN-h1, MBON-c2, MBON-f2, MBON-j2 and MBIN-m1; highlighted in red).

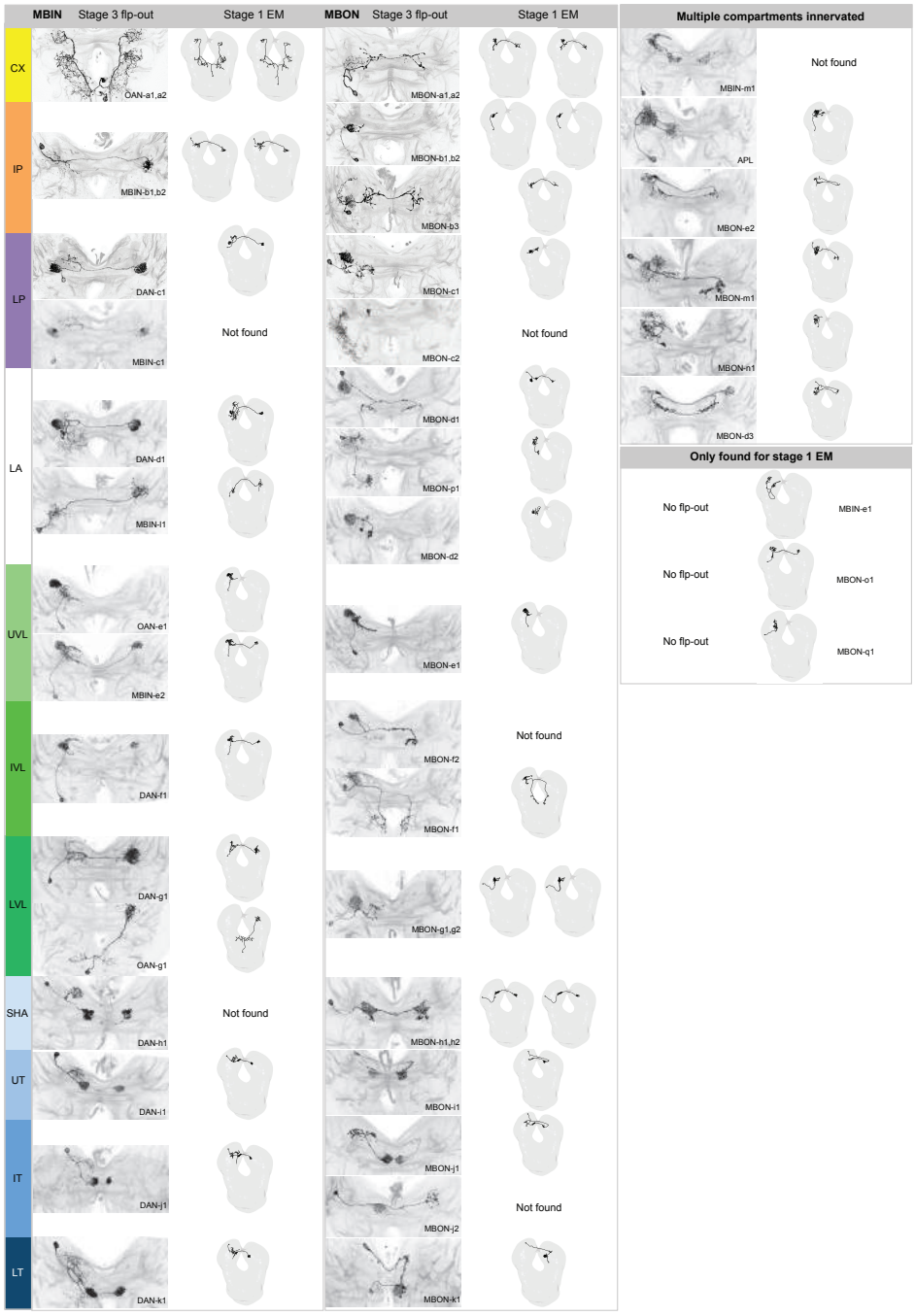

Supplemental Figure 2: Morphological organization of MBE neurons identified in stage 3 and stage 1 larvae.
For both stage 3 and stage 1 the morphological organization of mushroom body extrinsic neurons (MBEs) is shown. For stage 3 this is based on light microscopy brain scans from flp-out experiments (left panels), for stage 1 on electron microscopy reconstructions from Eichler et al. [2017] (right panels). In the case of OAN-a1 and OAN-a2 two cells were obtained in the flp-out experiment; the electron microscope reconstructions of both neurons are presented in the right hand panel. For the MBE double pairs only one flp-out is shown because the ipsilateral members of the double pair cannot be distinguished from light microscopy data; as they are separately revealed from the electron microscope reconstructions, however, they are both presented in the panels to the right.

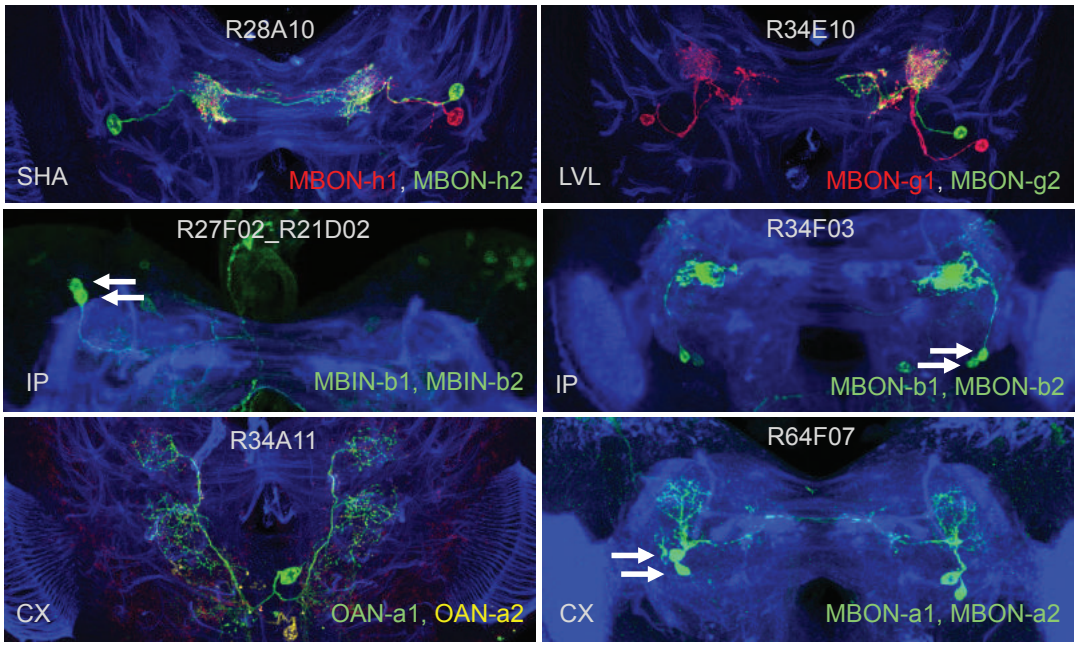

Supplemental Figure 3: MBE neuron (double) pairs and MBE symmetry.
In all but in the bottom left case, flp-outs from MBE double pairs are presented, showing strongly overlapping innervation patterns of the ipsilateral neurons of the double pair. In all but the two panels to the bottom left, the flp-outs of three or respectively four members of the double pair within the same brain directly reveal that MBE neurons are 'paired', i.e. are present in both hemispheres, and that the paired neurons in both hemispheres have symmetrical morphology. In all other cases, the paired nature of the MBEs and their symmetry was ascertained through independent flp-outs across brains, as well as from electron microscope reconstruction [Eichler et al., 2017]. The bottom left panel shows the segmentally homologous OAN-a1 and OAN-a2 neurons. Each panel shows a z-projection of the region of larval brain including the indicated MBEs. Anti-neuroglian staining (blue) provides a label for the brain. Individual neurons are shown as multi-color flp-outs in red, yellow and green depending on the expressed markers. Information about the Gal4 or split-Gal4 driver strain is given at the top of each panel. The identity of the MBEs and information about the innervated compartment is indicated within each panel. Arrows point to MBE cell bodies.

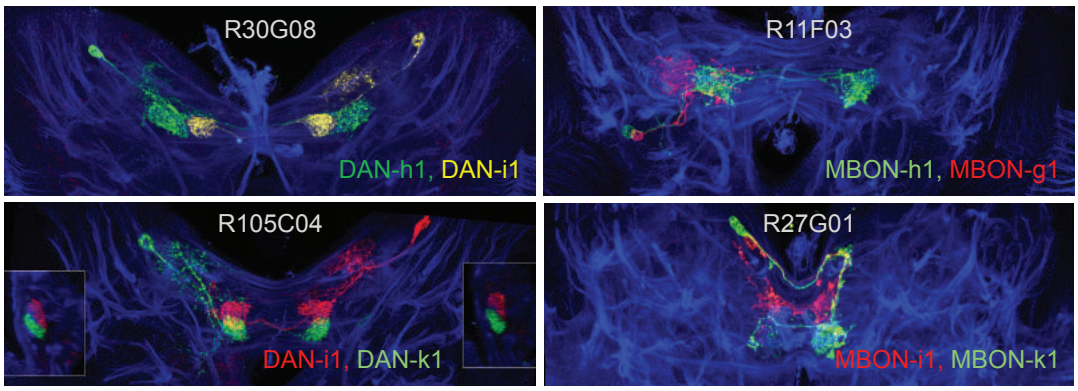

Supplemental Figure 4: MBE neurons cover compartments in a non-overlapping way.
Four examples of double flp-out events of MBE neurons that innervate neighboring compartments, showing their non-overlap. Each panel shows a z-projection of the larval brain region including the indicated MBEs. Anti-neuroglian staining (blue) provides a label for the brain. Individual neurons are shown as multi-color flp-outs in red, yellow and green depending on the expressed markers. Information about the Gal4 and split-Gal4 driver strain and the identity of the MBEs is given within each panel. For DAN-i1 and DAN-k1 the insets show a sagittal view of medial lobe innervation.

Supplemental Figure 5: Pre-screen results, combined for Gal4 strains covering the indicated MBE neuron.
(Panels 1-34) Gal4 strains including MBE neurons in their expression pattern were crossed to *UAS-shi^{ts}*. At restrictive temperature and thus under block of synaptic output from the respectively covered neurons larvae were trained in an odor-fructose reward associative learning task (panel 35; details as in Figure 2k). Appetitive odor-fructose memory is indicated by positive associative performance indices (PIs). Throughout panels 1-34, a schematic of the respectively indicated MBE neuron is shown in addition. The red shading indicates the 25/75 % quantile of the genetic control strain heterozygous for *UAS-shi^{ts}* but not expressing Gal4 (Ctrl). Sample sizes are indicated within the figure. * and ns refer to $P<0.05$ and $P>0.05$, respectively, in Mann-Whitney U-tests between control and the data combined across the experimental strains presented individually towards the right. The # symbol indicates that the strain yielded the respective cell as a flp-out clone, but that the cell cannot be discerned directly from the expression pattern of the Gal4 strain; this suggests stochastic and/ or weak transgene expression in the respective cell and strain.

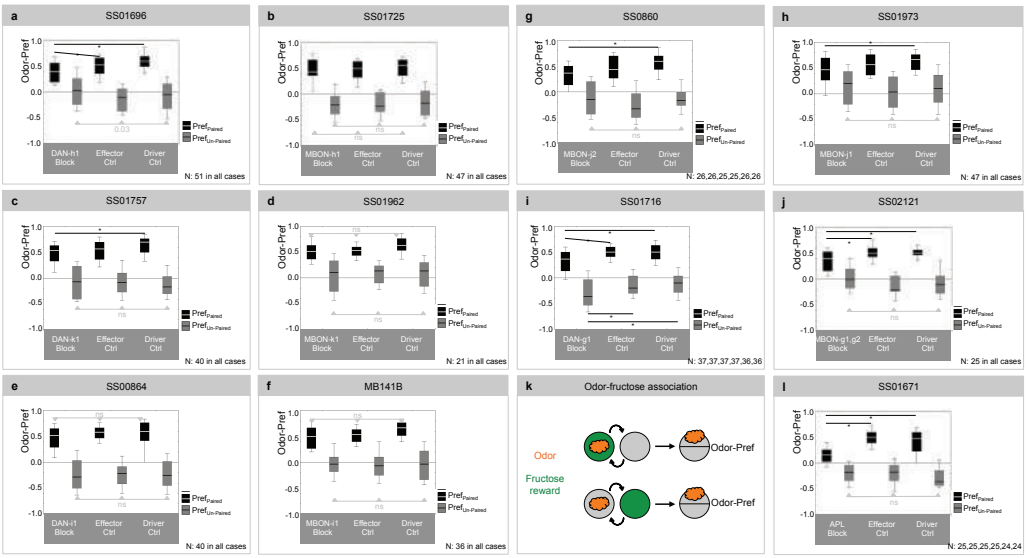

Supplemental Figure 6: Preference scores from odor-fructose association experiments upon silencing MBEs.
a-j Preference scores for the trained odor *n*-amylacetate (Odor-Pref) underlying the associative performance indices (PI) displayed in Figure 2a-j. A schematic of the training paradigm is shown in (k) (details as in Figure 2k).
l Same as in (a-j), regarding the associative performance indices (PI) displayed in Figure 4e. Sample sizes are indicated within the figure. * refers to P<0.05/2 in Mann-Whitney U-tests; ns refers to P>0.05 in Kruskal-Wallis tests.

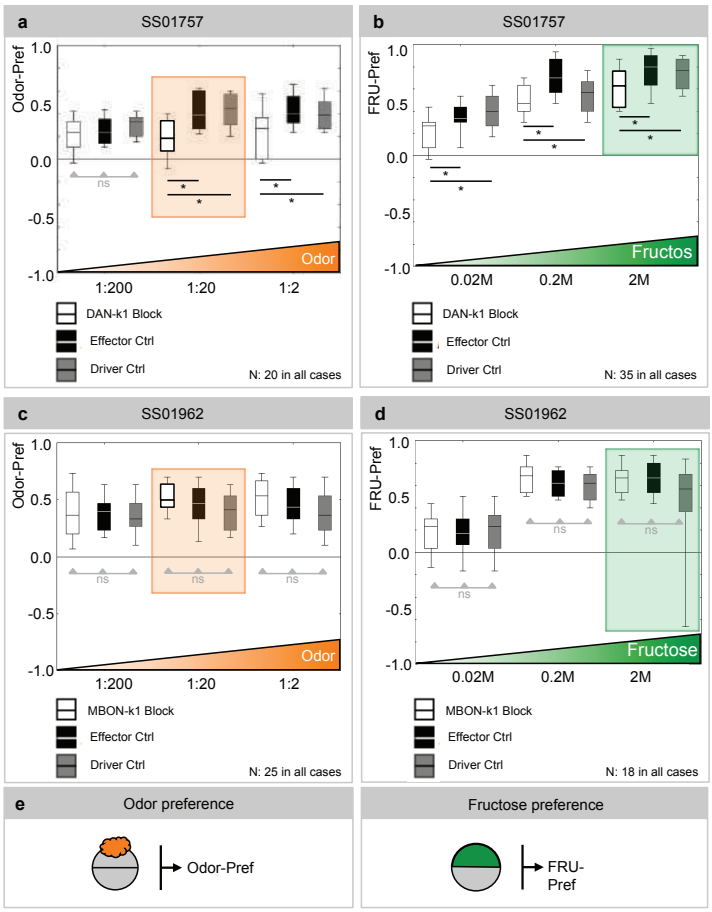

Supplemental Figure 7: Differential requirement of DAN-k1 but not MBON-k1 for innate odor- and fructose preference - extended.
a, b For the split-Gal4 strain covering the MBIN to the lower toe of the medial lobe (DAN-k1; SS01757), the panels show the preference scores of experimentally naïve larvae for the odor *n*-amylacetate (a; AM), or for fructose (b; FRU), at the indicated dilutions/concentrations. Larvae are either heterozygous for the split-Gal4 drivers as well as *UAS-Kir2.1::GFP* (DAN-k1 Block), or heterozygous for only the *UAS-Kir2.1::GFP* effector (Effector Ctrl), or heterozygous for the split-Gal4 drivers only (Driver Ctrl).
c, d Same as for (a, b), concerning the MBON of the same compartment (MBON-k1; SS01962).
e Schematics of the preference paradigms (details as in Figure 2k).
Please note that the data for *n*-amylacetate preference and fructose preference at the boxed dilution/concentration are also presented in Figure 2c for DAN-k1. Sample sizes are indicated within the figure. * refers to P<0.05/2 in Mann-Whitney U-tests; ns refers to P>0.05 in Kruskal-Wallis tests.

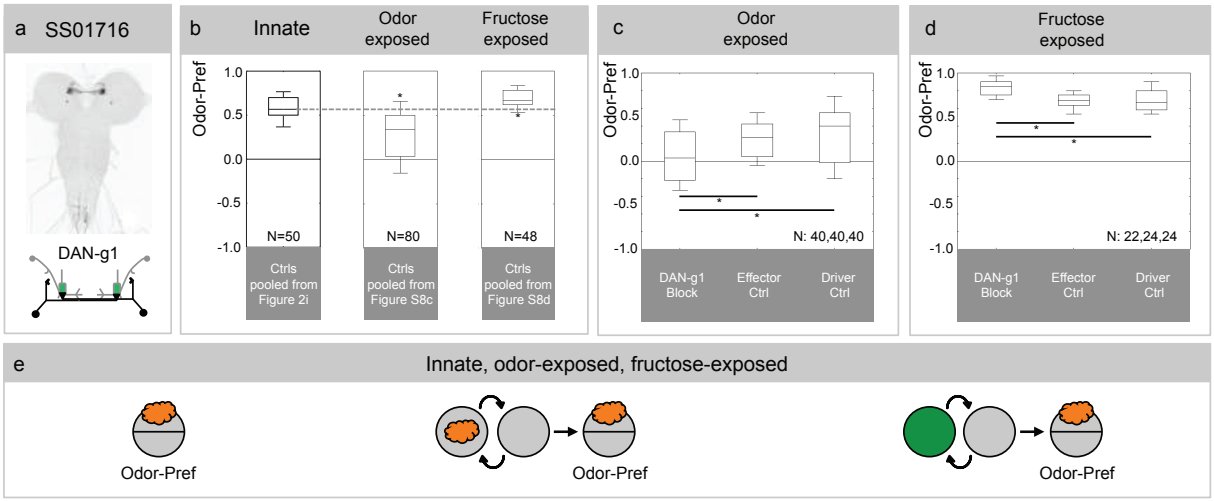

Supplemental Figure 8: Silencing DAN-g1 makes larvae more susceptible to the non-associative effects of stimulus-exposure.
a Expression pattern of the split-Gal4 strain covering the MBON of the lower vertical lobe (DAN-g1; SS01716). Regarding this neuron, a closer inspection of the odor-fructose association data upon its silencing suggests an unexpected function. That is, although innate odor preference remains intact (Figure 2i), odor preference scores are shifted towards the negative after both paired odor-fructose reward training and after unpaired presentations of odor and fructose (Figure S6i). In analyses of associative learning, such effects are intentionally averaged-out by calculating the difference in preference between paired versus unpaired-trained groups for the associative performance index (Figure 2i and k). Importantly, no such general, non-associative shift in preference towards the negative is seen for any other neuron of this study (Figure S6); in particular this is not the case for the output neuron double pair of the compartment innervated by DAN-g1 (MBON-g1,g2; Figure S6j). We thus wondered whether silencing DAN-g1 specifically affects odor preference after non-associative stimulus exposure.
b-d In genetic controls odor exposure decreases odor preference (b; Michels2005), an effect that is boosted upon silencing DAN-g1 (c). Fructose exposure increases odor preference in genetic controls (b; Michels2005, Saumweber2011b), an effect that likewise is boosted by silencing DAN-g1 (d). Thus, silencing DAN-g1 makes the larvae more susceptible to the effects of odor-only exposure and to the effects of fructose-only exposure; undisturbed activity in DAN-g1 thus appears to be required to partially 'buffer' olfactory behavior against non-associative effects of stimulus-exposure. Sample sizes are indicated within the figure. In (b) * refers to $P<0.05/2$ in Mann-Whitney U-tests versus innate odor preference. In (c, d) * refers to $P<0.05/2$ in Mann-Whitney U-tests.
e Schematic of the paradigms to measure innate odor preference in experimentally naïve larvae, odor preference after odor exposure, and odor preference after fructose exposure (details as in Figure 2k).

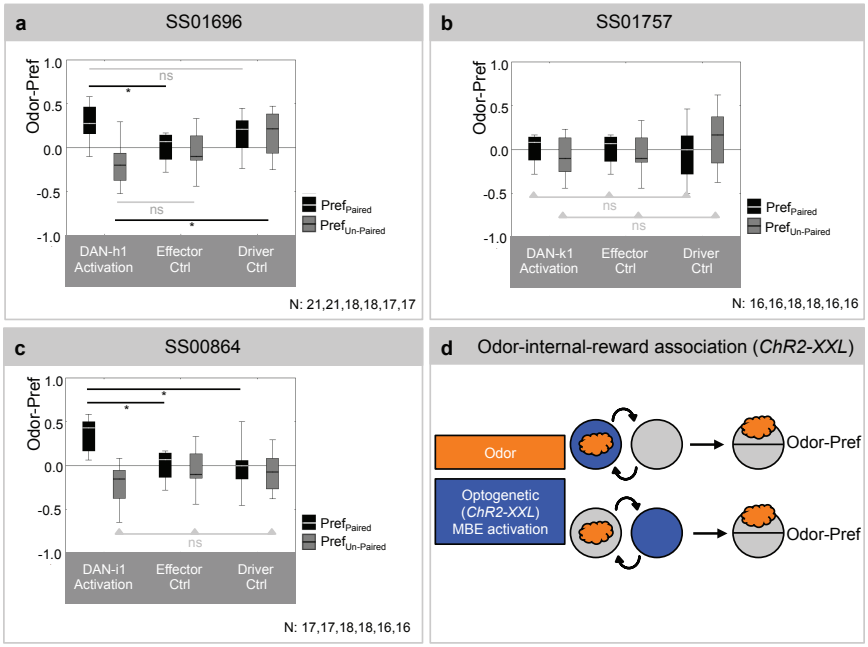

Supplemental Figure 9: Preference scores from odor-internal-reward association experiments using *ChR2-XXL*.
a-c Preference scores for the trained odor *n*-amylacetate (Odor-Pref) underlying the associative performance indices (PI) displayed in Figure 3a-c using *ChR2-XXL* for optogenetic activation of the indicated DAN as internal reward.
d Schematic of the training paradigm (details as in Figure 3d).
Sample sizes are indicated within the figure. At plain horizontal lines * refers to $P<0.05/2$ and ns to $P>0.05/2$ in Mann-Whitney U-tests; at horizontal lines with arrowheads, ns refers to $P>0.05$ in Kruskal-Wallis tests.

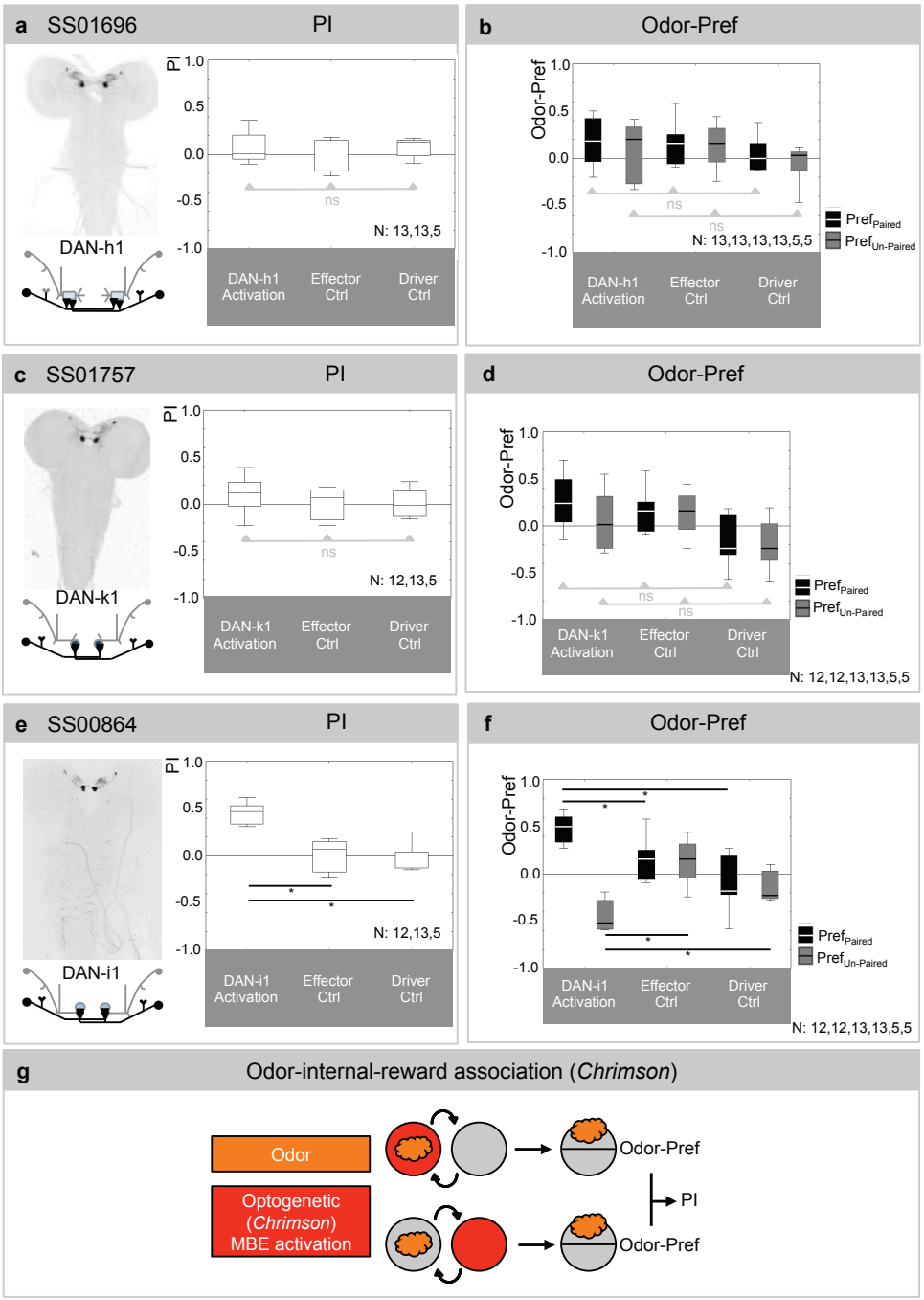

Supplemental Figure 10: Odor-internal-reward association experiments using Chrimson.
a-f Larvae are trained with odor stimulation and optogenetic activation of the indicated DANs as internal reward signal. The panels show the expression pattern of the indicated split-Gal4 strain and a schematic overview of the covered DAN, as well as the associative performance indices after internal-reward training (a, c, e), and the underlying preference scores (b, d, f). Larvae are either heterozygous for the split-Gal4 drivers as well as *UAS-Chrimson* (DAN-Activation), or heterozygous for the *UAS-Chrimson* effector only (Effector Ctrl), or heterozygous for only the split-Gal4 drivers (Driver Ctrl). Activation of DAN-h1 (a, b) as well as activation of DAN-k1 (c, d) is without measurable effect, while activation of DAN-i1 (e, f) is sufficient as internal reward.
g Schematic of the associative learning paradigm with odor and internal-reward (details as in Figure 3d, except that red light is used for the activation of neurons by Chrimson).
Sample sizes are indicated within the figure. * refers to $P<0.05/2$ in Mann-Whitney U-tests; ns refers to $P>0.05$ in Kruskal-Wallis tests.

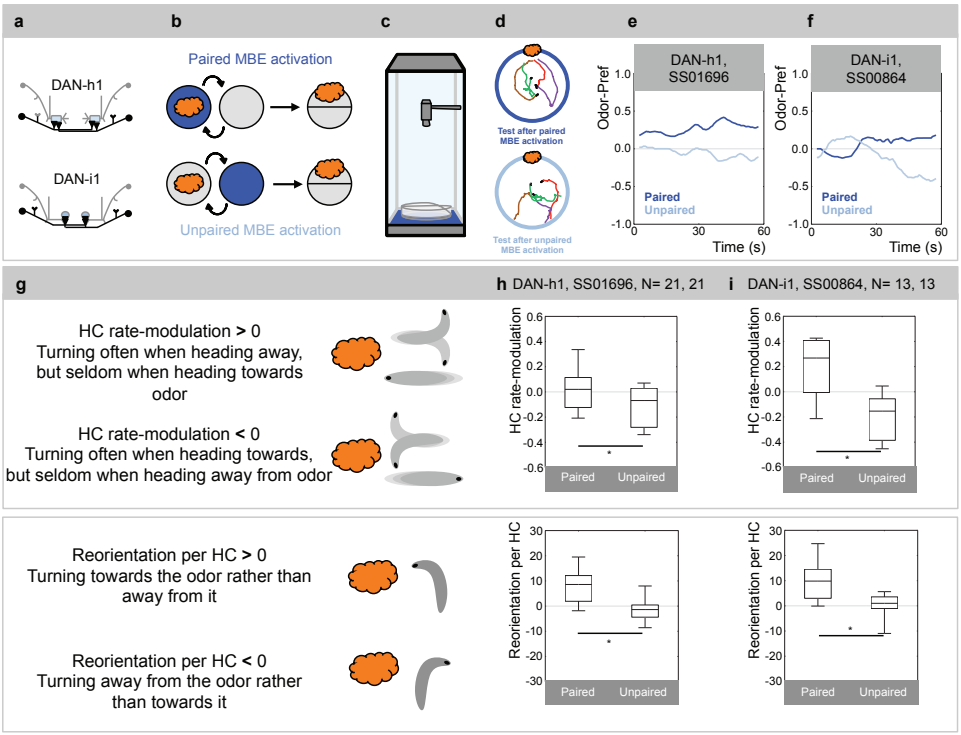

Supplemental Figure 11: Real-reward locomotor 'footprint' of memories established by optogenetic activation of either DAN-h1 or DAN-i1.

Given that optogenetic activation of either DAN-h1 or DAN-i1 is sufficient as an internal reward signal (Figure 3), we asked whether the established memories would have the same effects on chemotaxis as previously described for a real reward such as fructose [Schleyer et al., 2015b; Paisios et al., 2017]. After odor-DAN activation training, we recorded larval behavior during the test and analyzed it offline using custom-written software [Paisios et al., 2017].

a-f DANs, paradigm and data acquisition. Schematics of DAN-h1 and DAN-i1 (a) and of the odor-DAN activation association paradigm (b; details as in Figure 3d). Panels (c, d) sketch the experimental setup and 4 example tracks each of individual larvae recorded after paired (top) or unpaired (bottom) training with odor and DAN-i1 activation. After paired training with odor and either DAN-h1 or DAN-i1 activation, larvae have a higher preference for the odor than after unpaired presentations of odor and DAN activation (e, f). Displayed is the median preference of the full sample over time (sliding average 5 s). After the first minute, preferences remain stable (not shown). We therefore restrict our analysis to the first minute of the test during which larval preferences are most dynamic.

g-i Data analysis and results. (g) Analysis of larval locomotion according to under which stimulus conditions (top) and where-to (bottom) the larvae perform lateral head casts (HC). Both these aspects of locomotion are associatively modulated after training with a real fructose reward [Schleyer et al., 2015b; Paisios et al., 2017]. The associative modulation of the stimulus conditions under which animals head cast is captured by the HC rate-modulation (g, top):

HC rate-modulation = (#HC/s (heading away) -#HC/s (heading towards)) / (#HC/s (heading away)+#HC/s (heading towards))

This measure yields positive scores for attraction, that is when larvae systematically perform more HCs while they are heading away from the odor (odor concentration decrease) than while they are heading towards it (odor concentration increase) (#HC/s away $>$#HC/s towards), whereas it yields negative scores for aversion, i.e. when larvae perform more HCs while they are heading towards the odor than while they are heading away from it (#HC/s away $<$#HC/s towards). The associative modulation of where-to animals are head casting is measured by the reorientation per HC, that is how much on average HCs are biased towards versus away from the odor source (g, bottom):

Reorienation per HC =absheading angle before HC-absheading angle after HC

In this measure, the heading angle describes the orientation of the animal's head, with 0 °indicating that the odor is in front, and abs(180°) indicating that the odor is to the rear. Thus, this measure yields scores >0 for attraction, i.e. when the HCs get the larvae more on-target that away from it (abs(heading angle before HC) $>$abs(heading angle after HC)), while it would yield scores <0 for aversion. After paired training with either DAN-h1 activation or DAN-i1 activation the larvae perform more HCs while they are heading away from the odor than while they are heading towards it, measured as a positive HC rate-modulation; after unpaired training with either DAN-h1 activation or DAN-i1 activation the opposite effect is observed (h, i, top panels). Furthermore, larvae direct their HCs more towards the odor after paired training than after unpaired training, both after DAN-h1 training and DAN-i1 training (h, i, bottom panels). Thus, a memory induced by activation of either DAN-h1 or DAN-i1 as internal reward signal modulates the same aspects of chemotaxis as memories related to a real fructose reward [Schleyer et al., 2015b; Paisios et al., 2017].

Sample sizes are indicated within the figure. * refers to $P<0.05$ in Mann-Whitney U-tests.

Supplemental Figure 12: Preference scores upon silencing DAN-h1 or DAN-i1, compared between three different taste rewards.

a-c Preference scores for the trained odor *n*-amylacetate (Odor-Pref) underlying the associative performance indices (PI) displayed in Figure 3e, regarding the silencing of DAN-h1.

d-f Preference scores for the trained odor *n*-amylacetate (Odor-Pref) underlying the associative performance indices (PI) displayed in Figure 3f, regarding the silencing of DAN-i1.

g Schematic of the training paradigm (details as in Figure 3g).

Sample sizes are indicated within the figure. * refers to P<0.05/2 in Mann-Whitney U-tests; ns refers to P>0.05 in Kruskal-Wallis tests.

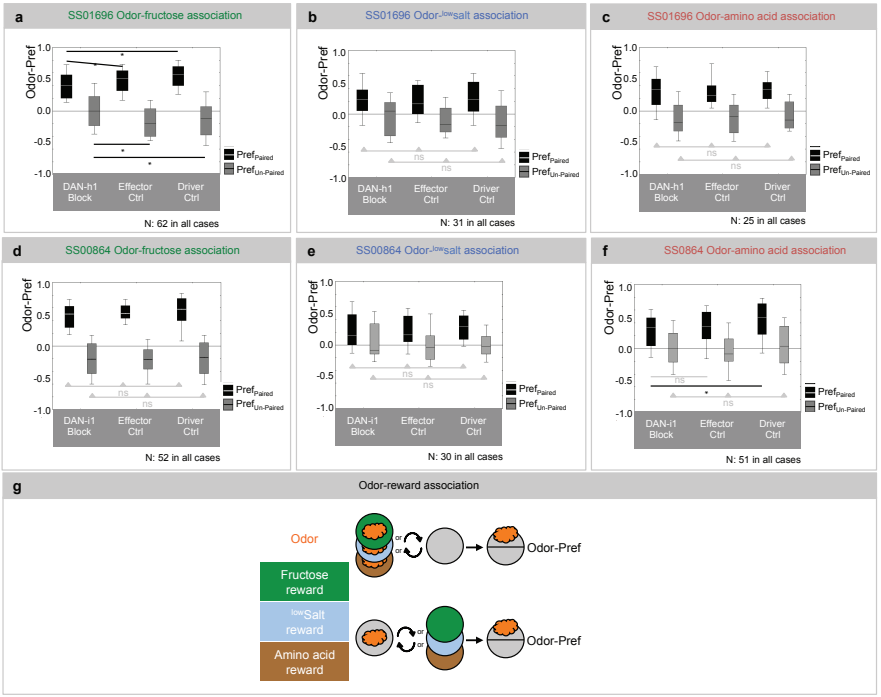

Supplemental Figure 13: Silencing DAN-i1 neither impairs odor-arabinose nor odor-sorbitol association.

a, b For a split-Gal4 strain covering the MBIN of the upper toe (DAN-i1; SS00864), the panels show the associative performance indices measuring odor-arabinose reward memory (a), and the preference indices underlying these associative performance indices (b) upon silencing DAN-i1 by means of *Kir2.1::GFP* expression.

c, d Same as in (a, b), for odor-sorbitol reward association.

e Expression pattern of the split-Gal4 strain and a schematic overview of DAN-i1 (left), and schematic of the training paradigm (right; details as in Figure 2k).

Sample sizes are indicated within the figure. In (a) * refers to P<0.05/2 and ns to P>0.05/2 in Mann-Whitney U-tests. In all other cases ns refers to P>0.05 in Kruskal-Wallis tests.

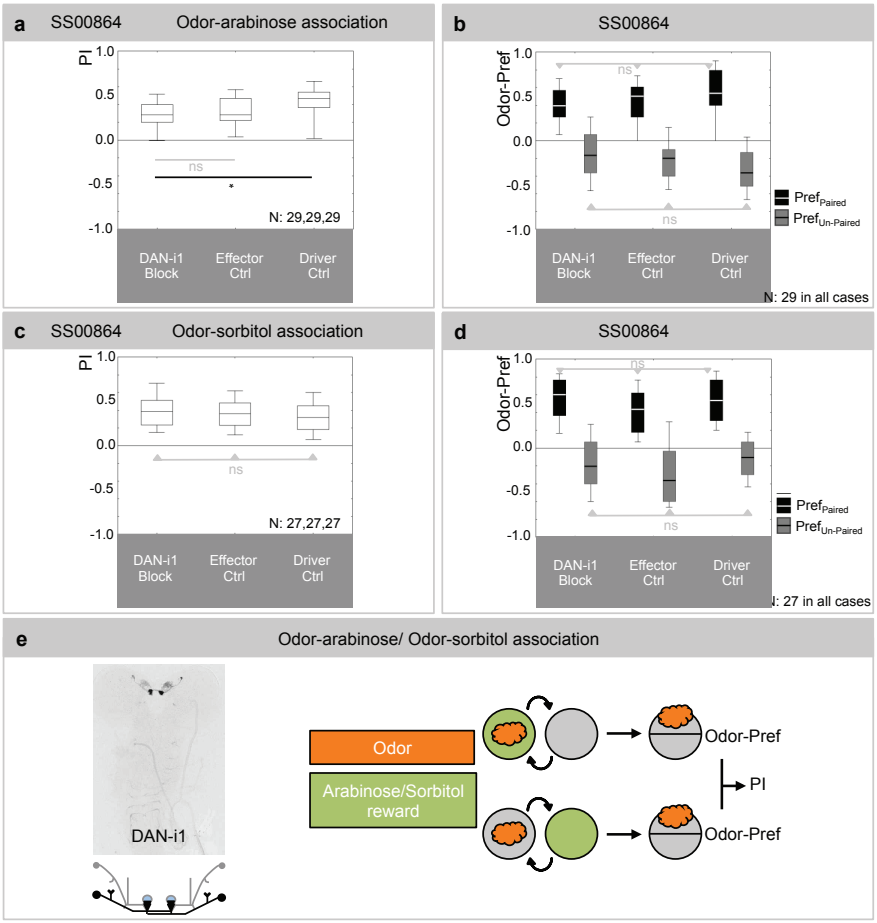

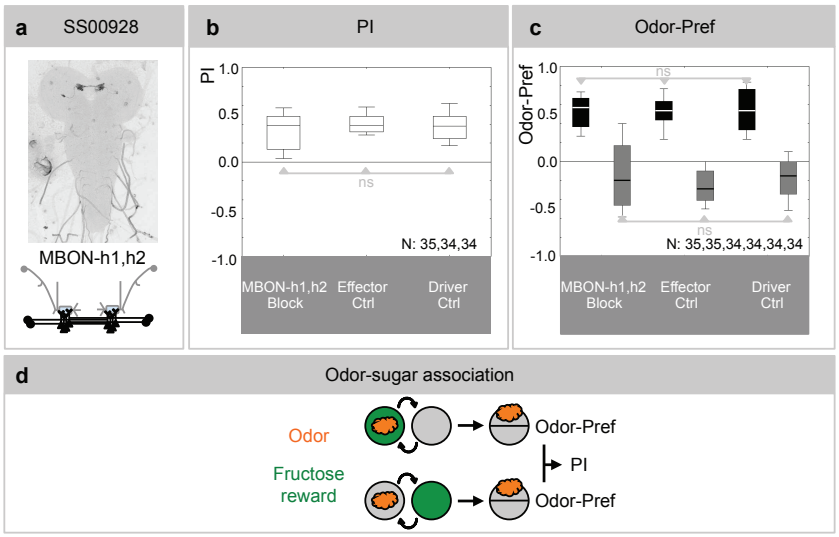

Supplemental Figure 14: Silencing MBON-h1,h2 does not affect odor-fructose association - revisited.
a-c For an additional split-Gal4 strain covering the medial lobe shaft MBON double pair (MBON-h1,h2; SS00928), the panels show the expression pattern of the strain and a schematic overview of MBON-h1,h2 (a), the associative performance indices measuring odor-fructose reward memory (b), and the preference indices underlying these associative performance indices (c) upon silencing MBON-h1,h2 by means of *Kir2.1::GFP* expression.
d Schematic of the training paradigm (details as in Figure 2k).
Sample sizes are indicated within the figure. ns refers to $P>0.05$ in Kruskal-Wallis tests.

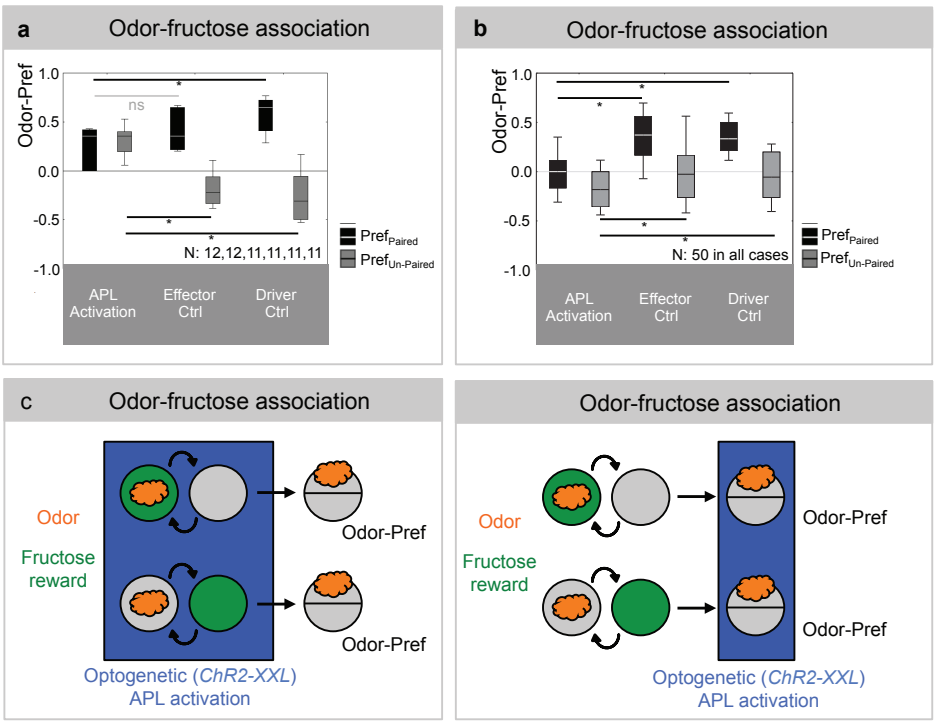

Supplemental Figure 15: Preference scores upon optogenetically activating the APL neuron during only training or only during testing.
a Preference scores for the trained odor *n*-amylacetate (Odor-Pref) underlying the associative performance indices (PI) displayed in Figure 4g, regarding the optogenetic activation of the APL neuron during only training.
b Same as in (a), but for optogenetic activation of the APL neuron during only testing; data relate to the PI scores in Figure 4i.
c, d Schematics of the behavioral paradigms (details as in Figure 4h and j).

Supplemental Figure 16: The APL neuron is remodeled and persists through metamorphosis.
a The APL neuron in the larva, revealed by anti-GFP staining (green) in offspring of a split-GAL4 driver strain expressing only in the APL neuron (GMR_SS01671) crossed to *UAS-GFP* as the effector strain. Neuropil structure is revealed using anti-N-cadherin (blue).
b Transgene expression in the APL neuron was induced late in larval life and then maintained into adulthood using a technique based on Harris et al. [2015]. A conditional flippase (hPRFlp) is expressed from the GMR_SS01671 split-Gal4 driver. The flippase is activated only late in the last larval stage by feeding larvae the progesterone mimic mifepristone (RU-486). The activated flippase removes a "stop" cassette from an actin-LexA driver, resulting in the constitutive expression of the tomato-RFP variant into the adult stage. To achieve this for the APL neuron, GMR_SS01671 was crossed to the three-transgene strain pJFRC48-13XLexAop2-IVS-myrtdTomato; Actin5Cp4.6>dsFRT>LexAp65; pJFRC108-20XUAS-IVS-hPRFlp-p10 respectively located to the attP8, attP5 and VK00005/ TM6 landing sites (available upon request). The image shows staining using anti-RFP (red); neuropil structure is revealed using anti-N-cadherin (blue).

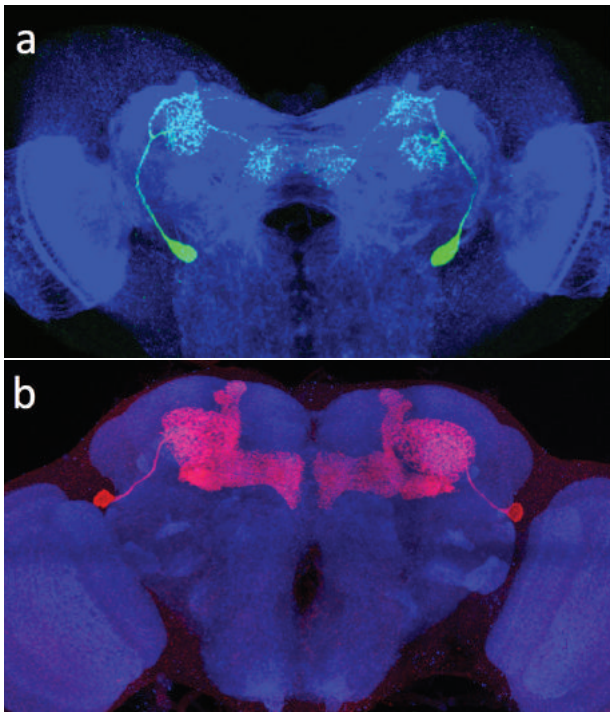

Supplemental Figure 17: Example of a polyadic complex with KCs, MBINs, MBONs, and the APL neuron.
Electron micrograph of a polyadic synaptic complex of a KC with the APL neuron, an MBIN and an MBON.

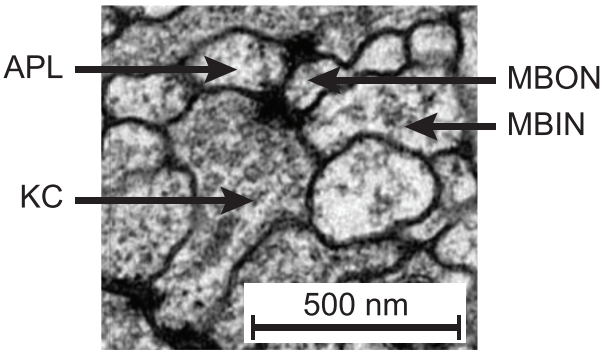

Supplemental Figure 18: MBON-j2 is glutamatergic.
Testing for the neurotransmitter properties of MBON-j2 by immunohistochemistry. At the top left the expression pattern of the SS00860 split-Gal4 driver strain and a schematic of MBON-j2 is shown. In addition, double labeling of MBON-j2 by anti-GFP in green with staining for respectively anti-GLUT (GLUT: vesicular glutamate transporter; top right), anti-GABA (GABA: gamma aminobutyric acid; bottom left), and anti-ChAT (ChAT: choline acetyltransferase; bottom right) is shown in magenta. Insets show the respective staining separately in black and white. MBON-j2 only stains for anti-GLUT and is therefore regarded as glutamatergic. Scale bars: 5 µm.

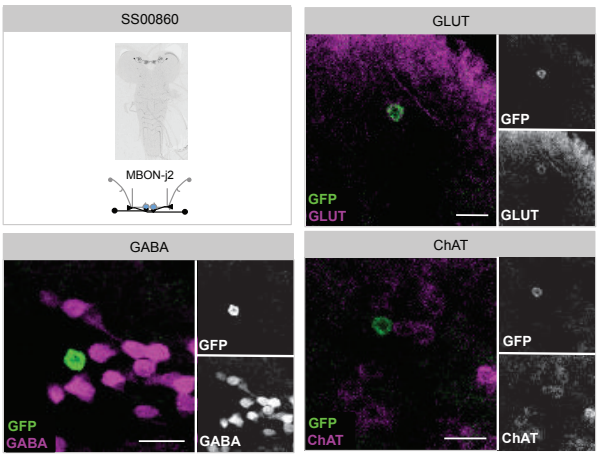

6.9 References

Apostolopoulou, A. A., Köhn, S., Stehle, B., Lutz, M., Wüst, A., Mazija, L., Rist, A., Galizia, C. G., Lüdke, A., and Thum, A. S. (2016). Caffeine taste signaling in drosophila larvae. *Frontiers in Cellular Neuroscience*, 10.

Apostolopoulou, A. A., Mazija, L., Wüst, A., and Thum, A. S. (2014). The neuronal and molecular basis of quinine-dependent bitter taste signaling in drosophila larvae. *Frontiers in behavioral neuroscience*, 8:6.

Apostolopoulou, A. A., Rist, A., and Thum, A. S. (2015). Taste processing in drosophila larvae. *Frontiers in integrative neuroscience*, 9:50.

Apostolopoulou, A. A., Widmann, A., Rohwedder, A., Pfitzenmaier, J. E., and Thum, A. S. (2013). Appetitive associative olfactory learning in drosophila larvae. *JoVE (Journal of Visualized Experiments)*, (72):e4334–e4334.

Aso, Y., Hattori, D., Yu, Y., Johnston, R. M., Iyer, N. A., Ngo, T.-T., Dionne, H., Abbott, L., Axel, R., Tanimoto, H., et al. (2014a). The neuronal architecture of the mushroom body provides a logic for associative learning. *Elife*, 3:e04577.

Aso, Y., Herb, A., Ogueta, M., Siwanowicz, I., Templier, T., Friedrich, A. B., Ito, K., Scholz, H., and Tanimoto, H. (2012). Three dopamine pathways induce aversive odor memories with different stability. *PLoS Genet*, 8(7):e1002768.

Aso, Y., Sitaraman, D., Ichinose, T., Kaun, K. R., Vogt, K., Belliart-Guérin, G., Plaçais, P.-Y., Robie, A. A., Yamagata, N., Schnaitmann, C., et al. (2014b). Mushroom body output neurons encode valence and guide memory-based action selection in drosophila. *Elife*, 3:e04580.

Aso, Y., Siwanowicz, I., Bräcker, L., Ito, K., Kitamoto, T., and Tanimoto, H. (2010). Specific dopaminergic neurons for the formation of labile aversive memory. *Current biology*, 20(16):1445–1451.

Baines, R. A., Uhler, J. P., Thompson, A., Sweeney, S. T., and Bate, M. (2001). Altered electrical properties in drosophilaneurons developing without synaptic transmission. *Journal of Neuroscience*, 21(5):1523–1531.

Barth, J., Dipt, S., Pech, U., Hermann, M., Riemensperger, T., and Fiala, A. (2014). Differential associative training enhances olfactory acuity in drosophila melanogaster. *Journal of Neuroscience*, 34(5):1819–1837.

Berck, M. E., Khandelwal, A., Claus, L., Hernandez-Nunez, L., Si, G., Tabone, C. J., Li, F., Truman, J. W., Fetter, R. D., Louis, M., et al. (2016). The wiring diagram of a glomerular olfactory system. *Elife*, 5:e14859.

Blenau, W. and Thamm, M. (2011). Distribution of serotonin (5-ht) and its receptors in the insect brain with focus on the mushroom bodies. lessons from drosophila melanogaster and apis mellifera. *Arthropod structure & development*, 40(5):381–394.

Bouzaiane, E., Trannoy, S., Scheunemann, L., Plaçais, P.-Y., and Preat, T. (2015). Two independent mushroom body output circuits retrieve the six discrete components of drosophila aversive memory. *Cell reports*, 11(8):1280–1292.

Brembs, B. and Heisenberg, M. (2001). Conditioning with compound stimuli in drosophila melanogaster in the flight simulator. *Journal of Experimental Biology*, 204(16):2849–2859.

Burke, C. J., Huetteroth, W., Owald, D., Perisse, E., Krashes, M. J., Das, G., Gohl, D., Silies, M., Certel, S., and Waddell, S. (2012). Layered reward signalling through octopamine and dopamine in drosophila. *Nature*, 492(7429):433–437.

Campbell, R. A., Honegger, K. S., Qin, H., Li, W., Demir, E., and Turner, G. C. (2013). Imaging a population code for odor identity in the drosophila mushroom body. *Journal of Neuroscience*, 33(25):10568–10581.

Chen, Y.-c. and Gerber, B. (2014). Generalization and discrimination tasks yield concordant measures of perceived distance between odours and their binary mixtures in larval drosophila. *Journal of Experimental Biology*, 217(12):2071–2077.

Chen, Y.-c., Mishra, D., Schmitt, L., Schmuker, M., and Gerber, B. (2011). A behavioral odor similarity “space” in larval drosophila. *Chemical senses*, page bjq123.

Choi, J., van Giesen, L., Choi, M. S., Kang, K., Sprecher, S. G., and Kwon, J. Y. (2016). A pair of pharyngeal gustatory receptor neurons regulates caffeine-dependent ingestion in drosophila larvae. *Frontiers in Cellular Neuroscience*, 10.

Claridge-Chang, A., Roorda, R. D., Vrontou, E., Sjulson, L., Li, H., Hirsh, J., and Miesenböck, G. (2009). Writing memories with light-addressable reinforcement circuitry. *Cell*, 139(2):405–415.

Cobb, M. (1999). What and how do maggots smell? *Biological reviews*, 74(4):425–459.

Cobb, M., Scott, K., and Pankratz, M. (2008). Gustation in drosophila melanogaster. *Insect Taste. SEB Experimental Biology Series*, 63:1–38.

Cohn, R., Morantte, I., and Ruta, V. (2015). Coordinated and compartmentalized neuromodulation shapes sensory processing in drosophila. *Cell*, 163(7):1742–1755.

Colomb, J., Grillenzoni, N., Ramaekers, A., and Stocker, R. F. (2007). Architecture of the primary taste center of drosophila melanogaster larvae. *Journal of Comparative Neurology*, 502(5):834–847.

Croset, V., Schleyer, M., Arguello, J. R., Gerber, B., and Benton, R. (2016). A molecular and neuronal basis for amino acid sensing in the drosophila larva. *Scientific Reports*, 6.

Das, G., Lin, S., and Waddell, S. (2016). Remembering components of food in drosophila. *Frontiers in integrative neuroscience*, 10.

Davis, R. L. (2004). Olfactory learning. *Neuron*, 44(1):31–48.

Dawydow, A., Gueta, R., Ljaschenko, D., Ullrich, S., Hermann, M., Ehmann, N., Gao, S., Fiala, A., Langenhan, T., Nagel, G., et al. (2014). Channelrhodopsin-2–xxl, a powerful optogenetic tool for low-light applications. *Proceedings of the National Academy of Sciences*, 111(38):13972–13977.

Demerec, M. and Kaufmann, B. P. (1965). *Drosophila guide: introduction to the genetics and cytology of Drosophila melanogaster*. Carnegie Institution of Washington Washington, DC.

Diegelmann, S., Klagges, B., Michels, B., Schleyer, M., and Gerber, B. (2013). Maggot learning and synapsin function. *Journal of Experimental Biology*, 216(6):939–951.

Eichler, K., Li, F., Litwin-Kumar, A., Park, Y., Andrade, I., Schneider-Mizell, C. M., Saumweber, T., Huser, A., Eschbach, C., Gerber, B., Fetter, R. D., Truman, J. W., Priebe, C., Abbott, L. F., Thum, A., Zlatic, M., and Cardona, A. (2017). The complete connectome of the mushroom body of a drosophila larva. *Nature*, In press.

Fanselow, M. S. (1998). Pavlovian conditioning, negative feedback, and blocking: mechanisms that regulate association formation. *Neuron*, 20(4):625–627.

Farris, S. M. (2011). Are mushroom bodies cerebellum-like structures? *Arthropod structure & development*, 40(4):368–379.

Filla, I. and Menzel, R. (2015). Mushroom body extrinsic neurons in the honeybee (apis mellifera) brain integrate context and cue values upon attentional stimulus selection. *Journal of neurophysiology*, 114(3):2005–2014.

Freeman, E. G. and Dahanukar, A. (2015). Molecular neurobiology of drosophila taste. *Current opinion in neurobiology*, 34:140–148.

Funayama, E. S., Couvillon, P., and Bitterman, M. (1995). Compound conditioning in honeybees: Blocking tests of the independence assumption. *Learning & behavior*, 23(4):429–437.

Galizia, C. G. (2014). Olfactory coding in the insect brain: data and conjectures. *European Journal of Neuroscience*, 39(11):1784–1795.

Gerber, B. and Aso, Y. (2017). Localization, diversity and behavioral expression of associative engrams in drosophila. In Menzel, R., editor, *Learning and Memory: A Comprehensive Reference*, volume In press.

Gerber, B., Biernacki, R., and Thum, J. (2013). Odor–taste learning assays in drosophila larvae. *Cold Spring Harbor Protocols*, 2013(3):pdb–prot071639.

Gerber, B. and Hendel, T. (2006). Outcome expectations drive learned behaviour in larval drosophila. *Proceedings of the Royal Society of London B: Biological Sciences*, 273(1604):2965–2968.

Gerber, B. and Smith, B. H. (1998). Visual modulation of olfactory learning in honeybees. *Journal of Experimental Biology*, 201(14):2213–2217.

Gerber, B. and Stocker, R. F. (2007). The drosophila larva as a model for studying chemosensation and chemosensory learning: a review. *Chemical senses*, 32(1):65–89.

Gerber, B., Stocker, R. F., Tanimura, T., and Thum, A. S. (2009). Smelling, tasting, learning: Drosophila as a study case. In *Chemosensory Systems in Mammals, Fishes, and Insects*, pages 187–202. Springer.

Gerber, B. and Ullrich, J. (1999). No evidence for olfactory blocking in honeybee classical conditioning. *Journal of Experimental Biology*, 202(13):1839–1854.

Gervasi, N., Tchénio, P., and Preat, T. (2010). Pka dynamics in a drosophila learning center: coincidence detection by rutabaga adenylyl cyclase and spatial regulation by dunce phosphodiesterase. *Neuron*, 65(4):516–529.

Grünewald, B. (1999a). Morphology of feedback neurons in the mushroom body of the honeybee, apis mellifera. *Journal of Comparative Neurology*, 404(1):114–126.

Grünewald, B. (1999b). Physiological properties and response modulations of mushroom body feedback neurons during olfactory learning in the honeybee, apis mellifera. *Journal of Comparative Physiology A: Neuroethology, Sensory, Neural, and Behavioral Physiology*, 185(6):565–576.

Guerrieri, F., Lachnit, H., Gerber, B., and Giurfa, M. (2005). Olfactory blocking and odorant similarity in the honeybee. *Learning & Memory*, 12(2):86–95.

Gupta, N. and Stopfer, M. (2014). A temporal channel for information in sparse sensory coding. *Current Biology*, 24(19):2247–2256.

Guven-Ozkan, T. and Davis, R. L. (2014). Functional neuroanatomy of drosophila olfactory memory formation. *Learning & Memory*, 21(10):519–526.

Hammer, M. (1993). An identified neuron mediates the unconditioned stimulus in associative olfactory learning in honeybees.–p. 59-63. Technical Report 6450, En: Nature (London)(United Kingdom).

Hammer, M. and Menzel, R. (1998). Multiple sites of associative odor learning as revealed by local brain microinjections of octopamine in honeybees. *Learning & Memory*, 5(1):146–156.

Hansson, B. S. and Stensmyr, M. C. (2011). Evolution of insect olfaction. *Neuron*, 72(5):698–711.

Harris, R. M., Pfeiffer, B. D., Rubin, G. M., and Truman, J. W. (2015). Neuron hemilineages provide the functional ground plan for the drosophila ventral nervous system. *Elife*, 4:e04493.

Hartenstein, V., Spindler, S., Pereanu, W., and Fung, S. (2008). The development of the drosophila larval brain. In *Brain development in Drosophila melanogaster*, pages 1–31. Springer.

Haynes, P. R., Christmann, B. L., and Griffith, L. C. (2015). A single pair of neurons links sleep to memory consolidation in drosophila melanogaster. *Elife*, 4:e03868.

Heimbeck, G., Bugnon, V., Gendre, N., Keller, A., and Stocker, R. F. (2001). A central neural circuit for experience-independent olfactory and courtship behavior in drosophila melanogaster. *Proceedings of the National Academy of Sciences*, 98(26):15336–15341.

Heisenberg, M. (2003). Mushroom body memoir: from maps to models. *Nature Reviews Neuroscience*, 4(4):266–275.

Hige, T., Aso, Y., Modi, M. N., Rubin, G. M., and Turner, G. C. (2015). Heterosynaptic plasticity underlies aversive olfactory learning in drosophila. *Neuron*, 88(5):985–998.

Holland, P. C. (1993). Cognitive aspects of classical conditioning. *Current opinion in neurobiology*, 3(2):230–236.

Holland, P. C. (1997). Brain mechanisms for changes in processing of conditioned stimuli in pavlovian conditioning: Implications for behavior theory. *Animal Learning & Behavior*, 25(4):373–399.

Honda, T., Lee, C.-Y., Yoshida-Kasikawa, M., Honjo, K., and Furukubo-Tokunaga, K. (2014). Induction of associative olfactory memory by targeted activation of single olfactory neurons in drosophila larvae. *Scientific reports*, 4:4798.

Honjo, K. and Furukubo-Tokunaga, K. (2009). Distinctive neuronal networks and biochemical pathways for appetitive and aversive memory in drosophila larvae. *Journal of Neuroscience*, 29(3):852–862.

Hosler, J. and Smith, B. H. (2000). Blocking and the detection of odor components in blends. *Journal of Experimental Biology*, 203(18):2797–2806.

Howard, J. D., Gottfried, J. A., Tobler, P. N., and Kahnt, T. (2015). Identity-specific coding of future rewards in the human orbitofrontal cortex. *Proceedings of the National Academy of Sciences*, 112(16):5195–5200.

Hückesfeld, S., Peters, M., and Pankratz, M. J. (2016). Central relay of bitter taste to the protocerebrum by peptidergic interneurons in the drosophila brain. *Nature Communications*, 7:12796.

Huser, A., Rohwedder, A., Apostolopoulou, A. A., Widmann, A., Pfitzenmaier, J. E., Maiolo, E. M., Selcho, M., Pauls, D., von Essen, A., Gupta, T., et al. (2012). The serotonergic central nervous system of the drosophila larva: anatomy and behavioral function. *PLoS One*, 7(10):e47518.

Ito, K. and Hotta, Y. (1992). Proliferation pattern of postembryonic neuroblasts in the brain of drosophila melanogaster. *Developmental biology*, 149(1):134–148.

Ito, M., Masuda, N., Shinomiya, K., Endo, K., and Ito, K. (2013). Systematic analysis of neural projections reveals clonal composition of the drosophila brain. *Current Biology*, 23(8):644–655.

Jenett, A., Rubin, G. M., Ngo, T.-T., Shepherd, D., Murphy, C., Dionne, H., Pfeiffer, B. D., Cavallaro, A., Hall, D., Jeter, J., et al. (2012). A gal4-driver line resource for drosophila neurobiology. *Cell reports*, 2(4):991–1001.

Kamin, L. J. (1969). Predictability, surprise, attention, and conditioning. In Campbell, B. A. and Church, R. M., editors, *Punishment and aversive behavior*, pages 317–332. New York: Appleton-Century-Crofts.

Keene, A. C., Stratmann, M., Keller, A., Perrat, P. N., Vosshall, L. B., and Waddell, S. (2004). Diverse odor-conditioned memories require uniquely timed dorsal paired medial neuron output. *Neuron*, 44(3):521–533.

Kim, H., Choi, M. S., Kang, K., and Kwon, J. Y. (2016). Behavioral analysis of bitter taste perception in drosophila larvae. *Chemical senses*, 41(1):85–94.

Kim, J. J., Krupa, D. J., and Thompson, R. F. (1998). Inhibitory cerebello-olivary projections and blocking effect in classical conditioning. *Science*, 279(5350):570–573.

Kim, Y.-C., Lee, H.-G., and Han, K.-A. (2007). D1 dopamine receptor dda1 is required in the mushroom body neurons for aversive and appetitive learning in drosophila. *Journal of Neuroscience*, 27(29):7640–7647.

Kitamoto, T. (2001). Conditional modification of behavior in drosophila by targeted expression of a temperature-sensitive shibire allele in defined neurons. *Journal of neurobiology*, 47(2):81–92.

Klapoetke, N. C., Murata, Y., Kim, S. S., Pulver, S. R., Birdsey-Benson, A., Cho, Y. K., Morimoto, T. K., Chuong, A. S., Carpenter, E. J., Tian, Z., et al. (2014). Independent optical excitation of distinct neural populations. *Nature methods*, 11(3):338–346.

Kunz, T., Kraft, K. F., Technau, G. M., and Urbach, R. (2012). Origin of drosophila mushroom body neuroblasts and generation of divergent embryonic lineages. *Development*, 139(14):2510–2522.

Kwon, J. Y., Dahanukar, A., Weiss, L. A., and Carlson, J. R. (2011). Molecular and cellular organization of the taste system in the drosophila larva. *Journal of Neuroscience*, 31(43):15300–15309.

Lak, A., Stauffer, W. R., and Schultz, W. (2014). Dopamine prediction error responses integrate subjective value from different reward dimensions. *Proceedings of the National Academy of Sciences*, 111(6):2343–2348.

Lee, P.-T., Lin, H.-W., Chang, Y.-H., Fu, T.-F., Dubnau, J., Hirsh, J., Lee, T., and Chiang, A.-S. (2011). Serotonin–mushroom body circuit modulating the formation of anesthesia-resistant memory in drosophila. *Proceedings of the National Academy of Sciences*, 108(33):13794–13799.

Li, H.-H., Kroll, J. R., Lennox, S. M., Ogundeyi, O., Jeter, J., Depasquale, G., and Truman, J. W. (2014). A gal4 driver resource for developmental and behavioral studies on the larval cns of drosophila. *Cell Reports*, 8(3):897–908.

Lin, A. C., Bygrave, A. M., De Calignon, A., Lee, T., and Miesenböck, G. (2014a). Sparse, decorrelated odor coding in the mushroom body enhances learned odor discrimination. *Nature neuroscience*, 17(4):559–568.

Lin, S., Owald, D., Chandra, V., Talbot, C., Huetteroth, W., and Waddell, S. (2014b). Neural correlates of water reward in thirsty drosophila. *Nature neuroscience*, 17(11):1536–1542.

Liu, C., Plaçais, P.-Y., Yamagata, N., Pfeiffer, B. D., Aso, Y., Friedrich, A. B., Siwanowicz, I., Rubin, G. M., Preat, T., and Tanimoto, H. (2012). A subset of dopamine neurons signals reward for odour memory in drosophila. *Nature*, 488(7412):512–516.

Liu, X. and Davis, R. L. (2009). The gabaergic anterior paired lateral neuron suppresses and is suppressed by olfactory learning. *Nature neuroscience*, 12(1):53–59.

Luan, H., Peabody, N. C., Vinson, C. R., and White, B. H. (2006). Refined spatial manipulation of neuronal function by combinatorial restriction of transgene expression. *Neuron*, 52(3):425–436.

Mackintosh, N. J. (1974). *The psychology of animal learning.* Academic Press.

Maes, E., Boddez, Y., Alfei, J. M., Krypotos, A.-M., D'Hooge, R., De Houwer, J., and Beckers, T. (2016). The elusive nature of the blocking effect: 15 failures to replicate. *Journal of Experimental Psychology: General*, 145(9):e49.

Martin, J. P., Beyerlein, A., Dacks, A. M., Reisenman, C. E., Riffell, J. A., Lei, H., and Hildebrand, J. G. (2011). The neurobiology of insect olfaction: sensory processing in a comparative context. *Progress in neurobiology*, 95(3):427–447.

Masuda-Nakagawa, L. M., Ito, K., Awasaki, T., and O'Kane, C. J. (2014). A single gabaergic neuron mediates feedback of odor-evoked signals in the mushroom body of larval drosophila. *Frontiers in neural circuits*, 8:35.

Masuda-Nakagawa, L. M., Tanaka, N. K., and O'Kane, C. J. (2005). Stereotypic and random patterns of connectivity in the larval mushroom body calyx of drosophila. *Proceedings of the National Academy of Sciences of the United States of America*, 102(52):19027–19032.

Menzel, R. (2001). Searching for the memory trace in a mini-brain, the honeybee. *Learning & Memory*, 8(2):53–62.

Menzel, R. (2014). The insect mushroom body, an experience-dependent recoding device. *Journal of Physiology-Paris*, 108(2):84–95.

Michels, B., Chen, Y.-c., Saumweber, T., Mishra, D., Tanimoto, H., Schmid, B., Engmann, O., and Gerber, B. (2011). Cellular site and molecular mode of synapsin action in associative learning. *Learning & Memory*, 18(5):332–344.

Michels, B., Saumweber, T., Biernacki, R., Thum, J., Glasgow, R. D., Schleyer, M., Chen, Y.-c., Eschbach, C., Stocker, R. F., Toshima, N., et al. (2017). Pavlovian conditioning of larval drosophila: An illustrated, multilingual, hands-on manual for odor-taste associative learning in maggots. *Frontiers in Behavioral Neuroscience*, 11:45.

Miller, R. R. and Matzel, L. D. (1988). The comparator hypothesis: A response rule for the expression of associations. In Bower, G. H., editor, *Psychology of learning and motivation*, pages 51–92. San Diego: Academic Press.

Mishra, D., Louis, M., and Gerber, B. (2010). Adaptive adjustment of the generalization-discrimination balance in larval drosophila. *Journal of neurogenetics*, 24(3):168–175.

Mishra, D., Miyamoto, T., Rezenom, Y. H., Broussard, A., Yavuz, A., Slone, J., Russell, D. H., and Amrein, H. (2013). The molecular basis of sugar sensing in drosophila larvae. *Current Biology*, 23(15):1466–1471.

Nern, A., Pfeiffer, B. D., and Rubin, G. M. (2015). Optimized tools for multicolor stochastic labeling reveal diverse stereotyped cell arrangements in the fly visual system. *Proceedings of the National Academy of Sciences*, 112(22):E2967–E2976.

Neuser, K., Husse, J., Stock, P., and Gerber, B. (2005). Appetitive olfactory learning in drosophila larvae: effects of repetition, reward strength, age, gender, assay type and memory span. *Animal behaviour*, 69(4):891–898.

Owald, D., Felsenberg, J., Talbot, C. B., Das, G., Perisse, E., Huetteroth, W., and Waddell, S. (2015). Activity of defined mushroom body output neurons underlies learned olfactory behavior in drosophila. *Neuron*, 86(2):417–427.

Owald, D. and Waddell, S. (2015). Olfactory learning skews mushroom body output pathways to steer behavioral choice in drosophila. *Current opinion in neurobiology*, 35:178–184.

Pai, T.-P., Chen, C.-C., Lin, H.-H., Chin, A.-L., Lai, J. S.-Y., Lee, P.-T., Tully, T., and Chiang, A.-S. (2013). Drosophila orb protein in

two mushroom body output neurons is necessary for long-term memory formation. *Proceedings of the National Academy of Sciences*, 110(19):7898–7903.

Paisios, E., Rjosk, A., Pamir, E., and Schleyer, M. (2017). Common microbehavioural 'footprint' of two distinct classes of conditioned aversion. In press.

Pauls, D., Selcho, M., Gendre, N., Stocker, R. F., and Thum, A. S. (2010). Drosophila larvae establish appetitive olfactory memories via mushroom body neurons of embryonic origin. *Journal of Neuroscience*, 30(32):10655–10666.

Pearce, J. M. and Hall, G. (1980). A model for pavlovian learning: variations in the effectiveness of conditioned but not of unconditioned stimuli. *Psychological review*, 87(6):532.

Perisse, E., Owald, D., Barnstedt, O., Talbot, C. B., Huetteroth, W., and Waddell, S. (2016). Aversive learning and appetitive motivation toggle feed-forward inhibition in the drosophila mushroom body. *Neuron*, 90(5):1086–1099.

Pfeiffer, B. D., Jenett, A., Hammonds, A. S., Ngo, T.-T. B., Misra, S., Murphy, C., Scully, A., Carlson, J. W., Wan, K. H., Laverty, T. R., et al. (2008). Tools for neuroanatomy and neurogenetics in drosophila. *Proceedings of the National Academy of Sciences*, 105(28):9715–9720.

Pfeiffer, B. D., Ngo, T.-T. B., Hibbard, K. L., Murphy, C., Jenett, A., Truman, J. W., and Rubin, G. M. (2010). Refinement of tools for targeted gene expression in drosophila. *Genetics*, 186(2):735–755.

Pitman, J. L., Huetteroth, W., Burke, C. J., Krashes, M. J., Lai, S.-L., Lee, T., and Waddell, S. (2011). A pair of inhibitory neurons are required to sustain labile memory in the drosophila mushroom body. *Current Biology*, 21(10):855–861.

Plaçais, P.-Y., Trannoy, S., Friedrich, A. B., Tanimoto, H., and Preat, T. (2013). Two pairs of mushroom body efferent neurons are required for appetitive long-term memory retrieval in drosophila. *Cell Reports*, 5(3):769–780.

Qin, H., Cressy, M., Li, W., Coravos, J. S., Izzi, S. A., and Dubnau, J. (2012). Gamma neurons mediate dopaminergic input during aversive olfactory memory formation in drosophila. *Current Biology*, 22(7):608–614.

Ren, Q., Li, H., Wu, Y., Ren, J., and Guo, A. (2012). A gabaergic inhibitory neural circuit regulates visual reversal learning in drosophila. *Journal of Neuroscience*, 32(34):11524–11538.

Rescorla, R. A. and Wagner, A. R. (1972). A theory of pavlovian conditioning: Variations in the effectiveness of reinforcement and nonreinforcement. In Black, A. H. and Prokasy, W. F., editors, *Classical conditioning II: Current research and theory*, pages 64–99. New York: Appleton-Century-Crofts.

Rohwedder, A., Wenz, N. L., Stehle, B., Huser, A., Yamagata, N., Zlatic, M., Truman, J. W., Tanimoto, H., Saumweber, T., Gerber, B., et al. (2016). Four individually identified paired dopamine neurons signal reward in larval drosophila. *Current Biology*, 26(5):661–669.

Roy, B., Singh, A. P., Shetty, C., Chaudhary, V., North, A., Landgraf, M., Vijayraghavan, K., and Rodrigues, V. (2007). Metamorphosis of an identified serotonergic neuron in the drosophila olfactory system. *Neural Development*, 2(1):20.

Saalfeld, S., Cardona, A., Hartenstein, V., and Tomančák, P. (2009). Catmaid: collaborative annotation toolkit for massive amounts of image data. *Bioinformatics*, 25(15):1984–1986.

Saumweber, T., Husse, J., and Gerber, B. (2011a). Innate attractiveness and associative learnability of odors can be dissociated in larval drosophila. *Chemical senses*, 36(3):223–235.

Saumweber, T., Weyhersmüller, A., Hallermann, S., Diegelmann, S., Michels, B., Bucher, D., Funk, N., Reisch, D., Krohne, G., Wegener, S., et al. (2011b). Behavioral and synaptic plasticity are impaired upon lack of the synaptic protein sap47. *Journal of Neuroscience*, 31(9):3508–3518.

Scherer, S., Stocker, R. F., and Gerber, B. (2003). Olfactory learning in individually assayed drosophila larvae. *Learning & Memory*, 10(3):217–225.

Schlegel, P., Texada, M. J., Miroschnikow, A., Schoofs, A., Hückesfeld, S., Peters, M., Schneider-Mizell, C. M., Lacin, H., Li, F., Fetter, R. D., et al. (2016). Synaptic transmission parallels neuromodulation in a central food-intake circuit. *eLife*, 5:e16799.

Schleyer, M., Miura, D., Tanimura, T., and Gerber, B. (2015a). Learning the specific quality of taste reinforcement in larval drosophila. *Elife*, 4:e04711.

Schleyer, M., Reid, S. F., Pamir, E., Saumweber, T., Paisios, E., Davies, A., Gerber, B., and Louis, M. (2015b). The impact of odor–reward memory on chemotaxis in larval drosophila. *Learning & Memory*, 22(5):267–277.

Schleyer, M., Saumweber, T., Nahrendorf, W., Fischer, B., von Alpen, D., Pauls, D., Thum, A., and Gerber, B. (2011). A behavior-based circuit model of how outcome expectations organize learned behavior in larval drosophila. *Learning & Memory*, 18(10):639–653.

Schneider-Mizell, C. M., Gerhard, S., Longair, M., Kazimiers, T., Li, F., Zwart, M. F., Champion, A., Midgley, F. M., Fetter, R. D., Saalfeld, S., et al. (2016). Quantitative neuroanatomy for connectomics in drosophila. *Elife*, 5:e12059.

Schroll, C., Riemensperger, T., Bucher, D., Ehmer, J., Völler, T., Erbguth, K., Gerber, B., Hendel, T., Nagel, G., Buchner, E., et al. (2006). Light-induced activation of distinct modulatory neurons triggers appetitive or aversive learning in drosophila larvae. *Current biology*, 16(17):1741–1747.

Schultz, W., Dayan, P., and Montague, P. R. (1997). A neural substrate of prediction and reward. *Science*, 275(5306):1593–1599.

Schwaerzel, M., Monastirioti, M., Scholz, H., Friggi-Grelin, F., Birman, S., and Heisenberg, M. (2003). Dopamine and octopamine differentiate between aversive and appetitive olfactory memories in drosophila. *Journal of Neuroscience*, 23(33):10495–10502.

Séjourné, J., Plaçais, P.-Y., Aso, Y., Siwanowicz, I., Trannoy, S., Thoma, V., Tedjakumala, S. R., Rubin, G. M., Tchénio, P., Ito, K., et al. (2011). Mushroom body efferent neurons responsible for aversive olfactory memory retrieval in drosophila. *Nature neuroscience*, 14(7):903–910.

Selcho, M., Pauls, D., Han, K.-A., Stocker, R. F., and Thum, A. S. (2009). The role of dopamine in drosophila larval classical olfactory conditioning. *PLoS One*, 4(6):e5897.

Selcho, M., Pauls, D., Huser, A., Stocker, R. F., and Thum, A. S. (2014). Characterization of the octopaminergic and tyraminergic neurons in the central brain of drosophila larvae. *Journal of Comparative Neurology*, 522(15):3485–3500.

Silva, B., Goles, N. I., Varas, R., and Campusano, J. M. (2014). Serotonin receptors expressed in drosophila mushroom bodies differentially modulate larval locomotion. *PloS one*, 9(2):e89641.

Smith, B. H. and Cobey, S. (1994). The olfactory memory of the honeybee apis mellifera. ii. blocking between odorants in binary mixtures. *Journal of Experimental Biology*, 195(1):91–108.

Steinberg, E. E., Keiflin, R., Boivin, J. R., Witten, I. B., Deisseroth, K., and Janak, P. H. (2013). A causal link between prediction errors, dopamine neurons and learning. *Nature neuroscience*, 16(7):966–973.

Stewart, S., Koh, T.-W., Ghosh, A. C., and Carlson, J. R. (2015). Candidate ionotropic taste receptors in the drosophila larva. *Proceedings of the National Academy of Sciences*, 112(14):4195–4201.

Stocker, R. F. (1994). The organization of the chemosensory system in drosophila melanogaster: a rewiew. *Cell and tissue research*, 275(1):3–26.

Strausfeld, N. J., Sinakevitch, I., Brown, S. M., and Farris, S. M. (2009). Ground plan of the insect mushroom body: functional and evolutionary implications. *Journal of Comparative Neurology*, 513(3):265–291.

Sutton, R. S., Barto, A. G., et al. (1981). Toward a modern theory of adaptive networks: Expectation and prediction. *Psychological review*, 88(2):135–170.

Tanaka, N. K., Tanimoto, H., and Ito, K. (2008). Neuronal assemblies of the drosophila mushroom body. *Journal of Comparative Neurology*, 508(5):711–755.

The Ol_1mpiad Consortium, ., Almeida-Carvalho, M. J., Berh, D., Braun, A., Chen, Y.-c., Eichler, K., Eschbach, C., Fritsch, P. M. J., Gerber, B., Hoyer, N., Jiangn, X., Kleber, J., Klämbt, C., König, C., Louis, M., Michels, B., Miroschnikow, A., Mirth, C., Miura, D., Niewalda, T., Otto, N., Paisios, E., Pankratz, M. J., Petersen, M., Ramsperger, N., Randel, N., Risse, B., Saumweber, T., Schlegel, P., Schleyer, M., Soba, P., Sprecher, S. G., Tanimura, T., Thum, A., Toshima, N., Truman, J. W., Yarali, A., and Zlatic, M. (2017). Concordance of behavioural faculties of stage 1 and stage 3 drosophila larvae. *Journal of Experimental Biology*, In press.

Thum, A. S., Leisibach, B., Gendre, N., Selcho, M., and Stocker, R. F. (2011). Diversity, variability, and suboesophageal connectivity of antennal lobe neurons in d. melanogaster larvae. *Journal of Comparative Neurology*, 519(17):3415–3432.

Tomchik, S. M. and Davis, R. L. (2009). Dynamics of learning-related camp signaling and stimulus integration in the drosophila olfactory pathway. *Neuron*, 64(4):510–521.

Turner, G. C., Bazhenov, M., and Laurent, G. (2008). Olfactory representations by drosophila mushroom body neurons. *Journal of neurophysiology*, 99(2):734–746.

Unoki, S., Matsumoto, Y., and Mizunami, M. (2006). Roles of octopaminergic and dopaminergic neurons in mediating reward and punishment signals in insect visual learning. *European Journal of Neuroscience*, 24(7):2031–2038.

Van Giesen, L., Hernandez-Nunez, L., Delasoie-Baranek, S., Colombo, M., Renaud, P., Bruggmann, R., Benton, R., Samuel, A. D., and Sprecher, S. G. (2016). Multimodal stimulus coding by a gustatory sensory neuron in drosophila larvae. *Nature communications*, 7.

Vasmer, D., Pooryasin, A., Riemensperger, T., and Fiala, A. (2014). Induction of aversive learning through thermogenetic activation of kenyon cell ensembles in drosophila. *Frontiers in behavioral neuroscience*, 8:174.

Vosshall, L. B. and Stocker, R. F. (2007). Molecular architecture of smell and taste in drosophila. *Annu. Rev. Neurosci.*, 30:505–533.

Waddell, S., Armstrong, J. D., Kitamoto, T., Kaiser, K., and Quinn, W. G. (2000). The amnesiac gene product is expressed in two neurons in the drosophila brain that are critical for memory. *Cell*, 103(5):805–813.

Waelti, P., Dickinson, A., and Schultz, W. (2001). Dopamine responses comply with basic assumptions of formal learning theory. *Nature*, 412(6842):43–48.

Wagner, A. R. (1981). Sop: A model of automatic memory processing in animal behavior. In Spear, N. E. and Miller, R. R., editors, *Information processing in animals: Memory mechanisms*, pages 5–47. Hillsdale: Erlbaum.

Wu, C.-L., Shih, M.-F. M., Lai, J. S.-Y., Yang, H.-T., Turner, G. C., Chen, L., and Chiang, A.-S. (2011). Heterotypic gap junctions between two neurons in the drosophila brain are critical for memory. *Current Biology*, 21(10):848–854.

Wu, C.-L., Shih, M.-F. M., Lee, P.-T., and Chiang, A.-S. (2013). An octopamine-mushroom body circuit modulates the formation of anesthesia-resistant memory in drosophila. *Current Biology*, 23(23):2346–2354.

Wu, Y., Ren, Q., Li, H., and Guo, A. (2012). The gabaergic anterior paired lateral neurons facilitate olfactory reversal learning in drosophila. *Learning & Memory*, 19(10):478–486.

Wystrach, A., Lagogiannis, K., and Webb, B. (2016). Continuous lateral oscillations as a core mechanism for taxis in drosophila larvae. *eLife*, 5:e15504.

Yamagata, N., Ichinose, T., Aso, Y., Plaçais, P.-Y., Friedrich, A. B., Sima, R. J., Preat, T., Rubin, G. M., and Tanimoto, H. (2015). Distinct dopamine neurons mediate reward signals for short-and long-term memories. *Proceedings of the National Academy of Sciences*, 112(2):578–583.

Young, J., Wessnitzer, J., Armstrong, J., and Webb, B. (2011). Elemental and non-elemental olfactory learning in drosophila. *Neurobiology of learning and memory*, 96(2):339–352.

Yu, D., Keene, A. C., Srivatsan, A., Waddell, S., and Davis, R. L. (2005). Drosophila dpm neurons form a delayed and branch-specific memory trace after olfactory classical conditioning. *Cell*, 123(5):945–957.

Yu, H.-H., Awasaki, T., Schroeder, M. D., Long, F., Yang, J. S., He, Y., Ding, P., Kao, J.-C., Wu, G. Y.-Y., Peng, H., et al. (2013). Clonal development and organization of the adult drosophila central brain. *Current Biology*, 23(8):633–643.

Chapter V: Odor-taste Learning in *Drosophila* Larvae

Annekathrin Widmann[2], Katharina Eichler[2], Mareike Selcho[1], Andreas S. Thum[2,$] and Dennis Pauls[1,$]

[1] Department of Neurobiology and Genetics, Theodor-Boveri-Institute, Biocenter, University of Würzburg, D-97074 Würzburg, Germany.

[2] Department of Biology, University of Konstanz, D-78464 Konstanz, Germany.

[$] These authors jointly supervised this work.

In Press: Journal of Insect Physiology (2017)

doi: 10.1016/j.jinsphys.2017.08.004

7.1 Abstract

The *Drosophila* larva is an attractive model system to study fundamental questions in the field of neuroscience. The larva offers - as the adult fly does - a seemingly unlimited genetic toolbox, which allows to artificially visualize, silence or activate neurons up to the single cell level. In combination with its simplicity in terms of cell number, the larva offers an interesting system to study the neuronal correlates of complex processes including associative odor-taste learning and memory formation. Here, we summarize the current knowledge about odor-taste learning and memory on the behavioral level and integrate the recent progress on the larval connectome to shed light onto the sub-circuits that allow *Drosophila* larvae to integrate present sensory input in the context of past experience and to elicit an appropriate behavioral response.

Keywords: learning and memory; mushroom bodies; *Drosophila* larva; connectome
Abbreviations: MB, mushroom body; KC, Kenyon cell; CS, conditioned stimulus; US, unconditioned stimulus; ORN, olfactory receptor neuron; LN, local neuron; PN, projection neuron; GRN, gustatory receptor neurons; SEZ, subesophageal zone; DA, dopamine; OA, octopamine; Syn, Synapsin; MBIN, mushroom body input neuron; MBON, mushroom body output neuron; cAMP, cyclic adenosine 3'5'-monophosphate; PKA, protein kinase A; PKC, protein kinase C

7.2 Introduction

For the last 50 years *Drosophila melanogaster* has become a favorable model system to study associative olfactory learning and memory (reviewed in Heisenberg [2003]; McGuire et al. [2005]; Keene and Waddell [2007]; Busto et al. [2010]; Schleyer et al.

[2011]; Owald and Waddell [2015]). Initially, *Drosophila* has been used as an organism that provides facile and unbiased access to genes. However, in the last two decades, there has been an outstanding emphasis on genetic tool development and consequential *Drosophila* has evolved from a suitable model for gene discovery to one offering the opportunity to integrate molecular genetics with systems neuroscience (Brand and Perrimon [1993]; Lai and Lee [2006]; Pfeiffer et al. [2010]; Yagi et al. [2010]; Potter and Luo [2011]; Jenett et al. [2012]; reviewed in Duffy [2002]; Elliott and Brand [2008]; Venken et al. [2011]). Thus, the current research focus lies -among others- on the molecular and neuronal pathways underlying the acquisition, storage and retrieval of memory at the systems level. Diverse factors have emphasized the *Drosophila* larva as a suitable model organism in neuroscientific research: First, a prerequisite is the elementary organization of the central larval nervous system that consists of only about 10,000 neurons [Dumstrei et al., 2003]. Second, the availability and robustness of behavioral assays [Aceves-Piña and Quinn, 1979; Scherer et al., 2003; Fishilevich et al., 2005; Luo et al., 2010; Apostolopoulou et al., 2013; Kane et al., 2013; Ohyama et al., 2013; Risse et al., 2013], and third the existence of transgenic techniques, which allow one to interfere with neuronal networks, small sets of neurons or even individually identified neurons [Li et al., 2014; Pauls et al., 2015]. These advantages together with the ongoing efforts toward the reconstruction of the complete larval connectome brings a full-brain, single-cell, and single-synapse understanding of learning and memory for the first time into reach [Heckscher et al., 2015; Ohyama et al., 2015; Berck et al., 2016; Fushiki et al., 2016; Jovanic et al., 2016; Schlegel et al., 2016; Schneider-Mizell et al., 2016; Zwart et al., 2016; Eichler et al., 2017].

In this review, we will summarize current knowledge and recent progress on odor-taste learning and memory in the *Drosophila* larva. We will describe different experimentally accessible types of odor-taste memories, and how in this respect relevant stimuli are

perceived and integrated. For that, we will revisit the underlying neuronal circuits and define sub-circuits that contribute and become substrate for modulation during conditioning. Finally, we will report on current findings obtained when genetically dissecting odor-taste learning and memory.

7.3 Odor-taste learning: Available paradigms and behavioral results

In 1974, Quinn and coworkers showed for the first time that electric shock can be used in adult *Drosophila* to reinforce the formation of aversive odor memories [Quinn et al., 1974]. Only a few years later, Aceves-Piña and Quinn described olfactory associative learning and memory in *Drosophila* larvae for the first time [Aceves-Piña and Quinn, 1979]. In this study, also larvae were trained to associate odor information with electric shock stimulation allowing to compare associative learning in different developmental stages. For the larva, however, these findings were somewhat forgotten [Heisenberg et al., 1985; Tully et al., 1994]. Only about one decade ago, due to the effort of Bertram Gerber and colleagues, research on larval learning and memory was intensified and put back into focus [Scherer et al., 2003; Neuser et al., 2005]. Since then, classical (or Pavlovian) appetitive olfactory learning is mainly analyzed using a two-odor, reciprocal training regime with three repetitions and usually 2M fructose reinforcement [Scherer et al., 2003; Saumweber et al., 2011]. More recently, different variations of the original experimental design were introduced that e.g. utilize only one-odor or non-reciprocal designs [Honjo and Furukubo-Tokunaga, 2005; Saumweber et al., 2011]. In addition, other sugars like sucrose, glucose, maltodextrin, sorbitol, xylose and arabinose were shown to fulfill a reinforcing function [Rohwedder et al., 2012].

The use of sugars is of particular interest as larvae are able to identify ”sweet” and

”energy-rich” sugar rewards, certainly, as flies do [Burke and Waddell, 2011; Rohwedder et al., 2012; Huetteroth et al., 2015; Ichinose et al., 2015; Musso et al., 2015; Yamagata et al., 2015]. In detail, larvae show concentration-dependent odor-taste memories for only-sweet sugars like xylose and arabinose. However, as these sugars do not offer a nutritional benefit, larvae do not change their feeding behavior and die as fast as food-deprived larvae. Contrary, larvae also associate only-nutritional sugars like maltodextrin or sorbitol that trigger feeding behavior and survival like sweet and nutritional sugars like fructose, sucrose or glucose [Rohwedder et al., 2012]. This also emphasizes the idea that different sugar stimuli provide diverse valence for distinct types of behaviors (e.g. learning, feeding or survival; Schipanski et al. [2008]; Schleyer et al. [2015a]). In addition to the various sugars, larvae can also sense and process low salt concentrations as well as amino acids (e.g. aspartic acid) as rewards [Niewalda et al., 2008; Schleyer et al., 2015a].

Certainly, larvae can establish aversive odor-taste memories. Bitter substances like quinine and caffeine as well as high salt (sodium chloride) concentrations were introduced as negative reinforcer [Gerber and Hendel, 2006; Niewalda et al., 2008; Schleyer et al., 2011; Apostolopoulou et al., 2014b, 2016]. Salt, however, turned out to be dichotomous. Low concentrations around 0.3M-0.4M can be utilized for appetitive odor-taste learning, while high salt concentrations peaking at 2M-4M induce the formation of aversive odor-taste associations (Niewalda et al. [2008]; Schleyer et al. [2011], but see also Russell et al. [2011]). In contrast, bitter substances such as quinine and caffeine are clearly aversive regarding preference behavior, feeding and associative conditioning [Schleyer et al., 2011; El-Keredy et al., 2012; König et al., 2015; Apostolopoulou et al., 2014b]. Noteworthy, in this sense the larva turned out to be particularly suited for aversive odor-taste learning, as flies usually deny these substances when purely presented. They ingest, however, salty or bitter tastants in mixtures with appetitive food compounds

and that may complicate the interpretation of the results [Meunier et al., 2003; Moon et al., 2006].

In most studies regarding larval associative learning and memory appetitive and aversive reinforcers are diluted in agarose, which is the main substrate larvae are exposed to during the behavioral experiment. Notably, other experimental procedures exist, where larvae are exposed to a reinforcer solution, rather than a reinforcer-agarose substrate (see Honjo and Furukubo-Tokunaga [2005]). Interestingly, recent work focusing on agarose as a potential reinforcer itself revealed that larvae are able to associate a specific agarose concentration with an odor stimulus [Apostolopoulou et al., 2014a]. Thus, although agarose is a non-metabolizable sugar, it offers a reinforcing function under certain conditions, which therefore, must be considered when comparing differences in larval behavior.

Additionally, not only taste provides a reinforcing function, as also light, temperature, vibration (buzz) and electric shock are used for olfactory conditioning in the larva. Accordingly, learning paradigms for each odor-sensory stimulus combination are available [Gerber et al., 2004; Pauls et al., 2010a; Eschbach et al., 2011; von Essen et al., 2011; Khurana et al., 2012]. Thus, on the behavioral level a comprehensive set of paradigms exists to study various aspects of appetitive and aversive odor-taste learning and memory (as well as for odor-non taste learning and memory) (Table 1).

Type of learning	Training procedure	Original reference
appetitive learning:		
odor-sucrose	en masse; 2-odor reciprocal paradigm	Rohwedder et al. 2012
odor-fructose	en masse; 2-odor reciprocal paradigm	Neuser et al. 2005
odor-maltodextrin	en masse; 2-odor reciprocal paradigm	Rohwedder et al. 2012
odor-sorbitol	en masse; 2-odor reciprocal paradigm	Rohwedder et al. 2012
odor-arabinose	en masse; 2-odor reciprocal paradigm	Rohwedder et al. 2012
odor-glucose	en masse; 2-odor reciprocal paradigm	Rohwedder et al. 2012
odor-xylose	en masse; 2-odor reciprocal paradigm	Rohwedder et al. 2012
odor-low salt	en masse; 2-odor reciprocal paradigm	Gerber and Hendel 2006
odor-fructose	individually; 2-odor reciprocal paradigm	Scherer et al. 2003
odor-fructose	en masse; 1-odor non-reciprocal paradigm	Honjo and Furukubo-Tokunaga 2005
aversive learning:		
odor-high salt	en masse; 2-odor reciprocal paradigm	Gerber and Hendel 2006
light-high salt	en masse; 2-odor reciprocal paradigm	von Essen et al. 2011
odor-medium salt	en masse; 2-odor reciprocal paradigm	Gerber and Hendel 2006
odor-quinine	en masse; 2-odor reciprocal paradigm	Gerber and Hendel 2006
odor-caffeine	en masse; 2-odor reciprocal paradigm	Apostolopoulou et al. 2016
odor-aspartic acid	en masse; 2-odor reciprocal paradigm	Schleyer et al. 2015
odor-agarose	en masse; 2-odor reciprocal paradigm	Apostolopoulou et al. 2014
odor-quinine	en masse; 1-odor non-reciprocal paradigm	Honjo and Furukubo-Tokunaga 2009
non-taste learning:		
odor-electric shock	en masse; 2-odor reciprocal paradigm	Aceves-Pina et al. 1979
odor-light	en masse; 2-odor reciprocal paradigm	von Essen et al. 2011
odor-buzz	en masse; 2-odor reciprocal paradigm	Eschbach et al. 2011
odor-heat learning	en masse; 2-odor reciprocal paradigm	Khurana et al. 2012
odor-electric shock	en masse; 1-odor reciprocal paradigm	Pauls et al. 2010a
odor-heat learning	en masse; 1-odor reciprocal paradigm	Khurana et al. 2012

Table 1: Behavioral paradigms to analyze learning and memory in *Drosophila* larvae.

7.4 Odor-taste learning: The neuronal circuits

Drosophila larvae can form odor-taste associations and store them in the central nervous system based on defined physio-chemical changes. Where do these learning dependent changes take place? Are these changes distributed over the entire central nervous system or are they localized at a specialized central brain area? Recent studies in larval and adult *Drosophila* clearly support the second case. There is strong evidence that the larval mushroom bodies (MBs) - similar to its adult counterpart - forms a specified brain region where olfactory and taste information merge (for the larva: Honjo and Furukubo-Tokunaga [2005]; Kaun et al. [2007]; Pauls et al. [2010b]; Michels et al. [2011]; Widmann et al. [2016]; for the fly reviewed in Heisenberg [2003]; McGuire et al. [2005]; Keene and Waddell [2007]; Owald and Waddell [2015]). The current assumption is that in this brain region learning and memory dependent plasticity occurs and is further relayed onto downstream premotor circuits.

7.4.1 Sub-circuit 1: Perception of odors

In the last decades, light microscopy studies combined with behavioral neurogenetics revealed that larvae receive olfactory stimuli by only 21 olfactory receptor neurons (ORN) housed in a single sensillum at its head, the dorsal organ [Oppliger et al., 2000; Python and Stocker, 2002; Fishilevich et al., 2005; Kreher et al., 2005]. The olfactory information from a given ORN is further conveyed at the larval antennal lobe in a direct one-to-one fashion to 21 projection neurons (PNs) that project to two second order olfactory brain centers: a) the lateral horn, a brain region that is thought to organize naïve olfactory behavior and b) the calyx region of the MB, comprised of MB intrinsic Kenyon Cells (KCs), neurons that are required for odor-taste learning [Ramaekers et al., 2005; Masuda-Nakagawa et al., 2009, 2010; Thum et al., 2011]. Recently these findings were

verified and completed by Berck and coworkers, who reconstructed the larval antennal lobe at synaptic resolution (connectome) using volume electron microscopy [Berck et al., 2016]. In total they identified 81 antennal lobe innervating neurons per hemisphere. In addition to the known canonical circuit consisting of 21 ORNs/ 21 uniglomerual PNs gain controlled via 5 GABAergic interneurons, they identified a second parallel circuit consisting of 14 multiglomerular PNs (mPNs) and hierarchically connected local neurons (LNs) that were only rudimentary described on light microscopy level [Thum et al., 2011]. Whether and how this second, parallel pathway participates in olfaction and odor-taste learning has to be analyzed.

7.4.2 Sub-circuit 2: Perception of taste

Sensory taste system

Drosophila larvae perceive taste stimuli via three external chemosensory organs positioned on the head and four internal organs located along the pharynx [Singh and Singh, 1984; Python and Stocker, 2002]. The seven sensory organs house about 81 gustatory receptor neurons (GRNs) and transfer taste information from the periphery to the subesophageal zone (SEZ) - the first-order taste center of the larval brain (Python and Stocker [2002]; Colomb et al. [2007]; Kwon et al. [2011]; Mishra et al. [2013]; Choi et al. [2016], reviewed in Apostolopoulou et al. [2015]). Whether these GRNs do signal ”taste-rewards” or ”taste-punishments” from the environment of the larvae is not entirely unraveled so far. For example, GRNs expressing bitter receptors Gr33a and Gr66a are necessary for the naïve avoidance of bitter substances like quinine, but they are not necessary for aversive odor-quinine learning [Apostolopoulou et al., 2014b]. On the contrary, this is not true for sensing bitter taste in general, as the same set of GRNs are necessary for aversive odor-taste learning reinforced by caffeine [Apostolopoulou et al., 2016]. The reception of caffeine triggering aversive reinforcement can even

be pinpointed to a single GRN of the dorsal pharyngeal organ [Apostolopoulou et al., 2016]. Nevertheless, additional mechanisms that are essential for the reception of taste dependent reinforcement must be considered especially as alternatives were recently proposed for adult *Drosophila* and honeybees [Ayestaran et al., 2010; Wright et al., 2010; Miyamoto et al., 2012; Dus et al., 2013; Gruber et al., 2013]. Furthermore, only little information is available about potential target neurons of larval taste afferents. Recent data suggests that neurons expressing the neuropeptide gene hugin signal bitter taste information to the protocerebrum and thereby regulate avoidance and feeding [Hückesfeld et al., 2016]. Also, octopaminergic (OA) interneurons receiving their input in the SEZ are suspects for distributing appetitive gustatory input as an internal reward signal [Honjo and Furukubo-Tokunaga, 2009; Selcho et al., 2014].

Taste reinforcement processing

In 1993, Hammer introduced a single OA VUM neuron as being essential in mediating sugar reward information within the honeybee brain [Hammer, 1993]. Ten years later Schwaerzel and coworkers showed in adult *Drosophila* that dopaminergic (DA) neurons mediate punishment information, while OA neurons mediate reward information [Schwaerzel et al., 2003]. More recently, it turned out that the suggested separation for OA (mediating reward) and DA (mediating punishment) does not pass intensive testing (reviewed in Waddell [2013]). For example, in larvae silencing a specific set of DA neurons conditionally during training abolished both aversive and appetitive odor-taste learning. This suggests that DA neurons mediate both, positive and negative reinforcer information [Selcho et al., 2009]. Interestingly, different DA receptors appear to allow reinforcer specificity, as a mutation in the dDA1 receptor affected both larval aversive and appetitive odor-taste learning, while a mutation in the DAMB receptor was specific for aversive odor-taste learning [Selcho et al., 2009]. In addition, recent work by Rohwedder and coworkers suggests that four neurons of the DA primary protocerebral anterior

medial (pPAM) cluster specifically mediate sugar reward information to the medial lobe of the MB [Rohwedder et al., 2016]. Consequently, DA mediates the relevant information for positive and negative reinforcers within the larval brain onto the MB. This mode of operations is conserved throughout development as it applies for adult *Drosophila* as well [Burke and Waddell, 2011].

So, what is the role of OA in *Drosophila* larval learning? With respect to odor-taste learning, the OA/TA circuitry turned out to be necessary mediating the sweetness of a sugar rather than the nutritional value, which is mediated by DA neurons [Selcho et al., 2014; Rohwedder et al., 2016]. Ablation of OA/TA neurons did not change odor-taste learning in larvae using fructose (both sweet and nutritious) or sorbitol (only nutritious) as rewarding stimuli. However, learning performance was impaired due to the ablation of OA/TA neurons using arabinose (only sweet) as a reinforcer [Selcho et al., 2014]. In line with recent results on adult *Drosophila* [Burke and Waddell, 2011; Ichinose et al., 2015; Musso et al., 2015; Huetteroth et al., 2015; Yamagata et al., 2015] it can therefore be concluded that only ”sweet” sugar information is processed by OA neurons upstream of the four DA pPAM neurons that in addition integrate the nutritional information of a sugar reward. The identity and detailed connectivity pattern of the potential signaling onto the pPAM cluster of these OA neurons remains elusive.

Modulation of taste dependent reinforcer information

Memory formation and retrieval is not only dependent on environmental stimuli, but also relies on the internal state of the animal. Conditional activation of neurons expressing dNPF (neuropeptide F, an ortholog of mammalian NPY) specifically during training reduced odor-fructose learning [Rohwedder et al., 2015]. In more detail, Rohwedder and colleagues suggest that artificial activation of dNPF neurons impairs sugar reward processing and by that the acquisition of memories. Interestingly, dNPF neurons seem

to be exclusively modulating appetitive memories as artificial activation of the same neurons did not alter aversive odor-taste memories, which appears reasonable as dNPF has a strong impact on feeding behavior in the larva [Wu et al., 2003, 2005]. Thus, it was hypothesized that dNPF neurons modulate odor-taste learning by targeting the sugar reward-signaling pathway, probably depending on the physiological state of the animal [Rohwedder et al., 2015]. In the end, the modulation of odor-taste learning appears important to match environmental information about food quality and quantity in relation to the current internal state of the animal. Under certain conditions this would allow the larva to ignore an actually irrelevant information of a tastant (good or bad), which typically comes along with stimuli such as sugar, salt or quinine.

7.4.3 Sub-circuit 3: Mushroom bodies

Mushroom bodies harbor a memory trace

Several findings suggest that the MBs harbor a memory trace for odor-taste learning in *Drosophila* larvae. Classical learning mutants like *dunce* and *rutabaga* are impaired in larval odor-taste learning [Honjo and Furukubo-Tokunaga, 2005; Widmann et al., 2016]. Gene products of both genes are enriched in MB KCs and serve as molecular substrates of cAMP signaling and by that for cellular plasticity in response to the coincidence detection of odor and taste stimuli [Crittenden et al., 1998]. Accordingly, blockage of synaptic output of MB KCs during odor-taste training and testing impaired learning and memory [Honjo and Furukubo-Tokunaga, 2005; Pauls et al., 2010b]. Even more, output of MB KCs was reported to be necessary only during test, but not during training [Honjo and Furukubo-Tokunaga, 2005]. In addition, MB function is also sufficient for appetitive odor-taste learning. Larvae of the rover allele of the foraging gene (encoding for a protein kinase G) showed lower initial scores for odor-taste learning than sitter larvae [Kaun et al., 2007]. The behavioral phenotype is based on a lower activity of the foraging gene

in sitter than in rover larvae and can be rescued from sitter to rover learning levels by boosting expression of the protein kinase G in the MB KCs [Kaun et al., 2007]. Although it is not clear if protein kinase G is directly related to synaptic plasticity, this is clearly the case for the synapsin (syn) gene product, a presynaptic vesicular phosphoprotein. syn mutants are impaired in odor-taste learning [Michels et al., 2011; Widmann et al., 2016]. Rescuing syn exclusively in MB KCs fully restored appetitive odor-taste learning [Michels et al., 2011]. Consequently: i) the larval MB provides a substrate for neuronal and cellular plasticity, ii) plasticity in the MB is necessary for odor-taste learning, iii) plasticity in the MB is sufficient for odor-taste learning, iv) acquisition of odor-taste memories is abolished if US signaling onto the MB KCs is impaired during training and v) odor-taste memories are abolished if the MB KCs cannot provide output during test. We therefore conclude that the MBs form a center for odor-taste learning and memory in the larval brain of *Drosophila*.

The mushroom body connectome

In 2003, Heisenberg introduced a minimal circuit model for odor memories in adult *Drosophila* [Heisenberg, 2003]. In the following, we will briefly introduce its concept and contrast the model with the results of the recently established larval MB connectome [Eichler et al., 2017]. The Heisenberg model assumes that odors are represented by the activation of a pattern of KCs. During training this representation occurs simultaneously with a modulatory reinforcement signal encoded by a DA (good or bad) or an OA (good) input neuron (MBIN), both MBINs connect to all KCs. Coincident activation of KCs in turn will strengthen the synaptic connectivity of KCs onto extrinsic MB output neurons (MBON). Thus, during conditioning, MBONs (that are initially latent) would come to act as odor-specific neurons that report the presence of a particular odor as an alerting signal for the conditioned behavior (Figure 1a).

The synaptic reconstruction of the larval MB ultrastructure confirms the minimal MBIN -

KC - MBON circuit model. First instar larvae have about 110 KCs per hemisphere that nearly all receive input from 7 DA neurons, 4 OA neurons, and 5 neurons of unknown neurotransmitter identity. At the same time, nearly all individual mature KCs synapse onto each of the 24 MBONs. Thus, the proposed MBIN - KC - MBON connectivity is confirmed by the larval MB connectome, it even includes distinct specifications for reward modulation at the medial lobe and punishment modulation at the vertical lobe [Schroll et al., 2006; Selcho et al., 2009; Rohwedder et al., 2016]. Yet, Eichler and coworkers also identified several remarkable additions to the proposed minimal circuit model (Figure 1b): i) there is not only a single bad and good MBIN - KC - MBON motif, rather several ones exist in parallel. The connectome reconstruction describes in total 16 motifs organized in 11 functional subunits. ii) KCs do not only connect to MBONs but also at the same time reconnect to MBINs. iii) MBINs do not only connect to KCs but also connect directly onto MBONs. iv) KCs can be divided in two subgroups: the first subgroup gets only input from a single PN, while the second subgroup collects information from multiple PNs. v) KCs are not isolated among each other as they synapse intensely onto each other. vi) Similarly, the 24 MBONs are neither separated, nor connect directly onto motor-circuits, they rather massively integrate the information of the parallel organized motifs by feed-forward excitation and inhibition [Eichler et al., 2017]. The function of these additional synaptic connections within the larval MB circuits is so far elusive. However, based on the complete anatomical description, one can now perform experiments in a targeted manner to inspect their potential function in the future. These functions may well expand beyond classical odor-taste learning.

7.4.4 Sub-circuit 4: Premotor circuits

The simple nervous system of the *Drosophila* larva is able to form associations between distinct stimuli. Moreover, it can generate many distinct motor patterns [Vogelstein

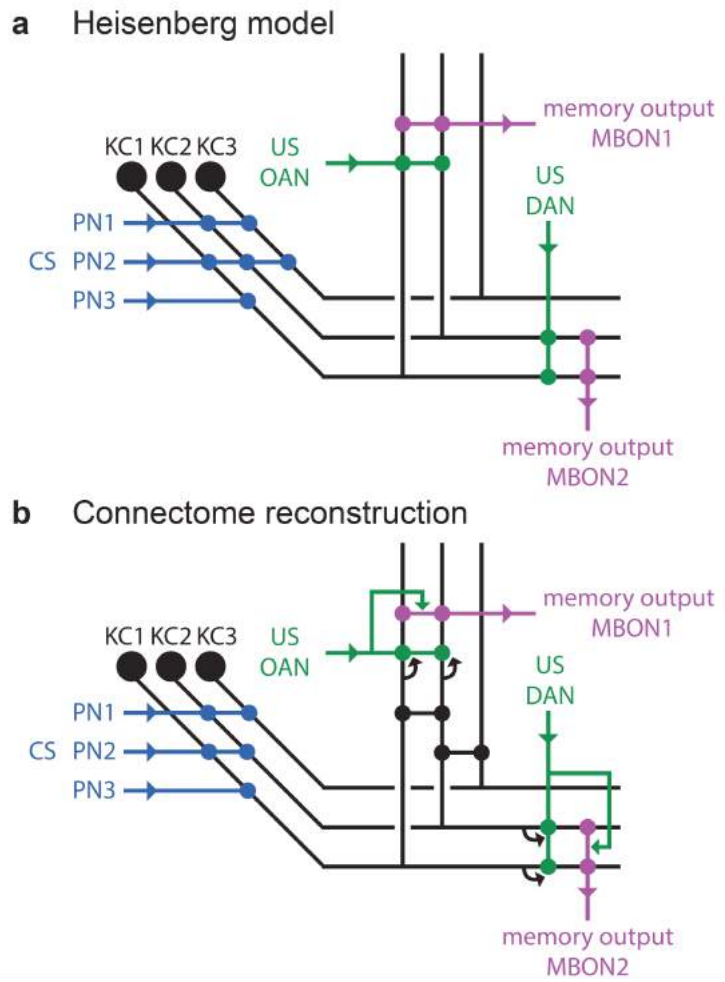

Figure 1: Comparison of the Heisenberg model and the connectome.
a In 2003, Heisenberg described that modulatory dopaminergic (DAN) and octopaminergic neurons (OAN) connect to the mushroom body (MB) Kenyon Cells (KCs) in order to signal reinforcer information, while KCs are activated by projection neurons (PNs) mediating odor information. In addition, MB KCs are connected to MB output neurons (MBONs) to elicit conditioned behavioral output in a kind of forward directed manner [Heisenberg, 2003].
b However, recent connectome data revealed two additional connections: KCs also synapse back onto DANs and OANs, while they directly connect to MBONs as well. Furthermore, KCs can be divided into two types: KCs that receive from multiple PNs (KC1 and KC2) and those that receive from only one PN (KC3). Strikingly, the study found that KCs synapse intensely onto each other [Eichler et al., 2017].

et al., 2014; Ohyama et al., 2015]. However, our current knowledge of the neuronal circuits downstream of the larval MB that activate appropriate motor patterns to drive conditional behavioral output is very limited. More work must be done to understand how the MBs connect with the motor circuits. Such approaches are now feasible given the considerable progress recently achieved for the larval motor systems. These findings include: i) the identification of muscles, motoneurons and sensory neurons, ii) the synaptic reconstruction (connectome), iii) the identification of command neurons and interneurons that coordinate and generate sequential motor patterns, iv) the description of multisensory circuits directly upstream of the motor circuit, and v) the identification of how these circuits select and maintain sensorimotor decisions [Couton et al., 2015;

Itakura et al., 2015; Ohyama et al., 2015; Jovanic et al., 2016; Zwart et al., 2016].

7.5 Odor-taste learning: The molecular network

Throughout the animal kingdom synaptic plasticity is essential for learning and memory and it is based on highly conserved molecular signaling pathways [Kandel, 2001; Dudai, 2004; Davis, 2005; Kandel et al., 2014]. Among many other important proteins and enzymes, odor-taste learning and memory in *Drosophila* larvae depends on the function of protein kinase A (PKA) and protein kinase C (PKC), which are involved in two highly conserved but different signaling pathways [Abel et al., 1997; Sacktor et al., 1987; Sossin et al., 1994; Atkins et al., 1998; Nguyen and Woo, 2003; Davis, 2005; Sacktor, 2008; Kandel et al., 2014; Widmann et al., 2016].

During odor-taste training larval MB KCs simultaneously receive an odor stimulus (CS: conditioned stimulus) via cholinergic PNs and reinforcer information (US: unconditioned stimulus) from DA neurons (and/or OA neurons; Gerber et al. [2009]; Selcho et al. [2009]; Honjo and Furukubo-Tokunaga [2009]; Selcho et al. [2014]). At the cellular level, binding of DA to its G-protein coupled receptor leads to a dissociation of the G-protein subunit from the corresponding G-protein coupled receptors (reviewed in Neve et al. [2004]). At the same time, the odor stimulus is perceived via acetylcholine receptors. Its activation leads to an opening of a voltage-dependent calcium channel and influx of Ca^{2+} (Figure 2). This mechanism is thought to be common in both the PKA and PKC signaling pathways [Widmann et al., 2016].

For the PKA pathway it is assumed that coincident KC stimulation by the CS and US pathways leads to an activation of type I adenylyl cyclase (AC; encoded by *rutabaga*) via Ca^{2+}/Calmodulin and DA dependent G-protein ($G_{\alpha}s$) signaling, respectively [Livingstone et al., 1984; Levin et al., 1992]. Active ACs increase intracellular cyclic adenosine

3'5'-monophosphate (cAMP) levels, which are negatively regulated through phosphodiesterases (encoded by *dunce*; Dudai et al. [1976]; Byers et al. [1981]; Chen et al. [1986]). cAMP serves as a regulatory signal for PKA [Taylor et al., 1990; Gervasi et al., 2010], which phosphorylates different substrates like potassium channels, the presynaptic vesicular phosphoprotein Syn or cAMP response element binding proteins (CREB) to induce cellular or synaptic plasticity [Yin et al., 1994; Godenschwege et al., 2004; Perazzona et al., 2004; Akbergenova and Bykhovskaia, 2007, 2010; Michels et al., 2011].

In contrast, only limited knowledge is available to what extent PKC signaling is involved in learning and memory dependent synaptic plasticity. Widmann and coworkers hypothesized that DA receptors coupled to $G_{\alpha}q$ regulate phospholipase C (PLC; Reale et al. [1997]; Beggs et al. [2011]; Widmann et al. [2016]). Activation of PLC increases intracellular inositol triphosphate (IP3) and diacylglycerol (DAG) levels. Whereas IP3 stimulates the release of Ca^{2+} from the endoplasmic reticulum, DAG is a physiological activator of PKC [Reale et al., 1997; Beggs et al., 2011]. Further, PKC is linked with Radish (Rsh) and potentially Bruchpilot (Brp) as direct or indirect downstream partners [Folkers et al., 2006]. This is so far hypothetical. Yet, a structural analysis on Rsh reported that it has several PKC phosphorylation sites [Folkers et al., 2006]. Ultimately, regulation of Brp via PKC signaling would change the organization of the active zone to provide a molecular substrate for presynaptic plasticity.

There is convincing data from different labs that both pathways are established for larval associative olfactory learning and memory, even when varying different parameters of the learning paradigms [Honjo and Furukubo-Tokunaga, 2005, 2009; Khurana et al., 2009; Widmann et al., 2016]. It seems that in most cases the PKA signaling pathway encodes for a short-lasting memory component (that may lead under certain circumstance to long term memory), whereas PKC signaling is essential to establish an anesthesia

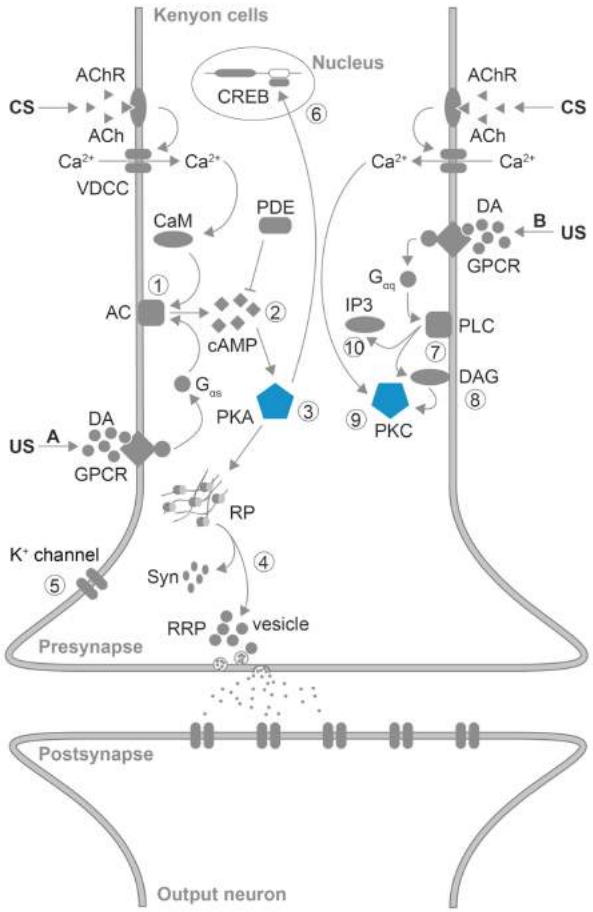

Figure 2: Proposed molecular network of learning and memory in *Drosophila* larvae.
Odor-taste learning and memory in *Drosophila* larvae involves at least the activity of two different protein kinases. Both protein kinases are parts of two different but conserved signaling pathways **(A,B)**. After classical olfactory conditioning MB KCs receive an olfactory stimulus (CS: conditioned stimulus) via cholinergic projection neurons, which is perceived through acetylcholine receptors (AChR). The activation of these receptors leads to an opening of voltage-dependent calcium channels (VDCC) and a subsequent influx of Ca^{2+}. The information of the reinforcer is mediated via dopaminergic neurons and the binding of dopamine (DA) to G-protein coupled receptors (GPCR) leads to the dissociation of G-protein subunits from their corresponding GPCRs. This mechanism seems to be shared between both pathways. In the classical pathway (1-6) coincidence stimulation of GPCRs and AChRs leads to an activation of type I adenylyl cyclase (AC) via Ca^{2+}/Calmodulin (CaM) and the G-protein subunit $G_{\alpha}s$, respectively (1). As a consequence an increase in intracellular cyclic adenosine 3'5'-monophosphate (cAMP) is ascertainable, which is negatively regulated through a phosphodiesterase (PDE) (2). cAMP serves as a regulatory signal for protein kinase A (PKA) (3), which phosphorylates different downstream targets (4-6) like potassium channels (4), the presynaptic vesicular phosphoprotein Synapsin (Syn) (5) or cAMP response element binding protein (6). In the alternative pathway (7-10) GPCR are coupled to another G-protein, $G_{\alpha}s$. The dissociation of this subunit leads to the activation of phospholipase C (PLC) (7), which increases the intracellular concentration of inositol triphosphate (IP3) (10) and diacylglycerol (DAG) (8). Simultaneous activation of VDCC leads to an increase in intracellular Ca^{2+}, which is strengthen through the release of Ca^{2+} from the endoplasmatic reticulum via IP3. Both, Ca^{2+} and DAG are physiological activator of protein kinase C (9). However, identifications of further downstream targets of PKC are far from resolved. ACh: Acetylcholin, RP: reserve pool, RPP: readily releasable pool.

resistant memory component [Honjo and Furukubo-Tokunaga, 2005, 2009; Khurana et al., 2009; Widmann et al., 2016]. Whether this dichotomy is indeed a general principle of associative olfactory learning requires further research.

7.6 Outlook

In the last decade, research on odor-taste learning and memory in *Drosophila* larvae was intensified on the behavioral, neuronal and molecular level. Based on the various examples discussed in this review, it is obvious that the larva is a useful and powerful system to address diverse questions in neuroscience quickly and precisely. Therefore,

the development of the ”model organism *Drosophila* larva” to unravel fundamental questions in neuroscience, such as the ones focusing on learning and memory, but also on brain science in more general terms, appears to be accelerating. The efforts made to reconstruct the entire connectome [Heckscher et al., 2015; Ohyama et al., 2015; Berck et al., 2016; Fushiki et al., 2016; Jovanic et al., 2016; Schlegel et al., 2016; Schneider-Mizell et al., 2016; Zwart et al., 2016], to analyze the function of identified cells due to specific Gal4 lines [Li et al., 2014], new molecular techniques such as single cell RNA sequencing [Nagoshi et al., 2010], CRISPR/Cas9 genome editing [Bassett et al., 2013; Gratz et al., 2013] or microfluidics based calcium imaging [van Giesen et al., 2016], and to improve behavioral approaches by automated, high resolution tracking systems [Ohyama et al., 2013; Risse et al., 2013; Schleyer et al., 2015b], will further improve our understanding on how the larval brain organizes behavior in general and learning and memory in particular.

7.7 Acknowledgements

This work was funded by the DFG grants [TH1584/1-1, TH1584/3-1], the Zukunftskolleg of the University of Konstanz and the Elite Program of the Baden-Württemberg Stiftung [all to AST].

7.8 References

Abel, T., Nguyen, P. V., Barad, M., Deuel, T. A., Kandel, E. R., and Bourtchouladze, R. (1997). Genetic demonstration of a role for pka in the late phase of ltp and in hippocampus-based long-term memory. *Cell*, 88(5):615–626.

Aceves-Piña, E. O. and Quinn, W. G. (1979). Learning in normal and mutant drosophila larvae. *Science*, 206(4414):93–96.

Akbergenova, Y. and Bykhovskaia, M. (2007). Synapsin maintains the reserve vesicle pool and spatial segregation of the recycling pool in drosophila presynaptic boutons. *Brain research*, 1178:52–64.

Akbergenova, Y. and Bykhovskaia, M. (2010). Synapsin regulates vesicle organization and activity-dependent recycling at drosophila motor boutons. *Neuroscience*, 170(2):441–452.

Apostolopoulou, A. A., Hersperger, F., Mazija, L., Widmann, A., Wüst, A., and Thum, A. S. (2014a). Composition of agarose substrate affects behavioral output of drosophila larvae. *Frontiers in behavioral neuroscience*, 8:11.

Apostolopoulou, A. A., Köhn, S., Stehle, B., Lutz, M., Wüst, A., Mazija, L., Rist, A., Galizia, C. G., Lüdke, A., and Thum, A. S. (2016). Caffeine taste signaling in drosophila larvae. *Frontiers in Cellular Neuroscience*, 10.

Apostolopoulou, A. A., Mazija, L., Wüst, A., and Thum, A. S. (2014b). The neuronal and molecular basis of quinine-dependent bitter taste signaling in drosophila larvae. *Frontiers in behavioral neuroscience*, 8:6.

Apostolopoulou, A. A., Rist, A., and Thum, A. S. (2015). Taste processing in drosophila larvae. *Frontiers in integrative neuroscience*, 9:50.

Apostolopoulou, A. A., Widmann, A., Rohwedder, A., Pfitzenmaier, J. E., and Thum, A. S. (2013). Appetitive associative olfactory learning in drosophila larvae. *JoVE (Journal of Visualized Experiments)*, (72):e4334–e4334.

Atkins, C. M., Selcher, J. C., Petraitis, J. J., Trzaskos, J. M., and Sweatt, J. D. (1998). The mapk cascade is required for mammalian associative learning. *Nature neuroscience*, 1(7):602–609.

Ayestaran, A., Giurfa, M., and de Brito Sanchez, M. G. (2010). Toxic but drank: gustatory aversive compounds induce post-ingestional malaise in harnessed honeybees. *PLoS One*, 5(10):e15000.

Bassett, A. R., Tibbit, C., Ponting, C. P., and Liu, J.-L. (2013). Highly efficient targeted mutagenesis of drosophila with the crispr/cas9 system. *Cell reports*, 4(1):220–228.

Beggs, K. T., Tyndall, J. D., and Mercer, A. R. (2011). Honey bee dopamine and octopamine receptors linked to intracellular calcium signaling have a close phylogenetic and pharmacological relationship. *PLoS One*, 6(11):e26809.

Berck, M. E., Khandelwal, A., Claus, L., Hernandez-Nunez, L., Si, G., Tabone, C. J., Li, F., Truman, J. W., Fetter, R. D., Louis, M., et al. (2016). The wiring diagram of a glomerular olfactory system. *Elife*, 5:e14859.

Brand, A. H. and Perrimon, N. (1993). Targeted gene expression as a means of altering cell fates and generating dominant phenotypes. *development*, 118(2):401–415.

Burke, C. J. and Waddell, S. (2011). Remembering nutrient quality of sugar in drosophila. *Current Biology*, 21(9):746–750.

Busto, G. U., Cervantes-Sandoval, I., and Davis, R. L. (2010). Olfactory learning in drosophila. *Physiology*, 25(6):338–346.

Byers, D., Davis, R. L., and Kiger, J. A. (1981). Defect in cyclic amp phosphodiesterase due to the dunce mutation of learning in drosophila melanogaster.

Chen, C.-N., Denome, S., and Davis, R. L. (1986). Molecular analysis of cdna clones and the corresponding genomic coding sequences of the drosophila dunce+ gene, the structural gene for camp phosphodiesterase. *Proceedings of the National Academy of Sciences*, 83(24):9313–9317.

Choi, J., van Giesen, L., Choi, M. S., Kang, K., Sprecher, S. G., and Kwon, J. Y. (2016). A pair of pharyngeal gustatory receptor neurons regulates caffeine-dependent ingestion in drosophila larvae. *Frontiers in Cellular Neuroscience*, 10.

Colomb, J., Grillenzoni, N., Ramaekers, A., and Stocker, R. F. (2007). Architecture of the primary taste center of drosophila melanogaster larvae. *Journal of Comparative Neurology*, 502(5):834–847.

Couton, L., Mauss, A. S., Yunusov, T., Diegelmann, S., Evers, J. F., and Landgraf, M. (2015). Development of connectivity in a motoneuronal network in drosophila larvae. *Current Biology*, 25(5):568–576.

Crittenden, J. R., Skoulakis, E. M., Han, K.-A., Kalderon, D., and Davis, R. L. (1998). Tripartite mushroom body architecture revealed by antigenic markers. *Learning & Memory*, 5(1):38–51.

Davis, R. L. (2005). Olfactory memory formation in drosophila: from molecular to systems neuroscience. *Annu. Rev. Neurosci.*, 28:275–302.

Dudai, Y. (2004). The neurobiology of consolidations, or, how stable is the engram? *Annu. Rev. Psychol.*, 55:51–86.

Dudai, Y., Jan, Y.-N., Byers, D., Quinn, W. G., and Benzer, S. (1976). dunce, a mutant of drosophila deficient in learning. *Proceedings of the National Academy of Sciences*, 73(5):1684–1688.

Duffy, J. B. (2002). Gal4 system in drosophila: a fly geneticist's swiss army knife. *genesis*, 34(1-2):1–15.

Dumstrei, K., Wang, F., Nassif, C., and Hartenstein, V. (2003). Early development of the drosophila brain: V. pattern of postembryonic neuronal lineages expressing de-cadherin. *Journal of Comparative Neurology*, 455(4):451–462.

Dus, M., Ai, M., and Suh, G. S. (2013). Taste-independent nutrient selection is mediated by a brain-specific na+/solute cotransporter in drosophila. *Nature neuroscience*, 16(5):526–528.

Eichler, K., Li, F., Litwin-Kumar, A., Park, Y., Andrade, I., Schneider-Mizell, C. M., Saumweber, T., Huser, A., Eschbach, C., Gerber, B., Fetter, R. D., Truman, J. W., Priebe, C., Abbott, L. F., Thum, A., Zlatic, M., and Cardona, A. (2017). The complete connectome of the mushroom body of a drosophila larva. *Nature*, In press.

El-Keredy, A., Schleyer, M., König, C., Ekim, A., and Gerber, B. (2012). Behavioural analyses of quinine processing in choice, feeding and learning of larval drosophila. *PloS one*, 7(7):e40525.

Elliott, D. A. and Brand, A. H. (2008). The gal4 system: a versatile system for the expression of genes. *Drosophila: Methods and Protocols*, pages 79–95.

Eschbach, C., Cano, C., Haberkern, H., Schraut, K., Guan, C., Triphan, T., and Gerber, B. (2011). Associative learning between odorants and mechanosensory punishment in larval drosophila. *Journal of Experimental Biology*, 214(23):3897–3905.

Fishilevich, E., Domingos, A. I., Asahina, K., Naef, F., Vosshall, L. B., and Louis, M. (2005). Chemotaxis behavior mediated by single larval olfactory neurons in drosophila. *Current Biology*, 15(23):2086–2096.

Folkers, E., Waddell, S., and Quinn, W. G. (2006). The drosophila radish gene encodes a protein required for anesthesia-resistant memory. *Proceedings of the National Academy of Sciences*, 103(46):17496–17500.

Fushiki, A., Zwart, M. F., Kohsaka, H., Fetter, R. D., Cardona, A., and Nose, A. (2016). A circuit mechanism for the propagation of waves of muscle contraction in drosophila. *Elife*, 5:e13253.

Gerber, B. and Hendel, T. (2006). Outcome expectations drive learned behaviour in larval drosophila. *Proceedings of the Royal Society of London B: Biological Sciences*, 273(1604):2965–2968.

Gerber, B., Scherer, S., Neuser, K., Michels, B., Hendel, T., Stocker, R. F., and Heisenberg, M. (2004). Visual learning in individually assayed drosophila larvae. *Journal of Experimental Biology*, 207(1):179–188.

Gerber, B., Stocker, R. F., Tanimura, T., and Thum, A. S. (2009). Smelling, tasting, learning: Drosophila as a study case. In *Chemosensory Systems in Mammals, Fishes, and Insects*, pages 187–202. Springer.

Gervasi, N., Tchénio, P., and Preat, T. (2010). Pka dynamics in a drosophila learning center: coincidence detection by rutabaga adenylyl cyclase and spatial regulation by dunce phosphodiesterase. *Neuron*, 65(4):516–529.

Godenschwege, T. A., Reisch, D., Diegelmann, S., Eberle, K., Funk, N., Heisenberg, M., Hoppe, V., Hoppe, J., Klagges, B. R., Martin, J.-R., et al. (2004). Flies lacking all synapsins are unexpectedly healthy but are impaired in complex behaviour. *European Journal of Neuroscience*, 20(3):611–622.

Gratz, S. J., Cummings, A. M., Nguyen, J. N., Hamm, D. C., Donohue, L. K., Harrison, M. M., Wildonger, J., and O'Connor-Giles, K. M. (2013). Genome engineering of drosophila with the crispr rna-guided cas9 nuclease. *Genetics*, 194(4):1029–1035.

Gruber, F., Knapek, S., Fujita, M., Matsuo, K., Bräcker, L., Shinzato, N., Siwanowicz, I., Tanimura, T., and Tanimoto, H. (2013). Suppression of conditioned odor approach by feeding is independent of taste and nutritional value in drosophila. *Current Biology*, 23(6):507–514.

Hammer, M. (1993). An identified neuron mediates the unconditioned stimulus in associative olfactory learning in honeybees.–p. 59-63. Technical Report 6450, En: Nature (London)(United Kingdom).

Heckscher, E. S., Zarin, A. A., Faumont, S., Clark, M. Q., Manning, L., Fushiki, A., Schneider-Mizell, C. M., Fetter, R. D., Truman, J. W., Zwart, M. F., et al. (2015). Even-skipped+ interneurons are core components of a sensorimotor circuit that maintains left-right symmetric muscle contraction amplitude. *Neuron*, 88(2):314–329.

Heisenberg, M. (2003). Mushroom body memoir: from maps to models. *Nature Reviews Neuroscience*, 4(4):266–275.

Heisenberg, M., Borst, A., Wagner, S., and Byers, D. (1985). Drosophila mushroom body mutants are deficient in olfactory learning: Research papers. *Journal of neurogenetics*, 2(1):1–30.

Honjo, K. and Furukubo-Tokunaga, K. (2005). Induction of camp response element-binding protein-dependent medium-term memory by appetitive gustatory reinforcement in drosophila larvae. *Journal of Neuroscience*, 25(35):7905–7913.

Honjo, K. and Furukubo-Tokunaga, K. (2009). Distinctive neuronal networks and biochemical pathways for appetitive and aversive memory in drosophila larvae. *Journal of Neuroscience*, 29(3):852–862.

Hückesfeld, S., Peters, M., and Pankratz, M. J. (2016). Central relay of bitter taste to the protocerebrum by peptidergic interneurons in the drosophila brain. *Nature Communications*, 7:12796.

Huetteroth, W., Perisse, E., Lin, S., Klappenbach, M., Burke, C., and Waddell, S. (2015). Sweet taste and nutrient value subdivide rewarding dopaminergic neurons in drosophila. *Current biology*, 25(6):751–758.

Ichinose, T., Aso, Y., Yamagata, N., Abe, A., Rubin, G. M., and Tanimoto, H. (2015). Reward signal in a recurrent circuit drives appetitive long-term memory formation. *Elife*, 4:e10719.

Itakura, Y., Kohsaka, H., Ohyama, T., Zlatic, M., Pulver, S. R., and Nose, A. (2015). Identification of inhibitory premotor interneurons activated at a late phase in a motor cycle during drosophila larval locomotion. *PloS one*, 10(9):e0136660.

Jenett, A., Rubin, G. M., Ngo, T.-T., Shepherd, D., Murphy, C., Dionne, H., Pfeiffer, B. D., Cavallaro, A., Hall, D., Jeter, J., et al. (2012). A gal4-driver line resource for drosophila neurobiology. *Cell reports*, 2(4):991–1001.

Jovanic, T., Schneider-Mizell, C. M., Shao, M., Masson, J.-B., Denisov, G., Fetter, R. D., Mensh, B. D., Truman, J. W., Cardona, A., and Zlatic, M. (2016). Competitive disinhibition mediates behavioral choice and sequences in drosophila. *Cell*, 167(3):858–870.

Kandel, E. R. (2001). The molecular biology of memory storage: a dialog between genes and synapses. *Bioscience reports*, 21(5):565–611.

Kandel, E. R., Dudai, Y., and Mayford, M. R. (2014). The molecular and systems biology of memory. *Cell*, 157(1):163–186.

Kane, E. A., Gershow, M., Afonso, B., Larderet, I., Klein, M., Carter, A. R., De Bivort, B. L., Sprecher, S. G., and Samuel, A. D. (2013). Sensorimotor structure of drosophila larva phototaxis. *Proceedings of the National Academy of Sciences*, 110(40):E3868–E3877.

Kaun, K. R., Hendel, T., Gerber, B., and Sokolowski, M. B. (2007). Natural variation in drosophila larval reward learning and memory due to a cgmp-dependent protein kinase. *Learning & Memory*, 14(5):342–349.

Keene, A. C. and Waddell, S. (2007). Drosophila olfactory memory: single genes to complex neural circuits. *Nature Reviews Neuroscience*, 8(5):341–354.

Khurana, S., Abubaker, M. B., and Siddiqi, O. (2009). Odour avoidance learning in the larva of drosophila melanogaster. *Journal of biosciences*, 34(4):621–631.

Khurana, S., Robinson, B. G., Wang, Z., Shropshire, W. C., Zhong, A. C., Garcia, L. E., Corpuz, J., Chow, J., Hatch, M. M., Precise, E. F., et al. (2012). Olfactory conditioning in the third instar larvae of drosophila melanogaster using heat shock reinforcement. *Behavior genetics*, 42(1):151–161.

König, C., Schleyer, M., Leibiger, J., El-Keredy, A., and Gerber, B. (2015). Bitter–sweet processing in larval drosophila. *Chemical senses*, 40(6):445–445.

Kreher, S. A., Kwon, J. Y., and Carlson, J. R. (2005). The molecular basis of odor coding in the drosophila larva. *Neuron*, 46(3):445–456.

Kwon, J. Y., Dahanukar, A., Weiss, L. A., and Carlson, J. R. (2011). Molecular and cellular organization of the taste system in the drosophila larva. *Journal of Neuroscience*, 31(43):15300–15309.

Lai, S.-L. and Lee, T. (2006). Genetic mosaic with dual binary transcriptional systems in drosophila. *Nature neuroscience*, 9(5):703–709.

Levin, L. R., Han, P.-L., Hwang, P. M., Feinstein, P. G., Davis, R. L., and Reed, R. R. (1992). The drosophila learning and memory gene rutabaga encodes a ca2+ calmodulin-responsive adenylyl cyclase. *Cell*, 68(3):479–489.

Li, H.-H., Kroll, J. R., Lennox, S. M., Ogundeyi, O., Jeter, J., Depasquale, G., and Truman, J. W. (2014). A gal4 driver resource for developmental and behavioral studies on the larval cns of drosophila. *Cell Reports*, 8(3):897–908.

Livingstone, M. S., Sziber, P. P., and Quinn, W. G. (1984). Loss of calcium/calmodulin responsiveness in adenylate cyclase of rutabaga, a drosophila learning mutant. *Cell*, 37(1):205–215.

Luo, L., Gershow, M., Rosenzweig, M., Kang, K., Fang-Yen, C., Garrity, P. A., and Samuel, A. D. (2010). Navigational decision making in drosophila thermotaxis. *Journal of Neuroscience*, 30(12):4261–4272.

Masuda-Nakagawa, L. M., Awasaki, T., Ito, K., and O'Kane, C. J. (2010). Targeting expression to projection neurons that innervate specific mushroom body calyx and antennal lobe glomeruli in larval drosophila. *Gene Expression Patterns*, 10(7):328–337.

Masuda-Nakagawa, L. M., Gendre, N., O'Kane, C. J., and Stocker, R. F. (2009). Localized olfactory representation in mushroom bodies of drosophila larvae. *Proceedings of the National Academy of Sciences*, 106(25):10314–10319.

McGuire, S. E., Deshazer, M., and Davis, R. L. (2005). Thirty years of olfactory learning and memory research in drosophila melanogaster. *Progress in neurobiology*, 76(5):328–347.

Meunier, N., Marion-Poll, F., Rospars, J.-P., and Tanimura, T. (2003). Peripheral coding of bitter taste in drosophila. *Journal of neurobiology*, 56(2):139–152.

Michels, B., Chen, Y.-c., Saumweber, T., Mishra, D., Tanimoto, H., Schmid, B., Engmann, O., and Gerber, B. (2011). Cellular site and molecular mode of synapsin action in associative learning. *Learning & Memory*, 18(5):332–344.

Mishra, D., Miyamoto, T., Rezenom, Y. H., Broussard, A., Yavuz, A., Slone, J., Russell, D. H., and Amrein, H. (2013). The molecular basis of sugar sensing in drosophila larvae. *Current Biology*, 23(15):1466–1471.

Miyamoto, T., Slone, J., Song, X., and Amrein, H. (2012). A fructose receptor functions as a nutrient sensor in the drosophila brain. *Cell*, 151(5):1113–1125.

Moon, S. J., Köttgen, M., Jiao, Y., Xu, H., and Montell, C. (2006). A taste receptor required for the caffeine response in vivo. *Current biology*, 16(18):1812–1817.

Musso, P.-Y., Tchenio, P., and Preat, T. (2015). Delayed dopamine signaling of energy level builds appetitive long-term memory in drosophila. *Cell reports*, 10(7):1023–1031.

Nagoshi, E., Sugino, K., Kula, E., Okazaki, E., Tachibana, T., Nelson, S., and Rosbash, M. (2010). Dissecting differential gene expression within the circadian neuronal circuit of drosophila. *Nature neuroscience*, 13(1):60–68.

Neuser, K., Husse, J., Stock, P., and Gerber, B. (2005). Appetitive olfactory learning in drosophila larvae: effects of repetition, reward strength, age, gender, assay type and memory span. *Animal behaviour*, 69(4):891–898.

Neve, K. A., Seamans, J. K., and Trantham-Davidson, H. (2004). Dopamine receptor signaling. *Journal of receptors and signal transduction*, 24(3):165–205.

Nguyen, P. and Woo, N. (2003). Regulation of hippocampal synaptic plasticity by cyclic amp-dependent protein kinases. *Progress in neurobiology*, 71(6):401–437.

Niewalda, T., Singhal, N., Fiala, A., Saumweber, T., Wegener, S., and Gerber, B. (2008). Salt processing in larval drosophila: choice, feeding, and learning shift from appetitive to aversive in a concentration-dependent way. *Chemical senses*, 33(8):685–692.

Ohyama, T., Jovanic, T., Denisov, G., Dang, T. C., Hoffmann, D., Kerr, R. A., and Zlatic, M. (2013). High-throughput analysis of stimulus-evoked behaviors in drosophila larva reveals multiple modality-specific escape strategies. *PLoS One*, 8(8):e71706.

Ohyama, T., Schneider-Mizell, C. M., Fetter, R. D., Aleman, J. V., Franconville, R., Rivera-Alba, M., Mensh, B. D., Branson, K. M., Simpson, J. H., Truman, J. W., et al. (2015). A multilevel multimodal circuit enhances action selection in drosophila. *Nature*, 520(7549):633–639.

Oppliger, F. Y., Guerin, P. M., and Vlimant, M. (2000). Neurophysiological and behavioural evidence for an olfactory function for

the dorsal organ and a gustatory one for the terminal organ in drosophila melanogaster larvae. *Journal of Insect Physiology*, 46(2):135–144.

Owald, D. and Waddell, S. (2015). Olfactory learning skews mushroom body output pathways to steer behavioral choice in drosophila. *Current opinion in neurobiology*, 35:178–184.

Pauls, D., Pfitzenmaier, J. E., Krebs-Wheaton, R., Selcho, M., Stocker, R. F., and Thum, A. S. (2010a). Electric shock-induced associative olfactory learning in drosophila larvae. *Chemical senses*, 35(4):335–346.

Pauls, D., Selcho, M., Gendre, N., Stocker, R. F., and Thum, A. S. (2010b). Drosophila larvae establish appetitive olfactory memories via mushroom body neurons of embryonic origin. *Journal of Neuroscience*, 30(32):10655–10666.

Pauls, D., von Essen, A., Lyutova, R., van Giesen, L., Rosner, R., Wegener, C., and Sprecher, S. G. (2015). Potency of transgenic effectors for neurogenetic manipulation in drosophila larvae. *Genetics*, 199(1):25–37.

Perazzona, B., Isabel, G., Preat, T., and Davis, R. L. (2004). The role of camp response element-binding protein in drosophila long-term memory. *Journal of Neuroscience*, 24(40):8823–8828.

Pfeiffer, B. D., Ngo, T.-T. B., Hibbard, K. L., Murphy, C., Jenett, A., Truman, J. W., and Rubin, G. M. (2010). Refinement of tools for targeted gene expression in drosophila. *Genetics*, 186(2):735–755.

Potter, C. J. and Luo, L. (2011). Using the q system in drosophila melanogaster. *nature protocols*, 6(8):1105–1120.

Python, F. and Stocker, R. F. (2002). Adult-like complexity of the larval antennal lobe of d. melanogaster despite markedly low numbers of odorant receptor neurons. *Journal of Comparative Neurology*, 445(4):374–387.

Quinn, W. G., Harris, W. A., and Benzer, S. (1974). Conditioned behavior in drosophila melanogaster. *Proceedings of the National Academy of Sciences*, 71(3):708–712.

Ramaekers, A., Magnenat, E., Marin, E. C., Gendre, N., Jefferis, G. S., Luo, L., and Stocker, R. F. (2005). Glomerular maps without cellular redundancy at successive levels of the drosophila larval olfactory circuit. *Current biology*, 15(11):982–992.

Reale, V., Hannan, F., Hall, L. M., and Evans, P. D. (1997). Agonist-specific coupling of a cloned drosophila melanogaster d1-like dopamine receptor to multiple second messenger pathways by synthetic agonists. *Journal of Neuroscience*, 17(17):6545–6553.

Risse, B., Thomas, S., Otto, N., Löpmeier, T., Valkov, D., Jiang, X., and Klämbt, C. (2013). Fim, a novel ftir-based imaging method for high throughput locomotion analysis. *PloS one*, 8(1):e53963.

Rohwedder, A., Pfitzenmaier, J. E., Ramsperger, N., Apostolopoulou, A. A., Widmann, A., and Thum, A. S. (2012). Nutritional value–dependent and nutritional value–independent effects on drosophila melanogaster larval behavior. *Chemical senses*.

Rohwedder, A., Selcho, M., Chassot, B., and Thum, A. S. (2015). Neuropeptide f neurons modulate sugar reward during associative olfactory learning of drosophila larvae. *Journal of Comparative Neurology*, 523(18):2637–2664.

Rohwedder, A., Wenz, N. L., Stehle, B., Huser, A., Yamagata, N., Zlatic, M., Truman, J. W., Tanimoto, H., Saumweber, T., Gerber, B., et al. (2016). Four individually identified paired dopamine neurons signal reward in larval drosophila. *Current Biology*, 26(5):661–669.

Russell, C., Wessnitzer, J., Young, J. M., Armstrong, J. D., and Webb, B. (2011). Dietary salt levels affect salt preference and learning in larval drosophila. *PloS one*, 6(6):e20100.

Sacktor, T., Kruger, K., and Schwartz, J. (1987). Activation of protein kinase c by serotonin: biochemical evidence that it participates in the mechanisms underlying facilitation in aplysia. *Journal de physiologie*, 83(3):224–231.

Sacktor, T. C. (2008). Pkmζ, ltp maintenance, and the dynamic molecular biology of memory storage. *Progress in brain research*, 169:27–40.

Saumweber, T., Husse, J., and Gerber, B. (2011). Innate attractiveness and associative learnability of odors can be dissociated in larval drosophila. *Chemical senses*, 36(3):223–235.

Scherer, S., Stocker, R. F., and Gerber, B. (2003). Olfactory learning in individually assayed drosophila larvae. *Learning & Memory*, 10(3):217–225.

Schipanski, A., Yarali, A., Niewalda, T., and Gerber, B. (2008). Behavioral analyses of sugar processing in choice, feeding, and learning in larval drosophila. *Chemical senses*, 33(6):563–573.

Schlegel, P., Texada, M. J., Miroschnikow, A., Schoofs, A., Hückesfeld, S., Peters, M., Schneider-Mizell, C. M., Lacin, H., Li, F., Fetter, R. D., et al. (2016). Synaptic transmission parallels neuromodulation in a central food-intake circuit. *eLife*, 5:e16799.

Schleyer, M., Miura, D., Tanimura, T., and Gerber, B. (2015a). Learning the specific quality of taste reinforcement in larval drosophila. *Elife*, 4:e04711.

Schleyer, M., Reid, S. F., Pamir, E., Saumweber, T., Paisios, E., Davies, A., Gerber, B., and Louis, M. (2015b). The impact of odor–reward memory on chemotaxis in larval drosophila. *Learning & Memory*, 22(5):267–277.

Schleyer, M., Saumweber, T., Nahrendorf, W., Fischer, B., von Alpen, D., Pauls, D., Thum, A., and Gerber, B. (2011). A behavior-based circuit model of how outcome expectations organize learned behavior in larval drosophila. *Learning & Memory*, 18(10):639–653.

Schneider-Mizell, C. M., Gerhard, S., Longair, M., Kazimiers, T., Li, F., Zwart, M. F., Champion, A., Midgley, F. M., Fetter, R. D., Saalfeld, S., et al. (2016). Quantitative neuroanatomy for connectomics in drosophila. *Elife*, 5:e12059.

Schroll, C., Riemensperger, T., Bucher, D., Ehmer, J., Völler, T., Erbguth, K., Gerber, B., Hendel, T., Nagel, G., Buchner, E., et al. (2006). Light-induced activation of distinct modulatory neurons triggers appetitive or aversive learning in drosophila larvae. *Current biology*, 16(17):1741–1747.

Schwaerzel, M., Monastirioti, M., Scholz, H., Friggi-Grelin, F., Birman, S., and Heisenberg, M. (2003). Dopamine and octopamine differentiate between aversive and appetitive olfactory memories in drosophila. *Journal of Neuroscience*, 23(33):10495–10502.

Selcho, M., Pauls, D., Han, K.-A., Stocker, R. F., and Thum, A. S. (2009). The role of dopamine in drosophila larval classical olfactory conditioning. *PLoS One*, 4(6):e5897.

Selcho, M., Pauls, D., Huser, A., Stocker, R. F., and Thum, A. S. (2014). Characterization of the octopaminergic and tyraminergic neurons in the central brain of drosophila larvae. *Journal of Comparative Neurology*, 522(15):3485–3500.

Singh, R. N. and Singh, K. (1984). Fine structure of the sensory organs of drosophila melanogaster meigen larva (diptera: Drosophilidae). *International Journal of Insect Morphology and Embryology*, 13(4):255–273.

Sossin, W., Sacktor, T., and Schwartz, J. (1994). Persistent activation of protein kinase c during the development of long-term facilitation in aplysia. *Learning & Memory*, 1(3):189–202.

Taylor, S. S., Buechler, J. A., and Yonemoto, W. (1990). camp-dependent protein kinase: framework for a diverse family of regulatory enzymes. *Annual review of biochemistry*, 59(1):971–1005.

Thum, A. S., Leisibach, B., Gendre, N., Selcho, M., and Stocker, R. F. (2011). Diversity, variability, and suboesophageal connectivity of antennal lobe neurons in d. melanogaster larvae. *Journal of Comparative Neurology*, 519(17):3415–3432.

Tully, T., Cambiazo, V., and Kruse, L. (1994). Memory through metamorphosis in normal and mutant drosophila. *Journal of Neuroscience*, 14(1):68–74.

van Giesen, L., Neagu-Maier, G. L., Kwon, J. Y., and Sprecher, S. G. (2016). A microfluidics-based method for measuring neuronal activity in drosophila chemosensory neurons. *Nature Protocols*, 11(12):2389–2400.

Venken, K. J., Simpson, J. H., and Bellen, H. J. (2011). Genetic manipulation of genes and cells in the nervous system of the fruit fly. *Neuron*, 72(2):202–230.

Vogelstein, J. T., Park, Y., Ohyama, T., Kerr, R. A., Truman, J. W., Priebe, C. E., and Zlatic, M. (2014). Discovery of brainwide neural-behavioral maps via multiscale unsupervised structure learning. *Science*, 344(6182):386–392.

von Essen, A. M., Pauls, D., Thum, A. S., and Sprecher, S. G. (2011). Capacity of visual classical conditioning in drosophila larvae. *Behavioral neuroscience*, 125(6):921.

Waddell, S. (2013). Reinforcement signalling in drosophila; dopamine does it all after all. *Current opinion in neurobiology*, 23(3):324–329.

Widmann, A., Artinger, M., Biesinger, L., Boepple, K., Peters, C., Schlechter, J., Selcho, M., and Thum, A. S. (2016). Genetic dissection of aversive associative olfactory learning and memory in drosophila larvae. *PLoS Genet*, 12(10):e1006378.

Wright, G. A., Mustard, J. A., Simcock, N. K., Ross-Taylor, A. A., McNicholas, L. D., Popescu, A., and Marion-Poll, F. (2010). Parallel reinforcement pathways for conditioned food aversions in the honeybee. *Current Biology*, 20(24):2234–2240.

Wu, Q., Wen, T., Lee, G., Park, J. H., Cai, H. N., and Shen, P. (2003). Developmental control of foraging and social behavior by the drosophila neuropeptide y-like system. *Neuron*, 39(1):147–161.

Wu, Q., Zhao, Z., and Shen, P. (2005). Regulation of aversion to noxious food by drosophila neuropeptide y–and insulin-like systems. *Nature neuroscience*, 8(10):1350–1355.

Yagi, R., Mayer, F., and Basler, K. (2010). Refined lexa transactivators and their use in combination with the drosophila gal4 system. *Proceedings of the National Academy of Sciences*, 107(37):16166–16171.

Yamagata, N., Ichinose, T., Aso, Y., Plaçais, P.-Y., Friedrich, A. B., Sima, R. J., Preat, T., Rubin, G. M., and Tanimoto, H. (2015). Distinct dopamine neurons mediate reward signals for short-and long-term memories. *Proceedings of the National Academy of Sciences*, 112(2):578–583.

Yin, J., Wallach, J., Del Vecchio, M., Wilder, E., Zhou, H., Quinn, W., and Tully, T. (1994). Induction of a dominant negative creb transgene specifically blocks long-term memory in drosophila. *Cell*, 79(1):49–58.

Zwart, M. F., Pulver, S. R., Truman, J. W., Fushiki, A., Fetter, R. D., Cardona, A., and Landgraf, M. (2016). Selective inhibition mediates the sequential recruitment of motor pools. *Neuron*, 91(3):615–628.

8 General discussion

Drosophila larvae have a small nervous system containing of about 10,000 neurons, yet display a large variety of behaviors (Vogelstein et al. [2014]; reviewed in Cobb [1999]; Diegelmann et al. [2013]; Gerber and Stocker [2007]; Schleyer et al. [2013]). The larval stage has all the same advantages as the adult stage: i) the genetic toolset [Brand and Perrimon, 1993], ii) a short generation time (reviewed in Markow [2015]), iii) inexpensive rearing in the laboratory and maintenance of stocks (reviewed in Stocker and Gallant [2008]) and iv) a high degree of homology to the human genome (reviewed in Bier [2005]). The reduced cellular complexity and redundancy makes *Drosophila* larvae an excellent model organism for investigating entire neuronal networks on an ultrastructure level. During my thesis work I mainly focused on reconstructing and analyzing the complete MB connectome consisting of the intrinsic KCs and extrinsic PNs, MBINs and MBONs. In the other part of my thesis I performed associative olfactory learning experiments with *Drosophila* larvae.

8.1 The mushroom body connectome

Chapter I describes the first complete reconstruction of a learning circuit. Here I show that the MB is formed by two distinct groups of intrinsic cells: single-claw and multi-claw KCs. The former are relays of olfactory signals from PNs and thus are stereotypic labeled-line connections. I show that the wiring of olfactory PNs and multi-claw KCs is random and bilaterally asymmetric. The model proposed in *Chapter I* shows that combining a random and a structured connectivity increases dimensionality and reduces the error rate in odor discrimination tasks. However, this is only true for systems with a small ratio of parallel fibers to inputs. For large ratios random connectivity was found to increase the dimension of the sensory representation [Litwin-Kumar et al., 2017].
Moreover in this chapter, I reveal a canonical circuit motif found in each MB compartment

with two unexpected connections. It was previously unknown that KCs synapse back onto MBINs and that MBINs have a direct connection to MBONs.

DANs were reported to be active in response to the US during training. Surprisingly, they also increase their activity as a response to the CS after training in insects (Riemensperger et al. [2005]; reviewed in Menzel [2012]) and monkeys (reviewed in Schultz [2015]). The KC-to-MBIN synapses could potentially explain their activity after learning.

The direct MBIN-to-MBON connections could encode for the outcome expectations described in Schleyer et al. [2011]. Larvae only display the full conditioned response after aversive olfactory training when an equally strong aversive reinforcer is also present in the test situation. Similarly larvae will not express the memory after appetitive training if the same and equally strong appetitive reinforcer is present in the test. Thus larvae only behaviorally express olfactory memory traces when they expect a gain from their actions (reviewed in Schleyer et al. [2011]).

Additionally I found MBON-to-MBIN feedback and feed-across motifs in the larval MB connectome similar to previously reported motifs in adult *Drosophila* [Ichinose et al., 2015; Das et al., 2014; Aso and Rubin, 2016]. These connections are implicated in the formation of long-term and conflicting memories in the adult. Such behaviors have not yet been described in larvae. Based on the available connectomics data one can now set out to investigate long-term memory in *Drosophila* larvae in a targeted way.

8.2 First instar larvae as a study case for anatomical and functional completeness

Testing the reconstructed neurons behaviorally is an important addition to the insight gained by the connectomics approach. A new tool that is being developed in Dr. An-

dreas S. Thum's laboratory will help with designing such experiments. The aim of his project is to establish a neuronal atlas describing the whole CNS on the light microscopy level. The first step was to create a larval standard brain on light microscopy level, called brainbase, by registering multiple brains into a common coordinate system. Then all known brain areas and neuroblast lineages were annotated by hand (by Dr. Volker Hartenstein, UCLA, USA). Subsequently, hundreds of GAL4 driver expression patterns are registered onto the standard brain. This allows for brain area or expression pattern based browsing of the standard brain. An important next step would also be the implementation of the EM connectome. Such a merged dataset will allow searching for GAL4 lines that express in neurons of interest based on the morphology of neurons reconstructed in the EM volume. Fast reconstruction together with a sophisticated search tool for GAL4 driver lines will enable complete description of neuronal networks on the single-synapse level and combined functional analysis of the neurons involved. It is expected that the motifs identified in the first instar larva connectome represent general features of the *Drosophila* MB, as the architecture of the larval and adult MB appear to be very similar. However, the reduced number of neurons in the larval brain enables a relatively rapid investigation of learning behaviors. Together with reconstruction efforts of the larval research community, the structure of other brain areas is being revealed one by one [Heckscher et al., 2015; Ohyama et al., 2015; Berck et al., 2016; Fushiki et al., 2016; Jovanic et al., 2016; Schlegel et al., 2016; Schneider-Mizell et al., 2016; Zwart et al., 2016].

Due to the relatively fast reconstruction of the small larval neurons a complete connectome of an entire brain is within reach. The brain circuitry of many of the sensory pathways described in the *sections 2.4 - 2.6* remain largely unknown. The whole brain connectome will help to reveal these pathways and uncover how sensory information is signaled to the MB. Also it will further enhance our understanding of how different parts

of the brain communicate with another and how neurons are wired to express a variety of behaviors on the system level. The small yet complex brain of larval *Drosophila* enables achieving anatomical and functional completeness with the first whole brain connectome and the ability of testing all neurons behaviorally using the collection of GAL4 and Split GAL4 fly strains available.

8.3 *Drosophila* as a study case for the development of neuronal networks

Reconstruction of whole networks is relatively fast in first instar larvae. The size of neurons and their number of synapses grow by a factor of about 5 from the first to the third larval stage. This increases the reconstruction time for the same neuron in different larval stages by a factor of about 4 (Dr. Casey Schneider-Mizell, personal communication). Therefore the development of suitable tools for automated reconstruction is an important next step. The laboratories of Dr. Albert Cardona and Dr. Stephan Saalfeld at Janelia Research Campus recently started to develop automated reconstruction and synapse-detection tools. Furthermore, there have been efforts of semi-automated reconstruction in adult *Drosophila*, this method remains laborious (seven column medulla dataset Takemura et al. [2015]; vertical lobe of the MB is in preparation, Dr. Gerald Rubin, personal communication). The further advancement of such tools will foster rapid reconstruction of neuronal networks in multiple life stages of *Drosophila*. This will make the fruit fly an excellent study case for the changes neuronal networks undergo during development and how neurons maintain or change their function and wiring in a developing brain.

8.4 Behavioral concordance of different larval stages

As mentioned before, I reconstructed the MB in an EM volume of a whole first instar larval brain (*Chapter I*). However most behavioral studies are performed with third instar larvae. Thus it is important to investigate if these two larval stages express similar behaviors and are comparable. *Chapter II* describes innate and learned behavior expression in first and third instar larvae. Interestingly, there are only small differences in behavior between these two stages and the results suggest concordance of the tested behaviors. The differences found are mostly due to the slower locomotion in the much smaller first instar larvae.

Importantly, when comparing performance indices for olfactory learning in first to third instar larvae no differences were found. As described in *Chapter I* a subset of KCs only forms a single dendritic claw each and receives from only one olfactory PN. Evidently these KCs are born first in the developing MB ensuring that all olfactory stimuli are represented in the KCs. During the development of the MB more and more multi-claw KCs are added encoding for combinations of stimuli and decreasing the error rate in odor discrimination tasks. It is expected that very young first instar larvae would perform badly when trained with two very similar odors, while older larvae have the ability to discriminate these odors well in such a task. Testing very young larvae (for example 6 hours after hatching, the age of the EM dataset larva) is experimentally very challenging, thus how well such young larvae with only few multi-claw KCs perform in learning and odor discrimination tasks remains unclear. However as shown by modeling experiments in *Chapter I* the composition of single- and multi-claw KCs already decreases error rate and increases dimensionality in a 6 hour old larva. This suggest that the performance of very young larvae in learning tasks might not differ from the performance shown in *Chapter II*.

Moreover, *Chapter IV* characterizes all MBINs and MBONs morphologically in third instar larvae with light microscopy. Comparing this light-microscopical neuronal atlas with the neurons reconstructed in the first instar larva (*Chapter I*) yields a high degree of similarity. Even though first instar larvae are missing one pair of MBINs and MBONs they can perform odor-fructose associations [Pauls et al., 2010], implicating a level of redundancy in the MB system.

8.5 Organization of reward and punishment signaling by MBINs

Chapter IV also describes the reward system of the MB in more detail. MBINs were found to be task specific, meaning that a different set of MBINs encodes for every type of reinforcer maintaining information about the reward identity in a labeled-line fashion. However, silencing these neurons only partially impairs memory in many cases, suggesting a partially redundant combinatorial code in the reward system. This has been found to be the case in adult *Drosophila* as well [Burke et al., 2012; Lin et al., 2014].

Chapter III describes the punitive effects of mechanosensory cues in third instar larvae. This work together with the MB reconstruction (*Chapter I*) and recent reconstruction efforts of the mechanosensory system [Jovanic et al., 2016; Ohyama et al., 2015] is guiding further investigation of the neuronal networks underlying odor-'buzz' learning in larvae. To date, the MBINs conveying punishment information onto the KCs are unknown. Recent studies in the laboratory of Dr. Marta Zlatic at Janelia Research Campus are investigating the role MB vertical lobe DANs and OANs play in the combinatorial code of aversive stimuli (it appears to be a similar case as in the appetitive system described in *Chapter IV*, Dr. Claire Eschbach, personal communication).

8.6 Review and concluding thoughts

Chapter V reviews the recent findings in the field of learning and memory of *Drosophila* larvae. This chapter points out that studying learning and memory in larvae as opposed to adult *Drosophila* has some clear advantages. One important difference between these life stages for aversive associative learning is that adult flies only ingest aversive food compounds (for example high-salt concentrations or quinine) when they are mixed with appetitive food compounds (sugar). That renders the conditioned response hard to interpret. Larvae will ingest aversive compounds when presented purely while crawling over the substrate. Moreover the reconstruction efforts in the whole brain of the larva in general and the MB connectome in particular for studying learning and memory are obvious advantages of the larva over the adult fly.

In summary, the studies included in my thesis are efforts made by many labs investigating behavior and reconstructing neuronal networks and strengthen *Drosophila* larvae in its role as a favorable model organism to study how information is processed in the brain. Accessibility to wiring diagrams of all brain areas will guide behavioral studies in the future. This will enable deciphering of how a whole brain functions and how all neurons of a brain work together to perform the entire behavioral repertoire of an animal in every day life.

Taken together, my thesis work provides a road map for future investigations of the learning and memory center in insects and will help understanding how a brain integrates sensory information to predict future events.

8.7 References

Aso, Y. and Rubin, G. D. (2016). Parallel dopaminergic neurons write and update memories with cell-type-specific rules. *eLife*.

Berck, M. E., Khandelwal, A., Claus, L., Hernandez-Nunez, L., Si, G., Tabone, C. J., Li, F., Truman, J. W., Fetter, R. D., Louis, M., et al. (2016). The wiring diagram of a glomerular olfactory system. *Elife*, 5:e14859.

Bier, E. (2005). Drosophila, the golden bug, emerges as a tool for human genetics. *Nature Reviews Genetics*, 6(1):9–23.

Brand, A. H. and Perrimon, N. (1993). Targeted gene expression as a means of altering cell fates and generating dominant phenotypes. *development*, 118(2):401–415.

Burke, C. J., Huetteroth, W., Owald, D., Perisse, E., Krashes, M. J., Das, G., Gohl, D., Silies, M., Certel, S., and Waddell, S. (2012). Layered reward signalling through octopamine and dopamine in drosophila. *Nature*, 492(7429):433–437.

Cobb, M. (1999). What and how do maggots smell? *Biological reviews*, 74(4):425–459.

Das, G., Klappenbach, M., Vrontou, E., Perisse, E., Clark, C. M., Burke, C. J., and Waddell, S. (2014). *Drosophila* learn opposing components of a compound food stimulus. *Current biology*, 24(15):1723–1730.

Diegelmann, S., Klagges, B., Michels, B., Schleyer, M., and Gerber, B. (2013). Maggot learning and synapsin function. *Journal of Experimental Biology*, 216(6):939–951.

Fushiki, A., Zwart, M. F., Kohsaka, H., Fetter, R. D., Cardona, A., and Nose, A. (2016). A circuit mechanism for the propagation of waves of muscle contraction in drosophila. *Elife*, 5:e13253.

Gerber, B. and Stocker, R. F. (2007). The *Drosophila* larva as a model for studying chemosensation and chemosensory learning: a review. *Chemical senses*, 32(1):65–89.

Heckscher, E. S., Zarin, A. A., Faumont, S., Clark, M. Q., Manning, L., Fushiki, A., Schneider-Mizell, C. M., Fetter, R. D., Truman, J. W., Zwart, M. F., et al. (2015). Even-skipped+ interneurons are core components of a sensorimotor circuit that maintains left-right symmetric muscle contraction amplitude. *Neuron*, 88(2):314–329.

Ichinose, T., Aso, Y., Yamagata, N., Abe, A., Rubin, G. M., and Tanimoto, H. (2015). Reward signal in a recurrent circuit drives appetitive long-term memory formation. *eLife*, 4:e10719.

Jovanic, T., Schneider-Mizell, C. M., Shao, M., Masson, J.-B., Denisov, G., Fetter, R. D., Mensh, B. D., Truman, J. W., Cardona, A., and Zlatic, M. (2016). Competitive disinhibition mediates behavioral choice and sequences in drosophila. *Cell*, 167(3):858–870.

Lin, S., Owald, D., Chandra, V., Talbot, C., Huetteroth, W., and Waddell, S. (2014). Neural correlates of water reward in thirsty drosophila. *Nature neuroscience*, 17(11):1536–1542.

Litwin-Kumar, A., Decker Harris, K., Axel, R., Sompolinsky, H., and Abbott, L. F. (2017). Optimal degrees of synaptic connectivity. *Neuron, in press*.

Markow, T. A. (2015). The secret lives of drosophila flies. *Elife*, 4:e06793.

Menzel, R. (2012). The honeybee as a model for understanding the basis of cognition. *Nature Reviews Neuroscience*, 13(11):758–768.

Ohyama, T., Schneider-Mizell, C. M., Fetter, R. D., Aleman, J. V., Franconville, R., Rivera-Alba, M., Mensh, B. D., Branson, K. M., Simpson, J. H., Truman, J. W., et al. (2015). A multilevel multimodal circuit enhances action selection in drosophila. *Nature*, 520(7549):633–639.

Pauls, D., Selcho, M., Gendre, N., Stocker, R. F., and Thum, A. S. (2010). Drosophila larvae establish appetitive olfactory memories via mushroom body neurons of embryonic origin. *Journal of Neuroscience*, 30(32):10655–10666.

Riemensperger, T., Völler, T., Stock, P., Buchner, E., and Fiala, A. (2005). Punishment prediction by dopaminergic neurons in *Drosophila*. *Current biology*, 15(21):1953–1960.

Schlegel, P., Texada, M. J., Miroschnikow, A., Schoofs, A., Hückesfeld, S., Peters, M., Schneider-Mizell, C. M., Lacin, H., Li, F., Fetter, R. D., et al. (2016). Synaptic transmission parallels neuromodulation in a central food-intake circuit. *eLife*, 5:e16799.

Schleyer, M., Diegelmann, S., Michels, B., Saumweber, T., and Gerber, B. (2013). 'decision making' in larval drosophila. In Menzel, R. and Benjamin, P., editors, *Invertebrate learning and memory*. Elsevier.

Schleyer, M., Saumweber, T., Nahrendorf, W., Fischer, B., von Alpen, D., Pauls, D., Thum, A., and Gerber, B. (2011). A behavior-based circuit model of how outcome expectations organize learned behavior in larval *Drosophila*. *Learning & Memory*, 18(10):639–653.

Schneider-Mizell, C. M., Gerhard, S., Longair, M., Kazimiers, T., Li, F., Zwart, M. F., Champion, A., Midgley, F. M., Fetter, R. D., Saalfeld, S., et al. (2016). Quantitative neuroanatomy for connectomics in drosophila. *Elife*, 5:e12059.

Schultz, W. (2015). Neuronal reward and decision signals: from theories to data. *Physiological Reviews*, 95(3):853–951.

Stocker, H. and Gallant, P. (2008). Getting started: an overview on raising and handling drosophila. *Drosophila: Methods and Protocols*, pages 27–44.

Takemura, S.-y., Xu, C. S., Lu, Z., Rivlin, P. K., Parag, T., Olbris, D. J., Plaza, S., Zhao, T., Katz, W. T., Umayam, L., et al. (2015). Synaptic circuits and their variations within different columns in the visual system of drosophila. *Proceedings of the National Academy of Sciences*, 112(44):13711–13716.

Vogelstein, J. T., Park, Y., Ohyama, T., Kerr, R. A., Truman, J. W., Priebe, C. E., and Zlatic, M. (2014). Discovery of brainwide neural-behavioral maps via multiscale unsupervised structure learning. *Science*, 344(6182):386–392.

Zwart, M. F., Pulver, S. R., Truman, J. W., Fushiki, A., Fetter, R. D., Cardona, A., and Landgraf, M. (2016). Selective inhibition mediates the sequential recruitment of motor pools. *Neuron*, 91(3):615–628.

9 Abbreviations

AD:	activation domain
AL:	antennal lobe
AM:	*n*-amylacetate
APL:	anterior paired lateral
BO:	bolwig's organ
CA:	calyx
Ca^{2+}:	calcium^{2+}
cAMP:	cyclic adenosine 3'5'-monophosphate
CNS:	central nervous system
CS:	conditioned stimulus
DA:	dopamine
DAN:	dopaminergic neuron
DBD:	DNA binding domain
DNA:	deoxyribonucleic acid
EA:	ethyl acetate
EM:	electron microscopy
FRU:	fructose
GFP:	green fluorescent protein
GR:	gustatory receptor
GRN:	gustatory receptor neuron
Hz:	Hertz
IAV:	inactive
IP:	intermediate peduncle
IT:	intermediate toe
IVL:	intermediate vertical lobe
KC:	Kenyon cell
L1:	first instar
L3:	third instar
LA:	lateral appendix
LH:	lateral horn
LN:	lateral neuron
LP:	lower peduncle
LT:	lower toe
LVL:	lower vertical lobe
MB:	mushroom body
MBIN:	mushroom body input neuron
MBON:	mushroom body output neuron
md:	class IV multidendritic
ML:	medial lobe
NaCl:	sodium chloride
NAN:	nanchung
NOMPC:	No mechanoreceptor potential C
OA:	octopamine
OAN:	octopaminergic neuron
OCT:	1-octanol
OR:	olfactory receptor
ORN:	olfactory receptor neuron
PI:	performance index
PKA:	protein kinase A
PKC:	protein kinase C
PN:	projection neuron
ppk:	pickpocket
PR:	photoreceptor
SEZ:	subesophageal zone
SHA:	shaft
shi^{ts}:	temperature sensitive shibire
Syn:	synapsin
TRP:	transient receptor potential
UAS:	upstream activation sequence
US:	unconditioned stimulus
UT:	upper toe
UVL:	upper vertical lobe
VL:	vertical lobe
VUM:	ventral unpaired median

10 Declaration of author's contributions

Chapter I: The complete connectome of the mushroom body of a *Drosophila* larva (Eichler et al., 2017, in press)

I reconstructed neurons, performed learning experiments, conceived the project, analyzed the data and wrote the manuscript.

Chapter II: The Ol$_1$mpiad: Concordance of behavioural faculties of stage 1 and stage 3 *Drosophila* larvae (The Ol$_1$mpiad consortium, 2017, in press)

I contributed to the experiments and analyzed data.

Chapter III: Immediate and punitive impact of mechanosensory disturbance on olfactory behaviour of larval *Drosophila* (Saumweber et al., 2014)

I contributed to the experiments.

Chapter IV: Functional architecture of reward learning in mushroom body extrinsic neurons of larval *Drosophila* (Saumweber et al., in revision)

I contributed electron microscopy data and analysis, experiments for Figure S5 and contributed to the writing of the manuscript.

Chapter V: Odor-taste Learning in *Drosophila* Larvae (Widmann et al., in revision)

I contributed to the figures and to writing the manuscript.

11 Acknowledgements

First and foremost I would like to thank my two supervisors Dr. Marta Zlatic and Dr. Andreas S. Thum for giving me the opportunity to work in both of their labs. Thank you Marta for the advice and support you gave me throughout all these years. I truly enjoyed the hours and hours spend in your office shaping this gigantic connectome dataset into a manuscript. Thank you Andi for the wonderful support you gave me from so far away and for trusting me to do this thesis remotely. Even though I have never been physically in your lab you always gave me the great feeling of being a part of it. I greatly appreciate all the advice and problem solutions that you gave me over Skype so many times.

I would also like to thank Dr. Albert Cardona for giving me the opportunity to reconstruct this truly fascinating area of the brain is his whole larval brain dataset. Thank you Albert for introducing me to coding and all the time spend fixing my errors and dealing with large amounts of data with me.

A big thanks goes to all the lab members of the Zlatic and Cardona labs. Thank you all for the collaboration and helpful inputs on my work and of course for the fun coffee breaks. A special thanks to Andrew Champion and Tom Kazimiers for always helping me with my computational problems and creating new useful ”buttons” in CATMAID for me. Furthermore thanks to Feng Li and Timo Saumweber for reconstructing the MB network with me. Also I would like to thank the rest of the larva brain tracing community for the support when I started to learn how to reconstruct and the endless hours of reviewing my first tracings.

Finally I would like to thank my parents Monika and Stefan Eichler and my sister Janina Eichler, to whom I dedicated this work. You have always been my biggest supporters and I thank you for all the encouragement through the years of undergrad and graduate work. Ich habe euch lieb!

Last but definitely not least I thank Samuel Nealy for his endless patience and help during the last months of my PhD thesis.